Factors affecting *de novo* formation of a yeast prion

by

Klement Stojanovski

University of Kent

A thesis submitted to the University of Kent for the degree of PhD in Biochemistry in the School of Biosciences

September 2011

Abstract

Prions are aggregates of misfolded proteins that have acquired an amyloid-like structure and ability to propagate through recruitment of new proteins. [*PSI*+], a prion form of eukaryotic release factor Sup35 (eRF1) is widely used as a model for research on prion formation and propagation and in this study [*PSI*+] is used to explore an effect of three previously identified proteins on *de novo* prion formation. One mechanism proposed to affect prion formation is direct interaction of Sup35p with its binding partners and search for proteins that interact with Sup35p identified Ppq1p, a putative Ser/Thr protein phosphatase (M.F. Tuite and T. von der Haar). Another approach was to identify proteins that function to protect translational apparatus from environmental and endogenous oxidative damage and this approach identified two ribosome associated peroxiredoxins, Tsa1p and Tsa2p (T. Sideri and C.M. Grant).

The data presented here shows that the deletion of *PPQ1* gene greatly increases the rate of *de novo* formation of [*PSI*+], but the mechanism by which loss of Ppq1p affects [*PSI*+] formation is not known. Analysis of the distribution of fluorescently-tagged Ppq1p showed that the protein co-localises with mitochondria. A further line of evidence linking Ppq1p to mitochondria was an observed reduction in respiratory capacity of a *ppq1Δ* strain.

That exposure to environmental sources of oxidative stress promotes [*PSI*+] prion formation was previously reported (Tyedmers *et al.*, 2008). Results presented here show that an endogenous source of oxidative stress, brought about by deleting the ribosomally-associated peroxiredoxins (Prx) encoded by genes *TSA1/2* (Trotter *et al.*, 2008; Sideri *et al.*, 2010), also increases the rate of *de novo* [*PSI*+] formation. This result provides a direct link between oxidative stress and the eukaryotic release factor Sup35p.

Declaration

No part of this thesis has been submitted in support of any other application for a degree or qualification of the University of Kent or any other University or Institute of learning.

Klement Stojanovski

September 2011

This thesis is composed of six chapters. The first chapter is an introduction to the topic and the second chapter is materials and methods. Chapters three, four and five are results chapters and chapter six is the general discussion chapter. I declare that I performed all the experimental work presented here with the exception of some genetic crosses that were done by Dr. B.S. Cox (University of Kent) and deletion strains done by T. Sideri (Manchester University) that are mentioned in text.

Part of data presented in Chapter 5 of this thesis was published in:

Sideri T.C., Stojanovski K., Tuite M.F., and Grant C.M. (2010) Ribosome-associated peroxiredoxins suppress oxidative stress-induced de novo formation of the [*PSI*⁺] prion in yeast. *Proc Natl Acad Sci U S A* **107**: 6394-6399.

Acknowledgments

Table of contents

Chapter I

Chapter II

Chapter III

Assaying *de novo* formation of the [*PSI*⁺] prion in wild type and mutant cells

Chapter V

The role of the Tsa1p/Tsa2p peroxiredoxins in _de novo_ formation of the [PSI⁺] prion

Chapter VI

List of Figures

List of Tables

Chapter I

Introduction

1.1   Prologue

Life is thought to have arisen soon after the environment on Earth became habitable, around 3.6 billion years ago. The process by which living organisms emerged is not understood, although hypotheses abound and can be divided into two groups: those that propose that the initial unit of living was a self-replicating hereditary molecule; and a second group that favours a "metabolism-first" explanation where a system of organic molecules did not carry hereditary information, but were able to oxidise inorganic molecules (e.g. Ferris, 2006; Shapiro, 2006). Regardless of whether metabolism or heredity preceded the other the next stage in evolution of life is thought to have been a system of molecules, presumably RNA that could perform both processes, self-replication and metabolism, i.e. the RNA world. Tentative evidence for this stage in evolution can still be found in living organisms (e.g. Ban *et al.*, 2000 and Nissen *et al.*, 2000). Since at least the time of the last common ancestor, storage of hereditary information and metabolism have been separated between two types of molecules, DNA and proteins. This division of heredity and metabolism was a central dogma of molecular biology (Crick, 1970) for decades, until it was challenged by the discovery of proteins that can do both, the prions.

1.2   Prions and protein-only hypothesis

1.2.1 Protein as a sole hereditary determinant

Scrapie, a disease that naturally occurs in sheep and goats, was first described almost 250 years ago, but it was not until 1939 that Cuille and Chelle proved that scrapie is an infectious disease. Similar diseases have also been described in humans: Creutzfeld-Jacob disease (1920) and its variant (vCJD; 1995), Gertzmann-Sträusler syndrome, fatal familial insomnia and kuru (1957). Various hypotheses on infectious particles were proposed to describe these peculiar human encephalopathies, e.g. "slow virus" (Gajdusek *et al.*, 1966). But the causative agent of scrapie was resistant to high temperature, UV radiation and formaldehyde treatment that inactivate nucleic acids (Chandler, 1961; Alper *et al.*, 1966) and these findings led to a proposal that the infectious particle is a protein (Griffith, 1967).

The idea was further elaborated by Prusiner and co-workers (Prusiner *et al.*, 1982; Prusiner, 1982) who introduced the term prion, a `small proteinaceus infectious particle which resists inactivation by procedures that modify nucleic acids'. Prusiner and colleagues were also the first to purify a prion protein and named it PrP. The prion and its native forms were later named PrP^{sc} and PrP^{c}, respectively. Despite huge interest by

science community in prions, they remained from biological perspective little more than a peculiar mammalian disease until 1994 when the protein-only prion hypothesis was proposed by Wickner to describe [*URE3*], an unusual non-mendelian trait of yeast *Saccharomyces cerevisiae* (Wickner, 1994). Several other fungal prions have been subsequently described: [*PSI*$^+$] (Wickner, 1994), [*HET-s*] (Coustou *et al.*, 1997), and [*RNQ*$^+$] (Sondheimer *et al.*, 2000) and linked to proteins Sup35p, HET-s, and Rnq1p, respectively. In recent years many new yeast prions were discovered and are described below (section 1.7).

1.2.2 Mechanism of prion appearance and propagation

Prions propagate by altering the normal structure of the cellular form of that protein (Griffith, 1967; Prusiner, 1982). In the *de novo* appearance of a prion, the natively folded protein adopts an alternative conformational state, either spontaneously or by interaction with other cellular factors. The detailed mechanism of *de novo* formation remains unknown, but it appears that interaction between prion proteins alone is sufficient for formation of a prion. Two alternative models have been proposed (Figure 1.1): the first model porposes that interaction between two monomers is sufficient for prion formation. This model was envoked to explain results of an experiment where researchers forced close proximity of two proteins and which was sufficient to induce conformational change. Such a dimer then served as a nucleus for conversion of other proteins to prion form and polymerisation into amyloid fibers (Goggin *et al.*, 2007; Roostaee *et al.*, 2009). Alternative model proposes that natively folded monomers are present in a cell in a dynamic equilibrium with partially misfolded monomers and oligomers. Metastable oligomeric species can undergo internal rearrangement into a stable amyloid species called propagon (Cox *et al.*, 2003) that facilitates conversion of other oligomers and that is capable of polymerisation into fibres (Serio *et al.*, 2000). Other cellular and environmental factors are therefore not necessary for prion formation, but could modulate this process.

Propagation of the prion form is thought to occur through a different mechanism and a typical lag phase is observed before the rapid polymerisation that precedes propagation. Evidence suggests that fragments of high molecular weight aggregates, polymers insoluble in sodium dodecyl sulphate (SDS; an ionic detergent) are necessary for the growth of prion polymers (Kryndushkin *et al.*, 2003). Once highly aggregated polymers are formed, subsequent polymerisation *in vitro* occurs through addition of monomers (Collins *et al.*, 2004) or oligomers (Serio *et al.*, 2000).
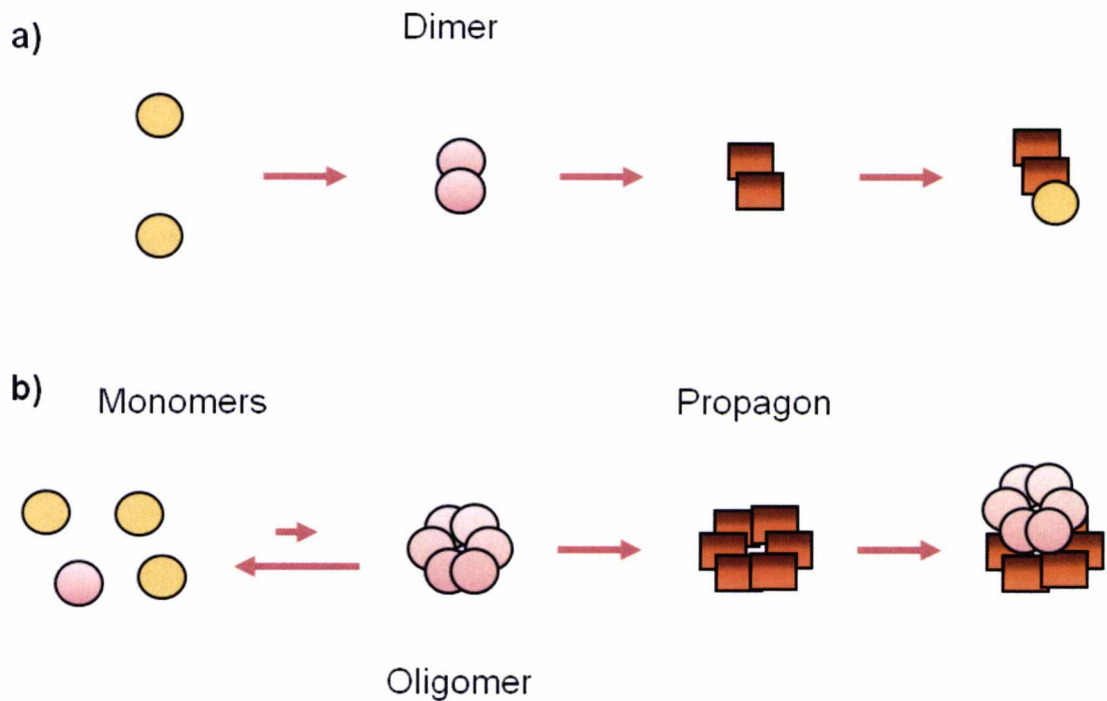
Figure 1.1: Two models of *de novo* prion formation. a) Close proximity of two monomers induces comformational change and an adoption of a stable amyloid structure. A dimer (and possibly a monomer) is capable of catalyzing comformational change of natively folded proteins; b) Folded monomers and partially unfolded monomers and oligomers are present in cells in equilibrium. Oligomers are metastable and can rearrange into a stable amyloid conformation. Such stable oligomers can catalyze structural change in other oligomers and possibly monomers; yellow circles – natively folded proteins, pink – partially misfolded proteins, dark red – a stable amyloid conformation.

1.2.3 Evidence for the protein-only hypothesis

To distinguish between nucleic acid replicons and prions in general, four genetic properties are expected to be found in the latter (Wickner, 1994) (NB: citations refer to studies that demonstrated a particular property for the eukaryotic release factor 3 (Sup35p) and its prion [*PSI*$^+$]):

1. The gene coding for the protein that gives rise to the prion is required for *de novo* formation and propagation of that prion. Cells lacking the protein cannot get infected or spontaneously generate that prion. This requirement cannot be demonstrated for Sup35p since the deletion of *SUP35* gene is lethal. The deletion of its prion forming domain (PrD) that is not necessary for Sup35p translation

termination function (see section 1.4) prevents prion formation (Doel *et al.*, 1994; Ter-Avanesyan *et al.*, 1994).

2. Presence of a prion results in a phenotype that is similar to that of the mutated or deleted gene. Aggregation of a protein leads to its inactivation and therefore, to a phenotype similar to that of cells with a non-functional protein. The *SUP35* gene is required for viability of the cell, but many mutants are known that reduce translation termination (Smirnov *et al.*, 1974; Cox, 1977).

3. Overproduction of a protein increases the frequency of *de novo* appearance of the prion presumably because there are more molecules of the protein that can undergo the necessary conformational change and establish the key protein: protein interactions (Chernoff *et al.*, 1993).

4. Cells exhibit reversible curability i.e. prions can be eliminated by some type of treatment that does not affect DNA, but unlike non-chromosomal nucleic acids, can then reappear spontaneously, by gene overexpression or other methods providing the protein that forms the prion is still present (Chernoff *et al.*, 1995).

A further line of evidence for the hypothesis is that *in vitro* generated aggregates can act as infectious agents. Aggregation of a purified soluble protein is induced *in vitro* and these aggregates can be used to infect [*prion⁻*] cells (King *et al.*, 2004; Tanaka *et al.*, 2004).

1.2.4 Prion strains/variants

Mammalian encephalopathies vary significantly in terms of incubation periods and neural degeneration patterns. That one conformation can cause a variety of diseases was seen as an evidence against protein only hypothesis by the opponents of the hypothesis. But it was eventually shown that prion proteins can adopt several alternative stable conformational states that correspond to different diseases. Bessen and Marsh (Bessen *et al.*, 1994) showed that two prion strains had different protease digestion patterns, indicating that overlapping, but not identical sequences of PrP protein were present in amyloid aggregates. Prion strains are in yeast called variants to avoid confusion with strains of different genetic backgrounds. Existence of not just two, but several different stable conformations appeared contra-intuitive, as the prevailing idea was that primary structure or amino acid (aa) sequence can only define one or two stable conformations. The challenge to the protein-only hypothesis was, therefore to explain the existence of different prion strains. The confirmation of multi-stable conformations hypothesis came

from studies of yeast prions, where King *et al.* (2004) and Tanaka *et al.* (2004) demonstrated a relationship between protein conformation and phenotype by creating polymers *in vitro* from isolated variant-specific seeds. These polymers were then used to infect yeast cells, which developed distinct, aggregate-specific phenotypes that were stably inherited.

Largely due to studies on yeast prions, the protein-only hypothesis is now widely accepted however some scepticism regarding mammalian prion still exist (Manuelidis *et al.*, 2007).

1.3   Amyloidogenesis

Amyloid fibrils significantly differ from other, amorphous protein aggregates, in that they are stable, ordered, filamentous aggregates that polymerise spontaneously. They can form large deposits and have been implicated in many human diseases e.g. Parkinson's disease. Amyloids were first described by Astbury (Astbury *et al.*, 1935), who examined an x-ray diffraction pattern of poached egg white and noted a reflection at ~4.7 Å along the stretched direction, and a perpendicular one at ~10 Å. This is indicative of β-strands perpendicular to the long axis of the fibril (Sunde *et al.*, 1997). Other properties of amyloids include their specific binding of thioflavin T and Congo red, which gives an apple-green birefringence under polarized light when bound to β-sheets (Chiti *et al.*, 2006).

Studies of amyloid macrostructure using transmission electron and atomic force microscopy have shown that amyloid fibrils vary in their shape; they can be rope-like and 7-13 nm wide or form long ribbons, 2-5 nm thick and up to 30 nm wide. Amyloid fibrils are usually made of 2-6 protofilaments each 2-5 nm in diameter (Bauer *et al.*, 1995; Saiki *et al.*, 2005; Pedersen *et al.*, 2006). Some amyloids also form higher-ordered structures (e.g. Jin *et al.*, 2003) with features found in classical polymers (Chiti *et al.*, 2006).

Other oligomeric species precede formation of the final amyloid state. These species contain β-sheets and bind Congo red and Thioflavin T (Walsh *et al.*, 1999), but are metastable and do not form stable fibrils. Although oligomeric species vary in macrostructure, a specific antibody can bind to oligomers of different proteins, but not to their monomeric or amyloid states, therefore proving that some common structure underlies the oligomeric species (Kayed *et al.*, 2003). Kayed *et al.* (2003) have also linked these species to cellular toxicity and consequently, disease pathology. Importantly, oligomeric species can represent intermediate steps towards fibril maturation (Harper *et al.*, 1997), but some appear to be `off-pathway´ and can form stable non-fibrilar

aggregates (Morozova-Roche *et al.*, 2004). Furthermore, fibril maturation can follow different paths simultaneously (Morozova-Roche *et al.*, 2004).

1.3.1 Factors affecting aggregation

Aggregation of proteins proceeds at different rates, depending on protein properties or intrinsic factors and on properties of the ionic environment (Chiti *et al.*, 2006). Studies on the effects of amino acid substitutions on the rate of aggregation of unstructured proteins have shown that amyloid formation is governed by simple physiochemical factors (Chiti *et al.*, 2006). Intrinsic factors affecting the change of rate are hydrophobicity, propensity to undergo a conformational transition from α to β structure (β-sheet propensity), and the net charge of the whole polypeptide chain (Chiti *et al.*, 2006). There are other, possible but disputed factors (Tartaglia *et al.*, 2004). Based on experimental data, algorithms have been developed that can indentify aggregation-prone regions within proteins and predict rate of fibril formation (e.g. DuBay *et al.*, 2004; Fernandez-Escamilla *et al.*, 2004). An algorithm described by the latter authors can be used to predict aggregation of folded proteins. Interestingly, this model predicts that highly aggregation-prone sequences are made of at least five consecutive residues populating the β-sheet. A similar sequence (GNNQQNY) was shown to form the core of Sup35p aggregates (Nelson *et al.*, 2005). Extrinsic factors, protein concentration, ionic strength and pH of the solution also play an important role in protein aggregation (DuBay *et al.*, 2004).

Many proteins are partly unfolded in their native state, including all known mammalian and fungal prions (Chiti *et al.*, 2006). Even fully folded proteins are transitionally unstructured during posttranslational folding, transport and stress (Dobson, 2003). Besides previously described factors, the accessibility of aggregation prone sequence to the solvent and conformational flexibility of the chain are important as well (Monti *et al.*, 2004). Interestingly, despite the importance of the above structural factors, partial unfolding is not necessary for aggregation of some fully structured proteins (Plakoutsi *et al.*, 2004).

Two main hypotheses are evoked to explain formation of alternate protein conformations in amyloidogenic proteins. The first proposes that refolded protein is stabilised mainly by backbone H-bonds (Fandrich *et al.*, 2001). Amino acid sequence is less important, although aa composition can affect the rate of fibrillisation and stability of aggregates. The alternative hypothesis proposes that aa side-chain interaction are more important for formation of aggregates. These can interact through H-bonds as proposed for Ure2p (Kajava *et al.*, 2004; Chan *et al.*, 2005) or stabilise the conformation through hydrophobic

interactions as demonstrated for the Sup35p-derived peptide GNNQQNY (Nelson *et al.*, 2005; van der Wel *et al.*, 2007). In their study of PrP protein Govaerts *et al.* (2004) proposed β-helix as a generic structure for aggregating proteins.

Two amino acids, glutamine (Gln) and asparagine (Asn) commonly found in amyloidogenic sequences were thought to have similar effect on propensity of the sequence to form an amyloid (Michelitsch *et al.*, 2000; Ross *et al.*, 2005a). New evidence suggests that Gln and Asn do not act in the same way on aggregation of prion proteins (Alberti *et al.*, 2009; Halfmann *et al.*, 2011). Replacing all Gln residues with Asn residues (all Asn) in Sup35p prion domain partly abolished the need for [*PIN*⁺] factor (see below) in [*PSI*⁺] prion formation presumably because Asn promoted aggregation (Halfmann *et al.*, 2011). Replacing all Asn with Gln (all Gln) residues in the same sequence on the other hand significantly reduced *de novo* formation of [*PSI*⁺] and produced an unstable prion that was readily lost (Halfmann *et al.*, 2011). In aggrement with their effect on *de novo* [*PSI*⁺] formation all Asn Sup35p proteins formed SDS-resistant aggregates, while all Gln did not. Previous studies have suggested that ordered amyloid fibres are not the toxic species and that toxicity to cells is cause by smaller presumably less structured oligomeric species (Kayed *et al.*, 2003). Study of all Gln and all Asn Sup35p sequences confirms this, since all Asn that readily forms amyloid aggregates was not toxic to the cell, while all Gln increase toxicity compared to wild type (wt) Sup35p (Halfmann *et al.*, 2011).

1.3.2 Does Sup35p form amyloids?

Several lines of evidence show that Sup35p, at least *in vitro*, does form amyloid fibres. *In vitro* generated fibres stain with amyloid-binding dyes Thioflavin T (Kimura *et al.*, 2003) and Congo red (King *et al.*, 1997). Aggregates are also SDS insoluble (Kryndushkin *et al.*, 2003) and are more protease resistant than the soluble form of Sup35p (King *et al.*, 1997). Inspection of aggregates using EM shows that they form fibres typical of amyloids (Glover *et al.*, 1997). Sup35pNM filaments also show X-ray diffraction (Serio *et al.*, 2000), X-ray fibre diffraction (Kishimoto *et al.*, 2004) and electron diffraction (King *et al.*, 2004) patterns consistent with cross-β structure. A detailed structure of GNNQQNY fragment from NQ-rich domain obtained by x-ray diffraction and solid state NMR revealed that the fragment can form amyloids *in vitro* (Nelson *et al.*, 2005; van der Wel *et al.*, 2007). Recently, amyloid fibres of the [*PSI*⁺] prion have also been detected *in vivo* in cells that expressed Sup35p under its native promoter (Kawai-Noma *et al.*, 2010).

A structure of Sup35p amyloid and of other yeast prions is still in dispute (Figure 1.2). Two competing models were proposed, a parallel in-register beta-sheet (Shewmaker *et al.*, 2006; Shewmaker *et al.*, 2008) and a cross beta-helix (Kishimoto *et al.*, 2004; Krishnan *et al.*, 2005; Nelson *et al.*, 2005). Current evidence favours the parallel in-register beta-sheet structure.
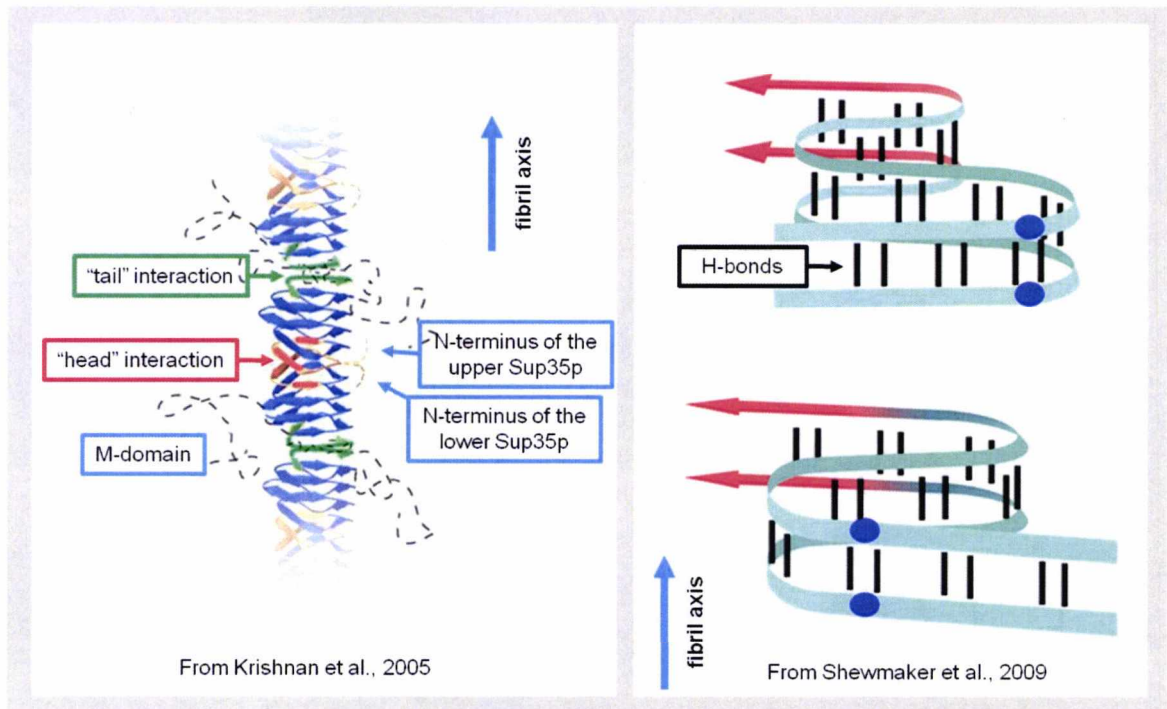
Figure 1.2: Alternative structures of Sup35p amyloids. left) Cross beta-helix: two Sup35p molecules interact with each other near N-terminus of N-domain (head) and with adjacent molecules in the fiber near M-domain (tail); right) Parallel in-register beta-sheet: two molecules are aligned along the sequence and interaction is stabilised with hydrogen bonds. Two alternative conformations that correspond to different prion variants are shown.

1.4 Sup35p and [*PSI⁺*] prion

Sup35p is also known as eukaryotic release factor 3 (eRF3) and functions as a translational termination factor in protein biosynthesis. Sup35p is a GTP-ase and interacts with Sup45p (eRF1) that decodes all three stop codons to form a complex that acts as a polypeptide chain release factor (Figure 1.3) (Stansfield *et al.*, 1995; Zhouravleva *et al.*, 1995). Only the C-terminal (C) domain of Sup35p is necessary for that function (Teravanesyan *et al.*, 1993) and while a NM domain truncated protein is fully functional, it is possible that the NM region also has a functional role (Teravanesyan *et al.*, 1993; Ter-Avanesyan *et al.*, 1994; Liu *et al.*, 2002; Hosoda *et al.*, 2003; Urakov *et al.*, 2006). Sup35p sequence is presented in Figure 1.4.
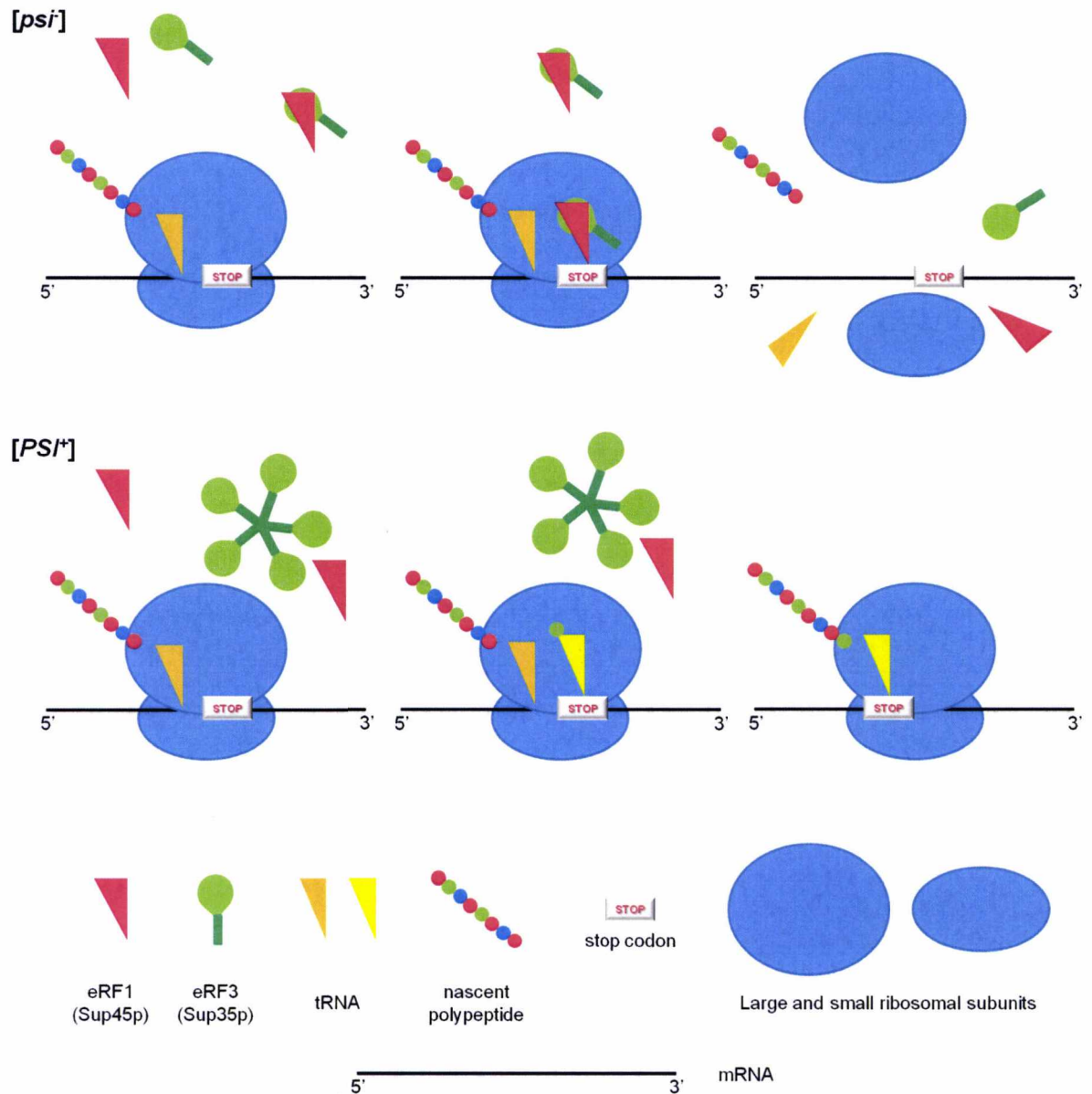
Figure 1.3: Translation termination in [*psi*] and [*PSI*+] cells. When a ribosome encounters a stop codon during translation it is decoded by Sup45p (eRF1) in a complex with Sup35p (eRF3). The translation stops and the nascent polypeptide is released. In [*PSI*+] cells, Sup35p is mostly present in form of prion aggregates and cannot form a complex with Sup45p. Stop codon is decoded by a near-cognate tRNA instead and translation continues to the next stop codon or until the ribosome reaches the end of mRNA.

1.4.1 [*PSI*+] phenotype

When Sup35p aggregates ([*PSI*+] phenotype), the C-domain retains its native structure (Krzewska *et al.*, 2007), but its function in translation termination is impaired (Figure 1.3). This loss of function results in the [*PSI*+] phenotype and is characterised by suppression of

nonsense mutations (Cox, 1965). Typical qualitative analyses of the prion status of Sup35p use colour difference of [*psi*⁻] (red) and [*PSI*⁺] (white) caused by nonsense suppression of *ade1-14* or *ade2-1* alleles (see Chapter 3 for detailed explanation).

a) Sup35p
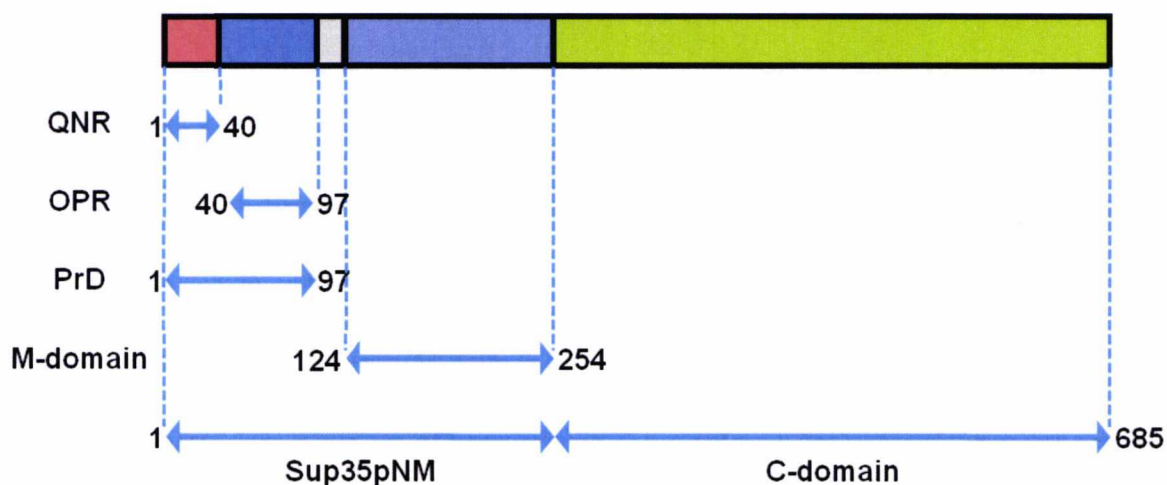
b) QNR

c) OPR

Figure 1.4: Primary structure of Sup35p protein of *S. cerevisiae.* a) Sup35p can be structurally and functionally divided into three domains: an aggregation-prone N-terminal (N) domain (amino acids 1-124), a highly charged middle (M) domain (124-254) and the C-terminal (C) domain (254-685) that is sufficient for translation termination. b) The Gln and Asn rich (QNR) region (amino acids 1-40) promotes initial aggregation of the protein. The amyloidogenic sequence is underlined. c) The oligopeptide repeats region (41-97) consists of 5 and a half repeats that are crucial for prion propagation. A mutation of indicated residue Gly[58] (*PNM2-1*) results in a failure to propagate the prion form and loss of prion. Numbers indicate position of an amino acid in the sequence.

1.4.2 Middle (M) domain

Middle (M) domain defines a highly charged and conformationally flexible sequence. Although initial data showed that the M-domain is not needed for prion appearance and

stable propagation (Ter-Avanesyan *et al.*, 1994), it might play a role in [*PSI⁺*] strain variation and mitotic propagation (Liu *et al.*, 2002). A deletion mutant constructed by Liu *et al.* (2002) and lacking the M-domain was mostly insoluble in its non-prion form, indicating that it has a possible role in the native protein to prevent spontaneous aggregation. Some evidence suggests a part of M-domain is within the minimal region required for maintenance of prion variants (Bradley *et al.*, 2004), although this is disputed (Shkundina *et al.*, 2006).

1.4.3 Prion-forming domain – structure and function

The prion forming domain (PrD) is located in the N-terminal region of Sup35p and spans amino acid residues from 1 – 97. It has an atypically high proportion of glutamine and asparagine residues. Structurally and functionally it can be divided into two domains, QNR (1 – 40), the glutamine/asparagine-rich or aggregation domain (DePace *et al.*, 1998; Liu *et al.*, 1999; Parham *et al.*, 2001; Osherovich *et al.*, 2004) and OPR (40 – 97), the oligopeptide repeats or propagation domain (Liu *et al.*, 1999; Parham *et al.*, 2001). The two domains function independently and are transferable between different prions (Parham *et al.*, 2001; Osherovich *et al.*, 2004). Overexpression of PrD, also referred to as N-domain is sufficient for induction of the [*PSI⁺*] prion (Derkatch *et al.*, 1996). Recent evidence suggests that the N-domain may also play a functional role in a deadenylation of the polyA tail in mRNAs, which leads to their degradation (Hosoda *et al.*, 2003), affects efficiency of translation termination (Volkov *et al.*, 2007) and it might also be involved in other cellular processes (Urakov *et al.*, 2006).

1.4.3.1 QNR region and protein aggregation

The QNR region mediates Sup35p protein-protein interactions and is responsible for seeding specificity and consequently the `species barrier´ (Chien *et al.*, 2001). Replacement with aggregation-prone polyglutamine does not impair proteins ability to aggregate (DePace *et al.*, 1998). Furthermore, the peptide GNNQQNY, which spans residues 7 – 13, readily forms amyloid fibrils *in vitro* (Nelson *et al.*, 2005).

1.4.3.2 OPR region and prion propagation

The OPR region defines the domain that is evolutionary conserved and consists of five and a half oligopeptide repeats (Parham *et al.*, 2001). In *PNM2-1* (`psi no more´) mutants, which contain a single aa substitution in the repeat 2, Sup35p is still able to aggregate but does not stably propagate in the prion form (Osherovich *et al.*, 2004). This suggests that propagation domain is necessary for chaperone-promoted fragmentation and generation of new seeds (Osherovich *et al.*, 2004; Shkundina *et al.*, 2006). Furthermore, increasing the number of peptides increases the frequency of *de novo* conversion to [*PSI*⁺] (Liu *et al.*, 1999). Similarly, carriers of PrP alleles with an increase in the number of repeats in the octapeptide region of PrP are predisposed to prion diseases (Goldfarb *et al.*, 1991). On the other hand, a random shuffling of the sequence of the PrD does not prevent formation or propagation of [*PSI*⁺], indicating that aa composition, and not a specific sequence defines its prion behaviour (Ross *et al.*, 2005b), although this conclusion is disputed (Halfmann *et al.*, 2011).

1.4.4   [*PSI*⁺] variants

Similar to a mammalian prion, [*PSI*⁺] can exist in distinct self-perpetuating prion variants within the same genetic background (Derkatch *et al.*, 1996; Derkatch *et al.*, 1997; Uptain *et al.*, 2001; Zhou *et al.*, 2001; Zhou *et al.*, 1999). Variants differ in mitotic stability (Derkatch *et al.*, 1996), ratio of soluble to aggregated Sup35p (Uptain *et al.*, 2001), efficiency of translation termination (Derkatch *et al.*, 1997) and interaction of Sup35p aggregates with other cellular factors, e.g. Rnq1p (Bradley *et al.*, 2003). [*PSI*⁺] prion variants are typically divided in two groups: weak and strong [*PSI*⁺] variant. The strong variant is more efficient at nonsense suppression than the weak variant and forms white colonies. The strong variant is mitotically stable that is frequency of loss of the [*PSI*⁺] prion is very low, $>10^{-4}$ per generation (Tuite *et al.*, 1981; Derkatch *et al.*, 1996). The weak variant has a lower efficiency of nonsense suppression and forms pink colonies. This variant is also mitotically less stable and cells lose the prion at frequency of 0.1-1%. The strong variant is more efficient at conversion of soluble NM into amyloid form than the weak one (Derkatch *et al.*, 1996; Uptain *et al.*, 2001). Molecular basis of [*PSI*⁺] variants are different conformations of PrD within aggregates (Parham *et al.*, 2001; Tanaka *et al.*, 2006; Toyama *et al.*, 2007).

1.4.5 *de novo* formation of [*PSI*⁺]

Sup35pNM can aggregate *in vitro* without any additional factors, but the presence of [*PIN*⁺] is an absolute requirement for *de novo* appearance of [*PSI*⁺] in intact cells (Derkatch *et al.*, 1997). Although initially defined as a factor that induces [*PSI*⁺] (PSI inducible) (Derkatch *et al.*, 1997), it is widely used to refer to [*RNQ*⁺] as it generally consists of aggregates of Rnq1p (Sondheimer *et al.*, 2000; Derkatch *et al.*, 2001; Osherovich *et al.*, 2001). Several other protein aggregates can also facilitate the *de novo* conversion of [*PSI*⁺], namely the [*URE3*] prion (Derkatch *et al.*, 2001), New1p (Osherovich *et al.*, 2001) and variants of huntingtin (Derkatch *et al.*, 2004). Although several researchers claimed to have generated [*PSI*⁺] in [*pin*⁻] strains (Derkatch *et al.*, 1997; Derkatch *et al.*, 2001) this might have been due to a lack of characterisation of [*PIN*⁺] aggregates at the time. Current opinion is that these aggregates act as an imperfect template on which misfolded Sup35p, aggregates (Derkatch *et al.*, 2004). This `cross-seeding´ interaction occurs only as the initial step and subsequently proteins do not co-aggregate (Bagriantsev *et al.*, 2004), with exception of some evolutionary closely related Sup35p (Chen *et al.*, 2007).

The spontaneous *de novo* formation of the [*PSI*⁺] prion occurs at a very low rate, ~5 x10⁻⁷ per generation (Lund *et al.*, 1981; Lancaster *et al.*, 2010). For more efficient prion formation a plasmid born Sup35p or only its prion domain can be expressed. Such *de novo* [*PSI*⁺] formation is called induced and the increase in the rate of *de novo* [PSI⁺] formation is proportional to the fold increase of Sup35p(/NM) in a cell (Chernoff *et al.*, 1993; Derkatch *et al.*, 1996). Overexpression needs to be transient because high levels of Sup35p are toxic in [*PSI*⁺] (Dagkesamanskaya *et al.*, 1991; Chernoff *et al.*, 1992; Derkatch *et al.*, 1996; Derkatch *et al.*, 1997).

de novo formation of the [*PSI*⁺] prion can be visualised using a green fluorescent protein (GFP) tagged to the plasmid expressed Sup35pNM domain or integrated into genomic *SUP35* gene (Figure 1.5). The prion formation progresses from diffuse Sup35p monomers through the formation of rings and ribbon-like structures to the formation of one or multiple dots (Patino *et al.*, 1996; Zhou *et al.*, 2001; Mathur *et al.*, 2010). Although rings/ribbons differ from dots in their macrostructure the underlying amyloid structure is the same (Tyedmers *et al.*, 2010). Rings and ribbons have been observed to form both at the cell periphery along the plasma membrane or internally along the vacuole (Ganusova *et al.*, 2006). Only about 20 – 25% of cells that exhibit rings or ribbons are viable though and grow into colonies. Rings eventually start to shrink and move from periphery to surround the vacuole, while ribbons collapse into one big aggregate. Mother cells usually retain rings and ribbons, while daughter [*PSI*⁺] cells typically have multiple tiny dots. Ring and

ribbon structures propagate [*PSI*⁺] less efficiently than dots resulting in higher proportion of daughter cells with diffuse Sup35p (Mathur *et al.*, 2010; Tyedmers *et al.*, 2010). Elimination of [*PSI*⁺] by overexpression of *HSP104*, the gene coding for the chaperone that is absolutely necessary for the propagation of yeast prions or inhibition of its ATPase activity by guanidine hydrochloride (GndHCl) reverses this process. Tiny aggregates form into rings and ribbons that start to shrink until only diffuse Sup35p is present (Zhou *et al.*, 2001; Tyedmers *et al.*, 2010). Whether the inhibition of ATPase activity actually eliminates [*PSI*⁺] from mother cells is unlikely since it has been shown that elimination of [*PSI*⁺] by GndHCl/hsp104 requires cell division and that the prion is lost because prion units (propagons) are diluted out of the population (Eaglestone *et al.*, 2000; Ness *et al.*, 2002; Byrne *et al.*, 2007).
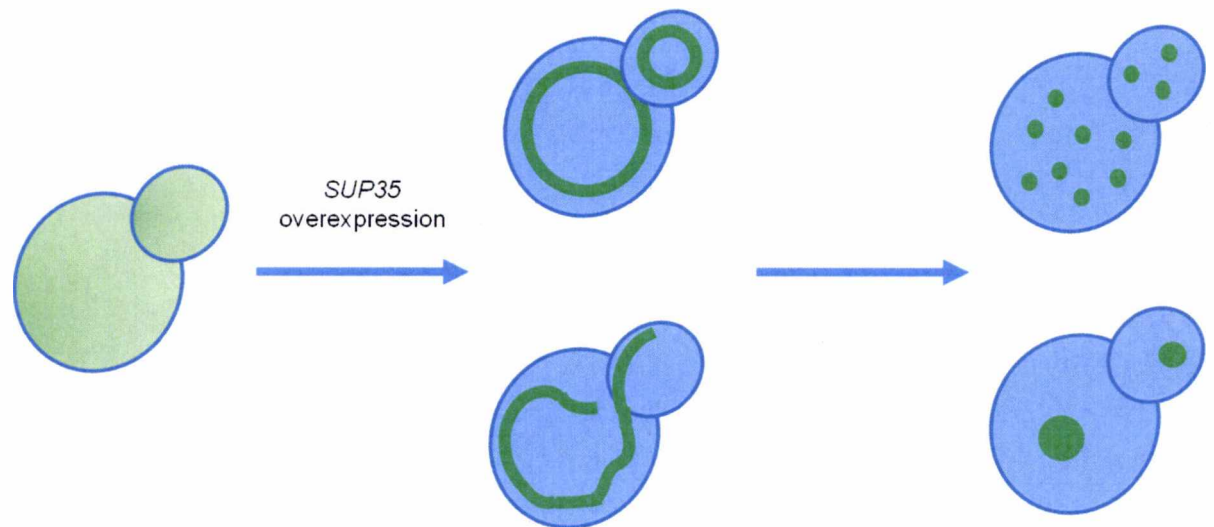
Figure 1.5: [*PSI*⁺] prion formation visualised with fluorescent protein. Sup35p-GFP is diffuse in cytoplasm of [*pin*⁻] cells. Overexpression of GFP tagged *SUP35* induces [*PSI*⁺] formation that proceeds through initial stage where Sup35p is present in elongated aggregates that latter fragment into foci.

Prion formation proceeds similarly for [Het-s]ᵧ (y indicates that the protein is expressed in *S. cerevisiae* rather than in *Podospora anserine*) prion (Coustou *et al.*, 1997) which also forms transient ring and ribbon structures that finally condense into two dots, indicating that the mechanism of prion formation is similar for all (fungi) prions (Mathur *et al.*, 2010). Interestingly, diffuse protein to ring/ribbon structures to protein aggregated in dots process is in case of [Het-s]ᵧ prion observed in [*pin*⁻] cells in which [*PSI*⁺] cannot form. In [*PIN*⁺] cells, on the other hand pHET-sᵧ forms dots without ring/ribbon intermediates (Mathur *et al.*, 2010).

Two cellular compartments have been identified that misfolded cytosolic proteins localise to (Kaganovich *et al.*, 2008). Prion aggregates and other amyloidogenic proteins that show poor solubility and are poorly ubiquitinated are sorted in specific compartment, called IPOD (insoluble protein deposit). Other misfolded proteins localise to a compartment at the cell nucleus called JUNQ (juxtanuclear quality control). IPOD and JUNQ are distinct compartments and have a separate function. Accumulation of misfolded proteins in JUNQ recruits cytosolic proteasomes, while proteasomes do not co-localise with IPOD. Both compartments contain Hsp104p (Kaganovich *et al.*, 2008), a yeast specific chaperone that is involved in resolubilisation of misfolded and aggregated proteins (Parsell *et al.*, 1994) and crucial for prion propagation (Chernoff *et al.*, 1995; Eaglestone *et al.*, 2000; Ferreira *et al.*, 2001; Ness *et al.*, 2002; Jung *et al.*, 2002; Byrne *et al.*, 2007).

Observation of diffusion of fluorescent protein (GFP/RFP) tagged proteins shows that proteins that were sorted to JUNQ can diffuse within this compartment and to the cytoplasm indicating that JUNQ localised proteins are soluble and can be refolded. Proteins in IPOD, on the other hand, do not diffuse within the compartment or to the cytoplasm suggesting that these proteins are present in insoluble aggregates. Therefore, as opposed to JUNQ where ubiquitinated misfolded proteins are temporarily sequestered and refolded or degraded, IPOD serves as a site of terminal sequestration (Kaganovich *et al.*, 2008) (Figure 1.6).

Ubiquitination plays a crucial role in sorting misfolded proteins and deciding their fate. For example, misfolded Rnq1p (that gives rise to [*PIN*$^+$]) is prone to aggregation and is one of a few yeast proteins that can form into a prion without a presence of additional [*PIN*$^+$] factors (see 1.4.1 and 1.5). This protein is upon overexpression typically sorted to IPOD compartment. Forcing ubiquitination of Rnq1p by attaching an ubiquitination signal sequence to the protein, results in a polyubiquitinated Rnq1p that sorts to JUNQ compartment and can be resolubilised. Both compartments are retained in the mother cell (Kaganovich *et al.*, 2008).

Single dot of Sup35p in *SUP35* overexpression-induced [*PSI*$^+$] *de novo* formation localises to IPOD, whereas multidot [*PIN*$^+$] and [Het-s]$_y$ induced under similar conditions localise to both, IPOD and JUNQ compartments (Mathur *et al.*, 2010; Tyedmers *et al.*, 2010). One possible hypothesis is that IPOD serves as a site of accumulation of misfolded aggregates of prion proteins and could possibly serve to nucleate initial stages of prion formation.

An alternative hypothesis was proposed by Ganusova *et al.* (2006), in which proteins aggregate to form prions at a site of actin patches/formation of endocytotic vesicles. Prion aggregates are then moved together with endocytotic vesicles to vacuole, where

aggregates form macrostructures such as rings and ribbons (Ganusova *et al.*, 2006; Section 1.4.3).
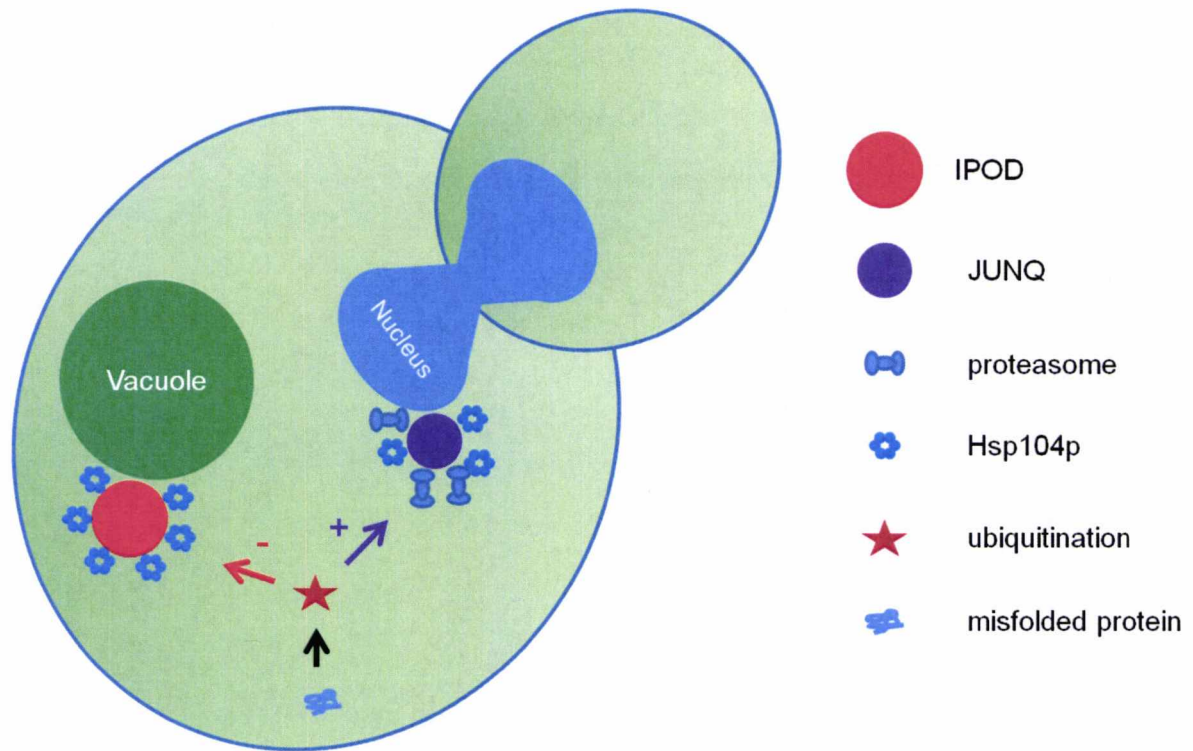
Figure 1.6: Misfolded proteins sort to IPOD or JUNQ compartments depending on ubiquitination. Misfolded proteins are ubiquitinated and ubiquitination results in their sorting to JUNQ (juxtanuclear quality control) compartment, where misfolded proteins are refolded or degraded by Hsp104p and proteasome systems. If proteins are not ubiquitinated and remain poorly soluble, they are sorted to IPOD (insoluble protein deposit) compartment that is peripheral to the vacuole where they are deposited as insoluble aggregates. Both compartments are retained in the mother cell.

1.4.6 [*PSI*⁺] prion propagation

Propagation of [*PSI*⁺] is a process distinct from prion formation and is not affected by factors that modulate prion formation, e.g. Sla1p, Sla2p that are required for assembly of cortical actin cytoskeleton and endocytosis (Ganusova *et al.*, 2006) or [*PIN*⁺] (Derkatch *et al.*, 2001). Prion aggregates can recruit new proteins on their own (e.g. King *et al.*, 2004; Tanaka *et al.*, 2004), but only at the end of the fibres (Collins *et al.*, 2004; Figure 1.1, Figure 1.2). Aggregates grow into larges structures and it is therefore crucial for prion propagation that prion fibres are broken into smaller fragments, propagons (Cox *et al.*, 2003) that can be transmitted to daughter cells. This function is thought to be done by a molecular chaperone Hsp104p (Chernoff *et al.*, 1995) that is necessary for propagation of yeast prions. Hsp104p acts through ATP hydrolysis-driven process to disaggregate

misfolded proteins (Parsell *et al.*, 1994; Glover *et al.*, 1998). Propagation is a finely balanced process, because insufficient rate of fragmentation of prion aggregates by Hsp104 would lead to large aggregates that could not be transmitted to daughter cells, while fragmentation that is faster than recruitment of new molecules to aggregates would lead to a loss of such aggregates. In agreement with this hypothesis overexpression or deletion of *HSP104* (Chernoff *et al.*, 1995) or inhibition of ATP-ase by addition of GndHCl (Tuite *et al.*, 1981; Eaglestone *et al.*, 2000) eliminates the [*PSI*⁺] prion. Interestingly, overexpression of this protein eliminates [*PSI*⁺] but not other yeast prions (Shorter *et al.*, 2006).

Chaperones from two other families, namely Hsp70 and Hsp40, are also implicated in [*PSI*⁺] propagation (Glover *et al.*, 1998). Hsp70 subfamilies Ssa and Ssb play a crucial role in regulating aggregation of proteins, formation and toxicity of amyloids and propagation of prions (e.g. Newnam *et al.*, 1999; Chacinska *et al.*, 2001; Meriin *et al.*, 2002; Allen *et al.*, 2005). The picture is further complicated since the effects these chaperones have on prions depend on prion variants (Kushnirov *et al.*, 2000), stress and can exhibit opposite effects on different prions (Schwimmer *et al.*, 2002; Allen *et al.*, 2005).

1.5   Factors influencing the *de novo* formation of [*PSI*⁺]

Factors shown to influence the *de novo* formation are [*PIN*⁺], Sup45p, several proteins involved in actin organisation/formation of endocytotic vesicles and proteins that function in chaperone-ubiquitin system. Proteins and their functions are summarised in Table 1.1.

1.5.1 [*RNQ*⁺] and Rnq1 protein

Rnq1p is a protein of unknown function, although it may be involved in regulation of ascus formation (Orlowska-Matuszewska *et al.*, 2006). It was first described by Sondheimer and Lindquist (Sondheimer *et al.*, 2000) who showed that the protein can aggregate and that its C-terminal domain can, in the context of prion behaviour, functionally substitute for the Sup35p PrD. Subsequently, Derkatch *et al.* (2001) showed that Rnq1p (and Ure2p) aggregates are the molecular basis for [*PIN*⁺], a factor described as necessary for induction of [*PSI*⁺] (Derkatch *et al.*, 1997). [*RNQ*⁺] is referred to as [*PIN*⁺] throughout this thesis.

Table 1.1: Factors affecting de novo formation of [*PSI*⁺]

Gene	Gene product	Cellular function	*Influence on the rate of the de novo formation of [PSI⁺]*
HSP104	Hsp104p	Resolubilisation of protein aggregates	ATP independent nucleation *in vitro*
SSB1	Ssb1	Cotranslational folding of the nascent polypeptide and protein turnover	Decreases the rate of the *de novo* formation
SSA subfamily	Ssa1p, Ssa2p, Ssa3p, Ssa4p	Protein folding; constitutively expressed and heat-shock induced	Promotes the *de novo* formation
SSE1	Sse1p	Nucleotide exchange factor for Hsp70 proteins	Promotes the *de novo* formation
UBC4	Ubc4p	Conjugating misfolded proteins to ubiquitin	Decreases the rate of the *de novo* formation
UBP6	Ubp6p	Deubiquitination, release of conjugated ubiquitin	Promotes the *de novo* formation
RNQ1	Rnq1p	Unknown, possibly controls prion formation	Prion form [*PIN*⁺] is necessary for the *de novo* formation
SUP45	Sup45p	Translation termination	Decreases the rate of the *de novo* formation
SLA1	Sla1p	Assembly of the cortical actin cytoskeleton	Promotes the *de novo* formation
SLA2	Sla2l	Membrane cytoskeleton assembly, cell polarization	Promotes the *de novo* formation
LAS17	Las17p	Actin assembly, localises to actin patches	Promotes the *de novo* formation
VPS5	Vps5p	Involved in transport of	Promotes the *de novo*

		membrane proteins to golgi aparatus	formation
SAC6	Sac6p	Organisation and maintenance of actin cytoskeleton	Promotes the *de novo* formation

The sequence of Rnq1p can be divided into the non-Q-rich N-terminal and the Q-rich C-terminal domain. In the latter domain which is sufficient for [*PIN*⁺] formation, Rnq1p has four hydrophobic regions and all are necessary for stable propagation, while only three are needed for co-aggregation with pre-existing wild type Rnq1p polymers (Vitrenko *et al.*, 2007a). Surprisingly, neither QG motif in the middle region of the protein nor the highly hydrophobic phenylalanine-rich motif at the C-terminus region, seem to have an effect on formation or propagation of [*PIN*⁺] (Resende *et al.*, 2003; Vitrenko *et al.*, 2007a). The role, if any, of other motifs is unknown. In contrast to other yeast prions, Rnq1p does not require the presence of another prion for [*PIN*⁺] formation. After curing, a prolonged incubation was sufficient for reappearance of [*PIN*⁺] (Derkatch *et al.*, 2000). On the other hand [*PIN*⁺], like [*PSI*⁺], cannot propagate in *hsp104Δ* mutants, confirming that a common mechanism underlies yeast prion propagation. [*PIN*⁺] can also exist in different variants characterised by the aggregation pattern of Rnq1p (Bradley *et al.*, 2003) and [*PSI*⁺] induction efficiency (Bradley *et al.*, 2002).

Two mechanisms could explain the necessity of Rnq1p aggregates for the *de novo* formation of [*PSI*⁺]. [*PIN*⁺] could act as imperfect template on which Sup35p aggregates (Figure 1.7) or could sequester factors preventing spontaneous aggregation of Sup35p. *In vitro* and *in vivo* studies have confirmed initial co-localisation of aggregates (Derkatch *et al.*, 2004; Vitrenko *et al.*, 2007b), but failed to observe heterologous aggregates expected in the sequestration hypothesis. A fusion of Sup35PrD to Rnq1p protein increased the frequency of *de novo* [*PSI*⁺] formation further confirming that the interaction of Sup35p and Rnq1p is driving [*PSI*⁺] formation (Choe *et al.*, 2009). Tyedmers *et al.* (2010) have shown that the interaction between Sup35p and [*PIN*⁺] is only necessary for initial aggregation of Sup35p and that the formation of visible ring/ribbon aggregates on [*PIN*⁺] is not necessary for [*PSI*⁺] formation (Tyedmers *et al.*, 2010). Interestingly, Resende *et al.* (2003) have observed that in *S. cerevisiae* strains carrying a deletion in the PrD of Sup35p, that prevents establishment of the [*PSI*⁺] state, the *RNQ1* gene is highly polymorphic. Interaction between the two proteins appears to constrain the *RNQ1* sequence evolution and might, therefore be of a functional nature.

Induction of [*PSI*⁺] seems to be [*PIN*⁺] variant specific. Bradley and co-workers (Bradley *et al.*, 2002) reported that in [*PIN*⁺] strains characterised by a single dot aggregation pattern of an Rnq1p-GFP fusion, an unstable [*PSI*⁺] was often induced. Further investigation showed that single dot [*RNQ*⁺] strains destabilise weak [*PSI*⁺] and that likewise, the *de novo* appearance of [*PSI*⁺] often eliminates the single dot [*PIN*⁺] (Bradley *et al.*, 2003). This evidence is difficult to interpret in the light of the above hypotheses; the sequestering inhibitory factors hypothesis seems unlikely, while in the template hypothesis destabilisation would require prolonged interaction of prions, an event not yet observed (Vitrenko *et al.*, 2007b).

1.5.2 Sup45 (eRF1)

Sup45p is a member of the eRF1 family of translation release factors and interacts with Sup35p to form a release factor complex responsible for translation termination (Stansfield *et al.*, 1995; Zhouravleva *et al.*, 1995), but may have other roles as well (Urakov *et al.*, 2006). The Sup35p binding site is located in the C-terminal region of eRF1 (Eurwilaichitr *et al.*, 1999), while the N-terminal region of a protein is involved in ribosome binding and termination-codon-dependent peptidyl-tRNA hydrolysis (Frolova *et al.*, 2000). The N-terminal region also interacts with Sup35p (Paushkin *et al.*, 1997).

Since Sup45p forms a complex with Sup35p the question arose whether Sup45p also affects the *de novo* formation of [*PSI*⁺]. Derkatch *et al.* (1998) have, by over-expressing the *SUP45* gene, shown that Sup45p levels modulate the *de novo* appearance of [*PSI*⁺] but do not have an effect on prion propagation. Sup45p could, by binding to Sup35p, stabilise its conformation and reduce the pool of Sup35p available for prion formation through protein misfolding, but not prevent polymerisation once [*PSI*⁺] seeds have been established. Alternatively, Sup45p could directly interact with other factors, chaperones, Rnq1p and/or [*RNQ*⁺].

1.5.3 Actin cytoskeleton and endocytosis

Several actin-related proteins have been shown to affect the *de novo* formation of the [*PSI*⁺] prion. Sla1p, an actin assembly protein interacts with N-domain of Sup35p (Bailleul *et al.*, 1999; Ganusova *et al.*, 2006). The deletion of *SLA1* gene decreases the frequency of *de novo* [*PSI*⁺] formation upon overexpression of the *SUP35* gene (Bailleul *et al.*, 1999). Interestingly, Sla1p contains oligopeptide repeats that resemble Sup35p OPR and are

located in the Sla1p C-domain, the domain that interacts with N-domain of Sup35 (Bailleul *et al.*, 1999). The significance of Sla1p oligopeptide repeats and their effect on *de novo* [*PSI⁺*] formation is not understood. Co-localisation studies showed that a significant fraction of Sla1p and Sla2p are present in cells in form of tiny foci (as judged by fluorescence of GFP tagged proteins) and co-localise with [*PSI⁺*] aggregates (Ganusova *et al.*, 2006). Other proteins that control actin dynamics, but are also involved in endocytosis (reviewed in Galletta *et al.*, 2009), namely Sla2, End3, Arp2, and Arp3 have also been shown to interact with the N-domain of Sup35p (Ganusova *et al.*, 2006), but have except for Sla2p not been reported to affect the rate of *de novo* prion formation.

Three additional proteins, Las17p, Vps5p and Sac6p were recently identified by searching for factors associated with actin cytoskeleton and endocytosis that affect the frequency of *de novo* [*PSI⁺*] formation (Manogaran *et al.*, 2011). Deletion of genes coding for these proteins (*LAS17*, *VPS5* and *SAC6*) reduces the frequency of *de novo* formation. Manogaran *et al.* (2011) showed that at least for deletion of these genes, the proportion of cells within a population that form rings and ribbons is significantly reduced. Additional confirmation that actin plays a crucial role in [*PSI⁺*] (and probably other prions) formation is that actin mutant *act1-R177A* also decreases the frequency of the induced *de novo* [*PSI⁺*] formation (Ganusova *et al.*, 2006).

1.5.4 Chaperones and ubiquitin system

Two ubiquitin related enzymes, Ubc4p and Ubp6p have been found to affect [*PSI⁺*] by preventing prion formation, but the mechanism is not known (Allen *et al.*, 2007). A role of ubiquitination and ubiquitin mediated degradation in sorting misfolded proteins to either JUNQ or IPOD (Kaganovich *et al.*, 2008) allows a speculation that deletion of genes coding for factors involved in ubiquitination/protein degradation would change a balance of sorting of misfolded protein towards IPOD compartment. IPOD is proposed to be the site of initial nucleation of prion aggregation (Mathur *et al.*, 2010; Tyedmers *et al.*, 2010) so the increase in levels of deposited misfolded prion proteins would promote prion formation. A deletion of factors involved in ubiquitination/protein degradation would therefore mimic a prion protein overexpression-induced prion formation.

Little is known about the role of chaperones on the *de novo* formation of prions, but since prions form through misfolding of cellular proteins, chaperones would be expected to tightly control this process. A *ssbΔ* strain indeed exhibit up to 10-fold higher frequency of *de novo* formation of [*PSI⁺*] (Chernoff *et al.*, 1999). On the other hand, overexpression of

the *SSA1* gene increases frequency of [*PSI*⁺] formation, an effect consistent with other studies and showing that enzymes of the Ssa subfamily might act as stabilisers of misfolded prion proteins (Allen *et al.*, 2005). Alterations of Sse1p levels, a nucleotide exchange factor for Hsp70, have a similar effect as alterations of levels of proteins of Ssa subfamily (Fan *et al.*, 2007; Sadlish *et al.*, 2008). Hsp104p seems to have no effect *in vivo* (Ness *et al.*, 2002), although it does promote aggregation *in vitro* in an ATP-independent manner (Shorter *et al.*, 2004).

Studies described above have demonstrated correlation between formation and propagation of [*PSI*⁺] and chaperones, but have not identified molecular species that chaperones interact with. Formation of matured amyloid fibrils is thought to be preceeded by aggregation of Sup35p into oligomeric species (Serio *et al.*, 2000) and it is likely that while some chaperones bind to monomers of Sup35p, others will interact with oligomers. In this hypothesis, different chaperones interact preferentially with different molecular species of Sup35p (and other prion proteins) and not only refolding misfolded proteins but also altering balance in favour of on- or off-pathway species and therefore promoting or inhibiting *de novo* formation of prions (Figure 1.7).

1.5.5 Environmental factors that affect prion formation

Environmental factors that cause stress in yeast cell can promote [*PSI*⁺] formation. Several stress-inducing conditions have been identified to date: conditions that cause osmotic stress (CaCl2, NaCl, KCl), oxidative (H_2O_2) or reductive (DTT) stress and other ($ZnSO_4$, LiCl, $MnCl_2$ and acetate) (Tyedmers *et al.*, 2008). Environmental stress factors probably affect prion formation directly by promoting prion protein misfolding and indirectly by increasing levels of misfolded proteins on a global level that overwhelms refolding/degradation systems.

1.6   The overview of prion formation

Prions form through several stages. Natively folded prion proteins are in dynamic equilibrium with partly misfolded monomeric and transient oligomeric species. At least some oligomeric species are unstable and can internally rearrange into more stable amyloid conformation. Once amyloid core is formed, it is capable of recruiting new oligomers and possibly monomers of the prion protein (Serio *et al.*, 2000; Figure 1.7-1). Chaperones and ubiquitin system affect this process by maintaining natively folded protein

1)

Monomers

natively folded protein	chaperone		amyloid
partially misfolded protein	oligomer		[PIN+] factor
binding partner (eRF1)	off-pathway oligomer		

2)

A

Vacuole

Nucleus

B

Vacuole

Nucleus
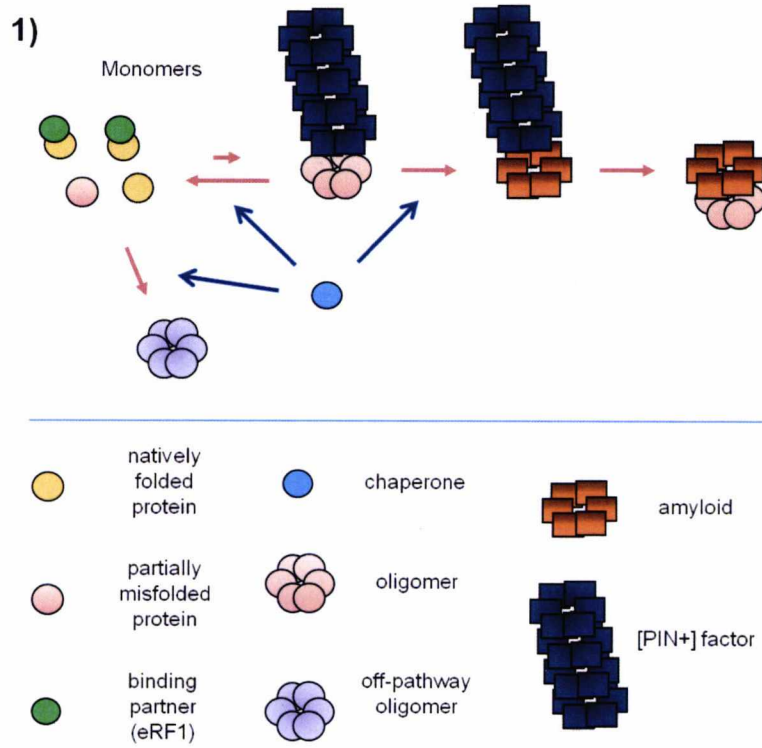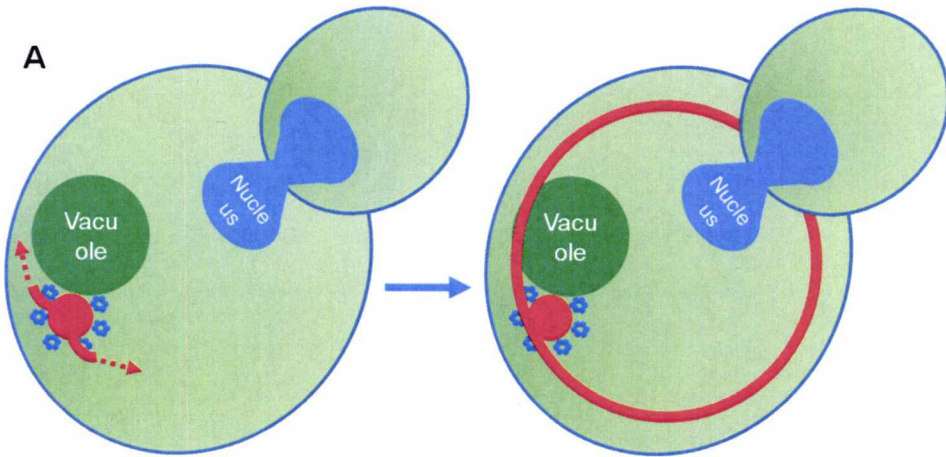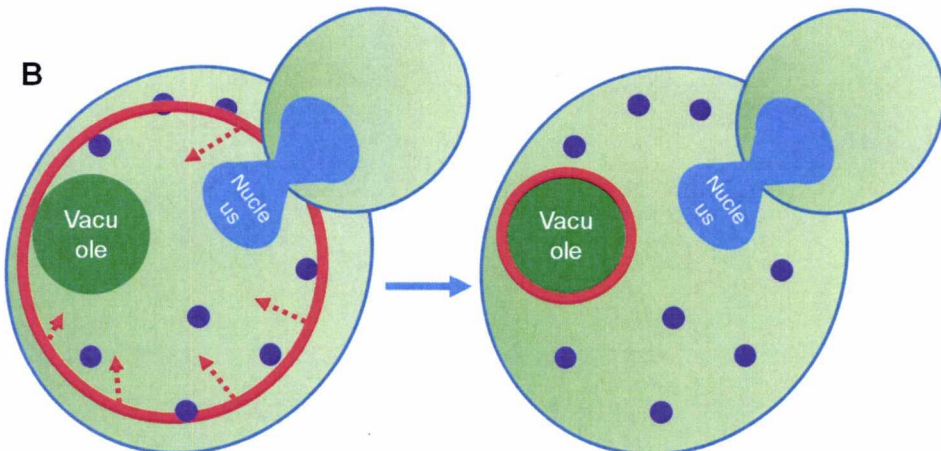
Figure 1.7: Overview of *de novo* [*PSI⁺*] prion formation. 1) [*PSI⁺*] (and other) prion probably forms through intermediate unstable oligomeric species that is in equilibrium with other monomeric species of Sup35p. Occasionally, the oligomeric species can refold into a more stable amyloid form, probably through interaction with [*PIN⁺*] factors. Chaperones can affect this process at any stage, preventing aggregation, refolding misfolded proteins and perhaps promoting prion conversion through stabilization of misfolded proteins. Sup35p interacting factors, such as Sup45p (eRF1) inhibit prion formation, presumably by stabilizing Sup35p in its native form through protein-protein interactions. Prionogenic (and amyloidogenic) proteins probably form other oligomeric species that do not progress towards amyloid conformation ("off-pathway"). 2) Two competing hypotheses have been proposed: A) misfolded proteins are shuffled to IPOD (insoluble protein compartment) where they form into visible aggregates (rings, ribbons). B) Aggregates alternatively form on actin patches and are then transferred with the assistance of components of endocytotic machinery.

conformations, refolding or targeting for degradation misfolded proteins and possibly stabilising some misfolded protein species. Environmental stress increases levels of misfolded prion and other proteins and therefore promotes prion formation directly and through sequestration of chaperones and ubiquitin system. The site of prion formation could be either the place of initial misfolding, cortical actin patches or perivacuolar IPOD compartment (Figure 1.7-2).

1.7   Other fungal prions

Several prions have been identified in yeast to date and only one in a non-yeast fungus, *Podospora anserina*. Fungal prions were initially seen as little more than few quirks of nature, but recent years have seen an enormous growth in number of described prions. Until a decade ago only [*PSI⁺*], [*URE3*] and [Het-s] were known, while in only the last three years, five new prions were described or their proteins identified. Several more have been suggested and the number of prions could easily be above 20 in *S. cerevisiae* alone (Alberti *et al.*, 2009). Majority of newly discovered prions and their effect on yeast are poorly understood (Table 1.2).

Table 1.2: Known fungal prions

Prion	Protein	Cellular function/ prion phenotype	Notes
[*PSI⁺*]	Sup35p	Translation termination factor eRF3 / nonsense suppression	Cox (1965) Wickner (1994)

[*URE3*]	Ure2p	Transcriptional regulator / uptake of poor nitrogen sources	Lacroute (1971)
			Wickner (1994)
[*PIN*⁺]	Rnq1p	Unknown / necessary for *de novo* formation of most yeast prions	Sondheimer *et al.* (2000)
			Derkatch *et al.* (1997)
			Derkatch *et al.* (2001)
[*ISP*⁺]	Sfp1p	Controls expression of ribosome genes / increased translational accuracy	Volkov *et al.* (2002)
			Rogoza *et al.* (2010)
[*SWI*⁺]	Swi1p	Subunit of the SWI/SNF chromatin remodelling complex / repression of transcription	Derkatch *et al.* (2001)
			Du *et al.* (2008)
[*MOT*⁺]	Mot3p	Nuclear transcription factor / derepression of transcription	Alberti *et al.* (2009)
[*OCT*⁺]	Cyc8p	Transcriptional co-repressor / derepression of transcription	Patel *et al.* (2009)
[*MCA*⁺]	Mca1p	Caspase, regulation of apoptosis / unknown	Nemecek *et al.* (2009)
[Het-s]	HET-s	Unknown / heterokaryon incompatibility	Coustou *et al.* (1997)

1.7.1 [*URE3*]

Ure2 protein is a negative regulator of transcription of nitrogen catabolic genes and acts by binding transcription factors Gln3p and Gat1p and preventing their translocation to nucleus (Courchesne *et al.*, 1988; Cunningham *et al.*, 2000). For example, cells with mutated gene for enzyme aspartate transcarbamylase require ureidosuccinate supplementation for growth. Uptake of ureidosuccinate from media is blocked in presence of ammonia through action of Ure2p. Ure2p is in its prion form, [*URE3*] inactive and cells are capable of uptake of poor nitrogen sources through expression of transporter genes. The phenotype of [*URE3*] prion resembles phenotype of *ure2* mutants (Wickner, 1994).

1.7.2 [*ISP*⁺]

[*ISP*⁺] prion was initially discovered as an antisuppressor, a phenotype opposite to that of the [*PSI*⁺] prion (Volkov *et al.*, 2002). [*ISP*⁺] differs from other yeast prions in that it does

not require Hsp104p for its propagation. Protein that gives rise to [*ISP*⁺] is a transcription factor Sfp1p and the prion is located in the nucleus (Rogoza *et al.*, 2010). Formation of [*ISP*⁺] does not cause a loss of function phenotype that is typical for other prions, since the deletion of *SFP2* gene causes suppressor phenotype. [*ISP*⁺] cells are also more resistant to translation interfering drugs and larger than cells of the *SFP2* deletion strain (Rogoza *et al.*, 2010).

1.7.3 [*SWI*⁺]

Swi1p was first identified as a possible prion in a screen that looked for genes which upon overexpression acted as [*PIN*⁺] factors (Derkatch *et al.*, 2001). Swi1p is a subunit of SWI/SNF chromatin remodelling complex and partial loss of function caused by switch to a prion form results in repression of transcription with an effect on global gene regulation (Du *et al.*, 2008).

1.7.4 [*MOT*⁺]

Mot3p is a zinc finger transcription factor that affects expression of a wide variety of genes (Grishin *et al.*, 1998). Alberti and colleagues have recently shown that it can form a prion (Alberti *et al.*, 2009). Prion appearance causes derepression of transcription similar to that of *mot3Δ* strain. [*MOT*⁺] differs from other prions in that it does not require presence of [*PIN*⁺] prion for the *de novo* formation (Alberti *et al.*, 2009).

1.7.5 [*OCT*⁺]

Cyc8p forms with Tup1p a transcription repression complex. Like SWI/SNF complex CYC8/TUP1 is a global transcription regulator, affecting transcription of more than 7% of yeast genes. Inactivation of Cyc8p by redistribution into insoluble aggregates is therefore likely to have a diverse effect on cells, although no phenotypes have been demonstrated yet (Patel *et al.*, 2009).

1.7.6 [MCA⁺]

Mca1p is a protease with a sequence similarity to mammalian caspases and functions in yeast apoptosis (Madeo *et al.*, 2002). Nemecek et al. (Nemecek *et al.*, 2009) showed that its Q/N-rich N-domain can form a prion, but the paper has been recently retracted. It is currently not know whether [*MCA*⁺] prion exists.

1.7.7 [Het-s]

[Het-s] is the only non-yeast fungal prion known to date. *Podospora anserina* has two allelic genes that code for proteins called pHET-S and pHET-s. pHET-s can transit from non-prion state [Het-s*] to a prion form [Het-s] (Coustou *et al.*, 1997). Only known phenotype of the protein is that it produces heterokaryon incompatibility, i.e. when two hyphae fuse and are of the opposite prion state the fusion dies. Interestingly, incompatibility is only present between hyphae with pHET-S which cannot form a prion and [HET-s] hyphae. [Het-s*] hyphae fusion with pHET-S hyphae is not toxic (Coustou *et al.*, 1997). It was suggested that this system might be a form of an immune system functionally similar to a plant immune system that causes hybrid necrosis (Paoletti *et al.*, 2009).

1.8   Evolutionary significance of prion inheritance or friend or foe controversy

A significant controversy has arisen in the decades since the discovery of yeast prions over possibility that [*PSI*⁺] and by extension other yeast prions have a beneficial effect on cells. [*PSI*⁺] has been shown to confer a growth advantage under several environmental conditions, such as high temperature, ethanol, DTT and KCl (Eaglestone *et al.*, 1999; Tyedmers *et al.*, 2008). Laboratory [*PSI*⁺] strains on the other hand exhibited increased sensitivity to chemicals, namely H_2O_2, $MgCl_2$, $CaCl_2$ and LiCl (Tyedmers *et al.*, 2008). Overall, [*PSI*⁺] was beneficial to cell growth and survival in approximately 25% of conditions tested (True *et al.*, 2000). Some evidence for beneficial role of the [*PSI*⁺] prion to cells therefore exist, although only for survival in laboratory conditions and it is unknown if conditions tested are relevant to yeast in natural settings. Another approach that could shed light on a role of prions in yeast is to look for [*PRION*⁺] cells in nature. No naturally occurring prions have been reported to date with an exception of [*PIN*⁺] (Nakayashiki *et*

al., 2005). This led some researchers to propose that similarly to PrP^{Sc} that causes mammalian encephalopathies, yeast prions are diseases as well (Nakayashiki *et al.*, 2005). On the other hand, prion forming domain of Sup35p has been conserved over long evolutionary time (Harrison *et al.*, 2007) and all yeast prions that were confidently identified have a global effect on protein expression and nutrient acquisition (Table 1.2). Conservation of prion forming sequences and regulatory functions such as regulation of transcription of proteins that are capable of prion formation suggest that prion formation might have a role in adaptation to environmental conditions.

1.9   Aims of the thesis

The review of literature in this chapter shows that prion formation is a complex process involving variety of cellular factors, such as actin/endocytosis related proteins, chaperones, protein ubiquitination and degradation systems and specific factors that interact with prion protein, which in case of Sup35p are Sup45p, Rnq1p/[*PIN*$^+$] and other yeast prions. Prion formation is also affected by environmental factors. Gene deletion has been proven to be a powerful tool in studies of cellular factors that affect prion formation (e.g. Ganusova *et al.*, 2006; Tyedmers *et al.*, 2008; Tyedmers *et al.*, 2010) and gene deletions were used as primary method of studying novel factors in this thesis as well.

Proteins that could affect [*PSI*$^+$] prion formation have been previously identified using two strategies. One strategy was to search for proteins that physically interact with Sup35p and to determine if their absence increases the rate of [*PSI*$^+$] formation. This strategy uncovered Ppq1p (M.F. Tuite and T. von der Haar, personal communication), a putative serine/threonine protein phosphatase (Chen *et al.*, 1993; Vincent *et al.*, 1994). The second strategy was to look for proteins that protect translational apparatus from environmental stress. Two proteins were identified, Tsa1p and Tsa2p that work in conjunction to protect translational apparatus from endogenous and exogenous stress (Wong *et al.*, 2002; Trotter *et al.*, 2008; Sideri *et al.*, 2010).

The aim of this thesis was to test for the effect of *PPQ1* and *TSA1 TSA2* gene deletions on *de novo* [*PSI*$^+$] formation. Aggregation of Sup35p into [*PSI*$^+$] impairs its function in translation termination that is characterised by suppression of nonsense mutations. Ability to grow on media lacking adenine caused by suppresson of *ade1-14* nonsense mutation was used to identify cells that exhibit nonsense suppression. Both gene deletions were expected to increase the number of non-[*PSI*$^+$] Ade$^+$ colonies detected by this assay and

the first step was to optimise an assay that differentiates between [PSI^+] and nuclear suppressor mutants.

In the second part of the thesis, the effect of *PPQ1* gene deletion on cellular processes was explored and fluorescent microscopy studies on Ppq1p localisation in cells were performed with an aim to elucidate the mechanism through which Ppq1p prevents [PSI^+] formation.

Chapter II

Materials and Methods

2.1   Yeast and bacterial strains

Table 2.1: *Saccharomyces cerevisiae* strains used in this study

Strain	Genotype	Notes	Reference
74-D694	*MATa ade1-14 trp1-289 his3Δ-200 ura3-52 leu2-3, 112 [pin⁻] [psi⁻]*	[pin⁻]	Chernoff *et al.*, 1995
74-D694	*MATa ade1-14 trp1-289 his3Δ-200 ura3-52 leu2-3, 112 [PIN⁺] [psi⁻]*	[PIN⁺]	Chernoff *et al.*, 1995
74-D694	*MATa ade1-14 trp1-289 his3Δ-200 ura3-52 leu2-3, 112 [PIN⁺] [PSI⁺]w*	Weak [PSI⁺]	Ferreira *et al.*, 2001
74-D694	*MATa ade1-14 trp1-289 his3Δ-200 ura3-52 leu2-3, 112 [PIN⁺] [PSI⁺]s*	Strong [PSI⁺]	Ferreira *et al.*, 2001
74-D694	*MATa ade1-14 trp1-289 his3Δ-200 ura3-52 leu2-3, 112 rnq1Δ::HIS3*	RNQ1 deleted	Koloteva-Levine, unp.
74-D694	*MATa ade1-14 trp1-289 his3Δ-200 ura3-52 leu2-3, 112 ppq1Δ::loxP [pin⁻]*	PPQ1 deleted	Created in this study
74-D694	*MATa ade1-14 trp1-289 his3Δ-200 ura3-52 leu2-3, 112 ppq1Δ::loxP [PIN⁺]*	PPQ1 deleted	Created in this study
BY4741	*MATa his3Δ1 leu2Δ0 met15Δ0 ura3Δ0 [PIN⁺]*		
BY4741	*MATa his3Δ1 leu2Δ0 met15Δ0 ura3Δ0 ppq1Δ::KanMX [PIN⁺]*	PPQ1 deleted	Open biosystems
BY4741	*MATa his3Δ1 leu2Δ0 met15Δ0 ura3Δ0 rnq1Δ::KanMX*	RNQ1 deleted	Open biosystems
BY4742	*MATα his3Δ1 leu2Δ0 lys2Δ0 ura3Δ0*		
W303-1A	*MATa ura3-52 leu2-3, 112 trp1-1 ade2-1 his3-11 can1-100 [PIN⁺]*		Rothstein
W303-1A	*MATa ura3-52 leu2-3, 112 trp1-1 ade2-1 his3-11 can1-100 tsa1Δ::LEU2 [PIN⁺]*	TSA1 deleted	Rand *et al.*, 2006
W303-1A	*MATa ura3-52 leu2-3, 112 trp1-1 ade2-1 his3-11 can1-100 tsa2Δ::KanMX [PIN⁺]*	TSA2 deleted	Sideri *et al.*, 2010
W303-1A	*MATa ura3-52 leu2-3, 112 trp1-1 ade2-1 his3-11 can1-100 tsa1Δ::LEU2 tsa2Δ::KanMX [PIN⁺]*	TSA1 TSA2 deleted	Sideri *et al.*, 2010
ATCC 201388	*Mata his3Δ-1 leu2Δ-0 met15Δ-0 ura3Δ-0 PPQ1-GFP*	PPQ1-GFP	Invitrogen

Table 2.2: *Escherichia coli* strains used in plasmid amplification and isolation of Gateway constructs

Name	Genotype
TOP10	F- *mcr*A Δ(*mrr-hsd*RMS-mcrBC) Φ80*lac*ZΔM15 Δ*lac*X74 *rec*A1 *ara*D139 Δ(*ara-leu*)7697 *gal*U *gal*K *rps*L (Str^R) *end*A1 *nup*G
Mach1-T1	F- Φ80*lac*ZΔM15 Δ*lac*X74 *hsd*R(r_k^-, m_k^+) Δ*rec*A1398 *end*A1 *ton*A
One Shot ccdB Survival 2 T1R	F- mcrA Δ(mrr-hsdRMS-mcrBC) Φ80lacZΔM15 ΔlacX74 recA1 araΔ139 Δ(ara-leu)7697 galU galK rpsL (Str^R) *end*A1 *nup*G fhuA::IS2

2.2 Plasmids

Table 2.3: plasmids used in this study

Name	Insert	Notes
p6442	*SUP35NM-GFP*	P$_{CUP1}$; T.Serio
Gateway entry vector; n. n.	*PPQ1*	pENTR/D-TOPO; this study
Gateway entry vector; n. n.	*PPQ1N*	pENTR/D-TOPO; this study
Gateway entry vector; n. n.	*PPQ1**	pDONR221; from PlasmID
pHS78	*COX4-RFP*	P$_{ADH1}$; pRS316; *LEU2*, CEN; Cerveny *et al.*, 2003
pYX142-mtGFP	*Mito-GFP*	P$_{TPI}$, *LEU2* or *URA3*, CEN
pYX142-mtRFP	*Mito-RFP*	P$_{TPI}$, *LEU2* or *URA3*, CEN
pTH575	*Renilla-Firefly*	Misincorporation: H245R in Firefly; Salas-Marco *et al.*, 2005
n.n.	*Renilla-Firefly*	Rate of translation; string of rare codons in Firefly gene; T von der Haar (unpublished)
n.n.	*Renilla-Firefly*	Ty1 (+1 frameshift) in the linker; Harger *et al.*, 2003
n.n.	*Renilla-Firefly*	L-A (-1 frameshift) in the linker; Harger *et al.*, 2003

pTH460	*Renilla-Firefly*	Readthrough: CAAC in the linker; Keeling *et al.*, 2004
pTH461	*Renilla-Firefly*	Readthrough: UAAC in the linker; Keeling *et al.*, 2004
pTH469	*Renilla-Firefly*	Readthrough: UAGC in the linker; Keeling *et al.*, 2004
pTH477	*Renilla-Firefly*	Readthrough: UGAC in the linker; Keeling *et al.*, 2004

2.3   Media

All media were dissolved in deionised water (dH$_2$O) and autoclaved at 121°C using the Prestige medical benchtop autoclave. Solid media (s – solid, l – liquid) were cooled down to ~50°C before pouring into Petri dishes. 2% (w/v) granulated agar (Difco) was added for solidification prior to autoclaving.

2.3.1 Yeast media

2.3.1.1 YEPD medium

2% (w/v) glucose, 1% (w/v) bacto-peptone and 1% (w/v) yeast extract were dissolved and sterilised. For selection of strains with KanMX cassette, G418 at a final concentration of 200µg/ml was added to media prior to pouring.

2.3.1.2 Alternative carbon source media

Media were prepared as describe for YEPD medium, except that glucose was replaced with 2% (w/v) galactose, 2% (v/v) ethanol or 2% (v/v) glycerol. Carbon sources were filter sterilised and added after autoclaving. YEDP used as a control was prepared in the same manner.

2.3.1.3 Minimal medium (MM)

2% (w/v) glucose, 0.67% (w/v) yeast-nitrogen base w/o amino acids (with ammonium sulphate) and Yeast synthetic complete drop-out media supplement (Formedium;

amounts according to suppliers instructions) to supplement with appropriate a.a./bases were prepared as described above.

2.3.1.4 Supplemented MM-Ade solid medium

Media was used for selection of [*PSI*⁺] cells. Solid minimal medium lacking adenine was prepared as described in 2.3.1.2 and after autoclaving supplemented with 1% or 2.5% (v/v) YEPD (l). 30ml of medium were poured per Petri dish.

2.3.1.5 ¼ YEPD and guanidine hydrochloride media

¼ YEPD 4% glucose medium increases colour definition of *ade1-14* (or *ade2-1 SUQ5*) strains, while addition of guanidine hydrochloride (GndHCl) blocks prion propagation (see introduction). 4% (w/v) glucose, 1% (w/v) bacto-peptone, 0.25% yeast extract and 2% granulated agar were dissolved in deionised water and autoclave-sterilised. Medium was left to cool down and poured or GndHCl was added prior to pouring to a final concentration of 3-5mM. Different final concentrations of GndHCl were used because toxicity of GndHCl to yeast varied between batches.

2.3.1.6 5-Fluoroorotic acid (5-FOA) medium

5-FOA solid medium was prepared in the same manner as MM-Ura, except for the addition of 1g of fluoroorotic acid and 10 ml of filter sterilised 0.2% uracil after autoclaved medium had cooled down. Medium was then mixed using a stirrer and poured into Petri dishes.

2.3.2 Bacterial media

2.3.2.1 Lysogeny broth (LB)

Growth medium for *E. coli* was made by dissolving 1% (w/v) bacto-tryptone, 0.5% (w/v) yeast extract and 1% (w/v) sodium chloride. For selection of plasmid transformed bacteria appropriate antibiotics were added after medium was cooled before pouring in case of solid medium and to broth just before use. Concentrations of antibiotics used were: ampicillin and geneticin – 100µg/ml and kanamycin – 50µg/ml.

2.3.2.2 Super optimal broth (SOC)

This medium was used for recovery of *E. coli* after transformation. Dissolved in distilled water was 2% (w/v) bacto-tryptone, 0.5% (w/v) yeast extract, 10mM NaCl and 2.5mM KCl.

2.4   Growth conditions

Yeast strain were grown on YEPD plates in 30°C incubator or in liquid YEPD media in conical flasks at the same temperature and shaken at 200rpm. Plasmid transformed cells were grown under the same conditions in minimal medium with appropriate drop-out supplement. Cells were harvested by centrifugation in benchtop centrifuge at room temperature (RT) at 3,600rpm for 5 min unless otherwise stated.

E. coli were grown on LB plates at 37°C or in LB broth at 37°C, 200rpm. Cells were harvested using benchtop centrifuge at RT at 12,000rpm for 1 min.

2.4.1   Determination of growth rates

For quantification of yeast growth 1ml cultures in 24 well microplates were incubated in BMG Labtech FLUOstar OPTIMA plate reader with a starting OD_{600} of 0.1. Doubling time was calculated by averaging four data points in logarithmic phase in MS excel. Growth in stationary phase (24h, 48h) was judged by comparison of OD_{600} densities of strains investigated with OD_{600} density of the wild type strain.

2.4.2   Cultures used in microscopy studies

Cultures were grown in 20ml of YEPD broth or in an appropriate selective medium to retain plasmids in 250ml conical flasks in a 30°C shaking incubator. 1ml of cultures in log phase, early (24h) or late (48h) stationary phase was harvested using benchtop centrifuge, resuspended in distilled H_2O and observed under microscope.

2.4.3 Stress conditions

2.4.3.1 Stress granule-inducing heat stress

Log phase cultures were heat-shocked as described in Grousl *et al.* (2009) at 46°C for 10 and 20 minutes.

2.4.3.2 Ppq1p foci formation-promoting stress

Cultures of ATCC 201388 *PPQ1-GFP* strain were grown into early stationary phase (24h) when MnCl$_2$ (to a final concentration of 10mM), ethanol [5% (v/v)], H$_2$O$_2$ (5mM) or sodium chloride (0.6M) were added or a culture was transferred into 37°C shaking incubator. After 2, 8 and 24 hours of incubation 1ml of culture was pelleted, resuspended in 50µl distilled water (ddH$_2$O) and observed under microscope.

2.5   DNA methods

2.5.1 Plasmid isolation from *Escherichia coli*

Cultures were grown overnight in 5ml LB broth with appropriate antibiotic added to retain a plasmid in a shaking incubator at 37°C. Cells were harvested at maximum speed and supernatant discarded. Qiagen QIAprep Spin Miniprep Kit (Cat. No. 27106) was used to isolate the plasmid according to manufacturer's instruction.

2.5.2 Genomic DNA extraction

A single colony was inoculated in YEPD broth and grown overnight in a shaking incubator at 30°C. 2ml of overnight culture was harvested by centrifugation and DNA extracted using the Puregene Yeast/Bact. Kit B (Qiagen, Cat. No. 158567) according to manufacturer's instructions.

2.5.3 Polymerase-chain reaction

Kits were bought from Roche; Taq DNA polymerase (Cat. No. 11 146 173 001) was used for analytical PCR and Expand High Fidelity PCR System (Cat. No. 11 732 641 001) for preparative PCR. Reaction mix was prepared according to manufacturer's instructions

and PCR performed using thermocycler. Temperature for primer alignment step was determined using Promega's BioMath web-tool (http://www.promega.com/techserv/tools/biomath/calc11.htm). Typical preparative setting for amplification of deletion cassette was:

Table 2.4: *PPQ1* deletion cassette amplification (660µl) using Roche Taq polymerase;

	Primer F	Primer R	pUG72	dNTPs	Buffer	Taq	ddH$_2$O
Stock	100 (µM)	100 (µM)	-	10 (mM)	10X	-	-
Vol	6.6	6.6	6.6	26.4	66	1.5	546.3

Table 2.5: PCR thermal cycling setting

Initial denaturation	No of cycles	Denaturation	Annealing	Elongation	Final extension
94°C 2'	35	95°C 40s	58°C 1'	72°C 2'45	72°C 15'

Table 2.6: Primers used in this thesis

Name	Sequence (5' – 3')	Notes
PPQ1 (gateway) F	caccATGAGAAGAAGCCCGT	Primer used for insertion of *PPQ1* into entry vector; lowercase letters indicate overhanging sequence
PPQ1 (gateway) R	CACTTTGGTTTTGTATAACTTC	Does not include stop codon
PPQ1N (gateway) R	ATTTGAAGAGGTATCATGAG	Primes at position 705 of PPQ1 ORF
PPQ-338-Bamf	gcggggatcc-GTTAACGTAATAAATGATAAATTATC	Lowercase sequence – restriction site; primer used for comfirmation of *PPQ1* deletion
PPQ+300-Pstr	gggggctgcag-ATTATCATTTATTTAGCCATAATGG	Lowercase sequence – restriction site; primer used for comfirmation of *PPQ1* deletion
scPPQ1-359 F	ACGAGGCGTATTTGTATAACCCGGT	Primer used for comfirmation of *PPQ1* deletion
scPPQ1+410 R	CCGGGGTTCGACTCCCCGTA	Primer used for comfirmation of *PPQ1* deletion

2.5.4 Agarose gel electrophoresis

1% (w/v) of molecular biology grade agarose (Melford) was dissolved in TAE buffer (40mM tris, 1mM EDTA, 20mM acetic acid, pH 8.5) by microwaving. The solution was left for 5 min to cool down and a SYBR Safe DNA gel stain (Invitrogen) was added in 1:10,000 (v/v) dilution. Still warm solution was poured into a gel tank, a comb was inserted and solution left to cool down. Once solid it was covered in TAE buffer and the comb was removed. Samples and a ladder (1kb Benchtop Promega or Hyperladder I Bioline) were loaded and run at 120V until the front was less than 1cm from the edge of the gel. Bands were visualised by UV transillumination.

2.5.5 Plasmid transformation

2.5.5.1 Bacterial

1μl of plasmid preparation was added to 100μl thawed *E. coli* in 1.5ml tube and gently swirled to mix. Transformation mix was incubated on ice for 30min and then transferred to 42°C water bath for 60s. The tube was put immediately back on ice for few minutes. 800μl of SOC media was added and the transformation mix was incubated in a shaking incubator at 37°C for one hour. 100μl of transformation mix was spread on LB plates with appropriate antibiotic added. Plates were incubated overnight at 37°C. Next day, colonies were picked up from a plate and plasmid isolated as described in section 2.5.1.

2.5.5.2 Yeast

Yeast transformation was done according to (Gietz *et al.*, 2007) with small modifications. Colonies were resuspended in 5ml of YEPD broth in 50ml tubes and grown overnight in a shaking incubator at 30°C. The next day 1ml of culture per transformation was pelleted and resuspended in a transformation mix as described in Gietz and Schiestl (2007) except for PEG-3350 and 100mM of 2-mercaptoethanol that were added to the transformation mix. Cells were heat-shocked in a water bath at 42°C for 20-40 minutes depending on yeast strain used, resuspended in distilled H₂O and spread on plates selective for the plasmid-born marker. Strains sensitive to heat shock were incubated at room temperature overnight instead and spread on appropriate plates. Plates were incubated at 30°C until colonies were visible or for up to 7 days.

2.5.6 Gateway cloning

Gateway cloning is based on a set of plasmids where PCR-amplified gene of interest is first cloned in-between two attL sites, resulting in an entry vector. Gene of interest is then shuffled into different destination vectors through att-site recombination in LR reaction.

2.5.6.1 Entry vector

Entry vector supplied in the kit (pENTR™ Directional TOPO® Cloning Kit) is linearised and cannot be propagated in cells without prior re-circularisation which is only achieved by integration of PCR amplified gene of interest. Primers were designed so that a gene of interest without the stop codon was amplified. Forward primer had a 4 nucleotide 5'-end extension necessary for directional cloning with Topo-isomerase enzyme. PCR fragment was amplified as described above (see 2.5.3) and the correct size was confirmed on agarose gel. Concentration of PCR product was estimated by comparison of intensity of fluorescence of bands with known dsDNA amounts to fluorescence of PCR bands using FLA-5100 imaging system (FujiFilm). Cloning reaction was done according to the protocol described in pENTR™ Directional TOPO® Cloning Kits manual – reaction solution (PCR+H$_2$0 = 4µl, salt buffer = 1µl, TOPO linearised plasmid = 1µl) was gently mixed and incubated for 5 minutes at room temperature. Two reactions were typically performed, one with 0.5:1 and the other 2:1 molar ratio of PCR product to TOPO vector because the method of estimating concentration described above is relatively imprecise and because the ratio that gives highest product yields varies between different PCR products. Cloning reaction mix was then transformed into competent *E. coli* as described in 2.5.5.1. Colonies growing on selective media were picked-up and plasmids isolated as described in 2.5.1. Correct size of candidate plasmids was confirmed by restriction digest followed by gel electrophoresis. Correct DNA fragment integration was confirmed by sequencing.

2.5.6.2 LR reaction

Usefulness of Gateway system lies in an ease of inserting PCR-amplyfied fragments into new plasmids and in a wide variety of available destination vectors. Combinations of different promoters, tags, markers and origins of replication available are presented in Figure 2.1. The LR reaction was performed according to Advanced Gateway Destination Vectors protocol. The LR mix was prepared by adding entry clone to 50-150ng (concentration was estimated from restriction digest gels as described in section 2.5.6.1),

destination vector at 150ng and supplied TE (pH 8) buffer up to 8µl. LR clonase mix was thawed, briefly vortexed and 2µl added to the mix. LR reaction mix was vortexed and incubated for one hour at room temperature. Proteinase K was added to inactivate clonase (37°C, 10 min). Mix was transformed into competent *E.coli* as described in 2.5.5.1.
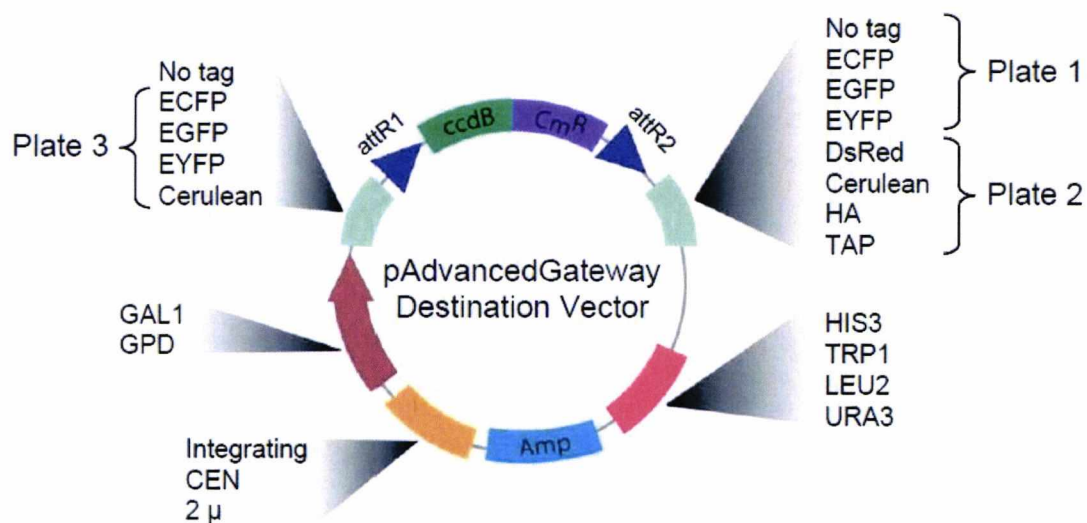
Figure 2.1: destination vectors (from Alberti *et al.*, 2007).

2.5.7 Gene deletion using *LoxP* deletion cassette

Method for gene deletion was described in (Gueldner *et al.*, 1996; Gueldener *et al.*, 2002). The *URA3* selective marker was PCR amplified from a pUG72 plasmid (section 2.5.3) using primers with 5' ends homologous sequences flanking the gene to be deleted with setting described by Gueldener. The gene of interest was replaced using a standard plasmid transformation method (2.5.5.2) with ~5ng of PCR product per transformation and selected on MM-Ura. Cells that lost the selective marker by spontaneous recombination at *LoxP* sites were selected for on 5-FOA plates.

2.6   Protein methods

2.6.1 Protein extraction

2.6.1.1 Quantitative proteomics method

This method of protein extraction was used for quantitative western blotting. The protocol was performed according to a method described in von der Haar (2007) in logarithmically growing cultures. 10^8 cells per sample from log phase culture were harvested by centrifugation at 3600rpm and resuspended in 200μl lysis buffer (0.1M NaOH, 0.05M EDTA, 2% SDS, 2% β-mercaptoethanol). Lysates were incubated in a heat block at 90°C for 10 min. 5μl of 4M acetic acid were added to lysates followed by 30s of vortexing at maximum speed. Lysates were then incubated for another 10 min at 90°C. After extraction, 50μl of loading buffer was added per lysate and samples were loaded on SDS-page gels.

2.6.1.2 Protein extraction for SDD-AGE and sedimentation analysis

Culture was grown to exponential phase and 8 ODU (~10^8 cells) were harvested. Cells were resuspended in ice-cooled lysis buffer (100mM NaCl, 2mM PMSF, 1 tablet of protease inhibitors without EDTA (Roche)/5ml of buffer, 10mM EDTA). 100μl of suspension was transferred to 1.5ml tubes and same volume of acid-washed glass bead (0.45-0.5mm diameter) added. Tubes were kept on ice throughout the procedure. Cells were broken using vortex at maximum speed in a cold room (4°C) for 30s and immediately put on ice. Procedure was repeated 3 times. 50μl of lysis buffer was added and tubes briefly vortexed. Cell debris was pelleted at 4°C for 3 min at 8000rpm in a benchtop centrifuge and supernatant collected into fresh tubes and immediately loaded on gel or liquid nitrogen frozen for storage.

2.6.2 Protein separation by sodium dodecyl sulfate polyacrylamide gel electrophoresis (SDS-PAGE)

SDS-PAGE enables separation of proteins on the basis of their molecular weight. Protocol for preparing SDS-PAGE gels was described in (Laemmli, 1970). Resolving gel (10%) was prepared by adding 42% (v/v) of 30% 29:1 acrylamide mix (Bio-Rad), lower Tris buffer (Tris (pH 8.8) with 0.4% SDS) to 375mM, 0.15% ammonium persulfate (APS), and 0.05% N,N,N',N'-tetramethylethylenediamine (TEMED). Gel was poured into a gel

cassette immediately after addition of TEMED to 0.5cm below comb, covered by 70% ethanol and left to solidify. Ethanol was then poured off and stacking gel prepared by mixing 250mM upper Tris buffer [Tris (pH 6.8) with 0.4% SDS, 0.23% APS, 0.07% TEMED] was poured on top of resolving gel to fill the cassette. A comb was inserted and the gel left to solidify. The cassette was transferred to a gel tank, comb removed and tank filled with running buffer [0.3% (w/v) Tris-base, 14.4% (w/v) glycine, 0.15% (w/v) SDS]. Protein extracts (prepared as described above) were mixed with 4x sample buffer [0.05M Tris (6.8), 1.6% SDS, 4% 2-mercaptoethanol, 25% glycerol, few grains of bromophenolblue] and 2-5µl loaded on gel. Gel was run at 180V until the dye-front reached the bottom of the gel.

2.6.3 Western blotting

Gel (sections 2.6.2 and 2.7.2.2) was immersed in transfer buffer (0.212% (w/v) Tris-base, 1.13% (w/v) glycine, 15% methanol). Blot was assembled by placing one piece of transfer buffer soaked 2mm Whatman GB005 gel blotting paper onto the bottom plate of Biometra Fast Blot. A piece of 0.45um Hybond C Super nitrocellulose membrane (Amersham) was rinsed in transfer buffer and added on top of Whatman papers. Protein gel was put on top and another piece of transfer buffer soaked Whatman paper was added. After each layer was added bubbles were removed using a roller. Finally, the upper plate of Biometra Fast Blot was placed on top. Transfer of proteins to the membrane was done at 25V for 30 min. For SDD-AGE gels (see below) the following modifications were used: transfer buffer T (transfer buffer with 0.1% SDS); two Whatman pieces on each side; PVDF membrane soaked in methanol then rinsed in ddH$_2$O; transfer of proteins to the membrane was done at 10V for 90 min.

Membrane was blocked in 5% (w/v) dry milk powder (Marvel) for at least 20 minutes with agitation and primary antibodies were added. The membrane was then incubated for 1h at RT or overnight at 4°C. Next, membrane was washed 3x with PBS and transferred to 5% milk with horseradish peroxidase conjugated (HPR) secondary antibodies (anti-rabbit, 1:60.000, Sigma – P6782) for an hour. Alternatively, membrane was incubated after washes with PBS in fresh PBS without milk and FITC (fluorescein) conjugated secondary antibodies (anti-rabbit, 1:1.000, Sigma – F9887) were added. After one hour incubation at RT membrane was washed with PBS three times.

2.6.3.1 Enhanced chemiluminiscence (ECL) detection

HPR conjugated antibodies were visualised using enhanced chemoluminiscence method. Solution 1 [2.5mM luminol (Fluka – 09235), 450uM coumaric acid (Sigma – C9008), 100mM Tris-HCl (8.5)] and solution 2 [0.02% (v/v) hydrogen peroxide (Sigma, H1009), 100mM Tris-HCl (8.5)] were prepared fresh and kept in dark. The two solutions were mixed together at 1:1 and membrane was incubated in the mix for 2 min. Membrane was then quickly dried using absorbent paper and Amersham Hyperfilm (GE healthcare, 28-9068-37) was exposed to it. The film was developed using Xenograph XL4.

2.6.3.2 Fluorescence detection

Once FITC antibodies were added the membrane was kept in dark throughout the incubation and briefly dried on absorbent paper. Fluorescence was visualised using FLA-5100 imaging system (FujiFilm).

2.6.4 Yeast two-hybrid assay

Yeast two hybrid assay is a method for determining protein-protein interactions. Transcription factor activation and binding domains (BD and AD, respectively) are encoded on two plasmids. The gene of interest – "bait" is fused to the binding domain while the other gene or gene library is fused to the activation domain of transcription activator. If the proteins of interest interact the reporter genes is activated resulting in transcription of one or more reporter genes, thus enabling yeast cells to grow on selective media. System used in this thesis was described in James $et\ al.$ (1996). PJ69-4a strain was transformed with activation and binding domain carrying plasmids (obtained from T. von der Haar) and grown on plates selective for plasmid markers. Single colonies were resuspended in distilled H_2O and spotted on plates selective for gene interaction markers (marker $GAL2$-$ADE2$: adenine deficient medium; marker $GAL1$-$HIS3$: histidine drop-out with addition of 1mM 3-Amino-1,2,4-triazole).

2.7 Prion methods

2.7.1 [PSI⁺] de novo assay

2.7.1.1 Adenine prototrophy and colony colour assay

Yeast cultures tested for the [PSI⁺] prion were spread on MM-Ade supplemented with 1% YEPD plates (unless otherwise stated) and incubated for 7 days. Colonies growing on plates were restreaked on MM-Ade + 1% YEPD and incubated until streaks/colonies became visible and velvetine replica plated on ¼ YEPD and ¼ YEPD + GndHCl plates. These plates were incubated for 3-4 days and put in a fridge for a day to increase colony colour difference. Colonies that were Ade⁺ and white to pink but reverted to strain's original red colony colour on GndHCl supplemented plates were scored as [PSI⁺]. Colonies that did not change colour on GndHCl plates compared to ¼ YEPD plates were scored as nuclear suppressor (SUP⁺) mutants.

2.7.1.2 Induced prion formation

Strains studied were transformed with p6442 plasmid (CUP1-SUP35NM-GFP URA3, 2u, section 2.2). Fresh transformants were resuspended in MM-Ura broth and grown overnight. Cultures were next day diluted to 0.2 OD_{600} in fresh MM-Ura medium with added copper sulphate ($CuSO_4$) to 25 or 50µM. Cultures were grown for 6h then pelleted and spread to MM-Ade + 1% YEPD plates at density of 10^4 cells per plate (unless otherwise stated) and on ¼ YEPD at 50 cells per plate. Colonies on ¼ YEPD plates were counted after 3-4 days and used to estimate the actual number of viable cells spread on MM-Ade + 1% YEPD plates. These plates were incubated for 7 days when number of colonies was counted. Ade⁺ colonies were restreaked on ¼ YEPD and ¼ YEPD with guanidine hydrochloride added to test for reversibility of phenotype to red colony colour. Colonies that reverted to red colour on guanidine medium were scored as [PSI⁺]. Frequency of de novo [PSI⁺] formation was calculated as number of [PSI⁺] number of cells spread on MM-Ade + 1% YEPD plates.

2.7.1.3 Spontaneous prion formation

Assay was performed and results analysed as described in induced de novo experiment except that strains were not transformed with a plasmid, were grown in YEPD broth,

diluted to OD_{600} 0.1 and $CuSO_4$ was not added to the medium. Cells were spread on MM–Ade + 1% YEPD plates at density of 10^5 and 10^6 cells per plate.

2.7.1.4 Rate of spontaneous *de novo* formation [*PSI*⁺]

Assay was done according to protocol in Lancaster *et al.* (2010). One fresh colony per sample was resuspended in distilled H_2O and cell density estimated using haemocytometer and spectrophotometer. Cells were transferred to 20ml YEPD broth at final density of 100 cells per sample and grown to OD~1.6 (late log phase, approximately 36 hours). Cells were spread on MM-Ade at 10^6-10^7 cells per plate and grown for 3-4 weeks (until no new colonies appeared). Rates were calculated using software provided by Lancaster and Masel. Program is based on calculations done by (Luria *et al.*, 1943), with integrated maximum-likelihood algorithm. This program was also used to estimate rates of *de novo* [*PSI*⁺] formation and *SUP*⁺ appearance for data from spontaneous and induced experiments (sections 2.7.1.2, 2.7.1.3).

2.7.2 Detection of prion aggregates

2.7.2.1 Sedimentation analysis

Cell extract was prepared as described in 2.6.1.2. 50µl of cell extract was transferred to 1.5ml tube and keep to ice. Another 50µl of cell extract was transferred to polycarbonate tube (Beckman) and centrifuged in pre-cooled TL100.3 rotor at 50,000rpm (100,000xg). Supernatant was collected into a fresh 1.5ml tube, while pellet was resuspended in 50µl of ice-cold lysis buffer. 3x loading buffer [180mM Tris-HCl (6.8), 15% glycerol, 6% SDS, few grains of bromophenol blue] was added and samples loaded on SDS-PAGE as described in 2.6.1.2.

2.7.2.2 Semi-denaturing detergent agarose gel electrophoresis (SDD-AGE)

SDD-AGE gel was prepared by dissolving 1.5% (w/v) of molecular biology grade agarose (Melford) in buffer G (20mM Tris-base, 200mM Glycine) and SDS added to final concentration of 0.1% (w/v). Gel was poured as described in 2.5.4. Gel tank was filled with Laemmli buffer [buffer G + 0.1% (w/v) SDS]. Cell extract was prepared as described in 2.6.1.2 and protein concentration measured using Bradford protein assay (Bio-Rad).

Samples were diluted to 5µg/µl in lysis buffer and 10µl of samples mixed with 3x loading buffer [180mM Tris-HCl (6.8), 15% glycerol, 6% SDS, few grains of bromophenol blue]. Preloading mix was incubated for 7min at RT and then loaded on gel. Electrophoresis was done at 125V until the dye was 1cm from the edge of the gel. Gel was transferred and developed as described in 2.6.3 and 2.6.3.1.

2.7.2.3 Visualisation of aggregates using fluorescent microscopy

Strain of interest was transformed with p6442. A colony was suspended in MM-Ura broth and grown overnight. Next day the culture was diluted to OD of 0.2 and $CuSO_4$ added to 25uM concentration. *SUP35NM-GFP* expression was induced for 2 hours when cells were pelleted and resuspended in distilled H_2O. GFP tagged Sup35pNM were visualised using green excitation filter on Olympus IX81 microscope with Hamamatsu Photonics Orca AG cooled CCD camera and UAPO 150x0/TIRFM-SP and UPLSAPO 60x0/1.35UPlanSAPO objectives.

2.7.3 Infectivity of prion aggregates – transfection method

Method was described in Tanaka *et al.* (2004). Sphaeroplast preparation: culture of 74-D694 [*psi-*] strain was grown to logarithmic phase (OD 0.6). Culture was pelleted and washed 1x with water and 1x with 1M sorbitol. Pellet was resuspended in 20ml SCE [1M sorbitol, 100mM Na citrate (pH 5.8) and 10mM EDTA]. DTT was added to 10mM and lyticase (Sigma, L4025) at 50 units / 10^7 cells. Cells were incubated at $30^{\circ}C$ shaking and periodically monitored by microscope. Sphaeroplasts are round compared to oval-shaped cells (in 1M sorbitol medium) and not visible in 0.1% SDS medium. When sphaeroplasts represented more than 90% of population (~30 min) culture was pelleted at 2000rpm for 10 min. Sphaeroplasts were washed 1x in STC (1.2M sorbitol, 10mM TrisHCl (pH 7.5), 10mM $CaCl_2$) and resuspended in 2ml STC. Transformation: 100µl of protoplast suspension was mixed with 1µl of pUG72 (*URA3* marker), 1µl of 10mg/ml ssDNA and 20 or 80µg of cell extract (see 2.6.1.2) and incubated at room temperature for 10 min. 0.9ml of PEG 8000 was added (sorbitol concentration has to remain >1M) transformation mix was mixed gently and incubated for another 30 min at room temperature. Sphaeroplasts were pelleted at 2000rpm for 5 min and supernatant discarded. Pellet was gently resuspended in 150µl of SOS [1M sorbitol, 25%YEPD, 7mM $CaCl_2$) medium and added to 8ml of top agar (MM-Ura with 3% agar, 1M sorbitol and 2% YEPD broth) in 15ml tubes

kept at 48°C (to prevent solidification) and immediately poured on sorbitol plates (top agar except for 2% agar). Colonies that grew in agar were picked out and streaked on ¼ YEPD and ¼ YEPD + GndHCl plates.

2.8   Luciferase luminescence assay

Cells transformed with appropriate Renilla-Firefly plasmids (see results) were grown in a 96 well microplate in 150µl of selective media per well and incubated (30°C, 1000rpm) overnight. 5µl of cultures was transferred to 145µl of fresh selective media and incubated for approximate 4h. 25µl of log phase culture were transferred to 96 well crosstalk-free plates. 20µl of Dual-Glo luciferase (Promega, E2920; at room temperature) and 5µl of Passive Lysis Buffer were added and mixed. The plate was well shaked (1000rpm) and left for 25 minutes at room temperature. Firefly luciferase luminescence was measured using BMG Labtech FLUOstar OPTIMA plate reader. Dual-Glo Stop & Glo substrate was diluted 1:100 in Stop & Go buffer and added 25µl per well. Crosstalk-free plate was shaken and incubated for 25 minutes at room temperature and Renilla luminescence was measured.

Measurements were calculated as a Firefly to Renilla luminiscence ratio. Typically four biological replicates were done per experiment and the outlying measurement was excluded. Plasmids used in the study were obtained from T. von der Haar:
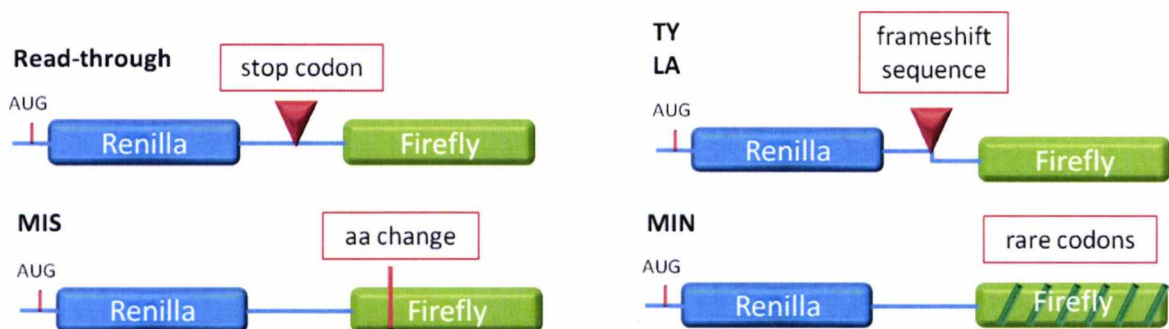
Figure 2.2: Dual luciferase system plasmids for studying various aspects of mRNA translation elongation and termination. A stop codon is inserted between the two genes (Keeling *et al.*, 2004); **MIS**: aa substitution renders Firefly non-functional. aa missincorporation is necessary for functional Firefly (Salas-Marco *et al.*, 2005); **TY** (yeast retrovirus Ty1), **LA** (yeast dsRNA virus L-A) +1/-1 ribosomal frameshifting signals: Firefly and Renilla are out of frame with frameshift sequence in the linker. Decrease in translational fidelity increases levels of Firefly (Harger *et al.*, 2003); **MIN**: Firefly is composed of rare codons that slow down the rate of translation. The system exaggerates the effect of mutations that slow down translation (von der Haar, unpublished).

2.9 Microscopy

2.9.1 Haemocytometer

Approximately 2μl of distilled H_2O was placed on cover slip and the slip pressed onto haemocytometer slide. 150μl of yeast culture was pipetted into one of the grooves and observed under microscope. Cells on 5 medium squares were counted and average number of cells calculated. Average number was multiplied by 250,000 to get an average number of cells per ml. In case of cultures used in respirometry experiments the procedure was repeated twice for each sample and average value calculated.

2.9.2 Fluorescent microscopy

2.9.2.1 Mitochondria visualisation

Strains investigated were transformed with pYX142-mtGFP plasmid carrying the mito-GFP gene. This gene has a sequence that targets the protein product to mitochondrial matrix attached to green fluorescent protein (pVT100U-mtGFP, 2μ, *URA3*) and the expression is under control of strong constitutive promoter *ADH1*. Loop-full of clone purified colonies were resuspended in 20ml of minimal medium and incubated at 30 °C at 200 rpm. Cultures were observed in logarithmic, early- and late-stationary phase (24 and 48 hours). 1ml of culture was pelleted, resuspended in 100μl distilled H_2O and mounted on a microscope slide. Slides were observed under microscope (Olympus IX81 microscope with Hamamatsu Photonics Orca AG cooled CCD camera and UAPO 150x0/TIRFM-SP and UPLSAPO 60x0/1.35UPlanSAPO objectives).

2.9.2.2 Phalloidin staining

A culture was grown to a desired growth phase (e.g. log-phase) as described for mitochondrial visualisation and fixative formaldehyde (Sigma) was added to a final concentration of 5% and left for 30 min at room temperature. Cells were pelleted and washed twice with PBS + 1mg/ml bovine serum albumin (BSA) + 0.1% Triton X-100. Cells were then resuspended in 40μl of the above PBS media and 1μl of Rd-Phalloidin (Texas Red-X phalloidin, Invitrogen) was added. Cells were incubated in dark for 30 min and washed twice with PBS + 1mg/ml BSA (w/o triton). Cells were finally resuspended in distilled H_2O, mounted on a slide and observed using Olympus IX81 microscope with

Hamamatsu Photonics Orca AG cooled CCD camera and UAPO 150x0/TIRFM-SP and UPLSAPO 60x0/1.35UPlanSAPO objectives.

2.10 Respirometry

Loop-full of colonies of the same strain were scraped and inoculated into 1ml of YEPD per well of a 24 well plate and incubated in BMG Labtech FLUOstar OPTIMA plate reader at 300rpm with 8-type shaking until cultures reached a desired growth phase. 5µl of culture was diluted in 495µl of water and number of cells counted with haemocytometer. Cells were diluted in minimal medium without amino acids and to a final concentration of 3.5×10^6 cells per ml. 2.5ml of cells in minimal medium were pipetted into a chamber of a respirometer (Oxygraph-2k, Oroboros). Chamber was washed with 70% ethanol then water three times and calibrated prior to use. After cells were pipetted into it the chamber was closed with a tube and excess liquid pipetted out. Cells were left until the measured O_2 flux [pmol/(s*mg)] curve levelled off (~20 min), the rate of O_2 consumption noted as routine respiration. Next 150µM TET (Sigma) an ATP synthase inhibitor was added. Any O_2 flux at this point can be attributed to membrane leakage. Addition of ionophore FCCP (Sigma) to 12µM increases inner mitochondrial membrane permeability and enables electron transport chain to reach its maximum capacity in so called uncoupled respiration (electron transport system capacity, ETS). Lastly, antimycin A, a cytochrome c reductase inhibitor was added to the final concentration of 2µM to account for any non-mitochondrial oxygen consumption. All data were recorded and analysed with DatLab software.

2.11 Tetrazolium red staining

Tetrazolium salt is a redox indicator that changes when reduced from soluble white coloured (tetrazolium) to water-insoluble red (formazan) substance. Level of colour change reflects the reductive capability of cells so the assay is typically used to test for electron transport system activity or deficiencies or simply for viability of cells. Cells were spotted on YEPD or Glycerol plates and incubated for 2-3 days when the plates were overlaid with 0.5 (w.v) tetrazolium red in 1% agar (cooled down to 42°C prior to pouring) and left to develop. After approximately two hours colonies were scored for colour.

2.12 Genetic crosses

2.12.1 Mating and diploid selection

The respiratory deficient and G418 resistant BY4741 MAT-a *ppq1Δ* strain was streaked on YEPD plate over a streak of the BY4742 MAT-alpha strain and incubated at 30°C for 5 hours. A mix of cells from the plates was restreaked on YEPGlycerol plate with 200µg/ml G418 that selected for diploid cells.

2.12.2 Tetrad dissection

Spore formation was induced in diploid cells by growing cells in YEPD medium and transferring the culture to 1% potassium acetate (pH 7.0). The culture was incubated at 25°C in a shaking incubator for approximately 7 days, when asci became visible under microscope. Culture was harvested and resuspended in 50U/ml lyticase and incubated for 10min at RT. 5µl of culture was spoted on YEPD plate and spread across the plate. Spores from a single ascus were micromanipulated using MSM System micromanipulator (Singer Instruments) and incubated at 30°C until visible colonies formed from spores.

Chapter III

Assaying the *de novo* formation of the [*PSI*⁺] prion in wild type and mutant cells

3.1   Introduction

The [*PRION*⁺] and [*prion*⁻] states are relatively stable in yeast although the switch from one state to the other can occur at a detectable frequency. In order to be able to determine the frequency of the switch from [*prion*⁻] to [*PRION*⁺] one needs a robust assay system that can detect the latter state in one in a million cells (Young *et al.*, 1975; Lund *et al.*, 1981; Lancaster *et al.*, 2010). Such an assay also needs to have a low rate of false positives, that is cells that phenotypically appear to be [*PRION*⁺] because of background nuclear mutations.

Mutation of factors that are involved in the termination of mRNA translation can affect the efficiency of termination. If mutations decrease the efficiency of termination, the frequency of events when the translational machinery continues to decode mRNA past the stop codon will increase. Such events can be monitored by use of marker genes that have a premature stop codon in their coding region, so-called nonsense mutations. Cells carrying such mutations can be auxotrophic for an essential compound e.g. amino acids and cannot grow on medium that is not supplemented with this compound. Ribosomes of cells that carry such a mutation that decreases efficiency of termination will occasionally continue protein synthesis past the nonsense mutation through a near cognate tRNA. This results in the synthesis of a functional protein and cells become partially or fully prototrophic for that essential compound. Marker genes with nonsense mutations are invaluable tools in research into translation termination.

The [*PSI*⁺] prion was initially discovered as a suppressor of nonsense mutations (Cox, 1965) and this phenotype is still used in high-throughput assays monitoring prion appearance. The [*PSI*⁺] prion was first discovered in a strain that carries a mutant *ADE2* allele called *ade2-1*. This allele has an ochre (UAA) nonsense mutation that results in a truncated protein product which for the *ADE2* gene is the enzyme phosphoribosylaminoimidazole carboxylase. This enzyme is part of the purine biosynthetic pathway. Cells carrying the *ade2-1* allele produce a C-terminally truncated protein and are unable to synthesize adenine, resulting in Ade⁻ phenotype. The resulting disruption in purine synthesis also causes a build-up of a coloured intermediate, giving cells which form red colonies. The [*PSI*⁺] prion is too weak a suppressor to suppress the nonsense mutation in *ade2-1* gene alone and requires a mutant allele of the *suq5*⁺ gene to do so. *suq5*⁺ codes for tRNA^*Ser* which normally decodes UCA codon and its allelic variation called *SUQ5* codes for a tRNA with a G to U substitution in the middle base of the anticodon and therefore decodes the ochre stop codon (Waldron *et al.*, 1981). Another, more recently described and more widely used auxotrophic marker for such studies is the *ade1-14* allele

which has an opal (UGA) nonsense mutation. [*PSI*⁺] cells do not require additional suppressors for suppression of this stop codon (Inge-Vechtomov *et al.*, 1988; Chernoff *et al.*, 1995) probably because the nonsense codon is in a 'leaky' 5'/3' nucleotide context.

A problem with the reporter genes described above is that they do not provide an option of selecting for loss of the [*PSI*⁺] prion, except assaying for a change to red colony colour which can only be screened visually. A reporter that can be used for assaying loss of [*PSI*⁺] is *can1-100*, a nonsense (UAA) allele of the *CAN1* gene that is widely used in laboratory yeast strains (Ono *et al.*, 1983). Canavanine, an arginine mimic, is toxic to cells that express functional Can1 protein, an arginine permease so the loss of the [*PSI*⁺] prion can be easily identified by resistance to this toxic amino acid analogue. As is the case in *ade2-1* marker, suppression of *can1-100* also requires *SUQ5*. Another reporter gene that allows for counter-selection is the *ura3-14* allele (Manogaran *et al.*, 2006). This gene construct, which has codons 234 to 254 of the *ade1-14* gene (UGA is at position 244) integrated immediately after the start codon of the *URA3* gene, allows similar selection for [*PSI*⁺] and can differentiate between prion variants. [*PSI*⁺] loss can be assayed on 5-FOA medium that is toxic to functional Ura3p-expressing cells (Boeke *et al.*, 1984; Manogaran *et al.*, 2006).

A significant problem in developing a *de novo* [*PSI*⁺] formation assay that relies on a nonsense suppression is the occurrence of nuclear suppressor mutations (*SUP*⁺), which arise at an approximately 4-fold higher rate than the de novo appearance of the [*PSI*⁺] prion (Lund *et al.*, 1981; Lancaster *et al.*, 2010). *SUP*⁺ mutants can appear due to mutations in a variety of genes and are divided into two classes: codon-specific tRNA mutants (e.g. *SUQ5*) or codon non-specific ribosomal suppressors (e.g. *SUP44* or *SUP46*), which include mutations in the release factor-encoding genes, *SUP35* or *SUP45*. Assays that can differentiate between *SUP*⁺ and [*PSI*⁺] mutants can be divided into two groups: (a) assays that rely on visualisation of prion aggregates, and (b) assays that utilise a reversible prion phenotype.

[*PSI*⁺] prion aggregates can be visualised either by direct *in vivo* observation of fluorescent protein tagged Sup35p using fluorescent microscopy or by assaying for the presence of SDS-resistant aggregates of the protein using the method of SDD-AGE (see methods section 2.7.2.2 and Figure 3.1). The first method requires strains to be engineered to express fluorescently labelled Sup35p typically with a plasmid carrying a *SUP35*-GFP gene fusion construct. The SDD-AGE assay is similarly impractical for testing large numbers of candidates.

The second approach relies on a much higher rate of [*PSI*$^+$] loss compared to the rate of appearance of antisuppressor mutations that would mask nuclear suppressor mutations. [*PSI*$^+$] is spontaneously lost at a frequency of $10^{-2} - 10^{-5}$ depending on the [*PSI*$^+$] variant (Tuite *et al.*, 1981; Derkatch *et al.*, 1996) and this loss can be readily observed by simply streaking cells on ¼ YEPD plates. Loss of the [*PSI*$^+$] prion can also be induced by exposing [*PSI*$^+$] cells to various conditions, most notably growing them in a medium with milimolar levels of guanidine hydrochloride (Tuite *et al.*, 1981). Guanidine hydrochloride (GdnHCl) is toxic at high concentrations, but mM levels inhibit ATPase activity of Hsp104p and thus blocks [*PSI*$^+$] propagation (Eaglestone *et al.*, 2000; Ferreira *et al.*, 2001). Typically, candidate cells (white, Ade$^+$) are spread on to ¼ YEPD plates and ¼ YEPD plates supplemented with 3 to 5 mM GdnHCl and colony colour is compared. If a colony colour remains white or pink on ¼ YEPD plate but reverts to red on GdnHCl plates, it can be concluded that the cells tested are [*PSI*$^+$]. Strains that have the *ura3-14* allele could also be tested on 5-FOA plates, since at least 100-fold higher numbers of Ura$^-$ cells from prion loss than genetic mutations could be expected. However, an assay using GdnHCl is preferable since the frequency of prion loss is 100% and it does not add selective pressure on [*PSI*$^+$] or *SUP*$^+$ cells.

In this chapter different parameters of the *de novo* [*PSI*$^+$] formation assay are explored. Supplementation of adenine-deficient medium with different concentrations of YEPD and density of cells per plate was found to affect both the estimates of rates of appearance of [*PSI*$^+$] prion and *SUP*$^+$ mutants. In the second part, the *de novo* [*PSI*$^+$] formation assay is used to estimate rates of spontaneous *de novo* appearance of the [*PSI*$^+$] prion and *SUP*$^+$ mutants in wild-type and *ppq1Δ* strains. Possible mechanisms through which Ppq1p could affect [*PSI*$^+$] formation are explored and followed up in subsequent chapters.

3.2   Optimisation of parameters of *de novo* [*PSI*$^+$] formation assay

The 74-D694 strain and its derivates ([*PSI*$^+$]/[*psi*$^-$] and [*PIN*$^+$]/[*pin*$^-$]/*rnq1Δ*) were used to test standard methods for assaying for the [*PSI*$^+$] prion (see section 3.1, Figure 3.1 and methods section 2.7). Additionally, the putative allosuppressor strain *ppq1Δ* (see chapter 4) and a strain with increased gene mutation rate i.e. *tsa1Δ tsa2Δ* (chapter 5), were used to evaluate the assays.
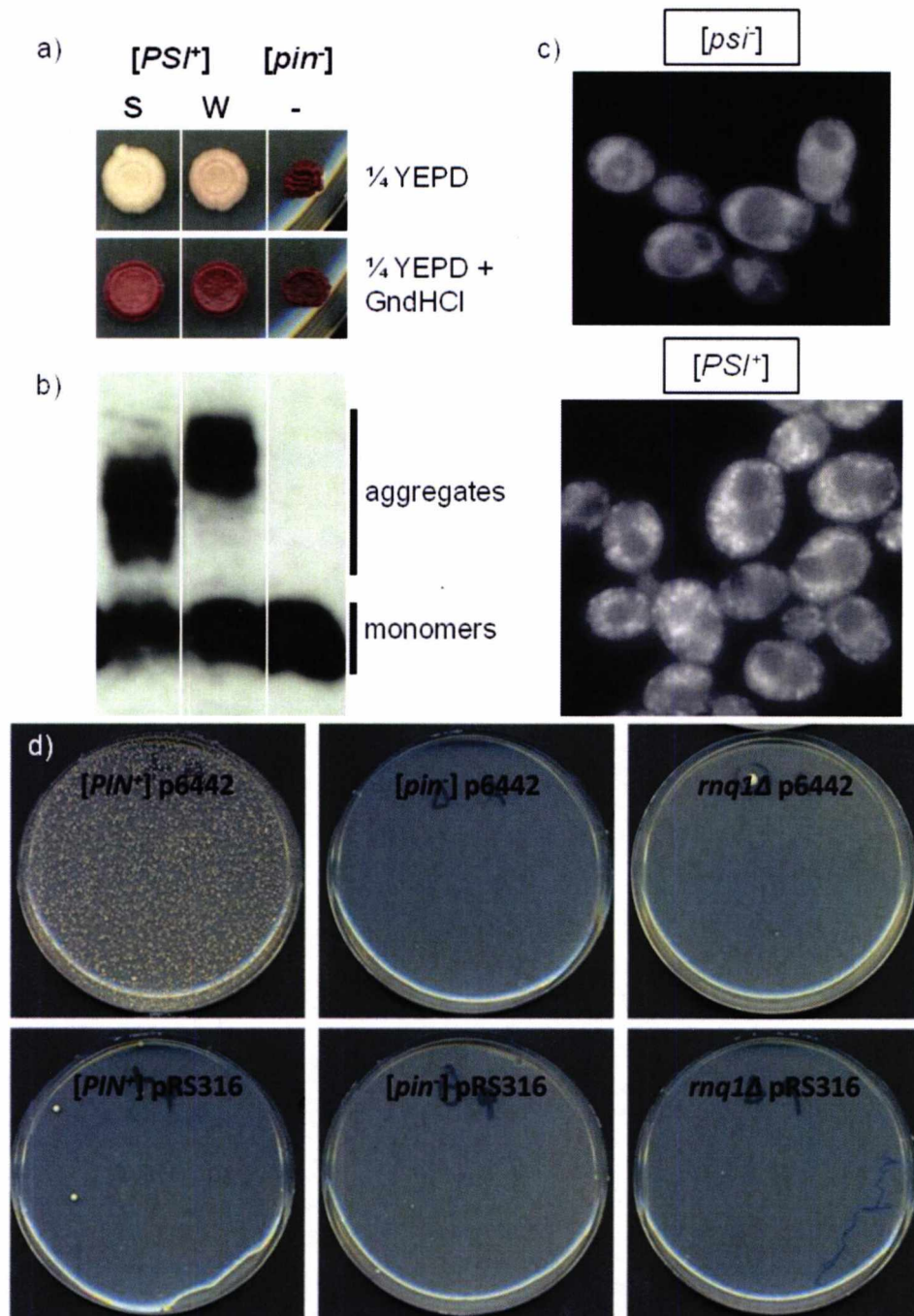
Figure 3.1: Assays used to identify presence or absence of [*PSI+*] prion. a) Difference in colony colour: [*PSI+*] strains on non-selective media (¼ YEPD 4% Glc) grow into pink (weak; W) to white (strong [*PSI+*]; S) coloured colonies, while [*psi-*] strains remain red (upper plate). Colony colour can be reversed to red by growing [*PSI+*] cells in presence of guanidine hydrochloride (GdnHCl) that blocks prion propagation (lower plate); b) Sup35p in [*PSI+*] strains is predominantly in form of SDS-resistant aggregates that can be visualised as less mobile smear in SDD-AGE method; c) Sup35p forms foci in [*PSI+*] cells that can be visualised by expressing fluorescent protein-labelled Sup35p. The Strain expresses chromosomal *SUP35-GFP* fusion; d) High levels of Sup35NM (or Sup35p) protein induce [*PSI+*] appearance with high frequency. [*PIN+*] is absolutely necessary for [*PSI+*] formation. Colony growth is shown on selective plates MM-adenine supplemented with 1% (v/v) YEPD; cells were spread on plates after 6h induction in 50µm CuSO₄; density of 10^6 cells per plate.

3.2.1 Selective medium complementation

A commonly used medium for the selection of [*PSI*+] cells from a [*psi*-] population is a YEPD supplemented, adenine-deficient minimal medium (MM-Ade + YEPD). The [*PSI*+] prion is a weak nonsense suppressor and cannot suppress the nonsense mutation in *ade1-14* sufficiently to grow without addition of a small amount of adenine. On the other hand excessive adenine supplementation would promote growth of Ade⁻ cells and inflate the numbers of [*PSI*+] and *SUP*+ colonies detected. For example, if there was sufficient adenine to allow every cell to divide twice before adenine in medium was exhausted, the effective number of cells spread on this medium would be 4x higher than estimated from ¼ YEPD plates and the rate of [*PSI*+] and *SUP*+ mutations would be overestimated by 4-fold. This effect could be further exaggerated in case of *SUP*+ mutants arising in strains such as those carrying the *ppq1Δ* mutation since *ppq1Δ* gives rise to an allosuppressor phenotype (Song *et al.*, 1987; see Chapter 4) while the *tsa1Δ tsa2Δ* strains have an elevated nuclear gene mutation rate (Iraqui *et al.*, 2009; see Chapter 5).

To explore the effect of supplementation of MM-Ade medium with YEPD, the wild type (wt), *ppq1Δ* and *tsa1Δ tsa2Δ* strains derived from 74-D694 were each grown from low cell number (~100 cells per culture) and then ~10⁶ cells were spread on MM-Ade plates either supplemented with 1%, 2.5% (v/v) or without YEPD broth added (Figure 3.2). Plates were incubated for 60 days and the number of colonies growing on plates counted. YEPD supplementation had a modest effect on the number of Ade⁺ colonies in the wt strain whereas the number of colonies on the 1% and 2.5% YEPD supplemented plates after 60 days of incubation were 30% and 60% higher than on the MM-Ade plates (Figure 3.3a). The number of Ade⁺ colonies in the *ppq1Δ* strain depended more on supplementation with YEPD where the number of colonies on MM-Ade with 2.5% YEPD plate was 2.3 times higher than on MM-Ade plates (88 vs 202 colonies). Similarly, *tsa1Δ tsa2Δ* strains had 4 times as many colonies on supplemented plate as on non-supplemented one (83 vs 327).

The majority of the difference in number of Ade⁺ colonies between the different media with the wt strain was due to *SUP*+ mutants rather than [*PSI*+] (Figure 3.3b) as judged by colony colour change on GdnHCl-containing plates. The number of *SUP*+ mutants almost tripled, while the number of [*PSI*+] colonies remained approximately the same. In the *ppq1Δ* strain, the number of [*PSI*+] colonies nearly tripled on MM-ade supplemented with 2.5% YEPD as compared to non-supplemented adenine-deficient medium and all additional [*PSI*+] colonies were scored as either very weak or dubious [*PSI*+].
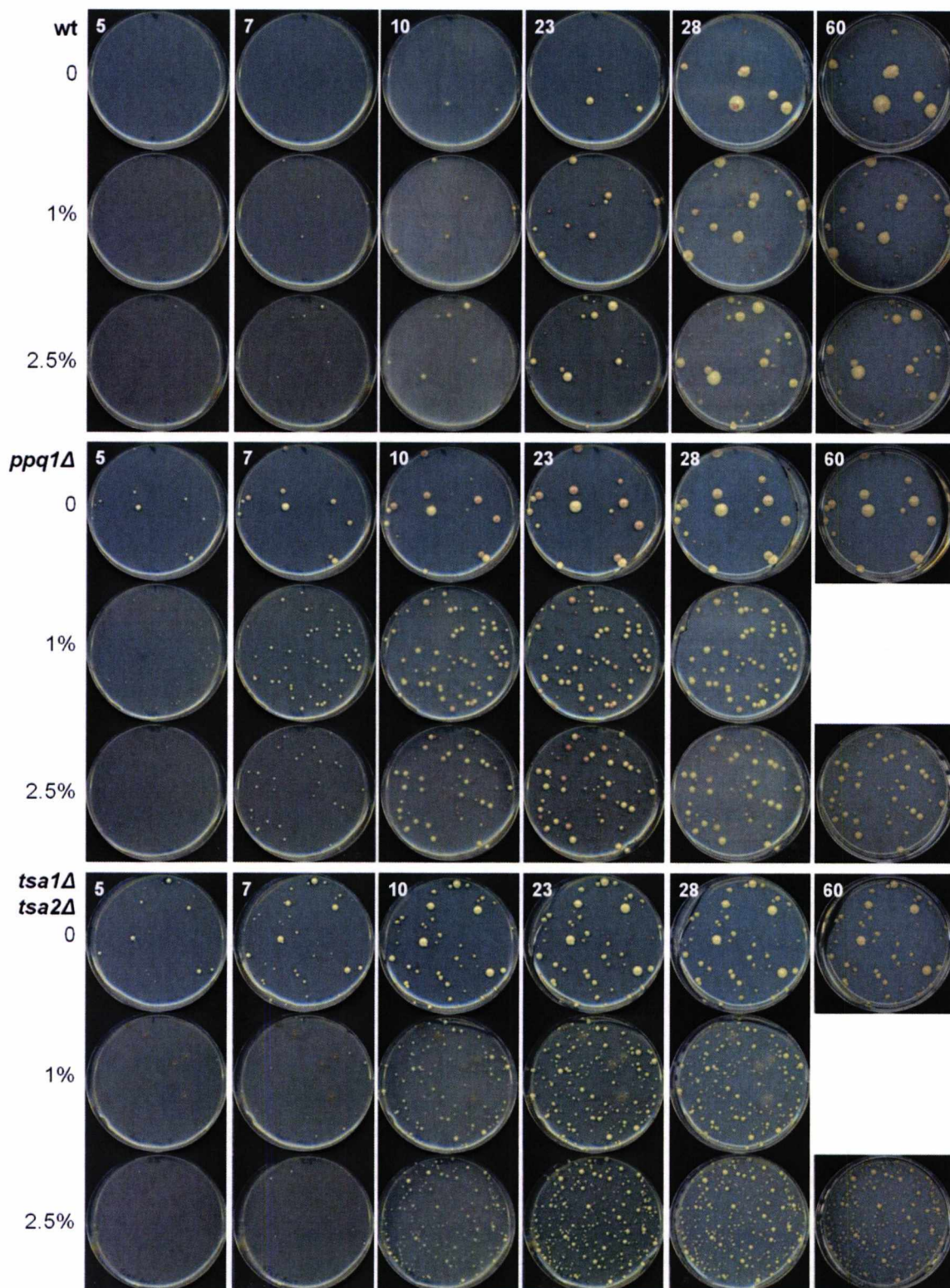
Figure 3.2: Effect of selective media complemented with different amounts of rich medium on growth of wt, *ppq1Δ* and *tsa1Δ tsa2Δ* strains. 0, 1% and 2.5% - minimal media without adenine, or supplemented with 1% (v/v) and 2.5% (v/v) YEPD, respectively; numbers in white indicate the day of incubation.

If Ade⁻ cells were capable of growth on YEPD supplemented adenine-deficient medium and the additional *SUP*⁺ mutants emerged during this growth, at least a 2-fold increase in number of *SUP*⁺ mutants would be expected compared to the number of *SUP*⁺ mutants on non-supplemented medium. The increase in the wt strain was much smaller, approximately 60% for MM-Ade + 2.5%YEPD compared to the number of *SUP*⁺ mutants on MM-Ade. The increase in number of colonies on supplemented medium is more likely to be due to the ability of cells with very weak suppressors to grow on such a medium.
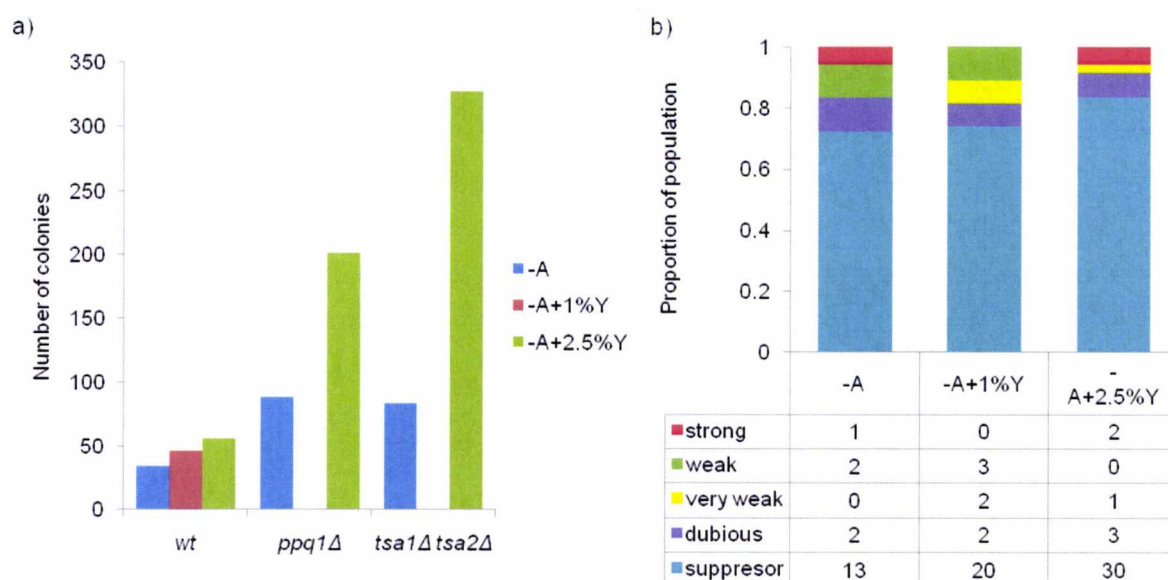
Figure 3.3: Effect of YEPD supplementation of selective medium on: a) number of colonies on each plate; b) different strains of [*PSI*⁺] prion or *SUP*⁺ mutations as a proportion of population (chart) or as a number of colonies (table). -A, -A+1%Y and -A+2.5%Y is minimal medium without adenine or supplemented with 1% (v/v) and 2.5% (v/v) YEPD broth, respectively; strong, weak, very weak and dubious are [*PSI*⁺] prion variants as judged by colony colour. Prion status of these colonies was not confirmed using other assays described above.

3.2.2 Growth on complemented selective media

Another parameter investigated was the time of incubation of the MM-Ade plates before counting and analysing Ade⁺ colonies. Results described above (Section 3.2.1) show that supplementation of an adenine-deficient medium does not allow for indiscriminate growth of cells. The test was not sensitive enough though to exclude a possibility that a small fraction of Ade⁻ cells did divide. Growth of cells on a selective medium also promotes accumulation of secondary mutations that further suppress *ade1-14* nonsense mutation. Such mutations could mask the presence of the [*PSI*⁺] prion (see below).The time of

incubation would therefore need to be short enough to reduce these problems, while still allowing for growth of [*PSI*⁺] and *SUP*⁺ mutant cells from the culture into visible colonies.

To test for the time needed for [*PSI*⁺] and *SUP*⁺ colonies to appear, four strains were tested: [*PSI*⁺] strong and weak variants were standard 74-D694-derived lab strains and two different nuclear *SUP*⁺ mutants isolated from previous experiments. The *SUP*⁺ mutants were categorised as strong and weak, based on their respective colony colour on ¼ YEPD i.e. white or pink. Cells were spotted on to plates in serial dilution from ~10^6 to ~10 cells per spot.

By day 3 of incubation, all [*PSI*⁺] and *SUP*⁺ strains formed clearly visible colonies on MM-Ade with 1% or 2.5% (v/v) YEPD (Figure 3.4). Strains grew significantly slower on non-supplemented MM-Ade plates and by day 5 only strong [*PSI*⁺] and *SUP*⁺ strains formed visible colonies at the lowest dilution. As judged from samples with higher cell density, the [*PSI*⁺] weak prion variants grew particularly slowly and it is possible that such variants would be suppressed in the *de novo* [*PSI*⁺] formation assay using non-supplemented MM-Ade plates. In general the rate of growth, as judged by appearance of colonies on selective plates was:

$$SUP^+ \text{ strong} > [PSI^+] \text{ strong} > SUP^+ \text{ weak} > [PSI^+] \text{ weak}$$
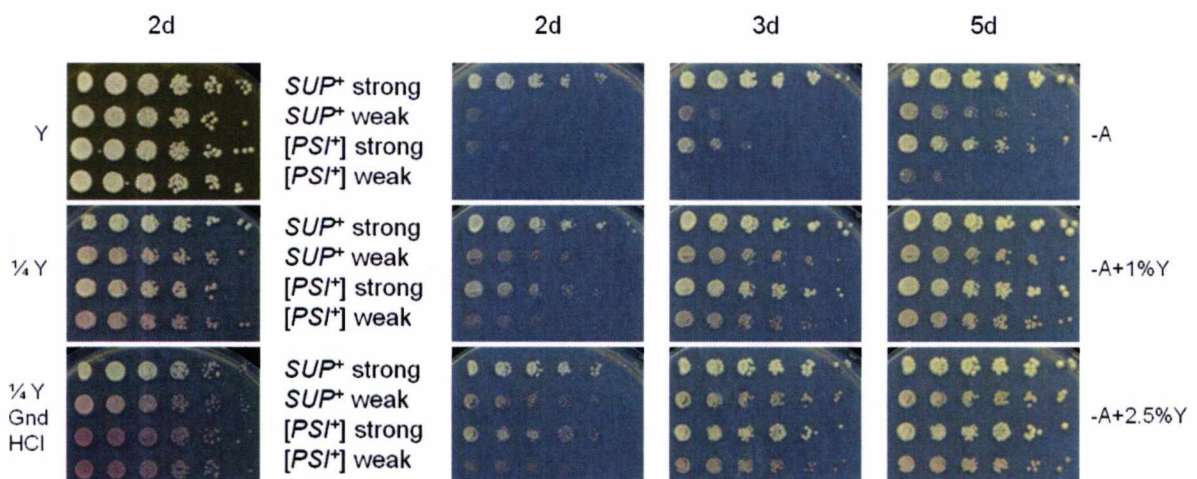
Figure 3.4: Comparison of growth of [*PSI*⁺] and *SUP*⁺ colonies on selective media (-A) complemented with different amounts of YEPD [+1%, 2.5% (v/v)]. Right: plates with different amounts of YEPD were incubated at 30°C and scanned after 2, 3 and 5 days; left – controls: top plate – strains grew equally fast on YEPD plate (Y), middle and bottom plates – ¼ YEPD (¼ Y) and ¼ YEPD with guanidine hydrochloride added (¼ Y GdnHCl) show that [*PSI*⁺] strains reverted to red colony colour on the latter plate while *SUP*⁺ strains did not.

These experiments lead to the conclusion that the lower incubation time limit that would allow for the identification of all [*PSI*⁺] colonies in the *de novo* assay was 5 days on a YEPD-supplemented selective medium. Longer incubation times would be expected to promote growth of additional *SUP*⁺ mutants. A number of *SUP*⁺ colonies start to appear after 7 days incubation that most likely are due to mutations that arose after the cells were plated (N. Koloteva-Levine, personal communication). Consequently, the optimal time of incubation was set at 7 days to allow for the slower growth of [*PSI*⁺] and *SUP*⁺ colonies on densely populated plates in the *de novo* [*PSI*⁺] formation assays described in method section 2.7.1.

3.2.3 Density dependence of *de novo* [*PSI*⁺] formation rates

The frequency of *de novo* formation of [*PSI*⁺] was previously observed to depend on the total number of cells spread per MM-Ade plate (N. Koloteva-Levine, personal communication). Experiments done previously in our laboratory showed that high plate densities ($>10^5$ cells per plate) negatively impact on the number of colonies that grow on MM-Ade + 1% YEPD plates. One possible explanation for this is that at high density, cells deplete the agar plates of nutrients before Ade⁺ cells can grow into visible colonies. If this were so, growth of less efficient nuclear suppressor (*SUP*⁺) mutations and the weak [*PSI*⁺] variants would be inhibited more than growth of strong nuclear suppressors and the strong variant of [*PSI*⁺].

To further investigate the effect of cell density on the appearance of Ade⁺ colonies, the levels of *de novo* [*PSI*⁺] were increased by overexpression of the NM region of Sup35p (Derkatch et al., 1996). Therefore, the 74-D694 [*PIN*⁺] [*psi*⁻] strain was transformed with the *URA3*-based plasmid p6442 as described in methods section 2.7.1.2. The transformed cells were grown in MM-Ura with added 50µM $CuSO_4$ to induce expression of the p6442-encoded Sup35pNM and then spread on MM-Ade + 1% YEPD plates at densities of 10^3, 10^4, 10^5 and 5×10^5. Cells were also spread at a density of 10^6 cells per plate, but colonies that grew on these plates were too small and too densely distributed to pick individually.

The frequency of *de novo* [*PSI*⁺] formation (i.e. [*PSI*⁺] cells appearing per 10^5 cells plated) showed a slight increase with increasing cell density although the difference was not statistically significant (Figure 3.5, average and mean values – green and red bars). In the case of the average frequency, an outlying value was excluded and only two samples were used for the calculations shown. Including the data from the third sample did

increase the frequency for the higher cell density plates, but standard deviations were greatly increased as well and the difference in frequencies was not significant.
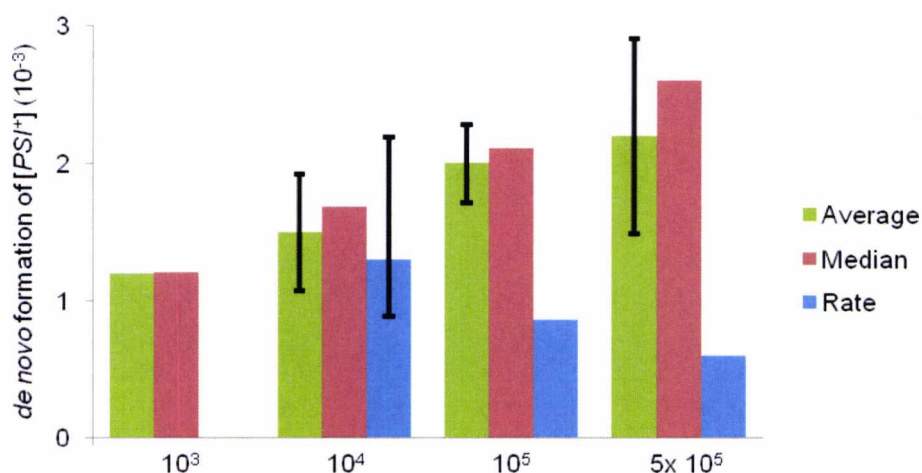
Figure 3.5: Estimated frequency (average and median) and rates for *de novo* [*PSI*$^+$] formation as a function of different cell densities. The average of two samples and median and rate for 3 samples are shown; 10^3 – 1000 cells per plate; average and median frequency are calculated as a number of [*PSI*$^+$] cells per number of all cells spread on MM-Ade – a ratio of [*PSI*$^+$] cells in population; Rate is calculated as a number of [*PSI*$^+$] formations events per generation; error bars in the case of "Average" represent standard deviation, while in the case of "Rate" they represent 95% confidence limits.

Following the publication of the study by Lancaster *et al.* (2010), the data were re-analysed using the software described by these researchers that uses a fluctuation test to estimate the rates of [*PSI*$^+$] prion formation. This resulted in evidence for a reverse trend i.e. the rate of *de novo* formation being lower at higher densities (Figure 3.5, rate – blue bars). Because a relatively low number of samples were used, this did not allow for boot-strap estimation of confidence limits except for 10^4 cells per plate sample. The difference between frequencies/rates for different cell densities was around 2-fold; Shaver and Sniegowski (unpublished, discussion to the program used for estimating the rate of prion formation) consider that experimental difficulties unavoidably produce bias in results and that differences smaller than 2 – 5-fold are less reliable.

The conclusion that one can draw from these experiments is that the density of cells plated on to MM-Ade did not affect the number of [*PSI*$^+$] colonies at the cell densities tested. Higher cell densities were not practical for induced *de novo* experiments because the Ade$^+$ colonies were too small and densely distributed to pick up from plates. Higher densities could be used to measure the spontaneous *de novo* rates where the number of [*PSI*$^+$] colonies are expected to be significantly lower (~1000x lower, see Section 3.2.2).

3.2.4 Elimination of the [*PSI*$^+$] prion by growth on guanidine hydrochloride supplemented plates

In the *de novo* [*PSI*$^+$] formation assays, Ade$^+$ colonies were streaked on ¼ YEPD containing either 3 or 5 mM GdnHCl to test for reversibility of colony colour in order to distinguish [*PSI*$^+$] colonies from *SUP*$^+$ mutant ones. Two approaches were tested:

> (a) streaking Ade$^+$ colonies from the initial MM-Ade + 1% YEPD plates on to fresh MM-Ade + 1% YEPD plates and then replica plating colonies on ¼ YEPD and ¼ YEPD+GdnHCl plates and;

> (b) inoculating colonies from initial plates directly into MM-Ade +1% YEPD broth in a 96 well microplate format and then spotting the various cultures on ¼ YEPD and ¼ YEPD GdnHCl plates using a replica plater.

The first approach enabled streaking from high to low cell density and hence a range from confluent growth to single colonies was observed. Observing single colonies was important because cells might acquire additional *SUP*$^+$ mutations during prolonged incubation on selective plates. Such colonies when re-streaked would grow into a mixture of red, white and pink colonies. In the case of a [*PSI*$^+$] colony with additional *SUP*$^+$ mutants, colour reversible and irreversible colonies would be observed on the GdnHCl plates. The disadvantage of this approach is that some [*PSI*$^+$] variants and weak *SUP*$^+$ mutants were found that grew slower than others (see Figure 3.4). Whilst the agar plates would have to be incubated long enough for slower growing variants to form visible colonies, this could cause strong [*PSI*$^+$] variants to grow confluently and when such variants are replica plated on YEPD + GdnHCl plates, they would not be able to grow for more than few generations. GdnHCl induces loss of [*PSI*$^+$] by blocking prion transmission to daughter cells and the process requires around 6 cell divisions or more (Eaglestone *et al.*, 2000; Byrne *et al.*, 2007) to generate a significant number of [*psi*$^-$] cells.

Growing cells in liquid broth avoids the variable growth rate issue, because cultures can be grown into stationary phase where cell densities do not vary significantly. Spotting cells is also faster and allows more samples to be tested per plate although the latter does not allow for single colony comparison which could be important if some cells in a colony from a selective plate have accumulated additional suppressor mutations.

[*PSI*$^+$] colonies were easily identified in the wt strain (Figure 3.6.1a) using the spot test. More problematic was the *ppq1Δ* strain where a mixture of colonies was visible in some spots (see Figure 3.6.1b). The presence of [*PSI*$^+$] colonies in the second spot of Figure

3.6.1b was confirmed by SDD-AGE (carried out by E Mansfield) that visualises SDS-resistant aggregates.

Streaking Ade+ colonies on plates (Figure 3.6.2) was problematic in cases of fast and slow growing [*PSI+*] variants. Fast growing [*PSI+*] variants achieved confluent growth before slow growing variants formed visible colonies and subsequently fast growing [*PSI+*] variants did not lose the [*PSI+*] prion on GdnHCl medium (Figure 3.6.2b) or consumed the adenine and became much darker on ¼ YEPD medium (Figure 3.6.2c). Another disadvantage of streaking Ade+ colonies on plates was that slower growing cells had lower initial cell densities when replica plated onto YPD + GdnHCl plates. Cells take up GdnHCl (e.g. Jones *et al.*, 2003) and presumably at high cell densities this can significantly reduce the concentration of GdnHCl in medium. Cells at low density might therefore be exposed to higher local concentrations of GdnHCl and since higher levels of GdnHCl (>5 mM) are toxic to cells (Tuite *et al.*, 1981) the growth defect of slow growing cells would be further exaggerated.
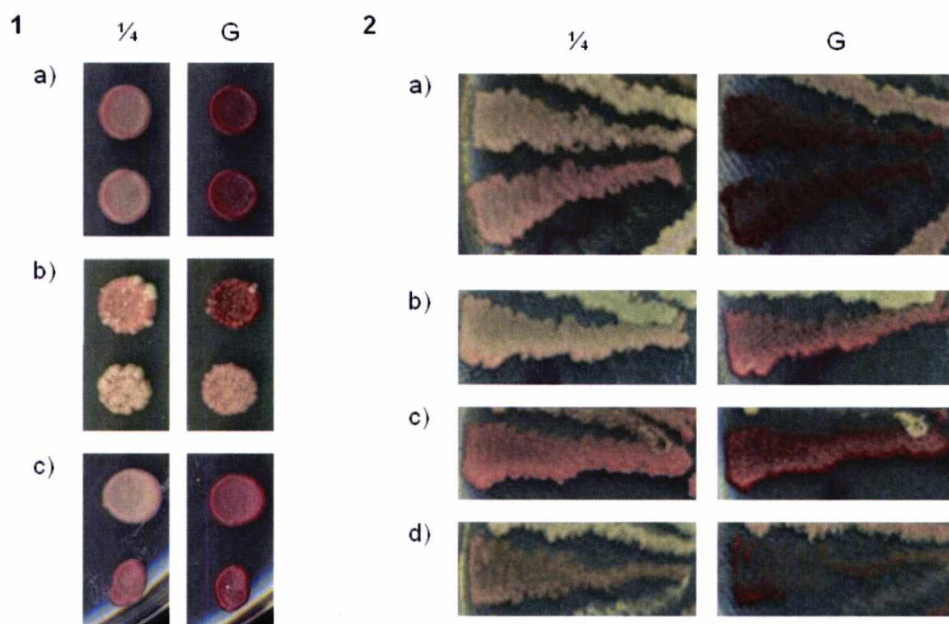
Figure 3.6: Colony colour assay using a "spotting" or "streaking" method. 1: Ade+ colonies were resuspended in MM-Ade + 1% YEPD broth, grown for 2-3 days and spotted on ¼ YEPD and ¼ YEPD + GdnHCl plates. Colony colour differentiation is simple in case of a wt strain (a), but mutant strain that are suppressors themselves (*ppq1Δ*, b) or have high mutation rate (*tsa1Δ tsa2Δ*, not shown) give rise to mixed-colony spots. The bottom colony of panel b had SDS-resistant Sup35p aggregates. c) strong and weak [*PSI+*] prion variant controls; 2: Ade+ colonies were restreaked on MM-Ade + 1%YEPD plates and replica plated on ¼ YEPD and ¼ YEPD + GdnHCl plates. a) a typical colony colour change; fast growing variants lose the [*PSI+*] prion only in cells on the edge of the streak (b), or can use up available adenine in ¼ YEPD medium and become darker (c), making colony colour differentiation less reliable (see text for explanation). Some variants grow

poorly and the effect is further exaggerated by locally higher concentrations of GdnHCl these variants are exposed to (c); ¼ – ¼ YEPD, G – ¼ YEPD + GdnHCl plates.

The optimal conditions identified in this section and used in subsequent experiments described in this thesis were: MM-Ade + 1% YEPD for selection of Ade⁺ colonies (only no YEPD supplementation had a strong negative effect on colony numbers); incubation time of 7 days; densities of up to 5 x10⁵ cells per plate (higher for spontaneous *de novo* [*PSI*⁺] experiments); "spotting" method for wt strain, while "streaking" method should be used for strains that promote nuclear mutations.

3.3   The effect of deletion of the *PPQ1* gene on *de novo* formation of [*PSI*⁺]

Ppq1p is a putative protein phosphatase that has been reported to affect accuracy of translation in yeast (Chen *et al.*, 1993; Vincent *et al.*, 1994). A mutation in the *PPQ1* gene, first identified as *sal6-1*, leads to an allosuppressor phenotype (Song *et al.*, 1987), i.e. *sal6-1* does not suppress nonsense mutations by itself, but allows for expression of other weak suppressors (Cox, 1977). Ppq1p might therefore affect translation at two steps, elongation and termination. Ppq1p has recently been shown to physically interact with Sup35p (T.von der Haar, personal communication) using the yeast two-hybrid assay. This analysis revealed that Ppq1p binds to the functional C-domain of Sup35p. Since Sup35p is the protein that misfolds to give rise to the [*PSI*⁺] prion, it was decided to test if a deletion of the *PPQ1* gene affects the rate of *de novo* [*PSI*⁺] formation. While working on determining the effect of such a *PPQ1* gene deletion on *de novo* prion formation, Tyedmers *et al.* (2008) reported a genome-wide screen for gene knockouts that resulted in an elevation of the frequency of *de novo* formation of the [*PSI*⁺] prion. They reported that a *ppq1* knockout gave the highest level of increase.

3.3.1 *PPQ1* gene deletion in the 74-D694 strain

The *PPQ1* gene was deleted using the protocol described by Gueldner *et al.* (1996, 2002) and is described in detail in Methods section 2.5.7. A *PPQ1* deletion cassette (DC) was amplified by PCR and the concentration of the product was estimated by agarose gel electrophoresis (Figure 3.7a). Approximately 5ng of the *PPQ1* DC was used to transform each strain and the cells were spread on to MM-Ura to select for putative *ppq1::URA3* knockouts. Ura⁺ colonies that grew on selective medium were clonally purified and spread

on 5-FOA plate to select for a loss of the *URA3* marker through spontaneous recombination at the *LoxP* sites (Figure 3.7b).
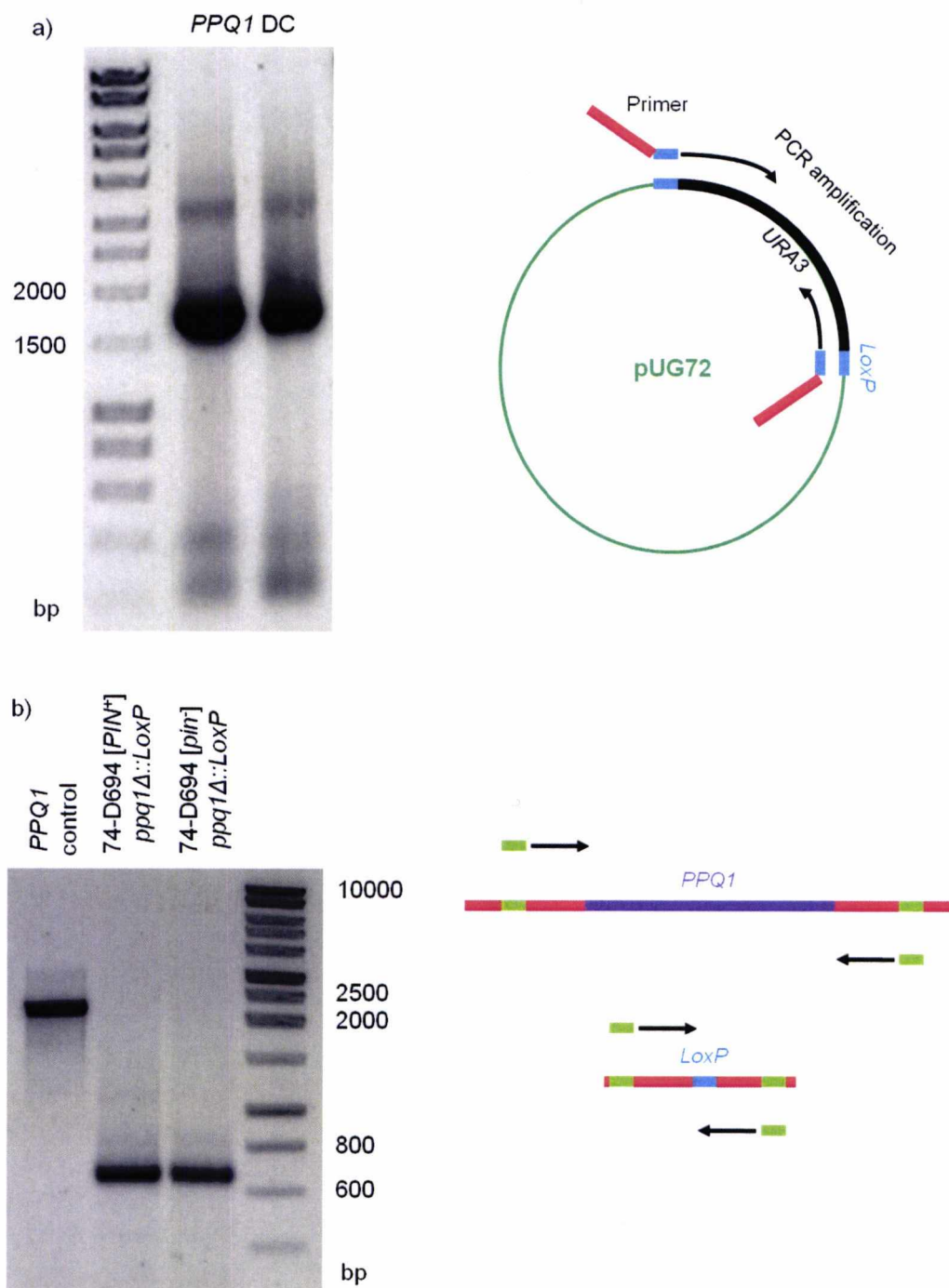
Figure 3.7: Creation of *PPQ1* deletion cassette and *PPQ1* gene deletion. a) deletion cassette (DC) was PCR amplified from pUG72 plasmid (*LoxP-URA3-LoxP*) using primers that had ~40bp on 5'-end homologous to sequences flanking *PPQ1* ORF. The resulting cassette was ~1.7kb long; b) after DC integration into genome deletion strains were grown on counter-selective media (5-FOA) to select for cells that lost *URA3* marker through homologous recombination of *LoxP* sites. Gene deletion was confirmed using primers up- and downstream of *PPQ1* ORF.

3.3.2 *PPQ1* gene deletion increases the rate *of de novo* [*PSI⁺*] formation

Spontaneous *de novo* [*PSI⁺*] formation was assayed using the 74-D694 strain, as described in Methods section 3.7.1.3. Cell densities tested in 3.2.3 were only up to 5 x10^5 cells per plate and were used here for induced [*PSI⁺*] formation. To test for the possibility that higher cell densities affect the rate of prion formation, cells were spread on to MM-Ade + 1% (v/v) YEPD selective media at densities of ~10^5 and 10^6 cells per plate. Eleven samples were assayed for each strain. The actual number of viable cells added per selective plate was calculated from the number of colonies on ¼ YEPD plates and multiplied by the dilution factor used. The average cell density for the wt strain was 8.4 x10^4 and 8.4 x10^5 cells per plate, and 8.9 x10^4 and 8.9 x10^5 for *ppq1Δ* strain.

The rate of spontaneous *de novo* [*PSI⁺*] formation was measured in the wt and the *ppq1Δ* [*psi⁻*] strains. The rate was significantly increased in the *ppq1Δ* deletion strain when comparing the results obtained when 10^5 cells per plate were used (Figure 3.8a). Using the method of Lancaster *et al.* (2010) the rate in the *ppq1Δ* strain was estimated at 8.5 x10^{-6} (95% confidence interval: 3.4 x10^{-6} – 1.7 x10^{-5}) per generation and in the wt strain at 4.6 x10^{-7} (1.1 x10^{-7} – 8.7 x10^{-7}) per generation, a difference in rates of approximately 19-fold (95% confidence interval: 4 – 150-fold increase). The rate of spontaneous *de novo* [*PSI⁺*] formation for the wt strain when a density of 10^6 cells per plate was used was similar to the rate seen for 10^5 cells per plate i.e. 4.1 x10^{-7} (95% CI: 1.1 x10^{-7} – 1.1 x10^{-6}) per generation. However, the *ppq1Δ* strain had a statistically significantly lower rate of spontaneous *de novo* [*PSI⁺*] formation compared to the rate estimated from 10^5 cells per plate experiment [1.7 x10^{-6} (8.9 x10^{-7} – 3.1 x10^{-6}) per generation; 5-fold lower rate]. The difference in rates of *ppq1Δ* and wt strain was only 4-fold.

The rate of *de novo* formation of [*PSI⁺*] obtained in these experiments for the wt *PPQ1⁺* strain were comparable albeit slightly lower to the rate published by Lancaster *et al.* (2010) i.e. 5.79 x10^{-7} (4.59 – 7.46) x10^{-7} per generation. Deletion of *PPQ1* gene increased the rate of *de novo* [*PSI⁺*] formation as was reported by Tyedmers *et al.* (2008) but the increase in the rate was higher in the experiments presented here (i.e. ~20-fold) compared to the 10-fold increase reported by Tyedmers *et al.* (2008).

3.3.3 *ppq1Δ* strain has an increased rate of *SUP⁺* mutations

Ade⁺ colonies that did not change colour and adenine prototrophy phenotype when grown on YEPD + 5mM GdnHCl plates were labelled as nuclear (*SUP⁺*) suppressor mutants.

The rate of appearance of SUP^+ mutants in the wt strain was comparable whether 10^5 or 10^6 cells were plated per plate; 1.6×10^{-6} (95% CI: 1.3×10^{-6} – 2.0×10^{-6}) and 1.3×10^{-6} (6.6×10^{-7} – 2.0×10^{-6}) per generation, respectively (Figure 3.9). The *ppq1Δ* strain had a significantly higher rate as calculated from 10^5 cells per plate experiment, estimated at 3.1×10^{-5} (2.7×10^{-5} – 3.7×10^{-5}) mutations per generation. The ratio of *ppq1Δ* to wt strain was 20:1 (95% CI: 14:1 – 28:1). Similarly to the rate of spontaneous *de novo* [*PSI*⁺] formation, the rate of SUP^+ mutations was approximately 9 times lower in *ppq1Δ* strain at a density of 10^6 cells per plate.
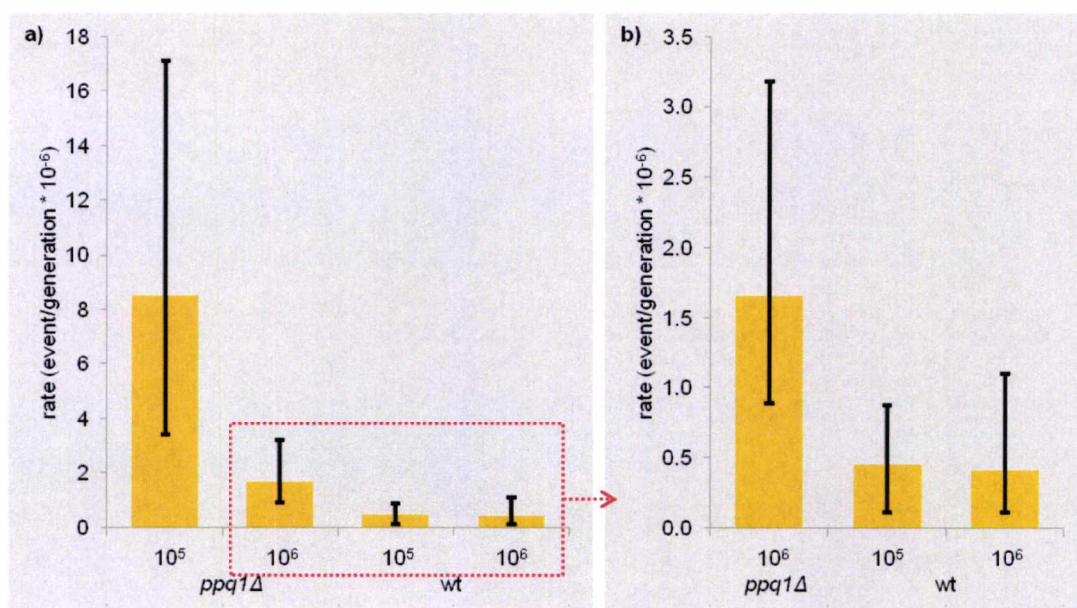
Figure 3.8: Comparison of spontaneous *de novo* [*PSI*⁺] formation rates in wt and *ppq1Δ* strains at two different densities, 10^5 and 10^6 cells per plate. (a) The rate of *de novo* formation was increased ~20-fold in *ppq1Δ* compared to wt strain when 10^5 cells per plate were spread on selective media, but only 4-fold at density of 10^6 cells per plate. b) A subset including all strains except *ppq1Δ* at 10^5 cells per plate; error bars represent 95% confidence intervals; 11 biological replicates were done per strain.

Ratios of SUP^+ to [*PSI*⁺] rates in 10^5 and 10^6 cells per plate experiments were 3.5:1 and 3.1:1 for wt and 3.7:1 and 2.1:1 for the *ppq1Δ* strain, respectively. Values from 10^5 cells per plate experiment (3.5:1 and 3.7:1) were close to Lancaster's (Lancaster *et al.*, 2010) estimate of ~4-fold larger rate of SUP^+. The 3.7:1 versus 2.1:1 ratios for the *ppq1Δ* strain indicated that SUP^+ cells were suppressed by high cell density more than their [*PSI*⁺] counterparts.
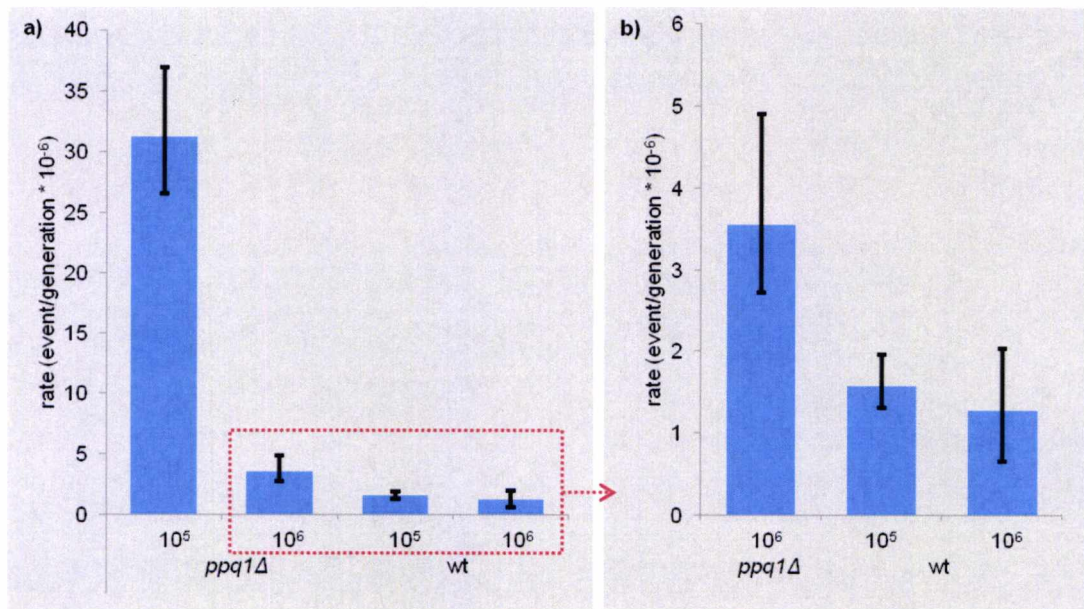
Figure 3.9: *PPQ1* gene deletion increased the rate of *SUP*⁺ mutants. Rates were compared between wt and *ppq1Δ* strains at two different densities, 10^5 and 10^6 cells per plate (a). The ratios of deletion to wt mutation rates were 20 and 3, respectively. b) A subset including all strains except *ppq1Δ* at 10^5 cells per plate; error bars represent 95% confidence intervals; 11 biological replicates were done per strain.

3.3.4 Selecting cells on non-supplemented MM-Ade medium

A similar experiment to the one described in section 3.3.2 using a plating density of 10^6 cells per plate was done using the same wt and *ppq1Δ* strains and selecting for Ade⁺ colonies on MM-Ade plates but without added YEPD. The protocol used was that described by Lancaster *et al.* (2010) and was similar to the protocol first described by Luria *et al.* (1943). The cell density on selective plates was calculated from ¼ YEPD plates as ~2 x10^6 cells per plate, approximately 2 times higher than the 10^6 cells per plate used in the experiment described in section 3.3.2.

The rate of *de novo* [*PSI*⁺] formation was found to be significantly lower on the non-YEPD supplemented selective medium being below the detection threshold in the wt strain: <5x10^{-8} (Figure 3.10a). Interestingly, the rate of *SUP*⁺ appearance was not affected by selection on non-supplemented medium. Similar results were obtained for the *ppq1Δ* strain (Figure 3.10b), where the rate of spontaneous *de novo* [*PSI*⁺] formation was almost 10 times lower in the non-supplemented medium. Again, the rate of *SUP*⁺ appearance was not affected by selection on non-supplemented medium.

Deletion of the *PPQ1* gene significantly increased the rate of spontaneous *de novo* [*PSI*⁺] formation and also increased the observed rate of *SUP*⁺ mutations. A dependence of rate

estimation on cell density was observed in the *ppq1Δ* strain at a density of ~10^6 cells per plate. Both rates of *de novo* [*PSI*⁺] formation and *SUP*⁺ mutations were decreased at this density. Selecting for Ade⁺ colonies on non-YEPD supplemented selective medium on the other hand only affected the rate of *de novo* [*PSI*⁺] formation by inhibiting growth of [*PSI*⁺] cells.
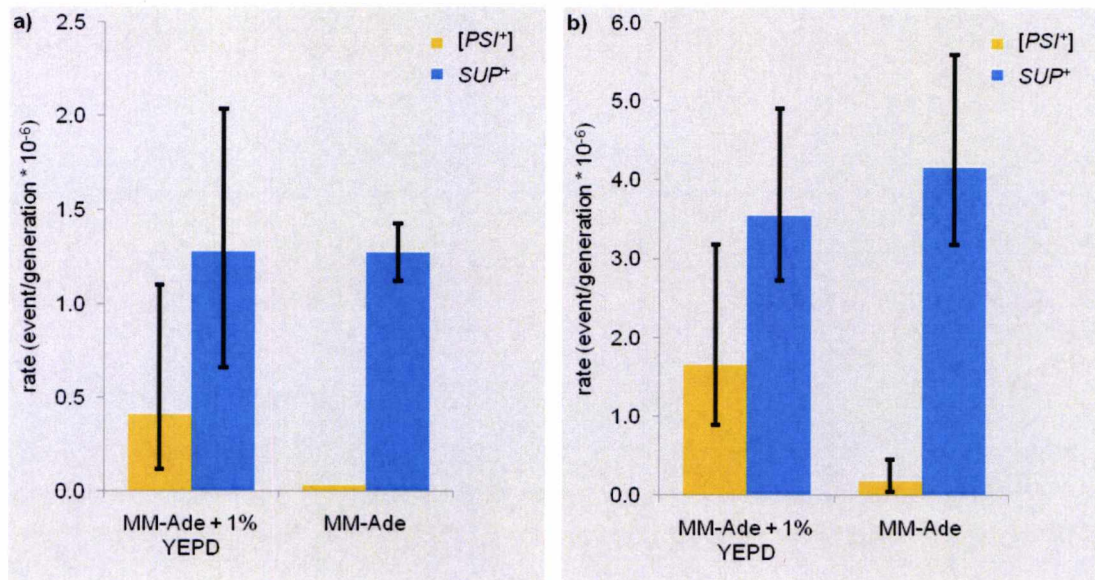
Figure 3.10: Effect of YEPD supplementation of adenine deficient medium on rates of [*PSI*⁺] and *SUP*⁺ appearance. Estimates of rates of *de novo SUP*⁺ appearance were similar in both media, while rates of *de novo* [*PSI*⁺] formation were significantly lower on non-complemented medium; a) effect on wt and b) on *ppq1Δ* strain.

3.3.5 Possible mechanisms through which Ppq1p affects *de novo* [*PSI*⁺] formation

The results described above confirm that loss of Ppq1p function increases the rate of *de novo* [*PSI*⁺] formation as was reported previously (Tyedmers *et al.*, 2008). Ppq1p thus prevents, either directly or indirectly, Sup35p from misfolding into its prion conformation however, the mechanism of action was not known. Several hypotheses were tested:

3.3.5.1 Ppq1p affects phosphorylation status of Sup35p

Phosphorylation of Sup35p has been observed *in vitro* (Fabret *et al.*, 2008) where Sup35p was incubated with the catalytic subunit of protein kinase A, radioactive labelled ATP and phosphorylation of the conserved T341 residue was found. However, in spite of several approaches being used, including testing both [*PSI*⁺] and [*psi*] strains, Fabret *et al.* (2008)

failed to detect phosphorylation of Sup35p *in vivo*. Furthermore, cells with full length Sup35p with a T341D mutation (D, aspartic acid mimics a phosphothreonine) were not viable. Similarly, our laboratory has not been able to detect *in vivo* phosphorylation of Sup35p (P. Mugnier, P.M. Herbert, M.F. Tuite, unpublished). One plausible hypothesis is that Sup35p is rapidly dephosphorylated *in vivo*, perhaps by Ppq1p. A comparative analysis of the effect of a *PPQ1* deletion on the yeast phosphoproteome has been undertaken by T. von der Haar (personal communication). By comparing protein extracts of wt and *ppq1Δ* strains on 2-dimensional gel and identifying changes in protein isoforms using mass spectrometry, this study identified several proteins whose phosphorylation status changed between the two strains although Sup35p was not one of them. It is therefore unlikely that the role of Ppq1p in suppressing *de novo* [*PSI*⁺] prion formation via direct dephosphorylation.

3.3.5.2 Deletion of *PPQ1* gene changes steady state levels of Sup35p

Another possibility is that Ppq1p affects Sup35 protein steady state levels. One consequence of elevating Sup35p levels is to increase the rate of *de novo* formation of the [*PSI*⁺] prion (Chernoff *et al.*, 1993). Levels of Sup35p were therefore measured in 5 strains: wt [*PIN*⁺] [*PSI*⁺], wt [*PIN*⁺], wt [*pin*⁻], *ppq1Δ* [*PIN*⁺] and *ppq1Δ* [*pin*⁻] (all 74-D694) to address this question. The approach was to use quantitative western blotting using seven biological replicates per strain (apart from the wt [*PIN*⁺] [*PSI*⁺] strain, where only 5 replicates were used). Sup35p levels were expressed as a ratio to the levels of phosphoglycerate kinase (Pgk1p), an abundant cytoplasmic protein, and then normalised to the levels in the wt [*pin*⁻] strain. Two outliers per strain were excluded from the calculations.

The levels of Sup35p did not differ significantly between wt [*PIN*⁺] and *ppq1Δ* [*PIN*⁺] strains (T test, two-tail, equal variance: p=0.76; F-test for unequal variance: p=0.45; Figure 3.11). These were the strains used for assaying the rate of *de novo* [*PSI*⁺] formation. The results suggest that the effect on *de novo* prion formation of the *PPQ1* deletion was not through significant changes (i.e. increases) in the levels of Sup35p. Interestingly, the *ppq1Δ* [*pin*⁻] strain had much lower levels of Sup35p than other strains (T test, two-tail, equal variance: p<0.01 compared to [*PIN*⁺] strain; F-test for unequal variance: p=0.49) although the significance of this in relation to the question being asked, is not immediately evident.

3.3.5.3 Ppq1p interacts with Rnq1p

Another possibility is that Ppq1p interacts with Rnq1 protein. Rnq1p gives rise to [*PIN*⁺] prion that is absolutely necessary for *de novo* [*PSI*⁺] appearance (Derkatch *et al.*, 1997), therefore any factors that affect Rnq1p and subsequently the formation and/or function of the [*PIN*⁺] prion, might be expected to have a significant effect on [*PSI*⁺] formation.

This hypothesis was tested using yeast two-hybrid assay. As positive controls previously confirmed Sup35p-Sup45p (Stansfield *et al.*, 1995), Sup35p-Ppq1p (von der Haar, unpublished) and Rnq1p-Sup35p (Tuite *et al.*, 2008) interactions were used. PJ69-4a strain was used in the experiment (James *et al.*, 1996) transformed with two plasmids, one with the binding domain attached to one gene and the other one with the activation domain attached to the other gene coding for potential interaction partners (see methods section 2.6.4). Sup35p-Sup45p and Sup35p-Ppq1p controls grew on selective media, but no interaction was observed for Rnq1p-Sup35p (Figure 3.12a).
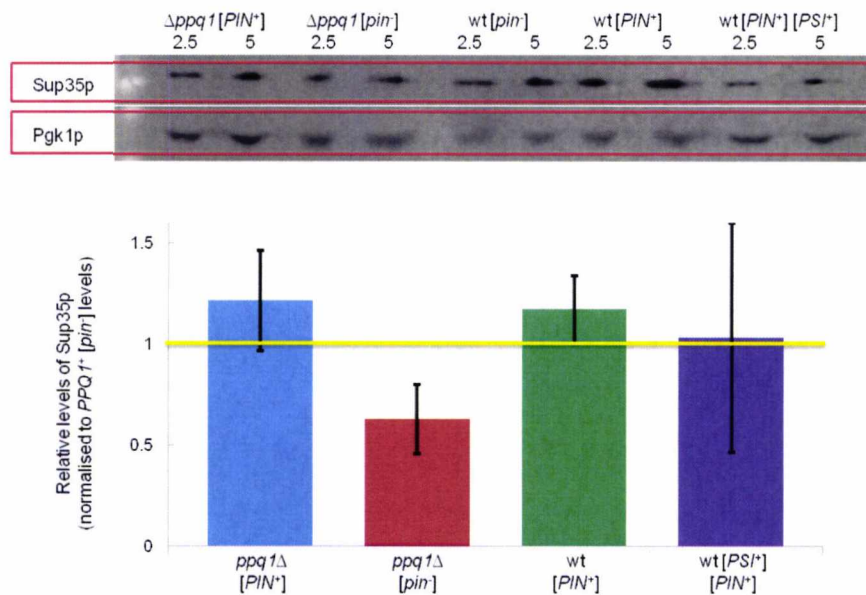
Figure 3.11. Sup35p levels in strains with wild-type or deleted *PPQ1* gene. Sup35p levels were estimated from fluorescence intensity using FITC conjugated secondary antibodies (see methods) in western blot analysis (above). Pgk1p was used as a loading control; below: relative levels of Sup35p where values were normalised to levels in the wt [*pin*⁻] strain; error bars represent one standard deviation.

One possibility is that interaction might be impaired as the strain used was probably [*PIN*⁺]. PJ69-4a strain was passaged through GdnHCl plate to eliminate possible [*PIN*⁺] prion (Figure 3.12b). The experiment was repeated in [*pin*⁻] strain, but again no

interactions could be observed for Rnq1p ruling out the possibility that the prion form of Rnq1p blocked a possible interaction with Rnq1p (Figure 3.12c).
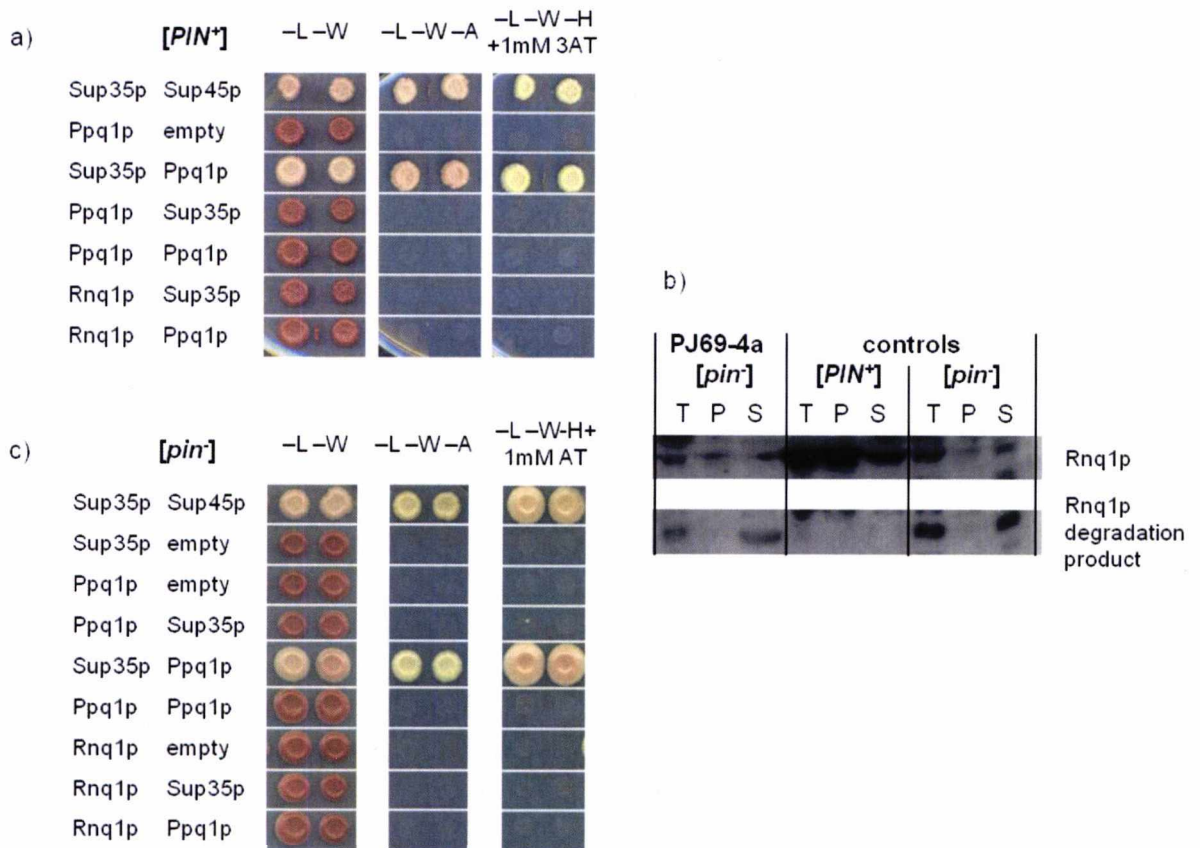
Figure 3.12. Testing Ppq1p and Rnq1p interaction in yeast two-hybrid assay. The interaction was tested in [*PIN*⁺] (a) and [*pin*⁻] (c) strains of PJ-69a; on the left are proteins with activation domain and on the right proteins with binding domain attached to them. −L −W: leucine and tryptophan drop-out media, selective for plasmid markers, −L −W −A: adenine deficient as well, −L −W −H + 1mM 3AT: leucine, tryptophan and histidine drop-out with competitive inhibitor of His3p; b) Sedimentation analysis: majority of Rnq1p is in soluble fraction confirming that GdnHCl passaged PJ69-4a strain is [*pin*⁻]; T, P, S − total cell extract, pellet fraction, soluble fraction, respectively. Majority of Rnq1p protein in soluble fraction was partially degraded (Rnq1 degradation product). Probed with anti-Rnq1p antibody.

3.4   Discussion

3.4.1 [*PSI*⁺] formation

Rates of spontaneous *de novo* [*PSI*⁺] formation and *SUP*⁺ mutations in the wt strain calculated in this study are: 4.6×10^{-7} [$(1.1 - 8.7) \times 10^{-7}$] and 1.3×10^{-6} [$(0.7 - 2.0) \times 10^{-6}$] per generation and are similar to previously reported rates. The high rate of *SUP*⁺ mutations is not surprising since mutations in many genes involved in translation could potentially

affect efficiency of termination at nonsense mutation: ribosomal proteins, tRNAs, translation termination factors, and proteins that affect accuracy of translation.

3.4.2 Optimising the *de novo* prion formation assay

3.4.2.1 The effect of media composition

Estimates of the rate of spontaneous *de novo* [*PSI*⁺] appearance were found to be highly dependent on the selective medium used. The rate, as estimated from YEPD supplemented, adenine-deficient medium, was at least 10-fold higher than the rate observed with MM-Ade alone. One possible explanation for this is that only strong [*PSI*⁺] variants are able to suppress the *ade1-14* allele sufficiently to allow growth on non-supplemented medium. A colony colour assay done on MM-Ade + 1% YEPD did not allow for differentiation of [*PSI*⁺] prion variants, therefore the ratio of strong to weak [*PSI*⁺] variants could not be calculated. However, no [*PSI*⁺] cells were observed on the non-supplemented MM-Ade medium and it seems unlikely that the wild-type strain generated only weak variants.

These findings suggest that non-supplemented MM-Ade medium suppresses growth of all [*PSI*⁺] variants. On the other hand, growth of [*PSI*⁺] strains on the different medium (Figure 3.4) showed that strong variants of [*PSI*⁺] can grow on MM-Ade, albeit much slower than strong nuclear-encoded suppressor mutant. Weak suppressor mutants grew slower than the [*PSI*⁺] strong variant, but the total number of SUP^+ mutants was not affected. Growth retardation therefore appears to be [*PSI*⁺] specific.

Another possibility is that the strong selection imposed on cells by use of a medium that is adenine deficient selects for cells that acquire SUP^+ mutations over [*PSI*⁺] mutants. In this model, [*PSI*⁺] would allow for a very slow growth, but the original [*PSI*⁺] cells would be eventually overgrown by SUP^+ [*PSI*⁺] cells. [*PSI*⁺] in these cells would be masked by the nuclear suppressors and undetectable using colony colour assay or lost completely when sufficient suppression was achieved through nuclear mutations.

3.4.2.2 The effect of cell density

The cell density used in the MM-Ade-based assay was comparable to MM-Ade + 1% YEPD (i.e. 10^6 cells per plate). At this density, spontaneous *de novo* [*PSI*⁺] formation rate in the wt strain was the same as the rate estimated when 10^5 cells per plate was used.

The various cell densities tested therefore do not affect the rate [*PSI⁺*] and *SUP⁺* mutations in the wt strain on the MM-Ade + YEPD supplemented medium, but could perhaps work in combination with complete adenine deficiency to suppress growth of [*PSI⁺*] cells. This hypothesis could be tested by repeating the experiments using unsupplemented MM-Ade plates with a density of 10^5 cells per plate.

The rate of spontaneous *de novo* [*PSI⁺*] formation in the *ppq1Δ* strain was much lower in the experiments where 10^6 cells were plated compared to when 10^5 cells were plated. The observed reduction is likely to be caused by an overcrowding effect (where cell exhaust available nutrients before they can grow into visible colonies) and was not observed with the wt strain possibly because of a lower number of [*PSI⁺*] colonies when compared to the *ppq1Δ* strain.

3.4.2.3 Appearance of *SUP⁺* nuclear-encoded suppressor mutants

As expected, the addition of YEPD to the MM-Ade selective medium increased the observed *SUP⁺* mutation rates, particularly at the highest level used i.e. supplementation with 2.5% (v/v) YEPD (Figures 3.2 and 3.3). Supplementation allows for growth of mutants with very weak suppressor mutations. To avoid growth of additional suppressor colonies on MM-Ade + 1% YEPD plates, colonies were scored and tested for colony colour after 7 days. The number of *SUP⁺* colonies corresponded closely to those on MM-Ade plates that were incubated for about 4 weeks (until no new colonies were appearing).

Different observed rates of *SUP⁺* mutation on 10^5 and 10^6 cells plates in the case of *ppq1Δ* strain show that growth of *SUP⁺* mutants is also suppressed by high densities. The overcrowding effect is stronger in the case of *SUP⁺* than [*PSI⁺*] cells. Again, as in case of [*PSI⁺*] rates, *SUP⁺* mutation rates in wt strain were not affected, presumably because of a smaller number of colonies that grew on each plate.

The rate of suppressor mutations was higher in the *PPQ1* deletion strain. Previous studies have shown that a *ppq1Δ* strain has an allosuppressor phenotype, i.e. enhances the efficiency of suppression for weak nonsense suppressors. In other words, nonsense suppression caused by the *PPQ1* deletion is too weak to be expressed on its own whereas *PPQ1* deletion-induced allosuppression allows for growth of cells with weak nonsense suppressors (Song *et al.*, 1987). Such weak suppressor mutations could not suppress nonsense mutations sufficiently in the wild-type background, hence the higher observed rate of *SUP⁺* in the deletion strain.

3.4.2.4 Spontaneous *de novo* [*PSI*⁺] formation protocol

Two different protocols were used to estimate the rate of *de novo* [*PSI*⁺] formation. The first protocol used was one adapted from lab protocol for induced *de novo* [*PSI*⁺] formation (N. Koloteva-Levine, personal communication). The second protocol was that described by Lancaster *et al.* (2010) (see methods section 2.7.1.4). Growing liquid cultures from low cell numbers was felt to be more appropriate than diluting them from an overnight experiments since the fluctuation test (first described by Luria *et al.*, 1943) assumes that the culture was started from a single [*psi*] (or non-mutated) cell. The results of the selective media comparison (section 3.2.1) indicate that the MM-Ade medium supplemented with 1% YEPD is the most appropriate medium for selection of various Ade⁺ cells, be they nuclear mutants or [*PSI*⁺]. Overcrowding effect might affect rate estimates therefore deletions/conditions that are expected to increase the rate of *de novo* [*PSI*⁺] formation should be tested at lower cell densities.

3.4.3 The role of the Ppq1 protein in *de novo* prion formation

Deletion of the *PPQ1* gene increased the rate of *de novo* formation of the [*PSI*⁺] prion (8.5 $\times 10^{-6}$) compared to the rate in wt strain (4.6 $\times 10^{-7}$ per generation). The increase in the rate compared to wt strain was 2-fold higher than reported previously (i.e. a 10-fold increase reported by Tyedmers *et al.*, 2008). Tyedmers and colleagues used in their experiment a strain variant of 74D-694, R2E2 that has an increased number of oligopeptide repeats in the prion domain (Liu *et al.*, 1999). R2E2 strain has an intrinsically increased rate of *de novo* formation of [*PSI*⁺] and this artefact could possibly account for a lower increase in the [*PSI*⁺] formation rate in *PPQ1* gene deletion strain they reported. The increase in the [*PSI*⁺] rate is mirrored in 28-fold increase in the rate of *SUP*⁺ appearance.

While the increase in the rate of appearance of *SUP*⁺ mutants can be explained by the allosuppressor effect of the *PPQ1* deletion, the mechanism behind the increased rate of [*PSI*⁺] formation is not immediately evident. Deletion of the *PPQ1* gene does not affect Sup35 protein levels in the cell nor does the proposed phosphatase activity of Ppq1p directly affect Sup35p since this protein has not been shown to be phosphorylated *in vivo*. The second eukaryotic release factor (eRF1 or Sup45p) is phosphorylated but its phosphorylation status is not affected by Ppq1p nor does phosphorylation of Sup45p affect allosuppression caused by *PPQ1* deletion (Kallmeyer *et al.*, 2006). Alternatively Ppq1p could interact with Rnq1p or compete with the protein for interaction with Sup35p. Ppq1p levels are very low in the cell (~300-fold lower than Sup35p levels (von der Haar,

2008; Ghaemmaghami *et al.*, 2003) so any effect based on physical interaction seems unlikely. In the next chapter, the effect of a *PPQ1* deletion on various cellular processes is explored with the intention of shedding light on the involvement of Ppq1p in [*PSI*⁺] prion formation.

3.4.4 Summary of findings

The experiments described in this chapter demonstrate that the choice of selective medium has a significant effect on the experimentally determined estimation of *de novo* [*PSI*⁺] formation rates. The [*PSI*⁺] prion causes weak nonsense suppression and levels of functional Ade1p generated by the suppression of the *ade1-14* allele are not sufficient for growth, on a non-supplemented adenine-deficient medium, for all [*PSI*⁺] variants that might arise spontaneously. Strong *SUP*⁺ mutants on the other hand can grow on selective medium without YEPD supplementation. Growth of both types of Ade⁺ cell also depends on cell density. Using the optimised *de novo* formation assay, deletion of the *PPQ1* gene was shown to lead to a significant increase in the rate of *de novo* [*PSI*⁺] prion formation and the observed rate of *SUP*⁺ mutation. In the case of the nuclear-encoded *SUP*⁺ mutations, the increase in rates was caused by the *ppq1Δ*-associated allosuppressor activity that allows growth of weak suppressor mutants to work more efficiently at translating their cognate stop codon rather than by increasing the mutation rate per se. While Ppq1p is known to interact physically with Sup35p, the mechanism of suppression of [*PSI*⁺] prion formation by the Ppq1p phosphatase is not known.

Chapter IV

The role of Ppq1 protein in cellular processes

4.1 Introduction

In a search for factors that affect the rate of *de novo* [*PSI*⁺] prion formation we identified Ppq1p as a potential factor on the basis of its interaction with the Sup35 protein (see Chapter 3). In parallel with our research, Tyedmers *et al.* (2008) identified that deletion of the *PPQ1* gene most affects the frequency of *de novo* [*PSI*⁺] formation. The mechanism by which loss of Ppq1p affects *de novo* [*PSI*⁺] formation is not understood, but this requires that we first understand the cellular role of this poorly studied protein. Ppq1p is a putative Ser/Thr phosphatase, but Sup35p is unlikely to be its target because there is no evidence that Sup35p is phosphorylated *in vivo* (Fabret *et al.*, 2008). The N-domain of Ppq1p is unusual in structure and could potentially promote aggregation of the protein perhaps in a prion-like manner. In this chapter I describe an investigation into the possible role of Ppq1p in mRNA translation, its effect on cellular processes other than protein synthesis and the possible role of N-domain in Ppq1p aggregation.

Ppq1p is a 549 amino acid long protein with two distinct domains. The sequence of the C-domain (235-549) is highly similar to type 1 Ser/Thr protein phosphatases with approximately 60% amino acid identity to the Glc7p phosphatase and approximately 65% identity to the C-domain of Ppz1p and Ppz2p phosphatases (Figure 4.1). The C-domain is distinct in that it is basic, while other phosphatase proteins are acidic (Chen *et al.*, 1993; Vincent *et al.*, 1994). Ppq1p has no closely related homologues in *S. cerevisiae* (Chen *et al.*, 1993; Vincent *et al.*, 1994), is present in cells at low levels (~270 molecules/cell) and is stable (von der Haar, 2008; Ghaemmaghami *et al.*, 2003).

The N-domain of Ppq1p is enriched in Ser and Asn representing 24% and 12% of amino acid residues, respectively. This amino acid composition bias towards Ser is similar to that seen in the N-domains of Ppz1p and Ppz2p (22-25%), while the former protein is also rich in Asn residues (11%). The N-domain of Ppz2p (Ppz2pN) on the other hand is arginine rich (9%) (Posas *et al.*, 1992; Hughes *et al.*, 1993; Chen *et al.*, 1993; Posas *et al.*, 1993; Vincent *et al.*, 1994). Beyond such an amino acid bias, the N-domain of Ppq1p does not share sequence similarities with Ppz proteins, but is more closely related to Aga1pN with 65% similarity in a 113 amino acid overlap (Vincent *et al.*, 1994). On the other hand, Chen *et al.* (1993) identified Gac1p, a regulatory subunit of Glc7p as showing a low level of sequence similarity to Ppq1pN. This sequence similarity does not extend to function since deletion or overexpression of *PPQ1* did not affect glycogen accumulation, a phenotype associated with a *glc7Δ* (Chen *et al.*, 1993).
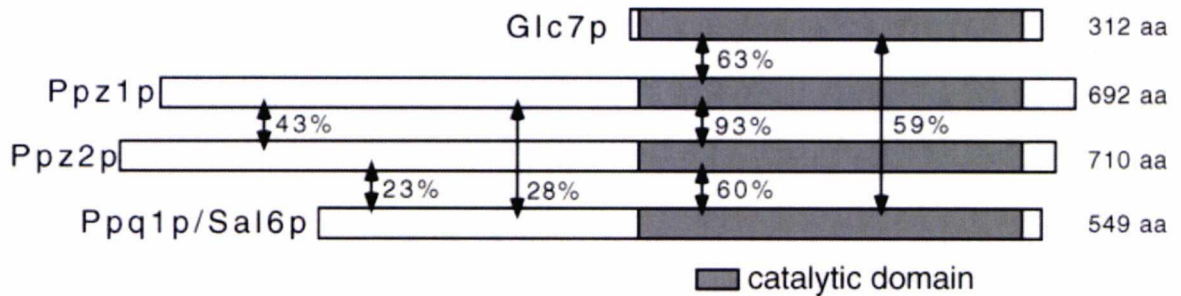
Figure 4.1: Domain structure and sequence similarity between related yeast PP1 and PP1-like phosphatases. Percentages indicate amino acid similarity; from Venturi *et al.* (2000).

The *PPQ1* gene was first identified through the *sal6-1* mutant allele that causes allosuppression in yeast (Song *et al.*, 1987) and was later shown to have a nucleotide insertion causing a frameshift (Vincent *et al.*, 1994). *sal6-1* was unable to suppress nonsense alleles used in their study on its own, but it enhanced suppression caused by the omnipotent suppressors *sup45-2* and *sup35-4*, which are point mutations in the genes encoding eRF1 and eRF3 (Sup35p) respectively. *sal6-1* mutants are not sensitive to various translation interfering drugs, such as cycloheximide (blocks translocation), paromomycin and G418 (elongation). In the presence of omnipotent suppressor mutants, *sal6-1* did slightly increase sensitivity to paromomycin and caused an increase in nonsense suppression and sensitivity to drugs in presence of some, but not all allosuppressors (i.e. *sal1*, *sal2-A*, *sal2-B*, *sal3*). In combination with [*PSI*⁺] however, the *sal6-1* allele did not affect any tested phenotypes beyond its effect attributed to the prion form of Sup35p (Song *et al.*, 1987). Deletion of the *PPQ1* gene can be complemented with expression of *PPQ1* gene with residues 111 – 240 of its N-domain deleted whereas overexpression of the gene had the opposite effect on translation termination causing antisuppression (Vincent *et al.*, 1994, Benko *et al.*, 2000).

The effect of Ppq1p on mRNA translation was further explored using drugs that inhibit protein synthesis. A *ppq1Δ SUP⁺* strain is sensitive to paromomycin, but not cycloheximide and G418 (Song *et al.*, 1987; Vincent *et al.*, 1994). On the other hand Chen *et al.* (1993) reported sensitivity to both cycloheximide and G418 in a strain lacking known nonsense suppressors. Both drugs inhibit protein synthesis at the elongation stage, rather than termination. Furthermore, deletion of *PPQ1* increased ribosomal +1 frameshift events on the transposon Ty1 by 2-fold, while *sup35* and *sup45* release factors mutants had no such effect (Burck *et al.*, 1999). A *PPQ1* deletion also affected the rate of translation, reducing it by 10-15% (Chen *et al.*, 1993). The sensitivity of the *ppq1Δ* strain to

paromomycin and the effects on both translation elongation and termination suggest that Ppq1p may modulate the accuracy of translation (Chen *et al.*, 1993; Vincent *et al.*, 1994). In agreement with their role in translation Ppq1p, Ppz1p and Ppz2p are the only Ser/Thr phosphatases expressed cyclically (i.e. show a pattern of expression that follows the cell cycle) in *S. cerevisiae*, in an expression pattern similar to some ribosomal and translation initiation factors. This emerged from a meta-analysis of microarray data reported by Dyczkowski *et al.* (2005).

Deletion of the *PPQ1* gene also affects the growth rate. Chen *et al.* (1993) reported a small growth defect of a *ppq1Δ* strain on rich and defined media using fermentable and non-fermentable carbon sources. Vincent *et al.* (1994) also observed a small reduction in growth of such mutants, but only on glycerol-based medium. These various *ppq1Δ* growth and translation phenotypes therefore appear to be strain specific. A stronger effect of a *PPQ1* gene deletion was observed in stationary phase cells where a *ppq1Δ* strain was found to grow significantly more slowly and ceased growth at a lower cell density (Chen *et al.*, 1993). During prolonged incubation in amino acid-deficient media, *ppq1Δ* cells were also reported to show a 'balloon-like' morphology (Chen *et al.*, 1993). The various effects of a *PPQ1* deletion or overexpression of the *PPQ1* gene are summarised in Table 4.1.

The N-terminal sequences of phosphatases might be important for specificity and/or for controlling the activity of the catalytic domain of the enzyme. For example, *PP1* cannot rescue temperature sensitivity of a *sit4* mutant – Sit4p a protein phosphatase that functions in progression from late G1 to S phase (Sutton *et al.*, 1991), whereas fusion of the N-domain of the *Drosophila melanogaster* phosphatase *PPV*, a *D. Melanogaster* orthologue of *SIT4* will complement these same phenotype (Mann *et al.*, 1993). The N-domain of Ppp5p on the other hand autoinhibits phosphatase activity of its C-domain by blocking the active site of the catalytic domain (Yang *et al.*, 2005).

The N-domains of Ppz1p and Ppz2p have a consensus sequence for myristoylation and they have been shown to be myristoylated *in vivo* (Hughes *et al.*, 1993; Clotet *et al.*, 1996). A *ppz1Δ* strain exhibits increased resistance to lithium toxicity and sensitivity to caffeine (Posas *et al.*, 1993), while (Clotet *et al.*, 1996) reported that deletion of a large region in the N-domain of Ppz1p downstream of this site complements the lithium resistance phenotype of *ppz1Δ* strain. Furthermore, expression of *PPZ1* with a mutated site for N-myristoylation in *PPZ1* deletion strain only slightly increased the sensitivity to lithium compared to a *ppz1Δ* strain (Clotet *et al.*, 1996). Another deletion in the N-domain (residues 241-318) of Ppz1p was able to partially complement the deletion phenotype. The effects of the two partial N-domain deletion constructs were reversed in the case of

sensitivity to caffeine indicating that different regions in Ppz1p have different roles (Clotet *et al.*, 1996). Venturi *et al.* (2000) on the other hand showed that the catalytic domain Ppz1p is sufficient for complementation of these phenotypes when expressed at higher levels. It is likely that N-myristoylation increases protein stability as is the case for the catalytic subunit of cAMP-dependent PK (Yonemoto *et al.*, 1993). The phenotypes reported by Clotet *et al.* (1996) were therefore probably a consequence of a lower concentration of the Ppz1 protein (Venturi *et al.*, 2000).

Table 4.1: Phenotypes described for *PPQ1* deletion / overexpression and comparison to *PPZ1/2*

Test	Phenotype	Notes	*ppz1/2Δ*	Notes
Effect on translation				
Translation termination	O (-)	Only in *SUP⁺*, 1, 3	-	(3-4x), 11; same in *ppz1Δ*
Trichodermin	O	1		
Rate of protein synthesis	-	2		
Accuracy	-	2-fold FS, 4	+	11
Paromomycin	O (-)	Only in *SUP⁺*, 1, 3;	++	In *ppz1Δ* as well, 11
Cycloheximide	O / -	1 / 2	O	11
G418	O / -	1 / 2		
Overexpression		Antisuppression, resistance to paromomycin, 3		Antisuppression, 13, 14
			Hygromycin	+; In *ppz1Δ* as well, 11
DNA, RNA				
Rifampicin	O	2		
Hydroxyurea	O	2		
DNA content	O	2	-	10
Growth				
YEPD	- / O	Homozygous, 2 / 3	O / - (OE)	Single and double, 9 12; / 15
YEP Glycerol	(-)	3		
SC Glc	-	Homozygous, 2		
SC Gal	-	Homozygous, 2		
SC gly	-	Homozygous, 2		
SC acetate	-	Homozygous, 2		
Low T	O / -	1, 3, 2 / in *SUP⁺*,	-	Only *ppz1/2Δ*, 5

		1, 3		
High T	O	1, 2, 3	- / (-)	8; Lysis at 37°C, 9
Heat shock	O	2		
from storage	-	Homozygous, 2		
Growth from spores	-	2		
Stationary phase growth	- -	Homozygous, 2	O	Increase in cell size, 9
Enlarged in stationary phase	O	2	+	Also in *ppz1Δ*, 9
Glycogen accumulation	O	2, 3	O	9
Starvation	-	Enlarged, cell wall distortion, 2		
Sorbitol	O	Does not rescue growth defects, 2	+	Partly rescues large cell and caffeine sensitivity phenotypes, 9
Filamentous growth	+ +	6	++ (OE)	*ppz1Δ*
Other				
mating pheromone sensitivity	O	2	O	9
mating efficiency	O	2		
sporulation frequency	O	2		
invertase levels	O	2		
sensitivity to UV	O	2		
Staurosporin (prot kinase inhib)	O	2		
SDS	O	2		
Caffeine	O	3, 2	-	Also in *ppz1Δ*, 9
acidic conditions	O	2		
NaCl	O	2		
MgCl$_2$	O	2		
CaCl$_2$	(-)	Above 30mM, 2		
Endocytosis	-	7		

Footnotes: "-" decrease, "O" no change and "+"increase; FS – frameshift; the list is not exhaustive for *PPZ1/2*; 1 – Song *et al.*, 1987; 2 – Chen *et al.*, 1993; 3 – Vincent *et al.*, 1994; 4 – Burck *et al.*,

1999; 5 – Venturi *et al.*, 2000; 6 – Jin *et al.*, 2008; 7 – Burston *et al.*, 2009; 8 – Posas *et al.*, 1992; 9 – Hughes *et al.*, 1993; 10 – Clotet *et al.*, 1999; 11 – ; 12 – Sopko *et al.*, 2006; 13 – Aksenova *et al.*, 2007; 14 – Ivanov *et al.*, 2008; 15 – Yoshikawa *et al.*, 2011

The function of Ppz1pN beyond a signal and the target for N-myristoylation is therefore not known. Similarly, no roles have been demonstrated for the N-domain of Ppq1p. In this chapter the phenotypes of *PPQ1* gene deletion and a possible function for Ppq1N are explored from the perspective of the protein's effect on [*PSI*$^+$] prion formation. Bioinformatic tools and searchable high-throughput databases are used to generate hypotheses that are then tested. Finally, a fluorescent protein tagged construct is used to visualise Ppq1p localisation under various conditions.

4.2   Bioinformatics

As a first step in an attempt to elucidate the function of Ppq1p with the emphasis on the protein's possible role in [*PSI*$^+$] prion formation, a range of bioinformatics tools were applied as described below. Information on conservation of the Ppq1p amino acid sequence and its predicted secondary and tertiary structural features could indicate the importance of the protein and its two domains, for the host organism. Identification of potential transcription factors that bind to *PPQ1* promoter region, predicted or confirmed post-translational modifications, analysis of gene expression patterns and *PPQ1* genetic/physical interaction and fitness interaction networks were all used to produce hypotheses on Ppq1p roles and hypothetical function of its N-terminal domain. The initial hypothesis was that N-domain might be implicated in self-aggregation and this was based on its Asn bias. Recent studies with the yeast Sup35p prion protein have clearly indicated the importance of Asn residues over Gln (Alberti *et al.*, 2009; Halfmann *et al.*, 2011).

4.2.1 Amino acid sequence comparison of Ppq1p within the genus *Saccharomyces* and in other fungi

The relative conservation of an amino acid sequence (i.e. how many amino acid changes per sequence length compared to an average sequence) reflects the importance of that protein or region for the fitness of the organism (e.g. Jordan *et al.*, 2002, but Hurst *et al.*, 1999).

In a recent study by Liti *et al.* (2009) a wide variety of *S. cerevisiae* strains were sequenced. This data set (available from http://www.sanger.ac.uk/Teams/Team118/sgrp/) was used to extract various Ppq1p amino acid sequences aligning them via the initiator methionine residues. Only two robust (present in more than one strain) amino acid changes were found in the 32 aligned Ppq1p sequences, one in each of the two domains of the protein. These changes are shown in Figure 4.2 next to a branch of a phylogram where they have most likely occurred. Two additional substitutions were present in a single strain but each was considered to be less reliable because they could be due to sequencing error (as indicated in Figure 4.2). Additionally, two sequences that were not aligned appeared to be a result of sequencing slip in a single nucleotide.
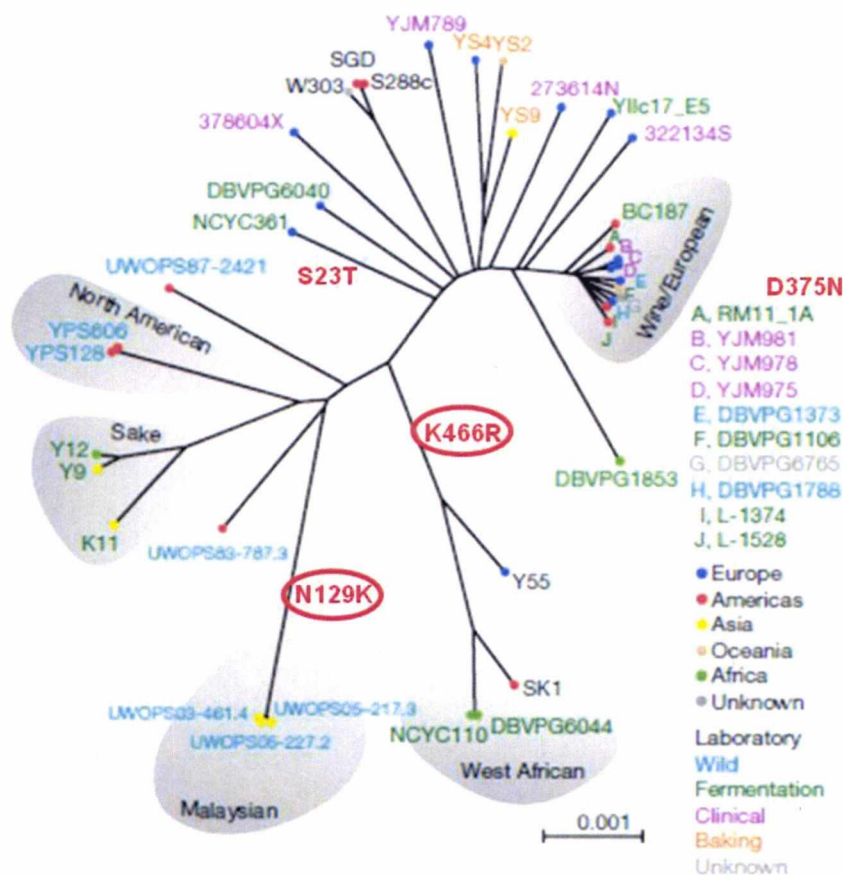
Figure 4.2: Alignment of Ppq1p sequences of 32 strains of *S. cerevisiae* plotted on a phylogenetic tree. Changes are presented as amino acid substitutions next to a branch where the substitution presumably occurred. Phylogram reproduced from Liti *et al.* (2009).

This result showed that a few amino acid changes have occurred in a wide range of *S. cerevisiae* strains from a wide range of ecosystems i.e. Ppq1p shows little polymorphism within *S. cerevisiae*. To try to better identify conserved regions within Ppq1p, an alignment of the protein with orthologues in other fungi was carried out. Figure 4.3 shows

that the Ppq1p C-domain is well conserved across fungal species compared to the N-domain. The conserved regions were visualised using a similarity plot (Figure 4.3b).

Vincent *et al.* (1994) reported that all tested phenotypes of a *PPQ1* gene deletion were complemented by plasmid-borne *PPQ1–ΔN* which lacked residues 111 – 240 (indicated in Figure 4.3a), while the sequence N-terminal to this, including the conserved region from residues 34 – 51, were left in-frame and intact. If any functions are specifically associated with the N-domain of Ppq1p, they could be localised to this conserved region.

Another possibility is that it is not the amino acid sequence that is important for the Ppq1p N-domain's hypothetical function but rather its composition. The amino acid composition of Ppq1pN is highly skewed towards Ser and Asn residues (see above). A comparison of

a)

b)

Figure 4.3: Similarity between Ppq1p and its orthologues in Fungi. a) NCBI BlastP, non-redundant protein database for Ppq1p – cut-off value was set at E-150. 1 Ppq1p [*Saccharomyces cerevisiae*], 2 hypothetical protein Kpol_1033p29 [*Vanderwaltozyma polyspora* DSM 70294], 3 KLTH0H05148p [*Lachancea thermotolerans*], 4 unnamed protein [*Kluyveromyces lactis*], 5 AFL051Wp [*Ashbya gossypii* ATCC 10895], 6 ZYRO0G03454p [*Zygosaccharomyces rouxii*], 7 unnamed protein [*Candida glabrata*]; Deletion within N-domain used in Vincent et al. (1994) study is indicated by a red square. The red arrow indicates predicted site of palmitoylation and the blue arrow a conserved phosphorylation site; b) a similarity plot (plotcon) of aligned sequences with a 10 amino acid window setting.

the relative abundance of the two amino acids (Table 4.2) showed that the percentage of Ser residues in the Ppq1p N-domain is similar between the different yeast species, while the abundance of Asn is less so.

Table 4.2: Proportion of Ser and Asn residues within N-domains of various fungi species.

Species	S (%)	N (%)
Saccharomyces cerevisiae	24.2	11.9
Vanderwaltozyma polyspora	21.7	16.2
Lachancea thermotolerans	16.9	5.8
Kluyveromyces lactis	23.3	8.2
Ashbya gossypii	23.0	6.0
Zygosaccharomyces rouxii	17.1	14.2
Candida glabrata	21.8	6.4
average	**21**	**10**
SD	**3**	**4**

Footnote: Sequences compared were identified by blast search (Figure 4.3). Ser residues do not only represent higher proportion of the sequence, but the proportion is also less variable between species than is the case for Asn residues

The amino acid sequence of the N-domain was also compared using Blast search against all non-fungal sequences in the NCBI database (http://blast.ncbi.nlm.nih.gov/Blast.cgi), but no significant hits were recorded suggesting that this domain might be unique to fungi.

4.2.2 Prediction of Ppq1p structure

Ppq1p has a long N-domain that is rich in Ser and the bias toward Ser residues appears to be relatively conserved within Fungi. In order to explore the structural features of the N-domain, a prediction of the folded protein was obtained using the web tool iTasser (Zhang, 2008). This software uses short sequences of proteins with known structure as a template and proceeds through several iterations calculating minimum free-energy states.

The secondary structure of the Ppq1p-N-domain predicted on the basis of amino acid properties was mostly coil (Figure 4.4). A model of the tertiary structure predicted a more folded domain with several α-helices. At the level of secondary structure, the Ppq1pN resembles yeast prion domains which are also made of mostly unfolded state promoting amino acids (Michelitsch et al., 2000; Alberti et al., 2009), but the tertiary structure of the prion domain of Sup35p obtained using the same software was unfolded (data not shown).

4.2.3 Domains/motifs and signal peptides

A resource available from the Saccharomyces Genome Database (http://www. yeastgenome.org/cgi-bin/protein/domainPage.pl?dbid=S000006100) allows one to summarise available information on domains/motifs, predicted transmembrane domains

A

```
MRRSPSRSNNNFAVPNCSTN SNSSQQQLTTPSDDLNSNEP NDPDDSRSLPTIKKFNNKHS INNYNTLASAGKNNNNKRAS
CCCCCCCCCCCCCCCCCCC CCCCCCCCCCCCCCCCCCC CCCCCCCCCCCCCCCCCCC CCCCCCCCCCCCCCCCHHH

NDNLLIPGENAHKQKIYTKD ENLKSLYLDIDVSVAKALSS SATAPKLINTARTSSTTTAT TSNNILTSPSYRESNYSSPS
HHHHHCCCCCCHHHCCHHHH CCCCCCCCCCCCCCCCSSCC CCCCCCHHCCCCCCCCCCCC CCHHHCCCCCCCCCCCCCC

SYSFSSYYSSATSASSSTSS FLKSSGLSSRVKSPSSSVKA GSFGAPSSPTSGIPNPKSSK KPIFLRRYSHDTSSN
CCCCCCCCCHHHHHCHHHHHCH CCCCCCCHCCCCCCCCHHH HHCCCCCCCCCCCCCCCCC CCCCCCCCCCCCCCCC
```

B

Figure 4.4: Predicted secondary and tertiary structure of Ppq1p. Model was constructed using iTasser software; N-domain (pink and blue) consists of long coils and α-helices; C-domain: green; A: predicted secondary structure and B: predicted tertiary structure.

and signal peptides for a given protein. It also provides a list of proteins that share the indentified domains/motifs. The Ppq1p C-domain was clearly identified as a protein phosphatase, while the N-domain of Ppq1p did not contain known sequences that could affect protein localisation.

Several prediction tools available through Expasy (www.expasy.org/tools/) were also used, namely MITOPROT-Prediction of mitochondrial targeting sequences, PATS, Predotar – service for identifying putative mitochondrial, plastid and ER targeting sequences, PTS1 predictor – peroxisomal targeting signal 1. None of these revealed any such domains, motifs or signal peptides within N-domain of Ppq1p. The sequence of Ppq1pN therefore does not have any known motifs or signal peptides.

4.2.4 Predicted posttranslational modifications

NetPhos 2.0, a programme that predicts phosphorylation sites in a protein (Blom *et al.*, 1999) (http://www.cbs.dtu.dk/services/NetPhos/) predicted more than 30 phosphorylation sites in Ppq1p. Only two of these sites have been observed to be phosphorylated using mass spectrometry of cellular proteins: Ser^{80} (Bodenmiller *et al.*, 2007) and Ser^{208} (Gruhler

et al., 2005). Ser[80] is a conserved residue when *PPQ1* orthologues in fungi are aligned (red arrow; Figure 4.3), while Ser[208] is not.

Ppq1p was not predicted to be myristoylated by the NMT - The MYR Predictor (http://mendel.imp.ac.at/myristate/SUPLpredictor.htm) yet the Ppz1p phosphatase was predicted to have myristoylation at two positions with high confidence. However, only the N-terminal prediction for Ppz1p has been experimentally confirmed (Clotet *et al.*, 1996).

The N-domain of Ppq1p was predicted to be palmitoylated; the CSS-Palm is software that predicts palmitoylated sites based on amino acid sequence (csspalm.biocuckoo.org; Ren *et al.*, 2008). The software predicted palmitoylation at Cys[17] with a high confidence (0.97) and at Cys[528] with a much lower confidence (0.31). The predicted site of palmitoylation is marked with red arrow in Figure 4.3, although this Cys residue is not conserved in the alignment between orthologues of fungi.

4.2.5   Promoters/conserved sequences upstream of *PPQ1* ORF

Identification of transcription factors (TFs) that bind to the promoter region of the *PPQ1* gene could provide clues to the process(es) in which Ppq1p is involved by clustering *PPQ1* with other genes whose transcription is activated by a particular TF. A curated repository called YEASTRACT (Abdulrehman *et al.*, 2011; http://www.yeastract.com/) lists TFs that have been confirmed to bind to specific DNA sequences and can be used to predict TF binding to those sequences. Inputting the *PPQ1* upstream sequence returned 3 confirmed and 41 predicted TFs.

To narrow down the list of potential TFs an alignment of the region upstream of *PPQ1* ORF for closely related species of the *Saccharomyces* genus was obtained using UCSC Genome Browser (Kent *et al.*, 2002; http://genome.ucsc.edu/cgi-bin/hgGateway; Figure 4.5). Two regions were defined as well conserved (circled in red). A highly conserved region immediately upstream of the *PPQ1* ORF was presumed to be 5' UTR and a transcription start site and corresponds to the mapping done by Vincent *et al.* (1994). With the expectation that TF binding sites are in conserved regions, a list of predicted TFs from YEASTRACT was reduced to 10 factors (Table 4.3). Two factors that were predicted to bind to less conserved regions indicated with yellow circles in Figure 4.5 were also included in the list.
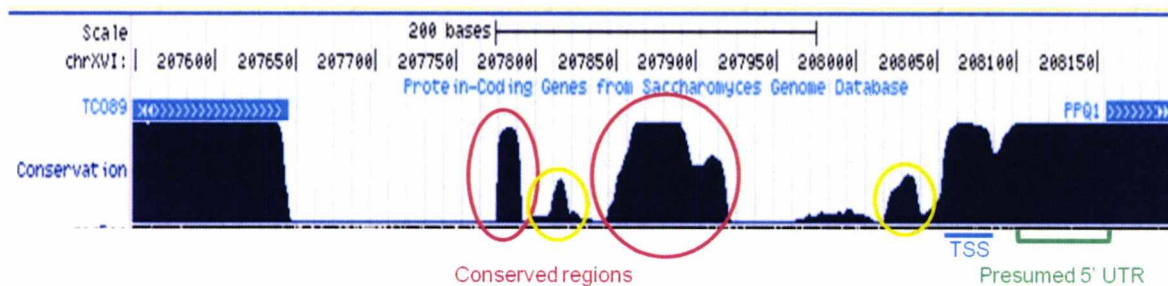
Figure 4.5: Conserved regions of the upstream sequence of *PPQ1* ORF. Alignment and conservation plot were obtained from UCSC Genome Browser (genome.ucsc.edu). 4 regions were defined – two highly conserved (red) and two less conserved (yellow). Conserved region directly upstream of *PPQ1* ORF corresponds to 5'UTR and a transcription start site identified by Vincent et al. (1994).

Chua *et al.* (2006) systematically overexpressed 55 different TFs in yeast and performed microarray analysis to determine changes in mRNA levels. None of the TFs tested in the study had an effect on *PPQ1* transcription. TFs that were tested in that study and appeared as potential TFs in the above analysis are indicated with (−) in Table 4.3. Overexpression of Ste12p, a TF that was experimentally confirmed to bind to upstream region of *PPQ1* (Lefrancois *et al.*, 2009; Zheng *et al.*, 2010), also had no effect on *PPQ1* mRNA levels (Chua *et al.*, 2006).

Table 4.3: Transcription factors that bind upstream of *PPQ1* ORF

OE	TF	SGD description
O	Azf1	Zinc-finger transcription factor, involved in induction of *CLN3* transcription in response to glucose; genetic and physical interactions indicate a possible role in mitochondrial transcription or genome maintenance
-	Cup2	Copper-binding transcription factor; activates transcription of the metallothionein genes *CUP1-1* and *CUP1-2* in response to elevated copper concentrations
-	Ecm22	Sterol regulatory element binding protein, regulates transcription of sterol biosynthetic genes; contains Zn[2]-Cys[6] binuclear cluster; homologous to Upc2p; relocates from intracellular membranes to perinuclear foci on sterol depletion
O	Fkh1	Forkhead family transcription factor with a minor role in the expression of G2/M phase genes; negatively regulates transcriptional elongation; positive role in chromatin silencing at HML and HMR; regulates donor preference during switching
O	Fkh2	Forkhead family transcription factor with a major role in the expression of G2/M phase genes; positively regulates transcriptional elongation; negative role in chromatin silencing at HML and HMR; substrate of the Cdc28p/Clb5p kinase

-	Hac1	Basic leucine zipper (bZIP) transcription factor (*ATF/CREB1* homolog) that regulates the unfolded protein response, via UPRE binding, and membrane biogenesis; ER stress-induced splicing pathway facilitates efficient Hac1p synthesis
O	Stb5	Transcription factor, involved in regulating multidrug resistance and oxidative stress response; forms a heterodimer with Pdr1p; contains a Zn(II)2Cys6 zinc finger domain that interacts with a pleiotropic drug resistance element in vitro
-	Upc2	Sterol regulatory element binding protein, induces transcription of sterol biosynthetic genes and of *DAN/TIR* gene products; Ecm22p homolog; relocates from intracellular membranes to perinuclear foci on sterol depletion
-	Abf1	DNA binding protein with possible chromatin-reorganizing activity involved in transcriptional activation, gene silencing, and DNA replication and repair
O	Rtg1	Transcription factor (bHLH) involved in interorganelle communication between mitochondria, peroxisomes, and nucleus
-	**Ste12**	Transcription factor that is activated by a MAP kinase signaling cascade, activates genes involved in mating or pseudohyphal/invasive growth pathways; cooperates with Tec1p transcription factor to regulate genes specific for invasive growth
O	**Gcr1/2**	Transcriptional activator of genes involved in glycolysis; DNA-binding protein that interacts and functions with the transcriptional activator Gcr2p

Footnote: Experimentally confirmed (bold) and predicted TF, OE: study by Chua *et al.*, 2006 found no effect of TF overexpression on (-) on *PPQ1* transcription or TF was not tested (O)

4.2.6 Predicting cellular processes Ppq1p affects using gene expression microarray datasets

The SPELL database/searching engine (http://spell.yeastgenome.org/; Hibbs *et al.*, 2007) gathers information from published microarray analysis data and enables one to search by gene or gene family. It also compares expression profiles and ranks genes according to their relative similarity in behaviour. *PPQ1* and one hundred genes so identified with similar expression profiles were analysed for GO term enrichment (a function available in SPELL). The highest scoring biological processes were: cellular cell wall organization or biogenesis, regulation of localization, fungal-type cell wall organization or biogenesis and biological regulation. For a group of 20 genes with the most similar expression profiles, the following processes are listed: glycosphingolipid biosynthetic, glycolipid metabolic, glycolipid biosynthetic, glycosphingolipid metabolic and metabolic process. The conclusion is that Ppq1p might function within or affect membrane or cell wall synthesis processes.

4.2.7 Predicting cellular processes Ppq1p affects from interactions

4.2.7.1 Physical and genetic interactions (BioGrid)

Data on physical and genetic interactions involving Ppq1p/*PPQ1* were retrieved from BioGrid (2011-07; http://thebiogrid.org/; Stark *et al.*, 2010) that lists 38 interactions, 4 of which are physical (*SDS22, YPI1, BZZ1, HEK2*). Other depositories (e.g. DryGin, BioPixie, etc) were also interrogated, but the overlap of proposed interactions for different databases was very low. Poor overlap and continuous change in lists of interacting genes within databases made use of more than one database impractical and therefore only the BioGrid database was used. Entering 38 genes and *PPQ1* into the SGD Gene Ontology Slim Mapper, a tool that maps annotations of groups of genes (www.yeastgenome.org/cgi-bin/GO /goSlimMapper.pl), returned a list of processes and components for this group of annotated genes. The list of highest scoring processes/components is given in Table 4.4 where processes/components are ranked according to enrichment; ratio of percentage of genes on the *PPQ1*-interacting genes list annotated with this term to percentage of all genes with the same annotation in the genome. For example, 17.9% of the genes that interact with *PPQ1* have been annotated as "Chromosome segregation" while only 2.1% of all the genes in *S. cerevisiae* have this annotation i.e. an 8.5-fold difference.

This approach did not identify protein synthesis as one of the processes that Ppq1p may be linked to. Rather, the majority of highest scoring processes and components indicated an involvement with various cytoskeleton-dependent processes.

Table 4.4: A list of processes and components that *PPQ1* and interacting genes cluster to.

Process - GO term	List/WG	Component - GO term	List/WG
Chromosome segregation	8.5	Microtubule organizing c.	6.4
Nucleus organization	5.7	Chromosome	4.3
Meiosis	5.1	Cytoskeleton	3.9
Pseudohyphal growth	5.1	Vacuole	2.2
Cytoskeleton organization	4.4	Site of polarized growth	2.1
Conjugation	4.1	Nucleus	1.9
Chromosome organization	4.0	Golgi apparatus	1.8

Cell cycle	3.1	Cellular bud	1.8
Protein modification process	3.0	Cytoplasm	0.9
Transcription, DNA-dependent	2.6	Membrane	0.5
Cellular carbohydrate metabolic process	2.5		
Vacuole organization	2.4		
Generation of precursor metabolites, energy	2.0		
Response to chemical stimulus	1.9		
Response to stress	1.9		
RNA metabolic process	1.9		
DNA metabolic process	1.6		

Footnote: GO terms are ranked according to fold difference that *PPQ1*-interacting genes present in each GO term compared to background of all *S. cerevisiae* genes

4.2.7.2 Fitness (FitDb) interaction networks

A different approach to exploring the possible cellular role(s) of Ppq1p is to identify phenotypes of a strain with the *PPQ1* gene deleted and look for gene deletions that result in similar phenotypes. Such a study was done by Hillenmeyer *et al.* (2008) where sensitivity to a variety of small molecules and conditions was systematically explored for whole-genome homozygous and heterozygous deletion collections. A depository at fitdb.stanford.edu also lists "co-fitness interactions", where gene deletion strains are ranked according to phenotypic similarity to a gene of interest.

Comparing results from homozygous and heterozygous collections showed that neither the conditions that *ppq1Δ* strains were sensitive to nor the lists of co-fitness interacting genes overlap between the two collections (Table 4.5 and Figure 4.6). This could be due to one of two possibilities: Ppq1p levels in heterozygous deletion might be sufficient for cellular processes in some but not all conditions, thus the effect is seen in only some of the conditions that processes involving Ppq1p are involved in. Alternatively, cells of the two strains compensate for single or double gene deletion by upregulation of different pathways. If the first hypothesis were true, the list of conditions a *PPQ1/ppq1Δ* heterozygous strain is sensitive to should form a subset in the list of conditions for *ppq1Δ/ ppq1Δ* homozygous gene deletion strain and same conditions would be expected to rank

high on both lists. This is not the case, but results are confounded by the fact that conditions tested for in the two collections do not overlap completely.

Table 4.5: List of conditions that cause highest fitness defect in homozygous and heterozygous *PPQ1* deletion strains.

Homozygous deletion /condition	Fitness Defect	Heterozygous deletion /condition	Fitness Defect
$MnCl_2$	20.0	clotrimazole	9.2
$CoCl_2$	16.0	5-fluorocytosine	5.0
$MnCl_2$	15.8	fluconazole	4.7
$MnCl_2$	13.4	latrunculin	4.2
$ZnCl_2$	13.3	bufexamac	4.1
$K_2Cr_2O_7$	13.1	bufexamac	4.0
LiCl	12.5	sulconazole nitrate	3.8
1,3-diallylurea	10.5	anisomycin	3.6
synthetic minimal media	8.7	latrunculin	3.5
sodium fluoride	8.7	latrunculin	3.5
sodium fluoride	8.2	methotrexate	3.4
synthetic minimal media	7.8	fluconazole	3.3
latrunculin	7.5	miconazole	3.2
synthetic minimal media	7.2	miconazole	3.2
rapamycin	7.0	lapachol	3.1
hydroxyurea	5.5	$CoCl_2$	3.0
rapamycin	5.4	LiCl	2.9
sorbitol	5.4	5-fluorocytosine	2.7
sorbitol	5.2	Bps	2.7
rapamycin	5.0	econazole nitrate	2.6

The two lists were thus analysed separately. Selection of co-fitness interacting genes i.e. genes with a high fitness correlation, was achieved by selecting 10 genes with highest co-fitness interaction score with *PPQ1* deletion and then selecting the top 10 co-fitness interacting genes for each of these. A list of selected genes and their phenotypic interactions was imported into Cytoscape (Shannon *et al.*, 2003) where a 'circular layout' option was used to visualise genes that cluster together (Figure 4.7). These core genes where then input in Gene Ontology Slim Mapper (http://www.yeastgenome.org/cgi-bin/GO/goSlim Mapper.pl) and the results ranked in terms of processes/components that have proportionally more genes assigned to from the list than would be from the whole genome (Table 4.6).

Homozygous co-fitness interactions   Heterozygous co-fitness interactions
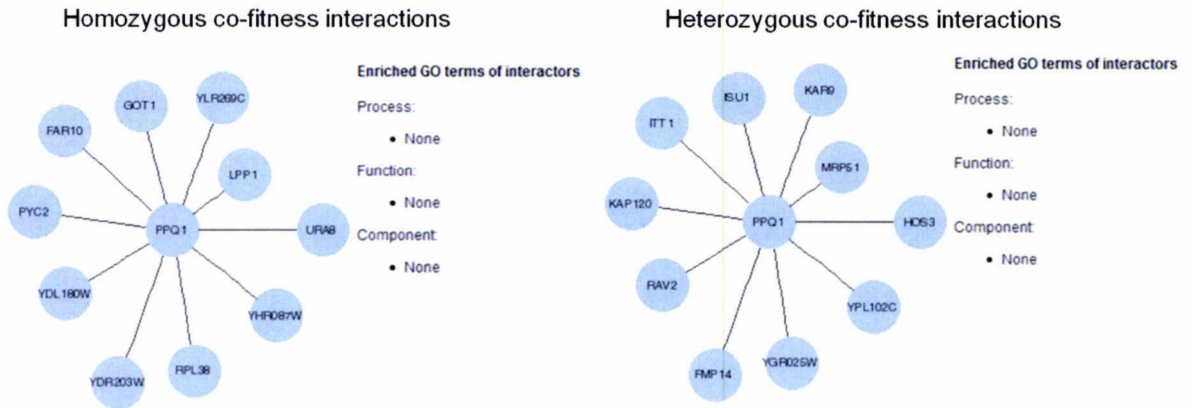
Figure 4.6: List of gene deletion strains that had similar fitness defect profile (FitDb). There is no overlap between lists for homozygous and heterozygous deletion collections.

Highest scoring processes and components for homozygous deletion suggest that *PPQ1* co-fitness interacting genes are involved in membrane-related processes. Heterozygous strains implicate various processes including mitochondria-related ones.
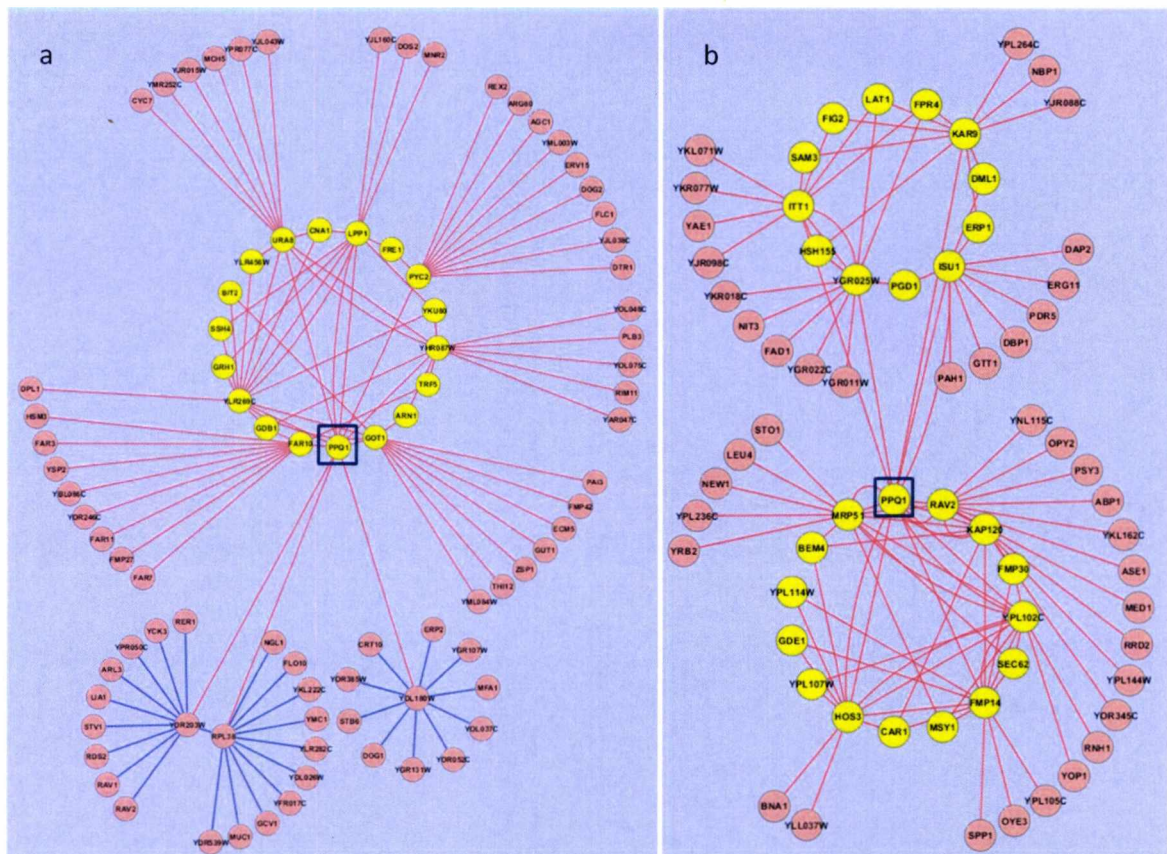
Figure 4.7: Representation of 1st and 2nd degree *PPQ1* co-fitness interactions with "circular" layout in Cytoscape – homozygous (a) and heterozygous (b) deletion collections. Some genes have more than one interaction and are clustered together as

"core" genes (yellow); only core genes were used in further analysis; *PPQ1* is highlighted in blue box.

Table 4.6: Slim Mapper Process and Component results for co-fitness interaction core genes in homo- and heterozygous collections

Homozygous deletion			
Process - GO term	**List/WG**	**Component - GO term**	**List/WG**
Conjugation	5.8	Cytoplasmic membrane-bounded vesicle	9.8
Cellular homeostasis	4.8	Golgi apparatus	3.8
Cellular lipid metabolic process	3.2	Plasma membrane	2.5
Vesicle-mediated transport	2.9	Endomembrane system	2.1
Cellular carbohydrate metabolic proc	2.6	Endoplasmic reticulum	1.9
Response to chemical stimulus	2.2	Membrane	1.5
Transport	1.7	Cellular component unknown	1.3
RNA metabolic process	1.2	Cytoplasm	1.0
Transcription	1.1	Nucleus	0.5

Heterozygous deletion			
Process - GO term	**List/WG**	**Component - GO term**	**List/WG**
Cellular homeostasis	3.2	Site of polarized growth	3.2
Cellular a. a. and derivative metabolic proc.	2.8	Mitochondrion	1.9
Cofactor metabolic process	2.7	Endomembrane system	1.4
Mitochondrion organization	2.3	Ribosome	1.3
Cellular lipid metabolic process	2.1	Cellular component unknown	1.2
Translation	1.3	Cytoplasm	1.1
Protein modification process	1.3	Nucleus	0.8
Chromosome organization	1.2	Membrane	0.6
RNA metabolic process	1.2		
Transcription	1.1		

Transport	1.1
Biological process unknown	0.9

Analysis of the Ppq1p sequence and the available data from various databases showed that: both domains of Ppq1p are conserved within *S. cerevisiae* strains, but the N-domain is less so within fungi. A conserved feature of N-domain is its Ser bias and the N-domain is predicted to be phosphorylated and possibly palmitoylated. Analysis of data from different databases clusters placed Ppq1p in several processes: cytoskeleton related processes, nucleus/chromosome organisation, membrane related processes, cellular homeostasis, and mitochondria related processes. mRNA translation was only identified in fitness database heterologous deletion list.

4.3   *PPQ1* deletion phenotypes

The initial objective was to see if the phenotypes previously reported by Chen *et al.* (1993) and Vincent *et al.* (1994) associated with a *ppq1Δ* in different genetic backgrounds could be replicated, and then subsequently to test the hypotheses generated in previous section i.e. that Ppq1p/*ppq1Δ* affects different aspects of mRNA translation, growth rate, sensitivity to manganese, effect on cell wall/cellular membranes, involvement in TORC1 pathway, effect on mitochondria. The strains used in this study were 74-D694 *ppq1Δ::LoxP* and BY4741 *ppq1Δ::KanMX* together with their respective wild type parental strains.

4.3.1 Effect of *PPQ1* deletion on translation

4.3.1.1 Translation elongation

The *ppq1Δ* strain (AY925) was shown (Chen *et al.*, 1993) to have a reduced rate of translation. Furthermore, it has been proposed that Ppq1p affects mRNA translation accuracy by presumably controlling phosphorylation levels of unknown target(s) (Chen *et al.*, 1993). Strain-specific effects were evident in earlier studies; for example, Chen *et al.* (1993) reported sensitivity of *ppq1Δ* strain to cycloheximide and G418, while Song *et al.* (1987) did not observe such sensitivity in *sal6-1* mutant. To evaluate whether or not a translation defect was created by the *ppq1Δ* in the 74D-694 strain background, a dual-luciferase plasmid-based reporter system was used to test whether *PPQ1* deletion affects

translational accuracy and to confirm the effect on rate of translation. Each reporter plasmid carries an insert of two linked in-frame luciferase coding sequence, Renilla and Firefly. Codon changes or other sequences are inserted in either the intergenic linker or the second luciferase coding sequence and the effects of such changes are measured by comparing luminescence of each of luciferases (see methods sections 2.2 and 2.8). Each of the following experiments was carried out with six independent transformants. In the subsequent analysis an outlier was excluded from the data set and the remaining five samples analysed using a T-test to assess the significance of the results (T-test: 1 tail, equal variance; F-test for unequal variance was p>0.05 for all experiments).

The rate of translation was measured using a plasmid where the second (i.e. downstream of the linker) luciferase (Firefly) coding sequence contained a string of rare codons (Figure 4.8, labelled as MIN). Translation would be predicted to slow down at rare codons because of lower levels of the cognate tRNAs in the cell that decode them. This analysis revealed that the rate of translation in the $ppq1\Delta$ strain was reduced by 40% compared to wt $PPQ1^+$ strain.
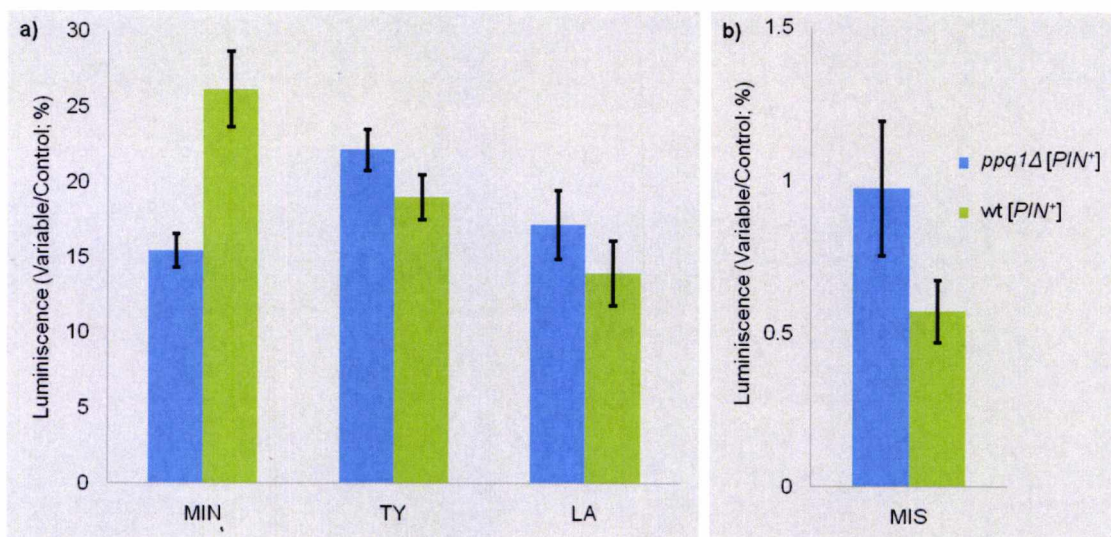
Figure 4.8: The effect of *PPQ1* deletion on rate and accuracy of translation elongation. 74-D694 wt and $ppq1\Delta$ strains were transformed with dual-luciferase plasmids and luminescence of cultures in log phase was recorded; a) MIN – rate of translation in firefly with a string of rare codons; TY – +1 frameshift sequence is inserted in the linker between Renilla and Firefly luciferases; LA – -1 frameshift sequence is inserted in the linker; b) MIS - H245R in Firefly. Amino acid missincorporation is required for a functional luciferase; all experiments show a statistically significant difference between wild-type and $ppq1\Delta$ strains with p< 0.001, 0.01, 0.05 and 0.01 respectively.

The accuracy of translation elongation was also reduced in the $ppq1\Delta$ strain. Translational accuracy was measured using plasmids with the Ty1 transposon +1 frameshift or L-A

dsRNA virus -1 frameshift sequence inserted into a linker between the two luciferase coding sequences or by using a plasmid with an His245Arg substitution in the Firefly luciferase (Methods Figure 2.2). In the case of the frameshift sequences, the Renilla and Firefly luciferase genes are out-of-frame and a ribosomal frameshift is required for functional Firefly luciferase to be generated. The assay for amino acid missincorporation was based on the ability of the cell to generate a functional luciferase from the inactive H245R mutant through mistranslation of the mutated codon. Levels of frameshift as measured by changes in luminescence were slightly, but statistically significantly increased in the *ppq1Δ* strain; for example, 17% increase in the +1 and 23% increase in the -1 frameshift events (Figure 4.8). This level is significantly lower than previously reported i.e. 2-fold increase for +1 frameshift in the *ppq1Δ* strain (Burck *et al.*, 1999). A decrease in accuracy of translation in the *ppq1Δ* strain was more evident in the case of amino acid missincorporation where there was a 70% increase in the luminescence compared to the wt control (Figure 4.8).

4.3.1.2 Translation termination

To evaluate whether a *ppq1Δ* deletion results in a defect in translation termination, nonsense suppression was measured using the dual-luciferase assay system in which one or other of the three stop codons is inserted in the intergenic linker between the Renilla and Firefly luciferase genes. In the constructs used (Methods, Figure 2.2) all stop codons had a C at position +4, a nucleotide context that increases stop codon readthrough significantly at all three stop codons (Namy *et al.*, 2001).

Twelve samples were tested for each transformant and 3 outliers excluded from the subsequent data analysis. The strains used were 74D-694 wt and a *ppq1Δ* derivative strain that was either [*PIN*$^+$] or [*pin$^-$*]. The effect of the [*PIN*$^+$] prion on termination accuracy was tested because it was noticed that colonies of *ppq1Δ* [*pin$^-$*] strain differed in colour from colonies of the other strains after prolonged incubation on ¼ YEPD plates (data not shown). In these assays nonsense suppression was expressed as a ratio of *ppq1Δ* to wt strain readthrough for each stop codon.

Deletion of *PPQ1* gene increased nonsense suppression at all three codons by almost two-fold compared to the wt *PPQ1*$^+$ strain (Figure 4.9). This finding matches the findings reported by others where a two-fold increase in growth rate for *sal6-1* in *sup45-2* background was observed (Song *et al.*, 1987). The growth rate difference observed in these tests is a consequence of different levels of functional marker proteins and therefore

reflects the level of suppression of nonsense mutations. In spite of the observed colony colour difference, the [*PIN*+] prion did not appear to alter the efficiency of termination in a *ppq1Δ* background.
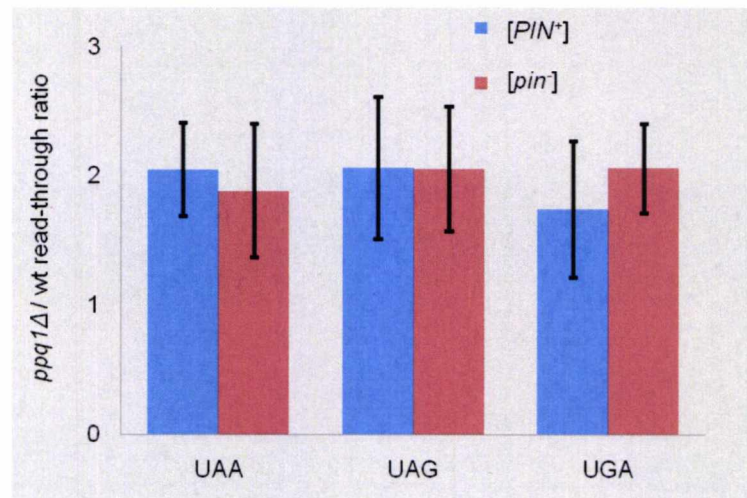
Figure 4.9: *PPQ1* deletion increases nonsense suppression. Stop codon readthrough was measured in four strains: 74D-694 wt / *ppq1Δ* and [*PIN*+] / [*pin*-]. Strains were transformed with plasmids carrying linked Renilla and Firefly luciferases that had one of the three stop codons inserted in the linker between two genes. Luminescence was measured in log phase and is expressed as ratio of luminescence in *PPQ1* deletion strain to wild-type strain. Nonsense suppression was increased two-fold at all codons.

4.3.1.3 Stop codon readthrough in presence of [*PSI*+]

Song *et al. (*1987) did not observe any differences in growth rates when comparing a *sal6-1* strain vs the parental wt strain carrying the same [*PSI*+] variant indicating that *sal6-1* mutation did not increase nonsense suppression caused by the [*PSI*+] prion. To confirm this a *ppq1Δ* strain with a [*PSI*+] strong variant was isolated in spontaneous *de novo* [*PSI*+] formation experiments (see chapter 3 section 3.3.2) and was transformed with the dual-luciferase stop codon plasmids and the levels of nonsense suppression in this strain compared to the levels in the *PPQ1* parent strain also carrying a strong variant of [*PSI*+]. It should be stressed that it is possible that although both were 'strong' [*PSI*+] variants, they may not necessarily be the same.

The levels of suppression of the ochre codon mutation (UAA) were slightly higher (17%) in a *ppq1Δ* [*PSI*+] strain compared to its wt counterpart (T-test: 2 tail, equal variance: $p < 0.001$; F-test: $p > 0.05$). The two strains did not differ in the levels of suppression of the amber codon, while suppression of opal (UGA) codon was significantly higher in the wt strain (T-test: 2 tail, equal variance: $p < 0.001$; F-test: $p > 0.05$) suggesting an

antisuppression phenotype linked to the *ppq1Δ* deletion Both strains had higher rate of stop codon readthrough compared to a *ppq1Δ* [*psi⁻*] strain; 3-fold for ochre and amber codons and 7-fold higher (*ppq1Δ*) or 13-fold higher (wt) for the opal codon (Figure 4.10).
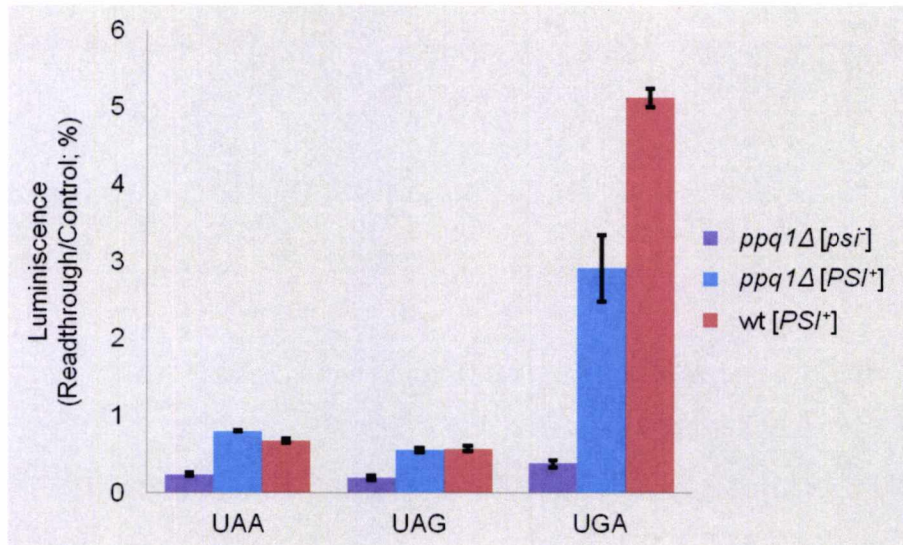
Figure 4.10: *PPQ1* deletion modulates nonsense suppression in [*PSI⁺*] background. Stop codon readthrough was measured in three strains: 74D-694 wt / *ppq1Δ* [*PSI⁺*] and *ppq1Δ* [*psi⁻*]. Strains were transformed with plasmids carrying linked Renilla and Firefly luciferases that had one of the three stop codons inserted in the linker between two genes. Luminescence was measured in log phase cells.

These results confirm previous observations that mutation of the *PPQ1* gene affects different aspects of translation; reduces the rate of translation and decreases the accuracy of both translation elongation and termination.

4.3.2 Growth rate of *ppq1Δ* strains

Chen *et al.* (1993) reported that deletion of *PPQ1* reduced the rate of growth in rich medium and on various carbon sources, while Song *et al.* (1987) and Vincent *et al.* (1994) did not report such an effect (see Table 4.1). In this section some of the reported phenotypes were reassessed in a BY4741 genetic background and two additional gene deletions were also tested.

Throughout this analysis the BY4741 wt and *ppq1Δ* strains were used. In the latter strain the *PPQ1* gene was replaced by the *kanMX* selection marker (see Methods, section 2.1) and the deletion was confirmed by PCR (Figure 4.11a).

4.3.2.1 Growth in log and stationary phase

Growth of the wt and *ppq1Δ* strains in YEPD medium was measured in 24 well microplates (1ml per well; methods section 2.4.1). While the rate of logarithmic growth was similar between the strains, the *ppq1Δ* strain grew significantly slower in early stationary phase i.e. the phase after diauxic shift which occurred between 10 and 12h (Figure 4.11b). Slow growth in stationary phase could indicate that the *ppq1Δ* strain failed to enter diauxic shift or that it cannot utilise non-fermentative carbon sources.

4.3.2.2 Growth rate on different carbon sources

Chen *et al.* (1993) reported a slow growth phenotype for their *PPQ1* deletion strain on a variety of carbon sources, while Vincent *et al.* (1994) only reported a slight defect upon growth in a rich glycerol-based medium. One explanation for the strong phenotype observed in Figure 4.11b in stationary phase for the *ppq1Δ* strain is that this strain is unable to metabolise non-fermentative carbon sources. Growth was therefore compared in media with a variety of different fermentative and non-fermentative carbon sources. An *rnq1Δ* derivative of BY4741 was included in this growth analysis because deletion of the *RNQ1* gene was shown to affect the levels of mitochondria related proteins (G.L.Staniforth, personal communication).
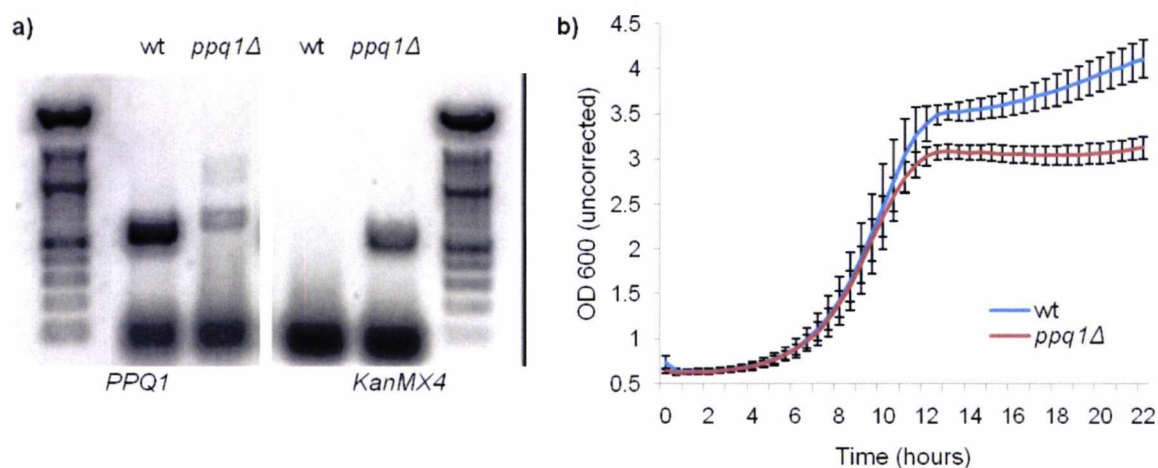
Figure 4.11: Confirmation of *PPQ1* gene deletion in BY4741 strain and growth of this strain in rich medium. a) strain from gene deletion collection has *PPQ1* gene replaced with KanMX cassette. Deletion was confirmed using primer that primes upstream of *PPQ1* ORF and either a primer that primes within *PPQ1* gene (left) or a primer that aligns to *KanMX* sequence (right); b) comparison of growth of wt and *ppq1Δ* strains. Error bars represent standard deviation.

Growth rates of the *ppq1Δ*, the *rnq1Δ* and the parent wt strains were measured during log phase growth and are presented as time required for a culture to double in Figure 4.12. No significant differences were observed between the *ppq1Δ*, the *rnq1Δ* strain and wt strains on any carbon source.

4.3.2.3 Deletion of *PPQ1* gene in *ppz1Δ* and *nrg1Δ* background

The Ppz1p and Ppq1p proteins share several structural and functional characteristics, including their effect on protein synthesis (see Table 4.1) where they have the opposite effect on accuracy of translation, whereas both deletions decrease the efficiency of translation termination (see Table 4.1). No genetic interaction has previously been reported between the two genes.

Nrg1p is a transcriptional repressor and is involved in glucose repression, but it also negatively regulates filamentous growth, which is significantly increased in a *ppq1Δ* strain (see Table 4.1). *NRG1* is also reported to have a positive genetic interaction with *PPQ1* (Costanzo *et al.*, 2010; from BioGrid).
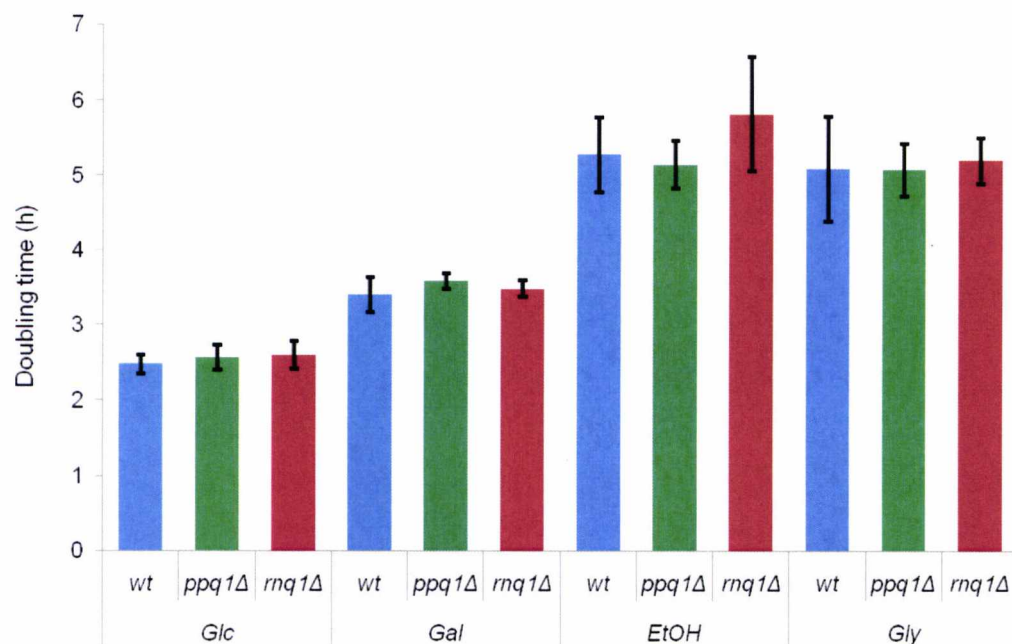
Figure 4.12: growth of wt, *ppq1Δ* and *rnq1Δ* strains on fermentative and non-fermentative carbon sources. Glc – 2% glucose, Gal – 2% galactose, EtOH – 2% ethanol and Gly - 2% glycerol.

The *PPQ1* gene was deleted from two gene deletion collection strains carrying either an *NRG1* or *PPZ1* gene deletion. The *PPQ1* gene was replaced with a deletion cassette carrying *URA3* marker as described in Methods, section 2.5.7. One colony was tested for each gene deletion using PCR per strain (Figure 4.13) and used in growth rate experiments.

4.3.2.4 Growth rate of double gene deletion strains

Deletion of the *PPZ1* gene had no observable effect on growth in rich medium at any phase of a batch culture compared to the wt (Figure 4.14a). A *ppq1Δ* strain grew slightly slower in the log phase than wt, but this difference was within the standard deviation of the replicates. Early stationary phase growth was significantly slower in a *ppq1Δ* strain as shown previously (Figure 4.11). Although the *ppz1Δ ppq1Δ* strain grew slightly slower in log phase compared to the wt strain, the difference was not significant whereas the double deletion strain grew significantly better in the early stationary phase and also underwent diauxic shift at higher cell density (Figure 4.14a). Similarly, the deletion of the *NRG1* gene did not have a significant effect on growth whereas the *nrg1Δ ppq1Δ* double mutant grew significantly slower in all phases (Figure 4.14b).
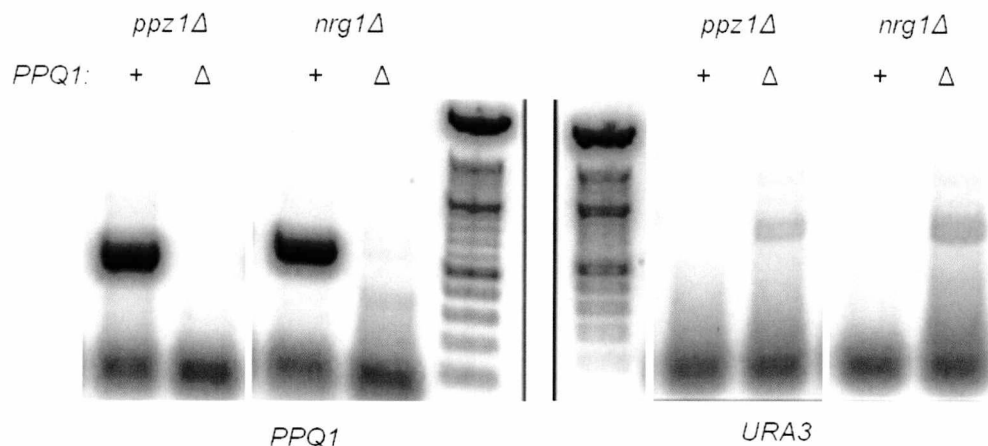
Figure 4.13: Confirmation of *PPQ1* gene deletion in BY4741 strain in *ppz1Δ* and *nrg1Δ* background. Deletion was confirmed using primer that primes upstream of *PPQ1* ORF and either a primer that primes within *PPQ1* gene (left) or a primer that aligns to *URA3* sequence (right); +: *PPQ1*, Δ: *ppq1Δ*.

The phenotype observed in *nrg1Δ ppq1Δ* double mutant is at odds with a previous report that *PPQ1* and *NRG1* exhibit a positive genetic interaction (Constanzo *et al.*, 2010; from BioGrid). The *ppz1Δ ppq1Δ* double mutant exhibited a positive genetic interaction indicating that Ppq1p and Ppz1p may have opposing functions during stationary phase.
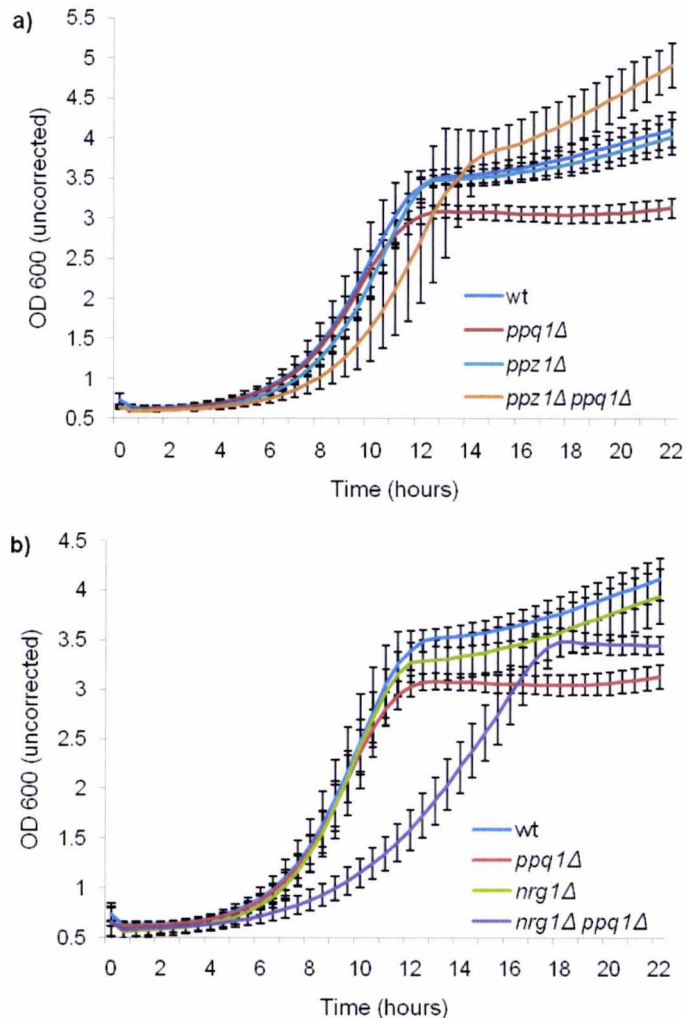
Figure 4.14: Effects of single and double gene deletions of *PPQ1* and *PPZ1* or *NRG1* genes on growth in log and stationary phases. Cells were grown from low density for 22h in YEPD medium on 24 well microplates at 30°C.

4.3.3 Sensitivity of *ppq1Δ* strain to various chemicals

4.3.3.1 Sensitivity to MnCl$_2$

Hillenmeyer *et al.* (2008) conducted a screen of a whole-genome deletion collection for sensitivity of each knockout strain to various small molecules. Conditions were ranked for each gene deletion strain according to a fitness defect they caused in that strain. The condition that caused the largest fitness defect in a homozygous *PPQ1* deletion strain was

the addition of manganese (Table 4.5). Manganese has a variety of effects on the cell, but at high concentrations it can also induce filamentous growth (Asleson *et al.*, 2000) a phenotype also identified in a *ppq1Δ* strain by Jin *et al.* (2008; Table 4.1). Also the transcription factor Ste12p, confirmed to bind upstream of the *PPQ1* ORF (Lefrancois *et al.*, 2009; Zheng *et al.*, 2010) also regulates filamentous growth and invasivity (Table 4.3; Roberts *et al.*, 1994). The sensitivity of the *ppq1Δ* strain to manganese was replicated in both YEPD broth and solid YEPD medium with the growth of the BY4741*ppq1Δ* mutant being inhibited in $MnCl_2$ supplemented medium. However, this was not observed with the 74-D694 *ppq1Δ* strain within the range of concentrations used (Figure 4.15a).
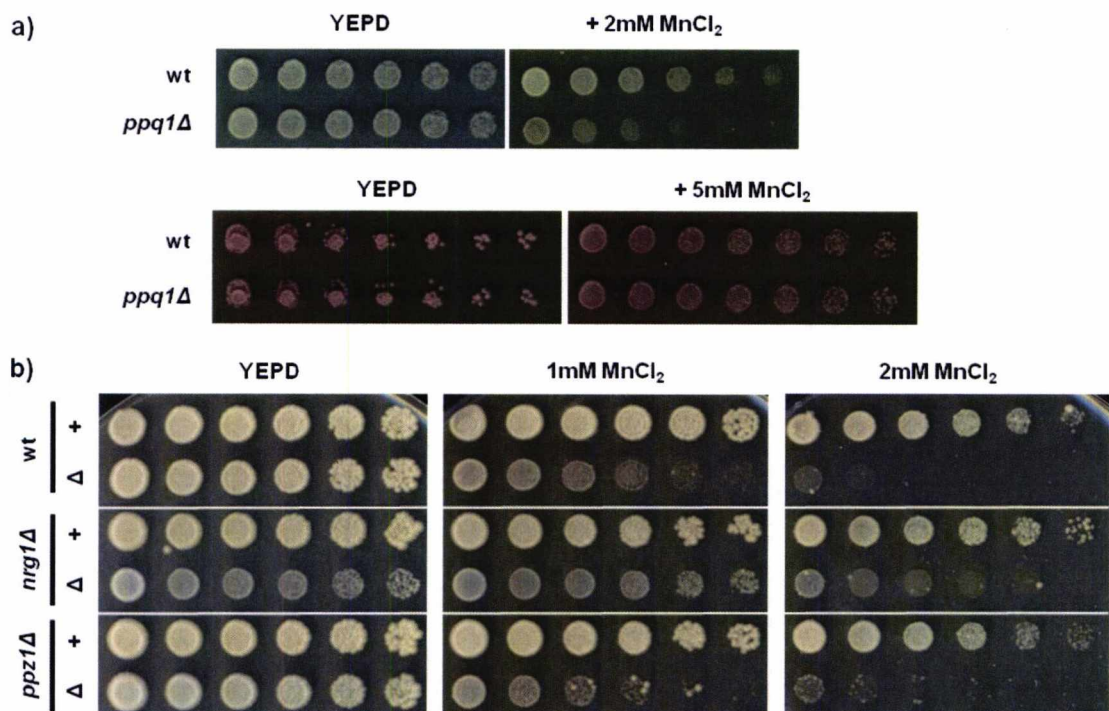
Figure 4.15: Sensitivity of *ppq1Δ* strain to manganese. a) *ppq1Δ* is sensitive to $MnCl_2$ in BY4741 background, but sensitivity was not observed in 74-D694 strain within concentrations tested; b) sensitivity to manganese was also observed in double deletion strains as shown.

4.3.3.2 Comparison of *ppq1Δ* segregation and sensitivity to $MnCl_2$

Co-segregation of *ppq1Δ* and sensitivity to manganese was tested by crossing BY4741 *ppq1Δ::kanMX* to a BY4742 *PPQ1⁺* strain. To select for diploid cells the following strategy was used: the BY4741 *ppq1Δ::kanMX* mutant strain was grown on a plate in presence of 0.5μg/ml ethidium bromide to induce loss of mitochondria. The so-treated cells were plated onto YEPD and then their petite phenotype confirmed by their inability to grow on

glycerol-based medium (YEPG). One such [*rho*] petite strain was crossed to respiratory competent [*RHO*⁺] BY4742 strain which has the opposite mating type and the resulting diploid cells were selected by their ability to grow on glycerol medium and their resistance to G418 (due to the *ppq1Δ::kanMX* allele which is partially dominant). The resulting diploid strain BY4743 was induced to sporulate and a number of asci were dissected by micromanipulation. The segregation of the *ppq1Δ::kanMX* and *PPQ1* alleles in tetrads was monitored by the G418 resistance phenotype. Three complete tetrads were isolated although subsequent analysis of one of these tetrads (tetrad III) proved that the spores were most likely not from the same ascus (Figure 4.16 and data not shown).

Since only two complete and verified tetrads were obtained, all spores were used (i.e. including those from incomplete tetrads) to test for sensitivity to manganese (Figure 4.17). Sensitivity of spores to manganese did not show absolute correlation with the *ppq1Δ::kanMX* marker although the majority (10 out of 13, 77%) of the *ppq1Δ* spores were sensitive to $MnCl_2$, while majority of wt were not (i.e. 10 out of 11). This would suggest that one or more additional alleles in this genetic background may modulate this sensitivity.
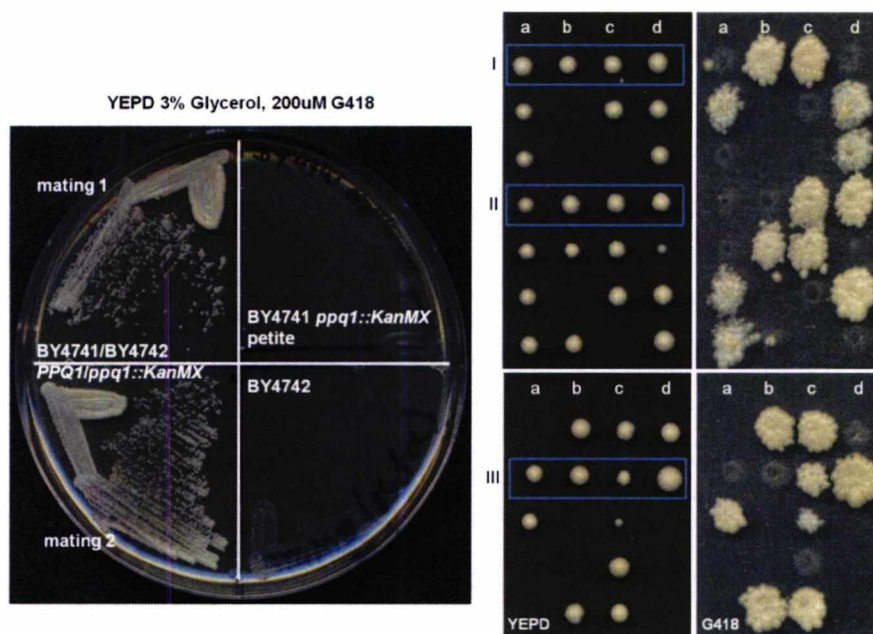
Figure 4.16: Crossing BY4741 *ppq1Δ::KanMX* and BY4742. Left: strategy for selection of diplods. G418 resistant petite BY4741 colony was crossed with respiratory competent BY4742 strain; right: tetrad dissection and selection on G418 medium to follow KanMX marker segregation. Full tetrads are indicated by the blue boxes.

The *PPZ1* and NRG1 genes were also deleted in the BY4741 background and both double deletion (*ppz1Δ ppq1Δ*, *nrg1Δ ppq1Δ*) strains showed sensitivity to manganese that was comparable to the original BY4741 *ppq1Δ* strain (see Figure 4.15). It is therefore likely that additional alleles that affect sensitivity to manganese were present only in the BY4742 strain although this was not tested due to the lack of availability of a *ppq1Δ* derivative of BY4742. Thus while it can be concluded that sensitivity to manganese is a *ppq1Δ* – associated phenotype, it is also evident that there are as yet undefined genetic modifiers that may influence this phenotype.
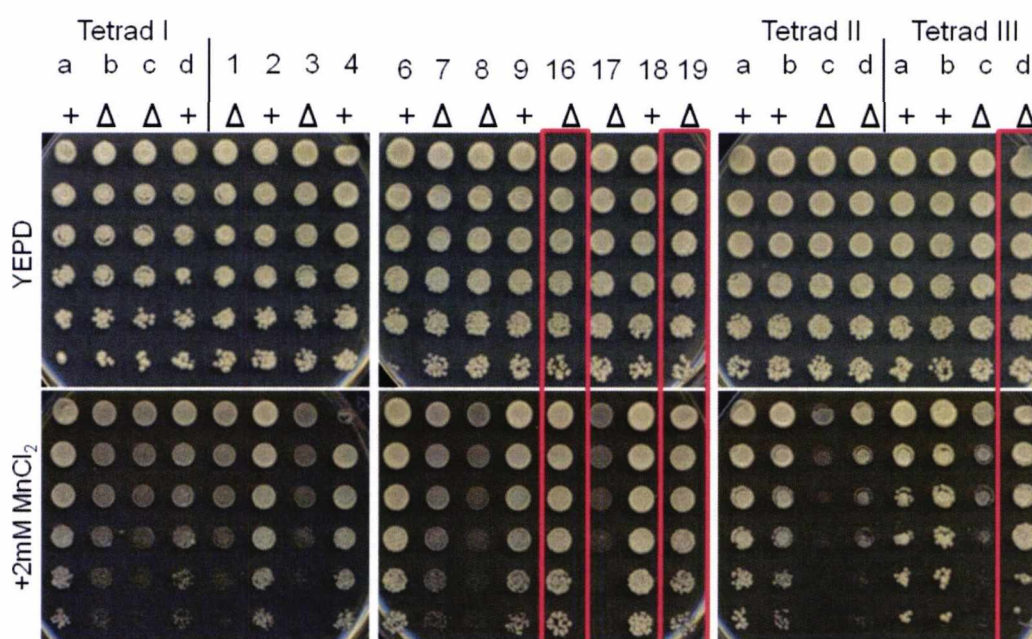
Figure 4.17: Sensitivity of wt and *ppq1Δ* spores to MnCl₂. Marker segregation only partially coincides with sensitivity to MnCl₂, although majority of *ppq1Δ* spores are somewhat sensitive to manganese. Spores that show resistance comparable to wt spores are indicated with red squares; +: *PPQ1⁺* and Δ: *ppq1Δ*.

4.3.3.2 Sensitivity to SDS

A comparison of gene expression profiles in the SPELL database (see section 4.2.6) listed several processes related to glycolipids and cell walls as the GO terms that selection of genes with similar gene expression pattern clustered to. Mutants with defects in cell wall or plasma membrane are more sensitive to SDS, an anionic detergent. Although Chen *et al.* (1993) reported that their *ppq1Δ* strain was not sensitive to SDS it was here investigated whether this phenotype was also dependent on the strain background. SDS also induces mitochondrial petites and the experiments were carried out on agar plates with glycerol as sole carbon source to select for respiratory competent

cells. The *ppq1Δ* strain was not more sensitive to SDS than wt in the BY4741 background (Figure 4.18).

4.3.3.3 Sensitivity to rapamycin

One of chemical agents the homozygous *ppq1Δ/ppq1Δ* deletion strain was reported to be sensitive to was rapamycin (FitDb). This phenotype is interesting because *TOR1* is also listed as one of the genes that functionally interacts with the *PPQ1* gene (BioGrid). Tor1p is a protein kinase inhibited by rapamycin and is a subunit of the TORC1 complex that controls growth in response to environmental stimuli.
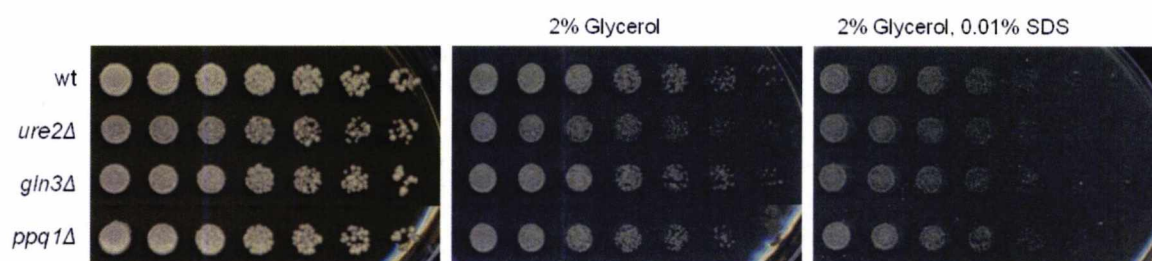
Figure 4.18: *PPQ1* deletion does not affect sensitivity to the cellular membrane disrupting agent SDS. Overnight cultures of the strains indicated (BY4741) were diluted to the same density and spotted (5μl) on YEPD, glycerol and glycerol + 0.01% (w/v) SDS plates.

To confirm the sensitivity to rapamycin phenotype in the BY4741 haploid strain, the strains were grown on YEPD solid medium with 25nM rapamycin using *ure2Δ* and *gln3Δ* strains as controls. Gln3p is a transcriptional activator and the deletion of *GLN3* gene induces resistance to rapamycin, while Ure2p is an inhibitor of Gln3p and deletion of *URE2* gene increases sensitivity to rapamycin (Cardenas *et al.,* 1999). In the BY4741 background the sensitivity of the *ppq1Δ* mutant to rapamycin was similar to that of the wt strain (Figure 4.19).

Results presented in this section agree with previously reported effect of the *PPQ1* deletion on mRNA translation. The *ppq1Δ* strains were also found to be sensitive to manganese, a chemical with various effects on cells, including induction of filamentous growth and loss of mitochondria (see below). Growth of *ppq1Δ* mutant was significantly slower in stationary phase, but these cells could grow on non-fermentable carbon sources

at rates comparable to the wt strain. Contrary to previous reports, the *ppq1Δ* strain was not sensitive to rapamycin at least in the BY4741 genetic background nor was the *ppq1Δ* strain sensitive to SDS indicating that cell wall and plasma membrane are not affected in this strain.
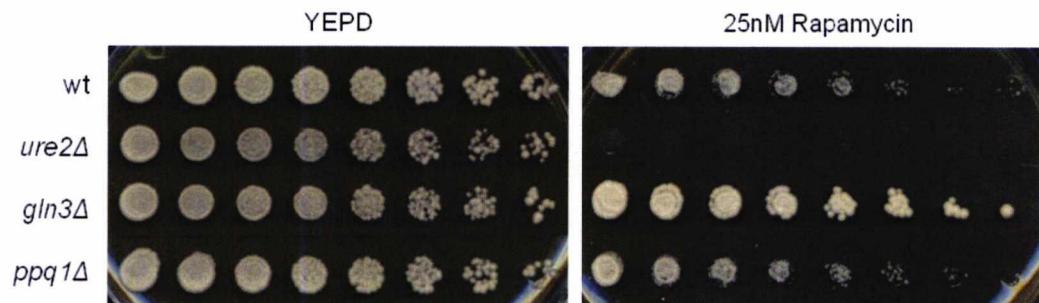
Figure 4.19: *ppq1Δ* strain is not sensitive to rapamycin. Overnight cultures were diluted to the same density and spotted (5µl) as a serial dilution on YEPD and YEPD + 25nm rapamycin. The *ure2Δ* strain was used as a rapamycin sensitive control and the *gln3Δ* strain as a rapamycin resistant control.

4.4   Distribution of Ppq1 protein in a cell

In chapter 3 it was shown that deletion of the *PPQ1* gene increased the rate of *de novo* [*PSI⁺*] formation, confirming similar findings reported by Tyedmers *et al.* (2008), but the mechanism of suppression of prion formation by Ppq1p is not understood. One possibility is that N-domain of Ppq1p has a role in promoting Sup35p aggregation since this domain has a skewed amino acid composition with a strong bias towards Ser and Asn residues. Prion domains are typically Asn rich and Asn residues have been predicted to be more important than Gln residues for propagation of prions (Alberti *et al.*, 2009; Halfmann *et al.*, 2011). On the other hand, the predicted tertiary structure of the N-domain of Ppq1p (Figure 4.4) shows a relatively folded domain with several alpha-helices, while prion domains are typically unfolded.

In the following section I describe experiments aimed at identifying the subcellular distribution of Ppq1p by means of microscopy looking in particular whether the N-domain plays a role in the sub-cellular distribution of the protein. The hypotheseis being tested were (a) that Ppq1p is not strictly diffuse within cytoplasm and (b) that the N-domain of the phosphatase influences its distribution and (c) possibly promotes aggregation of Ppq1p.

4.4.1 Engineering new tagged alleles of Ppq1p

In order to probe Ppq1p localisation within a cell, new constructs with fluorescent protein tagged to *PPQ1* gene were created. Creation of tags was necessary because an anti-Ppq1p antibody is not available. Oligonucleotide primers that align to the both ends of *PPQ1* gene (excluding the stop codon) and to the end of N-domain (at position 705) of the gene were designed and synthesised (MWG Eurofins Operon; see Table 4.7) These primers were used to PCR-amplify the *PPQ1* gene including its N-domain from the 74-D694 strain and the amplification confirmed by agarose gel electrophoresis (Figure 4.20). A *PPQ1** entry vector (pDONR221; * indicates that a stop codon was included) was obtained from PlasmID (plasmid.med.harvard.edu/PLASMID/).

Table 4.7: Primers used in construction of *PPQ1* and *PPQ1N* Gateway entry vectors

Primer	Sequence (5' – 3')
PPQ1 (gateway) F	caccATGAGAAGAAGCCCGT
PPQ1 (gateway) R	CACTTTGGTTTTGTATAACTTC
PPQ1N (gateway) R	ATTTGAAGAGGTATCATGAG

Footnote: Capital letters denote the *PPQ1* sequence, while lower case letters indicate a sequence needed for integration into the entry vector.
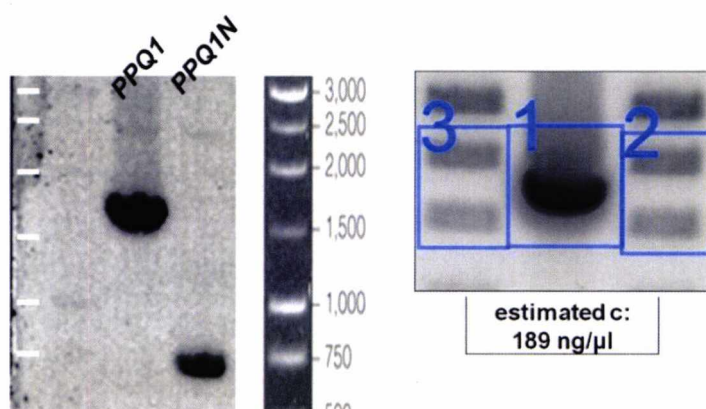
Figure 4.20: Confirmation of PCR amplification of *PPQ1* and *PPQ1N* sequences from 74-D694. Bands on the agarose gel correspond to the expected sizes of *PPQ1* (1650bp) and *PPQ1N* (705bp) (left); comparison of fluorescence of a sample to fluorescence of bands with known amounts of dsDNA was used to estimate concentration of PCR products (right).

The amplified DNA fragments were inserted into the entry vector pENTR/D-TOPO (see Methods, section 2.5.6.1 for details) and confirmed by DNA sequencing. The oligonucleotode primers used for the later were 'M13 forward' and 'M13 reverse' and an internal primer (CTGTCGCTAAAGCCCTATCC, priming at 338-357).

The *PPQ1*$^{(*)}$/*PPQ1N* inserts were then transferred from the entry vector into destination vectors (Table 4.8) using LR reaction (see methods section 2.5.6.2). Successful transfer of inserts into destination vectors was confirmed by a restriction digest (data not shown).

Table 4.8: List of destination vectors

PCR insert	Backbone	Copy number	Selection marker	Promoter	Product
PPQ1	pAG415	CEN	*LEU2*	*GAL1*	*PPQ1-DsRed*
					PPQ1-GFP
	pAG423	2μ	*HIS3*	*GAL1*	*PPQ1-DsRed*
	pAG425	2μ	*LEU2*	*GAL1*	*PPQ1-DsRed*
PPQ1*	pAG415	CEN	*LEU2*	*GAL1*	*GFP-PPQ1*
PPQ1N	pAG415	CEN	*LEU2*	*GAL1*	*PPQ1N-GFP*
	pAG425	2μ	*LEU2*	*GAL1*	*PPQ1N-DsRed*

Footnote: *PPQ1*$^{(*)}$/*PPQ1N* inserts were shuffled from entry to destination vectors in an LR reaction; * indicates stop codon present.

4.4.2 Distribution of tagged Ppq1p in different strains

Either N-terminal GFP or C-terminal GFP or DsRed tags and under P_{GAL1} control on centromeric plasmid, was tested in both the [*PIN*$^+$] and [*pin*$^-$] derivatives of the 74-D694 strain with wt or deleted *PPQ1* gene. Initial observations were that tagged Ppq1p was present in cells at low levels that were largely indistinguishable from the intrinsic autofluorescence in the [*psi*$^-$] cells (Figure 4.21a). In some cases fluorescent foci were observed in the *ppq1Δ* [*PIN*$^+$] and wt [*pin*$^-$] strains (e.g. Figure 4.21b), but this was not reproducible between experiments and cells with fluorescent foci were only rarely observed. Such foci were never observed in cells transformed with destination vectors without a *PPQ1* insert (ccdB-tag; Figure 4.21c). Foci could be observed with both Ppq1p-GFP (Figure 4.21b) and Ppq1p-DsRed (Figure 4.21d) when used as C-terminal tags, but

not with the *GFP-PPQ1* construct with the GFP at the N-terminus. Appearance of foci and the occasional ribbon-like structures did not depend on the concentration of the inducer galactose used (Figure 4.21e) within the range 0.1% to 0.4% (w/v) of galactose in the medium. This is contrary to what would be expected of the behaviour of a prion domain where high protein levels promote aggregation. No discernable DsRed was observed in standard 2% raffinose 1% galactose medium using a multicopy, 2μ-based plasmid. Expression of the GFP tagged Ppq1p N-domain was sufficient for the formation of foci in BY4741 *PPQ1* (Figure 4.21f; NB: the second picture is a z-stack projection). The conclusion reached was that Ppq1p is mostly diffuse within the cytoplasm, but can under undefined conditions relocate to distinct foci with the N-domain sufficient for the relocalisation to foci (Figure 4.21f).
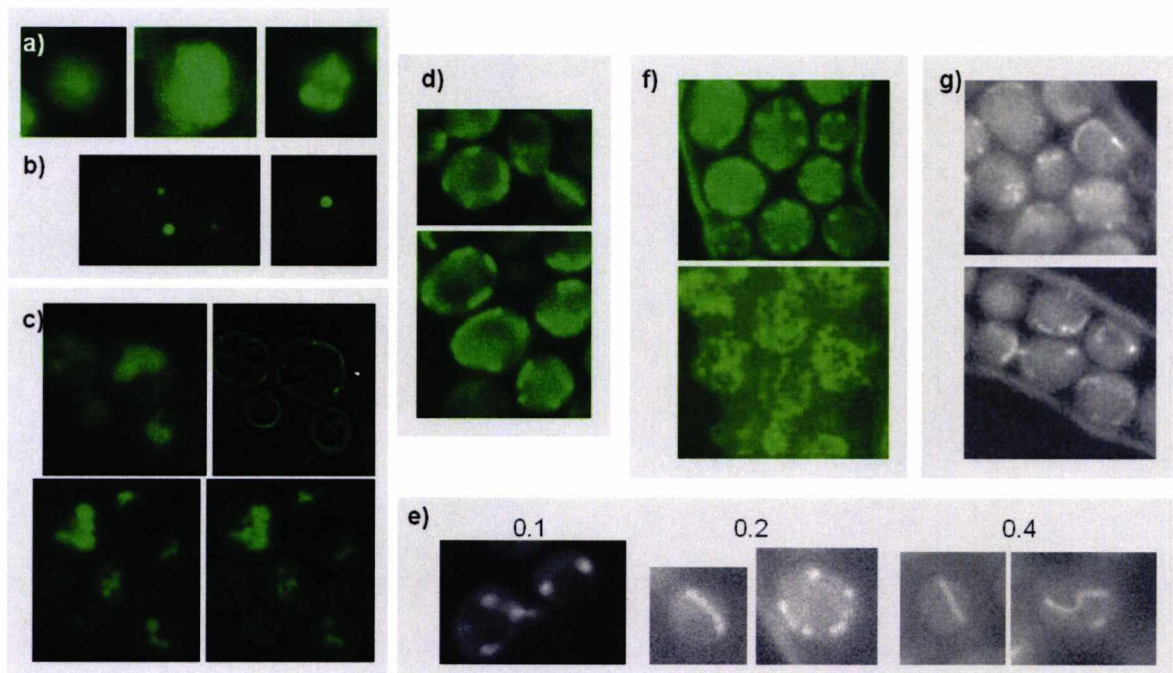
Figure 4.21: Distribution of Ppq1p within a cell. Ppq1p is mostly diffuse within a cell (a), but in some cases forms one to few foci (b); c) cells transformed with destination vectors without a *PPQ1* insert do not exhibit foci. Left: green channel, right: green channel with light in visible spectra; d) Ppq1p-DsRed fusion: foci are observable independently of the type of fluorescent tag or channel used; e) intensity of fluorescence or presence of foci/other structures does not depend on concentration of galactose [0.1% - 0.4% (w/v) of galactose]; f) *PPQ1N* domain is sufficient for formation of foci. Single plain (above) and z-stack projection (below) pictures; g) *GFP* tag was fused to 3' end of chromosomal *PPQ1*; Foci were mostly observed near water-air boundary (e.g. f-g); cells carrying a low copy number plasmid encoding *PPQ1-GFP* under *GAL1* promoter control were grown to logarithmic phase when galactose was added and cells incubated for additional 5 (a-e) or 24h (f); g) 24h old culture in YEPD. Cells were pelleted, resuspended in distilled water and mounted on microscope slides; the colour of pictures is arbitrary.

Since the fluorescent signal could not be reliably distinguished from background fluorescence when diffuse, it could not be verified whether Ppq1p is diffuse in most experiments or simply not expressed. To confirm expression of the *PPQ1*-fusion proteins western blot analysis of cell-free extracts from induced cells was undertaken using an anti-GFP antibody, but no signal was detected. Although that could be a consequence of very low levels of expression combined with relatively weak binding of the antibody to GFP epitope(s), overexpression of *PPQ1* with any of the tags or *PPQ1* with the stop codon, did not affect growth rate of transformants. Overexpression toxicity of *PPQ1* has been previously reported (Sopko *et al.*, 2006). There are three possible explanations: Ppq1p constructs were either not expressed, not catalytically active or BY4741 and 74D-694 strains are not sensitive to overexpression of *PPQ1*.

To avoid *PPQ1* expression issues a strain with GFP integrated downstream of the genomic *PPQ1* sequence was used (ATCC 201388; Methods, section 2.1). Similar fluorescent structures were observed in this strain that expresses a *PPQ1-GFP* fusion gene using the native *PPQ1* promoter (Figure 4.21g). Because of the problems with reproducibility of foci, only the ATCC 201388 strain was used in subsequent experiments in order to ensure consistent expression.

Again the appearance of fluorescent foci from chromosomal *PPQ1-GFP* was sporadic i.e. it was observed in cells in some experimental replications and not at all in other replications under the same conditions. Foci were mostly observed in older cultures (i.e. after 24h growth in YEPD) and almost exclusively near water-air boundary that formed on the slides prepared for microscopy. As opposed to the fluorescence sometimes observed in vacuoles, the fluorescent foci and ribbon-like structures were only observable in the appropriate channel (a system of lenses that filters out light but for a small range of wavelength spectra; green channel enables visualisation of GFP, but filters out RFP and other signals): in the green channel but not the red one when Ppq1p was tagged with GFP and the red but not the green channel when DsRed tag was used. Fluorescence observed was therefore not a non-specific autofluorescence exhibited by yeast cells.

4.4.3 Co-localisation of Ppq1p-GFP with various cytoplasmic foci

High levels of overexpression of the various *PPQ1* fusions did not promote foci formation as would be expected in case of aggregation triggered by a prion domain. Ppq1p is also a low abundance protein (~300 molecules/cell; von der Haar, 2008; Ghaemmaghami *et al.*, 2003) and thus unlikely to from large foci on its own. Conditions that promote

relocalisation of Ppq1p to foci were not identified in the previous section and an alternative approach was used to identify these conditions. There are different cytoplasmic foci-like structures that involve translation factors, namely P-bodies and stress granules (reviewed in Balagopal *et al.*, 2009) and it is possible that Ppq1p decorates such aggregates when they form (see below). If Ppq1p co-localises with any of these structures the conditions that promote formation of said structures should also promote Ppq1p relocalisation to foci. To explore this hypotheses fluorescent protein labelled markers of various structures were used to test whether Ppq1p co-localised with any of the known cellular structures.

4.4.3.1 Co-localisation with [*PSI*⁺] aggregates

Microscopic analysis (Figure 4.21) suggested that the structures Ppq1p might co-localise to resemble the foci seen with prion aggregates. Ribbon-like structures (see Figure 4.21e) in particular have been shown to represent early stages of prion formation (Zhou *et al.*, 2001; Tyedmers *et al.*, 2010; Mathur *et al.*, 2010). Since Ppq1p foci formation did not depend on gene expression levels, it is possible that Ppq1p does not aggregate on its own, but rather interacts with aggregates of other prions. Ppq1p interacts with Sup35p (chapter 3 section 3.3.5.3 and M.F. Tuite and T. Von der Haar, personal communication) and it is possible that such an interaction pulls it into the Sup35p-based [*PSI*⁺] aggregates. To test this hypothesis, the 74-D694 strain with *GFP* inserted to C-terminus of *SUP35* was transformed with the plasmid carrying a galactose-inducible *PPQ1-DsRed* gene (see section 4.4.1 Table 4.8) and the distribution of Ppq1p followed in both [*psi*⁻] and [*PSI*⁺] strains. If Ppq1p were to interact with aggregates, distribution of the protein should change from diffuse in the [*psi*⁻] strain to foci-like in [*PSI*⁺]. As can be seen in Figure 4.22, the distribution of Ppq1 protein was not affected by prion status of cells.

4.4.3.2 Co-localisation of Ppq1p with P-bodies and stress granules

P-bodies (PB) and stress granules (SG) are cytoplasmic structures that contain translation factors. Both classes of structures contain proteins with prion-like domains that promote aggregation (Gilks *et al.*, 2004; Reijns *et al.*, 2008). Since Ppq1p is involved in protein synthesis, it is plausible that it is also present in either of these types of cytoplasmic bodies.

PBs are present in cells under normal growth conditions, while SGs form in yeast cells following certain stresses, e.g. prolonged heat-shock (46°C for 10 min, Grousl *et al.*,

2009). A plasmid carrying a *PPQ1-DsRed* fusion (see section 4.4.1 Table 4.8) was transformed into BY4741-based strains with either *DCP2* (PB marker) or *PAB1* (SG) fused to GFP and integrated into the genome. The transformants were grown in MM-Leu under normal laboratory conditions or subjected to heat stress conditions (46°C for 10 min), respectively. Ppq1p did not co-localise with either the PBs or SGs (Figure 4.23), since neither of conditions tested resulted in the appearance of Ppq1p-DsRed fluorescent foci. The BY4741 strain used required incubation at 46°C for 20 instead of 10 minutes to induce formation of Pab1p-containing granules.
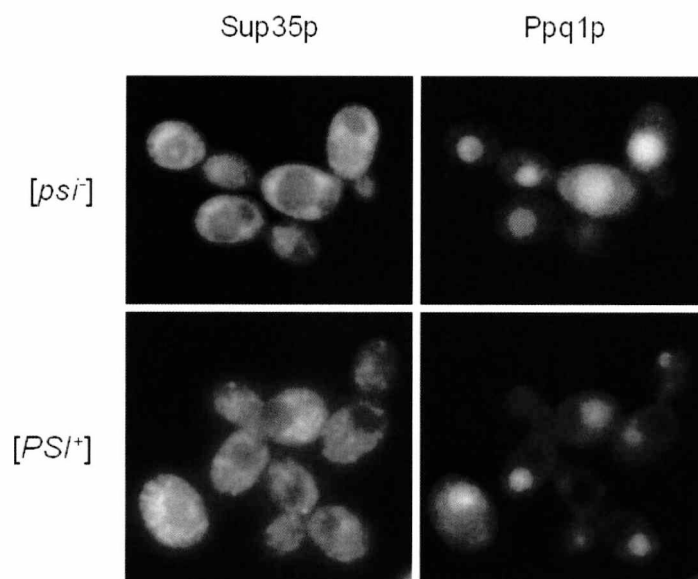
Figure 4.22: Co-localisation of Ppq1p with Sup35p. Despite Ppq1p and Sup35p interacting *in vivo* Ppq1p does not co-localise with [*PSI*⁺] aggregates.

4.4.3.3 Co-localisation of Ppq1p with mitochondria

The location and shape of Ppq1p foci resembled mitochondria that, in a single plane, look like foci but in a z-stack projection resemble a reticular network (in stationary phase). To test the hypothesis that Ppq1p co-localises with mitochondria, a strain with a GFP-tagged chromosomal *PPQ1* allele (ATCC 201388 strain) was transformed with a plasmid encoding the mitochondrial marker *COX4-RFP* – where Cox4p is a subunit of cytochrom c oxidase (Maarse *et al.,* 1984). Cultures were grown under conditions that promote localisation of Ppq1p to foci (i.e. cultures between 24h and 48h) and observed as described in Methods section 2.9.3.1. Ppq1p and Cox4p co-localised in some, but not all cases (Figure 4.24). Co-localisation was also tested using DAPI stain that binds to DNA. Ppq1p and DAPI localised to foci that appeared identical by size and distribution within a cell, yet both signals were almost never present within the same cell: with cells having

either DAPI-stained foci or GFP foci (Figure 4.24e). In rare cases, localisation to foci for both Ppq1p-GFP and DAPI-stain could be observed (Figure 4.24f) and in such cases Ppq1p-GFP and DAPI containing foci overlap.
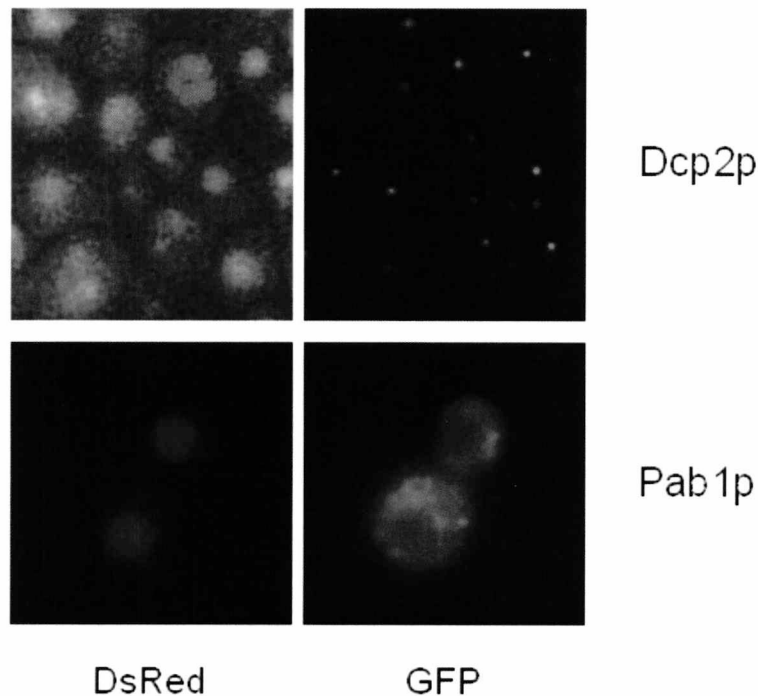
Figure 4.23: DsRed labelled Ppq1p does not co-localise with P-bodies (Dcp2p) or stress granules (Pab1p) markers. BY4741 DCP2-GFP strain was grown under normal laboratory conditions while 20 minute incubation at 46°C was necessary to induce formation of Pab1-containing foci.

Formation of [*PSI⁺*], stress granules or P-bodies did not induce re-localisation of Ppq1 to these structures. Ppq1p-GFP co-localised with mitochondria, typically with fragmented and non-DAPI stained, although occasionally Ppq1p-GFP also co-localised with reticular types of mitochondria. To understand the significane of colocalisation of Ppq1p and mitochodrial markers conditions that promote it needed to be identified.

4.4.4 Factors promoting Ppq1p foci formation

In section 4.4.3.3 it was shown that Ppq1p relocalises to mitochondria, but the conditions that trigger such relocalisation were not elucidated. If it is assumed that Ppq1p localisation to mitochondria was of functional significance and not just an experimental artefact, then

data on processes affected by *PPQ1* deletion or overexpression can be used to predict conditions that promote such a localisation. One possibility is that growth stage of the culture is important, since data presented above (Figure 4.21g and Figure 4.24) indicated that Ppq1p-GFP was mostly observed in foci in non-log phase stages of a batch culture, when the GFP-tagged *PPQ1* was expressed from its native promoter. Growing a culture for 1-6 days in YEPD did not promote relocalisation of Ppq1p-GFP to foci on its own (data not shown) meaning that entering the stationary phase is not sufficient for relocalisation of Ppq1p.
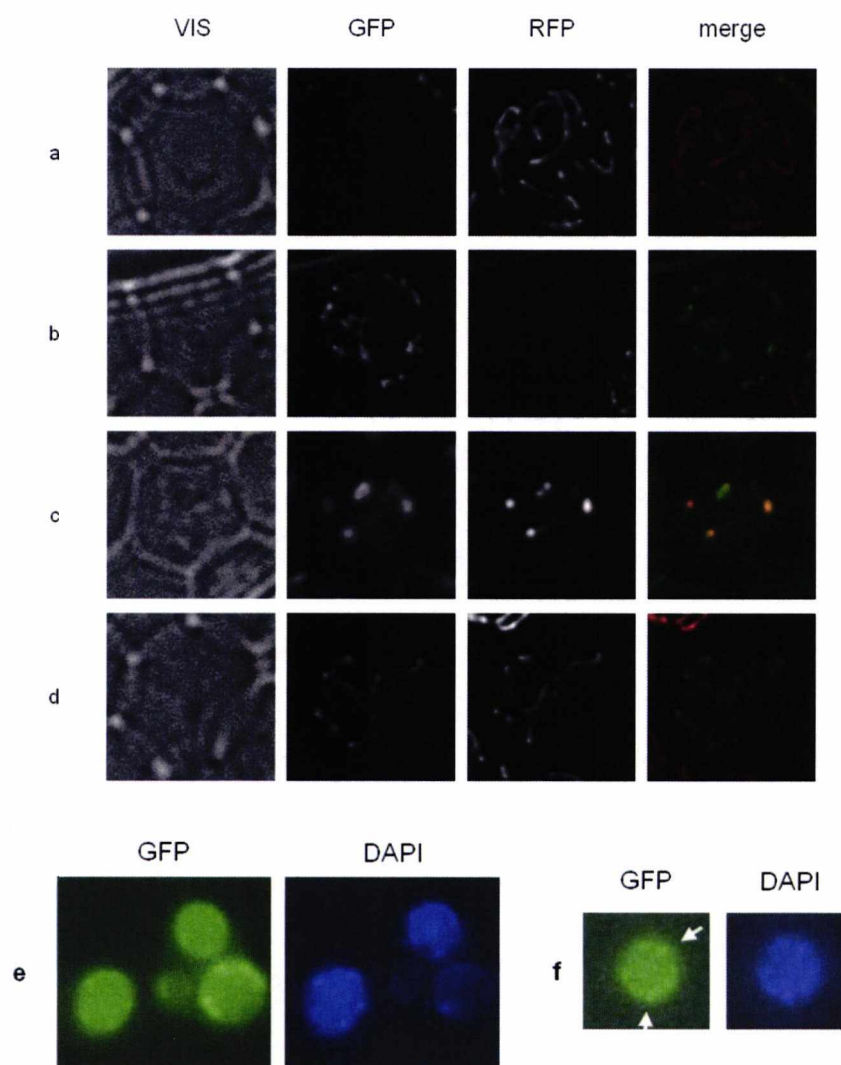
Figure 4.24: Co-localisation of Ppq1-GFP and mitochondria in stationary phase cultures. Cox4-RFP: Ppq1p localises to foci and ribbon-like structures in cells near water-air boundary; some cells exhibit Cox4p-RFP distribution consistent with reticular mitochondrial networks (a, b and d), while some have fragmented mitochondria (c). Ppq1p co-localises with both types of mitochondria (c and d); pictures are z-stack projections; DAPI stain: Ppq1p mostly localises to foci in cells that do not stain with DAPI and vice versa (e), but in rare cases co-localisation of Ppq1p-GFP and DAPI-stained mitochondria can be observed (f).

One important factor that could promote re-localisation of Ppq1p-GFP to mitochondrial foci is stress. *PPQ1* exhibits genetic interactions with the genes *YPD1, SCH9* and *ANP1* all of which are involved in cellular responses to osmotic stress (BioGrid interactions http://thebiogrid.org/36003/summary/saccharomyces-cerevisiae/ppq1.html). Ppq1p redistributes to foci mostly near the water-air boundary when mounted on a slide (Figure 4.21f,g) and osmotic stress could be one of conditions present at the water-air boundary. Two alternative possibilities tested are that these cells are exposed to either heat or oxidative stress.

Cultures of ATCC 201388 were therefore grown in rich glucose-based medium for 24h and then exposed to one of the five conditions tested for their ability to induce relocalisation of Ppq1p-GFP to foci; growth at 37°C or in presence of sodium chloride, hydrogen peroxide, manganese or ethanol. Cells from cultures were harvested and observed microscopically (Methods section 2.9) after 2, 8 and 24h of growth under the various conditions. All experiments were done in duplicate.

4.4.4.1 Effect of manganese and ethanol on Ppq1p relocalisation

The set of conditions that could induce Ppq1p relocalisation to mitochondrial foci are those that induce filamentous growth, since this behaviour is increased in a *ppq1Δ* strain (Jin *et al.*, 2008). Both manganese and ethanol can induce filamentous growth in yeast (Asleson *et al.*, 2000; Lorenz *et al.*, 2000). A concentration of 5mM of manganese was used, compared to 10mM used by Asleson *et al.* (2000) because the ATCC strain 201388 containing the integrated *PPQ1-GFP* allele, showed sensitivity to concentrations used in the experiments described in section 4.3.3.1. Ethanol was used at 5% (v/v) since no effect on Ppq1p-GFP distribution was observed in preliminary experiments at a concentration of 1% as used by Lorenz *et al.* (2000).

Growth of cells in either ethanol or manganese induced Ppq1p-GFP foci formation, but only after prolonged growth in supplemented medium (Figure 4.25). The proportion of the population that contained such fluorescent foci was relatively low, ~30% in manganese treated culture and ~20% in ethanol treated culture. Foci observed in the EtOH-treated cells experiment were also much smaller and consequently fainter.

4.4.4.2 Effect of Hydrogen peroxide, heat stress and sodium chloride on Ppq1p relocalisation

A different approach was taken to search for factors that could potentially cause re-localisation of Ppq1p in cells to mitochondria. Conditions that could have arisen on desiccated slides (i.e. slides with water-air boundary) were predicted to be either oxidative, temperature or osmotic stress. Cultures of the ATCC 201388 strain were therefore incubated as described above, adding either 5mM hydrogen peroxide or 0.6M sodium chloride final concentrations. Heat-stress of the cultures was induced by growing cells at $37^\circ C$.
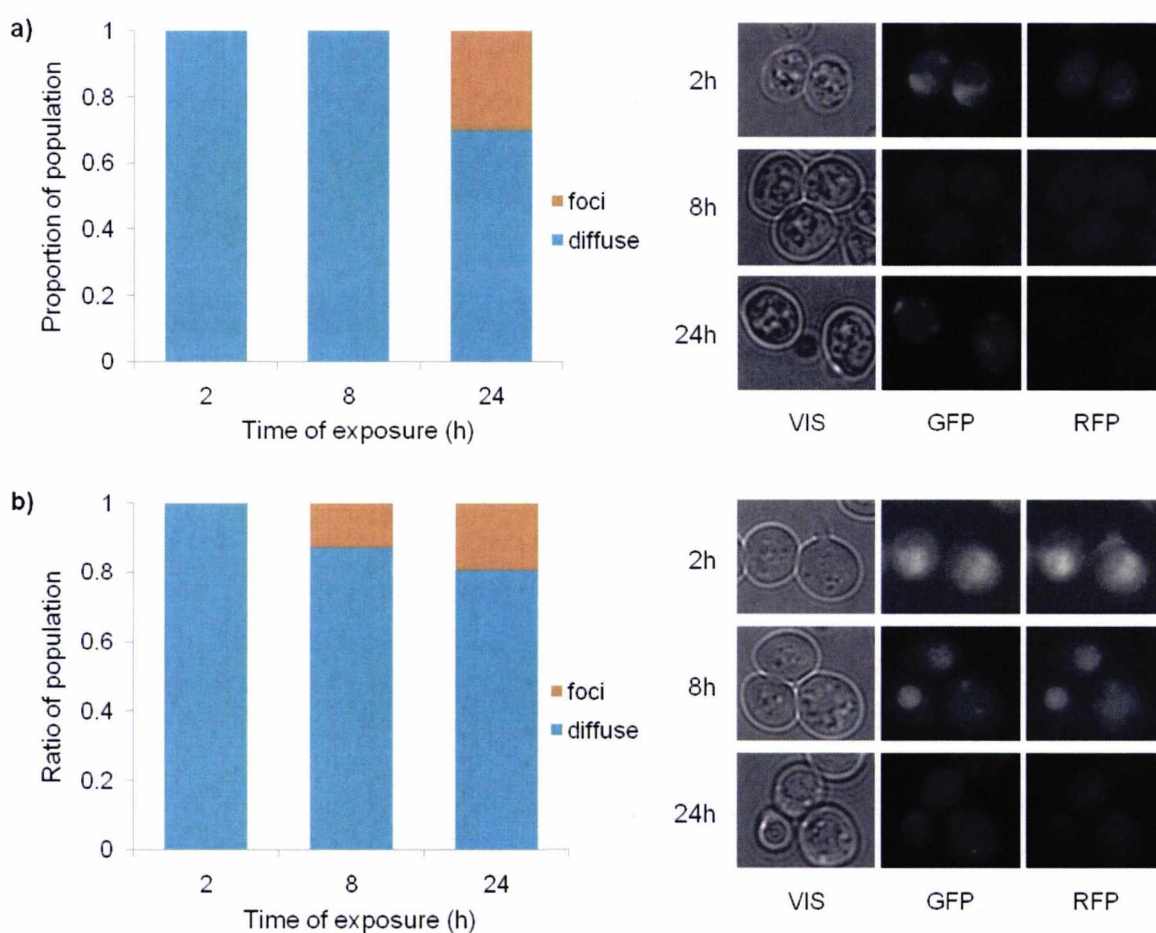
Figure 4.25: Addition of manganese (10mM; a) or ethanol [5% (v/v); b] to post-log phase cultures induces re-localisation of Ppq1p to foci. Left: proportion of cells that show diffuse distribution of Ppq1p versus those that have foci during incubation in supplemented YEPD. Average of two replicates was taken; Right: distribution of Ppq1p-GFP within cells. Red channel was used as a control for unspecific fluorescence. Red and green channel pictures are maximum intensity projections of image stacks; VIS – bright-field, GFP – green channel, RFP – red channel.

Hydrogen peroxide induced foci in approximately 30% of the cells examined (Figure 4.26a) and the foci were also brighter than in cells exposed to the other treatments examined. Sodium chloride induced foci in much larger proportion of the cells; almost 60% on average (Figure 4.26b) although the variability between two replicates was large for these experiments. A mild heat shock had no effect on distribution of Ppq1p-GFP, which remained diffuse throughout cells during 24h of incubation (data not shown).

Although the majority of conditions tested promoted re-localisation of Ppq1p to foci, these were only observed after prolonged incubation i.e. 8h. This contrasts with the immediate appearance of such foci in initial experiments (see Figure 4.21). The cultures were therefore also tested for early foci formation i.e. within 10 min of exposure to the relevant conditions. To induce re-localisation of Ppq1p-GFP to foci, the conditions used in this experiment were more extreme, that is: incubation at $50^{\circ}C$ for 5-10min for the heat-shock, 5 M NaCl for osmotic stress, 20 mM $MnCl_2$ and 10 mM H_2O_2 for oxidative stress. No foci were observed under any of the conditions tested (data not shown).
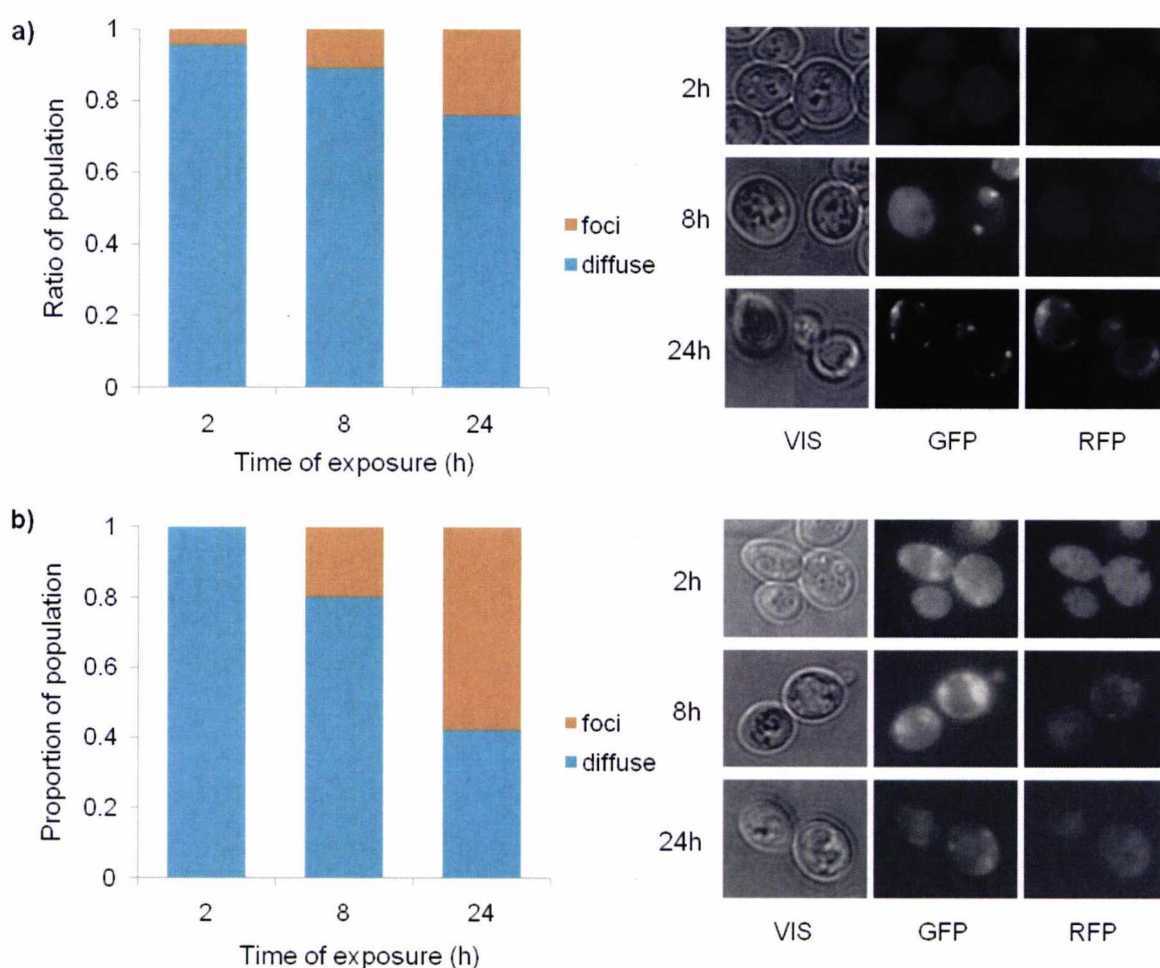
Figure 4.26: Addition of 5mM hydrogen peroxide (a) or 0.6M sodium chloride (b) induces in post-log cultures re-localisation of Ppq1p to foci. Left: proportion of cells

that show diffuse distribution of Ppq1p versus those that have foci during incubation in MnCl$_2$ or NaCl supplemented YEPD; Right: distribution of Ppq1p-GFP within cells. Red channel was used as a control for unspecific fluorescence. Green and red fluorescence pictures at 24h time point (a) were deconvolved using Huygens software with 2 iterations and 40 signal to noise setting. Red and green channel pictures are maximum intensity projections of image stacks; VIS – bright-field, GFP – green channel, RFP – red channel.

Conditions that promoted Ppq1p-GFP relocalisation to foci were filamentous growth inducing conditions – manganese and ethanol, and oxidative and osmotic stress conditions – hydrogen peroxide and sodium chloride. A prolonged exposure to these conditions was needed, typically at least 8h.

4.4.4.3 Manganese-induced Ppq1p foci co-localise with mitochondrial marker Cox4p

The experiments described above identified several conditions that promoted the re-localisation of Ppq1p to distinct structures or foci. There are several differences to previously the foci previously observed (see Figure 4.21). First, the foci observed in cells at the water-air boundary formed within minutes of addition of cells on slides, while prolonged incubation of cells (for > 8h) for all of the conditions described above, was necessary to observe distinct Ppq1p-GFP foci. Second, these foci appeared to differ in size between themselves, in particular ethanol induced foci appeared much smaller. Third, no ribbon-like structures were observed.

To establish whether these foci corresponded to the same structures observed in the previously described experiments, the ATCC 201388 strain was transformed with a plasmid coding for RFP tagged Cox4 (pHS78) and grown in rich medium supplemented with 5 mM manganese as described in section 4.4.4.1 above. Green fluorescent foci appeared as in the previous experiment and these mostly co-localised with the Cox4p mitochondrial marker (Figure 4.27).

Ppq1p-GFP relocalises to foci during filamentous growth (ethanol, manganese) or stress-inducing (hydrogen peroxide, sodium chloride) conditions and the Ppq1-GFP containing foci, at least in case of manganese-induced relocalisation of Ppq1p, appeared to correspond to mitochondria.
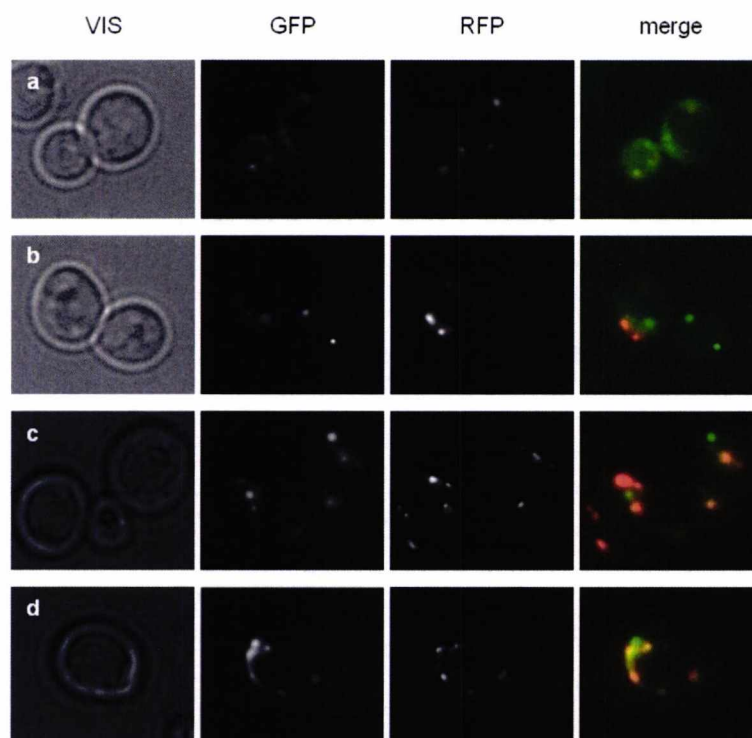
Figure 4.27: Co-localisation of Ppq1-GFP and Cox4-RFP foci in cultures incubated in rich media for 24h and for another 24h after addition of MnCl$_2$ media. Cells with different distributions of the two protein fusions were observed: a) Ppq1p is diffuse while Cox4p foci are visible; b) Ppq1p foci in the cell where no Cox4-RFP is visible; Ppq1p and Cox4 signals can partially (c) or fully (d) overlap; GFP and RFP pictures are maximum intensity projections of image stacks deconvolved with iterations, signal-noise ratio setting of 2, 40 except for RFP c and d where 50, 40 setting was used; VIS – bright-field, GFP – green channel, RFP – red channel.

In summary: the distribution of Ppq1p within a cell was explored in this section. Ppq1p is diffuse in cytoplasm, but relocates to foci under certain conditions. Relocalisation was observed with both GFP and DsRed fluorescent proteins and the N-domain of Ppq1p was sufficient for relocalisation. Foci (and in some cases ribbon-like structures) were found to overlap with mitochondria, as judged by the mitochondrial marker Cox4p and mtDNA stained by DAPI. Conditions that promote relocalisation of Ppq1p to mitochondrial foci were prolonged exposure to filamentous growth-inducing chemicals (manganese and ethanol) and exposure to oxidative (hydrogen peroxide) and osmotic (sodium chloride) stress. Conditions that promote immediate relocalisation of Ppq1p to mitochondria at water-air boundary on microscope slides were not identified.

4.5 Effect of *PPQ1* and *RNQ1* gene deletion on mitochondrial structure and function

Clustering of the genes from the FitDb heterozygous database (see section 3.3.4) had suggested that Ppq1p might be involved in mitochondrial organisation (Table 4.6). Impairment of mitochondrial function is also a plausible explanation for the slow growth phenotype of the *ppq1Δ* strains in the post-diauxic shift stages of a batch culture when respiratory metabolism becomes important. Growth in a medium with alternative carbon sources, e.g. glycerol and ethanol, was not retarded though. Earlier described results (section 4.4) also showed that Ppq1p localises to mitochondria when cells are exposed to stress conditions. The hypothesis tested in this section was that deletion of *PPQ1* gene affects mitochondria, either its structure and/or function.

An *rnq1Δ* strain was also included in these experiments because the Rnq1 protein has several functional similarities with Ppq1p; both proteins interact with Sup35p and have a role in the *de novo* formation of the [*PSI*⁺] prion. Rnq1p has also been proposed to be involved in mitochondrial processes (G.L. Staniforth, personal communication).

4.5.1 Mitochondrial morphology in a *ppq1Δ* mutant

The structure and function of mitochondria are tightly linked and a defect in mitochondrial morphology can generate problems in mitochondrial replication (e.g. Hermann *et al.*, 1998) or a functional defect linked, for example, to early stages of apoptosis (Leadsham *et al.*, 2009). To test this hypothesis a plasmid encoding GFP fused to a mitochondrial-targeting sequence was used. The protein, mito-GFP is transported to the mitochondrial membrane and can be used to visualise mitochondrial network (Westermann *et al.*, 2000).

Changes in mitochondrial organisation occur during different stages of the yeast growth cycle (Visser *et al.*, 1995). In log phase, when cells predominantly ferment, mitochondria form a single unbranched tube. This fermentative morphological type of mitochondrion starts to branch during diauxic shift resulting in appearance of a reticular network. Several causes, e.g. defects in fusion, fission or entry into apopototic pathways, can lead to a change in the morphology of mitochondria, but for purposes of this study, which is to test for any defects in mitochondrial morphology in *ppq1Δ* mutant, they were defined in a single category: fragmented/swollen type of mitochondria (Figure 4.28).
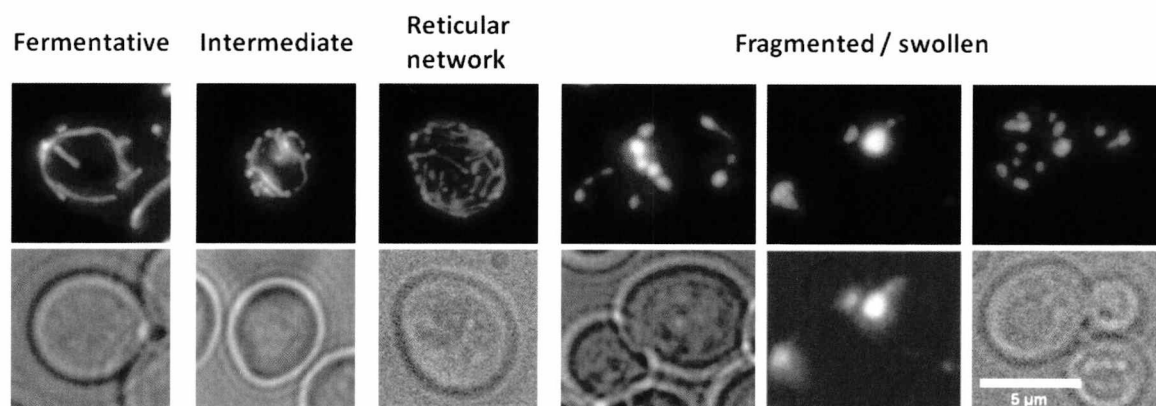
Figure 4.28: different types of mitochondrial morphology as defined in this study. The fermentative, intermediate and reticular type represent typical mitochondrial morphology during log (fermentative), diauxic-shift and early stationary (oxidative) growth, respectively (e.g. Visser *et al.*, 1995); fragmented / swollen mitochondria can be a result of structural and/or functional defects.

The BY4741 wt, *ppq1Δ* and *rnq1Δ* strains were transformed with the mito-GFP expressing plasmid and mitochondrial morphology assessed at different growth phases: logarithmic phase ($OD_{600}<1$), early- and late-stationary phase (24 and 48 hr old cultures respectively). Deletion of the *PPQ1* gene did not have a significant effect on mitochondrial morphology (Figure 4.29) although the *ppq1Δ* cells were slightly rounder at 48h than wt cells as noted previously by Chen *et al.* (1993). The significance of this phenotype was not explored.

A statistically significant increase in proportion of cells exhibiting fragmented/swollen mitochondria at 48h in the *rnq1Δ* strain was observed compared to the wt strain (Figure 4.30), while at 24h both strains had a large proportion of cells with fragmented/swollen mitochondria. The *rnq1Δ* strain had a lower number of reticular mitochondria partly due to a higher proportion of fragmented mitochondria, but also due to a higher proportion of the fermentative type of mitochondria. In 48h old cultures the majority of mitochondria in the *rnq1Δ* strain were fragmented/swollen. A 48 hour culture of *rnq1Δ* and wt strains was spotted on to YEPD and YEPglycerol and overlaid with tetrazolium red stain (see methods section 2.11) to test whether *RNQ1* deletion strain had a lower reducing power than the wt strain, an indicator of mitochondrial dysfunction. The opposite effect was observed, indicating that respiration was higher in the *rnq1Δ* strain under these conditions (Figure 4.30).

4.5.2 Effect of *PPQ1* and *RNQ1* deletion on respiration

Deletion of *PPQ1* did not have a significant effect on mitochondrial morphology (see above) but this does not rule out the possibility that it could still have an effect on respiration. On the other hand, the *rnq1Δ* deletion strain had significantly altered mitochondrial morphology, but did not seem to show any defect in respiration as judged by the tetrazolium stain. To further explore the possible effects of *PPQ1* or *RNQ1* deletions on the structure and also function of mitochondria, several aspects of respiration in the two strains were measured.
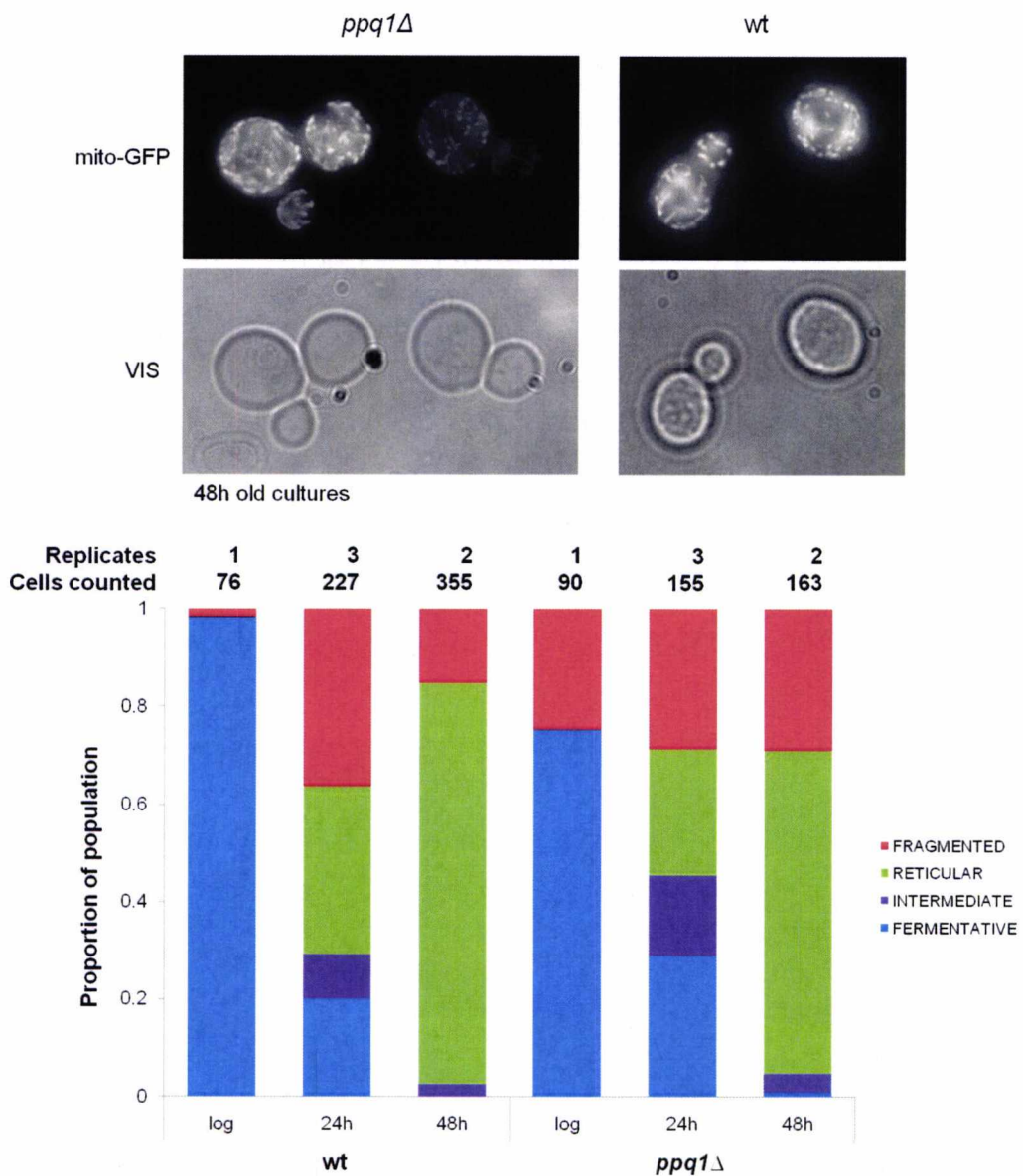
Figure 4.29: Effect of loss of Ppq1p on mitochondrial morphology. Upper, typical *ppq1Δ* and wt mitochondrial morphology in 48h old cultures. Lower; number of cells with different mitochondrial types presented as a proportion of population. There are no statistically significant differences between the two strains.

Respiration in the intact cells was measured using an Oxygraph-2k (Oroboros) respirometer that measures changes in oxygen concentration in the cell culture. Cells from log, early stationary (24h) or late stationary (48h) phase were used to measure routine respiration, leak (respiration attributed to diffusion of protons through inner mitochondrial membrane) and uncoupled respiration (maximum respiratory capacity; Figure 4.31). Only data from 48h old cultures was used in further analysis because data at this time point showed less variability between biological replicates.
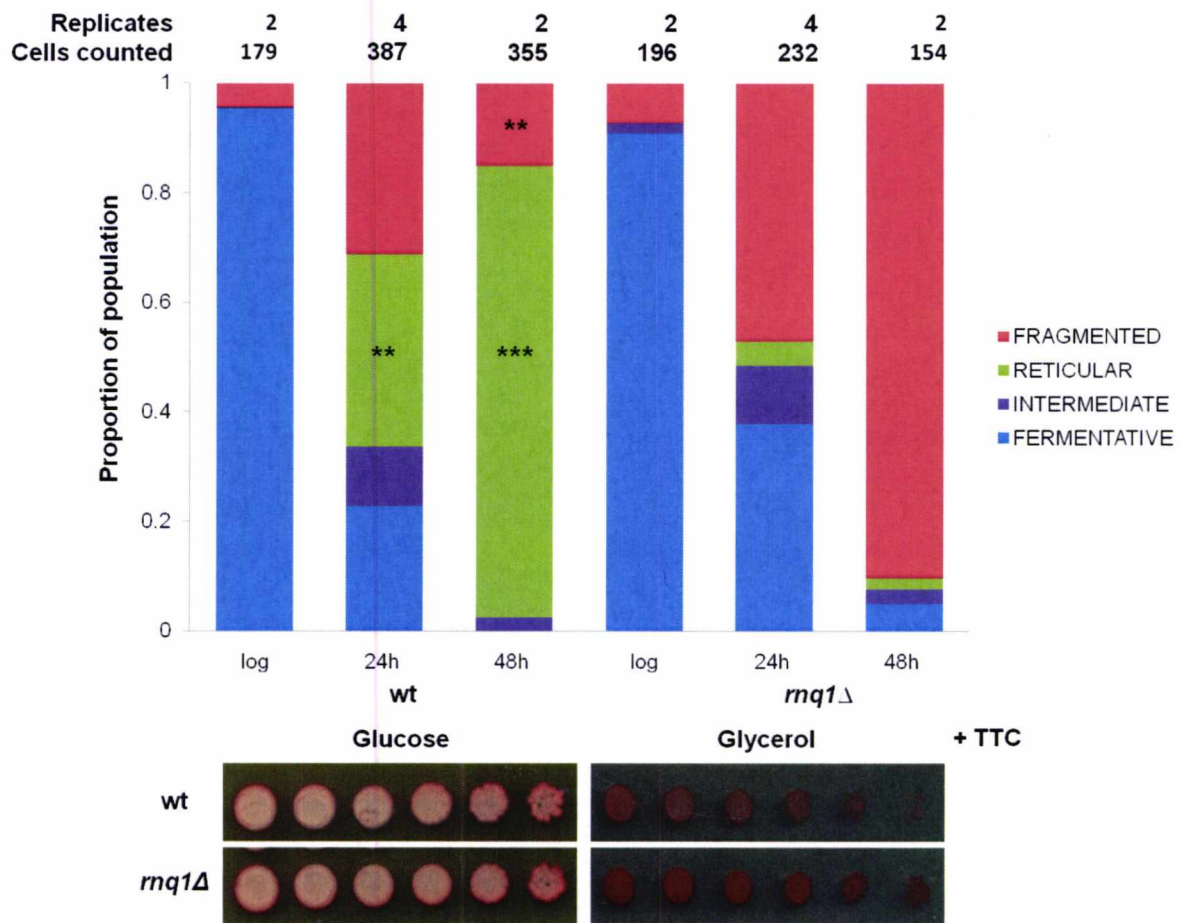
Figure 4.30: Effect of *RNQ1* gene deletion on mitochondrial morphology. Upper; mitochondrial morphology types as a proportion of population during different growth phases. Diauxic shift at ~11h; asterisks indicate types of mitochondria that represent a statistically significant proportion of population in *rnq1Δ* compared to wt strain; Statistical tests: t-test, one tail, equal variance (F-test two sample was done to test for unequal variance, all samples: p>0.05); stars indicate as follows: ** p<0.01, *** p<0.001; *rnq1Δ* stains darker than wt strain when overlaid with tetrazolium red dye.

Routine respiration (Figure 4.32 green columns) of 48 h old cultures of *rnq1Δ* and *ppq1Δ* strains was not significantly different to the respiration of the wt strain (T-test, one-tail, equal variances; p=0.053 and 0.23 respectively). Uncoupled respiration on the other hand

was significantly decreased in both deletion strains (t-test, one-tail, equal variances; *rnq1Δ*: p=0.02 and *ppq1Δ*: p=0.01). A higher routine to uncoupled respiration ratio (R/E) means that cells were respiring closer to their maximum capacity and this can be a consequence of increased energy demand, higher intrinsic uncoupling or reduced respiratory capacity due to damage in electron transport system. The cause of high R/E was not explored.

red line - rate of O2 consumption
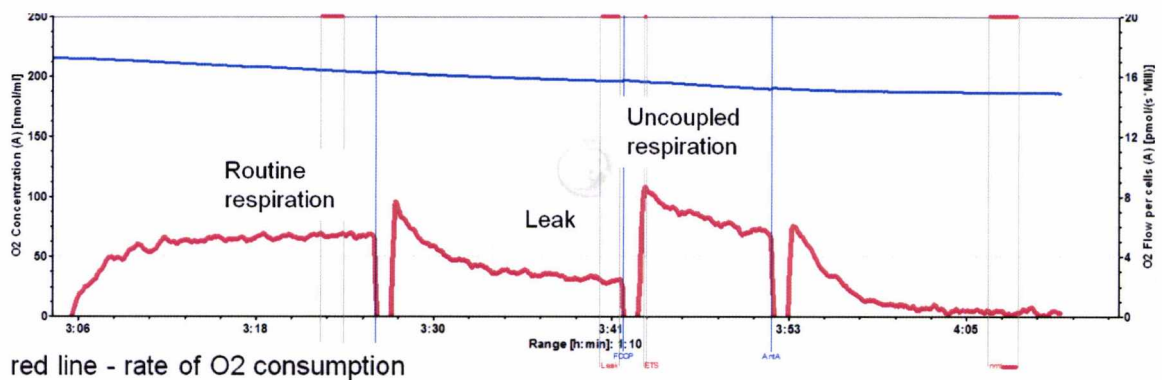
Figure 4.31: Measuring respiration in intact cells. Routine respiration of the culture was measured in minimal medium without a carbon source. Next, TET was added to measure leakiness of mitochondrial inner membrane and finally FCCP was used to note maximum respiratory capacity of cells (see methods for details).
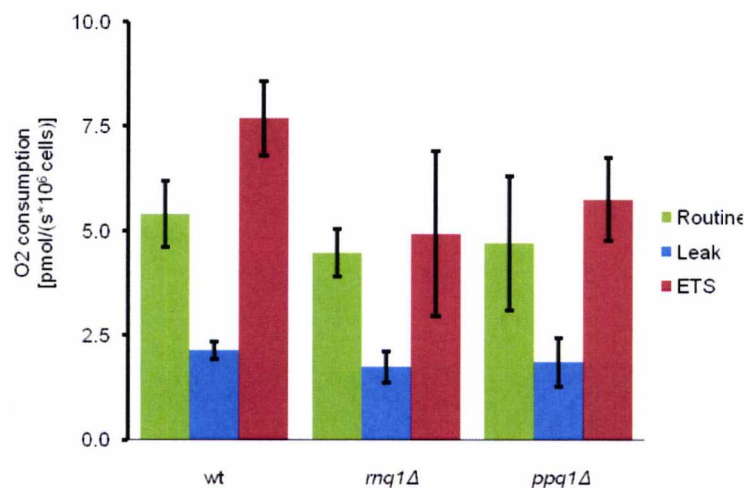
Figure 4.32: Respiration of wt, *rnq1Δ*, *ppq1Δ* strains grown to late stationary phase (48h). For each strain routine (green columns), leak (blue) and uncoupled respiration (red, ETS) were determined. Difference in routine respiration is not statistically significant, while decrease in uncoupled respiration for both deletion strains is seen.

4.5.3 Co-segregation of respiratory defects with *ppq1Δ* allele in a genetic cross

To confirm that respiration defects observed above for the *ppq1Δ* and *rnq1Δ* strains were a consequence of the corresponding gene deletion, one complete tetrad for each of the deletion strains was analysed. The respiration experiments were then carried out on each of the four spore cultures from one complete tetrad per gene deletion. Tetrad II (see section 4.3.3.4) was used to test for an effect of *PPQ1* deletion, while a tetrad obtained from crossing BY4741 *rnq1Δ* to BY4742 was used to confirm results for *rnq1Δ* strain. This tetrad was provided by Dr B.S. Cox. Three replicates were done for each deletion and wt pair in each tetrad.

The observed respiration phenotype in the *rnq1Δ/+* tetrad was similar for all four spores (Figure 4.33), where uncoupled respiration was lower than routine respiration. This effect is associated with excess uncoupler (FCCP) concentration, but has not been previously observed in BY4741 strains at the concentration used (i.e. 12 uM; J.E. Leadsham, personal communication). This suggested that the respiratory phenotype segregated in a non-mendelian fashion, i.e. 4:0.
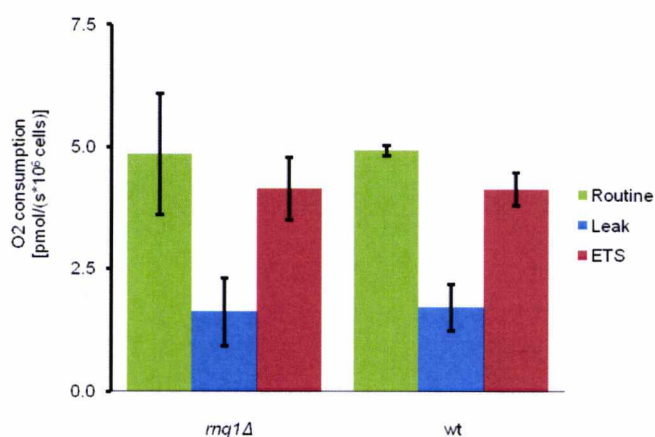
Figure 4.33: Respiration in a tetrad obtained by sporulation of BY4743 *rnq1Δ/RNQ1* strain. Respiration of all four spores of one tetrad was measured and is presented as an average of two spores for each strain.

No conclusions could be made for the *ppq1Δ/+* tetrad (Figure 4.34). While it seemed that the wt spores respired at a lower rate, the variability observed was large and was not dependent on the spore used. The *ppq1Δ* spores on the other hand had a high rate of respiration, but similarly to *rnq1Δ,* a lower rate of uncoupled respiration.

The *PPQ1* deletion strain did not have significantly altered mitochondrial morphology compared to the wt strain, nor was the routine respiration rate affected in the *ppq1Δ* strain. The maximum respiratory capacity on the other hand was significantly lower in *ppq1Δ* strain compared to the wt strain. Co-segregation of respiratory defects with *ppq1Δ* allele could not be confirmed and it is possible that the tetrad used carried additional mutations that affected respiration (see also section 4.3.3.2). The *rnq1Δ* strain had a significantly higher proportion of fragmented/swollen mitochondria in late stationary phase (48h) compared to the wt strain. The *rnq1Δ* strain also had a significantly lower respiratory capacity than the wt strain. Again, co-segregation of respiratory defects was not confirmed, since the "*rnq1Δ*" respiration phenotype segregated in a 4:0 non-mendelian fashion.
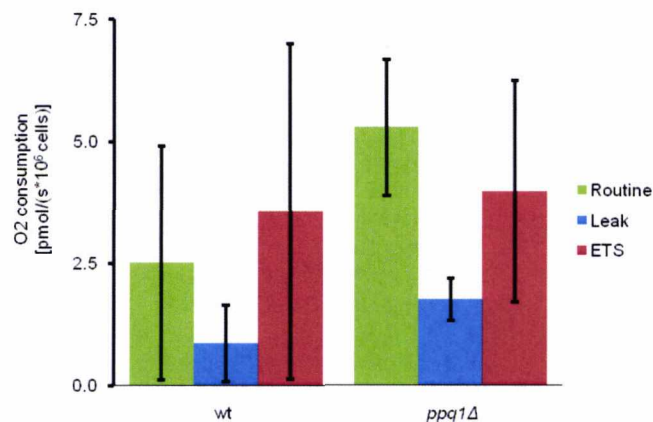
Figure 4.34: Respiration in tetrads from BY4743 *ppq1Δ/PPQ1* strain. Respiration of all four spores of one tetrad was measured and is presented as an average of two spores for each strain.

4.6 Discussion

4.6.1 Sequence and database analysis

The Ppq1p protein sequence was found to be highly conserved within a wide range of strains of *Saccharomyces cerevisiae*. By comparison, one of its binding partners Sup35p, showed 5 amino acid changes across the same number of strains. The N-domain of Ppq1p in particular only had one amino acid change compared to 4 for the prion domain of Sup35p (data not shown). The N-domain of Ppq1p was much less conserved across fungal species. Thus while the Ppq1p C-domain shows a high degree of similarity with

orthologues in other fungi, the N-domain seems to have only its Ser-rich composition conserved.

The predicted secondary structure of Ppq1p showed some similarity to the aggregation-prone domains (e.g. Sup35 prion domain) which are also biased in amino acid composition and mostly unstructured (Michelitsch *et al.*, 2000; Alberti *et al.*, 2009). They differ, for example, in that the N-domain of Ppq1p is rich in Ser, an amino acid not typically connected to sequences known to aggregate. Ppq1p also contrasts the Sup35p prion domain by not being particularly rich in Gln residues. The N-domain of Ppq1p was predicted to be somewhat unstructured (see Figure 4.4), but also to have 8 helices, unlike to prion domain of Sup35p which was predicted to be mainly unfolded (not shown).

Interestingly, the top template used by iTASSER for modelling the protein structure of Ppq1p N-domain was Ppp5p, a phosphatase with a long N-domain that includes a number of tetratricopeptide repeats involved in the regulation of protein activity. This domain functions with the C-terminal region of the protein to block the catalytic site in C-domain (Yang *et al.*, 2005), although there is currently no evidence for such a function in Ppq1p.

Different bioinformatic approaches were used in an attempt to identify cellular processes that Ppq1p affects, although these analyses failed to provide strong evidence for any one process. For example, in analysing the data from BioGrid scores (section 4.2.7.1), the processes predicted were nuclear and chromosomal organisation and functionally overlapped with some potential TFs such as Abf1p, Fkh1p and Fkh2p.

Another highly enriched group of processes identified were related to the cytoskeleton. In particular, homozygous and heterozygous *ppq1Δ* strains have been reported to be sensitive to latrunculin, a drug that interferes with actin polymerisation (Coue *et al.*, 1987). Ppq1p also physically interacts with Bzz1p, a protein involved in regulation of actin polymerisation (Soulard *et al.*, 2002). Filamentous growth was also supported by evidence from multiple sources; for example a *PPQ1* deletion results in an increase in filamentous growth in *S. cerevisiae* (Jin *et al.*, 2008). Another process that appeared high on a list for both types of co-fitness interactions was cellular homeostasis. The effect of Ppq1p on any of these processes was not tested experimentally.

In general, the variety of processes identified could be a consequence of Ppq1p's role in translation, since this process through synthesis of proteins affects all other cellular processes. However, in the bioinformatic and systems-level analyses carried out, translation was only indentified in heterozygous deletion interactions. Never-the-less, because of a demonstrated interaction between Ppq1p and the translation termination

factor Sup35p (chapter 3 section 3.3.5), a detailed analysis of translation in a wt vs *ppq1Δ* was carried out.

4.6.2 A role for Ppq1p in translation?

The potential role of Ppq1p in translation, and in particular translation termination, has been documented before (Song *et al.*, 1987; Vincent *et al.*, 1994). The problem with these previous studies was that translation termination was measured solely on the basis of growth on selective media and the accuracy of termination was measured through sensitivity to the aminoglycoside antibiotic paromomycin. There was also some disagreement whether a *ppq1* deletion had a phenotypic effect without additional nonsense suppressor mutations having to be present in the same strain (see introduction and Table 4.1). Here this problem was avoided by quantitatively measuring different aspects of translation using plasmid-based reporters.

The efficiency of translation termination was found to be reduced two-fold at all three stop codons – UAA, UAG and UGA in 74-D694 strain and it was further shown that deletion of *PPQ1* decreased the accuracy of translation. As was previously shown by (Burck *et al.*, 1999) the frequency of +1 frameshift increased in a *ppq1* deletion (section 4.3.1.1). As another measurement of translation accuracy, the rate of amino acid missincorporation was assayed and also found to increase in the *ppq1Δ* deletion strain, while data from the translation of a rare-codon-based firefly luciferase (section 4.3.1.1) suggested that the rate of mRNA translation is reduced in the absence of Ppq1p. This confirms previous reports (Chen *et al.*, 1993), but considering that the general accuracy of translation was decreased in the *ppq1* knockout strain, it is possible that rare codons were mistranslated more often than the commonly used codons and that this test reflects an effect on the accuracy rather than the rate of translation.

The observed effect of the *ppq1* gene deletion on both elongation and termination suggests a common mechanism whereby Ppq1p perhaps affects ribosomes or factors that in turn play a role in both stages of translation (e.g. *TEF4* and *TEF5* which encode subunits of eEF1B; Valouev *et al.*, 2009). Alternatively, since Ppq1p physically interacts with Sup35p, it could also interact with eEF1A (Tef1/2p), a translation elongation factor since this protein shares sequence identity with the C-domain of Sup35p (Kushnirov *et al.*, 1988).

Deletion of either the *PPQ1* or *PPZ1* genes decreases the efficiency of translation termination, but gene deletions have the opposing effect on translation accuracy; the *ppq1* mutant had decreased accuracy of translation, while the *ppz1* mutant exhibits an increased accuracy of translation (Song *et al.,* 1987; Vincent *et al.,* 1994, Burck *et al.,* 1999; Venturi *et al.,* 2000; de Nadal *et al.,* 2001). It was demonstrated here that *PPQ1* and *PPZ1* also interact genetically (section 4.3.2.4). Ppz1p probably does not affect the same targets in translation as Ppq1p does, because deletion of both genes increased nonsense suppression, but deletion of the *PPZ1* gene had the opposite effect on the accuracy of translation to that seen in the *ppq1Δ* strain. Deletion of the *PPZ1* gene affects the phosphorylation status of eEF1Bα (*TEF5*) although direct dephosphorylation of the elongation factor by Ppz1p has not been reported (de Nadal *et al.,* 2001). One possibility is that either Ppq1p or Ppz1p works upstream of the other, affecting the other protein and additional targets. For example, Ppz1p could dephosphorylate Ppq1p that would in turn dephosphorylate eEF1Bα. An important question remains unanswered though; Why was the growth of the *ppq1 ppz1* double mutant better on rich medium than the growth of the wt strain (see Figure 4.14).

4.6.3 Co-localisation of Ppq1p with mitochondria

The initial hypothesis being tested was that N-domain of Ppq1p promotes protein self-aggregation and perhaps constitutes a prion-like domain. Although typical prion domains are well defined, the existence of prions such as HET-s and PrP shows that variety of sequences can support prion phenotype (Tuite *et al.,* 2010). Even within "classical" prion domains, some properties are not well understood. While Asn and Gln are considered equivalent in their prionogenic capacity, recent studies suggested that Asn is more important (Alberti *et al.,* 2009; Halfmann *et al.,* 2011). Data on the amino acid conservation of the N-domain of Ppq1p (Ppq1pN) showed that it is Ser residues that are conserved across fungi species rather than Asn and this lends further support to the notion that the Ppq1p-N-domain might function in connection with phosphorylation, rather than promoting self-aggregation. On the other hand, Ser is also a polar amino acid, a property that is the basis of formation of a polar zipper (Perutz *et al.,* 1994).

The hypothesis that the N-domain of Ppq1p is an aggregation prone domain was tested by tagging the protein C-terminally with the fluorescent protein GFP. No discernable fluorescence was observed with a high-copy number plasmid, while a CEN-based plasmid produced weak fluorescence that could not be reliably distinguished from non-specific

background fluorescence in diffuse state. Furthermore, probing western blots using an anti-GFP antibody did not detect the Ppq1p-GFP protein, neither from plasmid-borne copies or when an integrated allele of the *PPQ1-GFP* was present in the strain. The only confirmation of *PPQ1* gene expression was through the observation that Ppq1p localised to foci or ribbon-like structures in some cells of these strains. It is perhaps not surprising that *PPQ1-GFP* expressed under control of the native *PPQ1* promoter could not be observed on western blots in total cell extracts as Ppq1p is predicted to be present in cells at extremely low levels (~300 molecules/cell; von der Haar, 2008; Ghaemmaghami *et al.*, 2003). One alternative approach would be to express *PPQ1* under control of the efficient and inducible *CUP1* promoter, which consistently produces strong expression in case of *SUP35* (see chapter 5 Figure 5.4), but since localisation of Ppq1p to foci/ribbon-like structures seemed to be dependent on environmental/physiological conditions more than the level of expression, the issue of *PPQ1* expression was not pursued further and natively expressed *PPQ1-GFP* was used in all subsequent studies described.

The lack of discernable Ppq1p-GFP fluorescence outside of foci/ribbon-like structure could cast some doubt on whether the signal in these structures was produced by tagged Ppq1p. For example, the signal could be caused by other sources such as autofluorescence of mitochondria that could be induced by environmental stresses. This was controlled for by expressing *PPQ1* tagged with either GFP or DsRed proteins (section 4.4.2). In each case, the fluorescence localised to foci/ribbon-like structures and was only observed in the channel that corresponded to fluorescent protein used, but not to a control channel. The fluorescence signal was weak – as would be expected for a low abundance protein – and in contrast to other cellular sources of fluorescence (such as red pigment in *ade1-14* mutants) the fluorescence was rapidly photobleached. Furthermore, such GFP/DsRed fluorescence was not observed in any other experiments reported in this thesis. Co-localisation was also not dependent on the tag used since results were obtained with both GFP and DsRed tags.

Co-localisation experiments with *PPQ1-GFP* expressed under its native promoter showed that the structures Ppq1p co-localised to were mitochondria. The problem was that conditions which promote this co-localisation were not apparent. Two groups of conditions that could potentially promote mitochondrial co-localisation were tested: conditions that promote filamentous growth and conditions that were associated with dessication. In both cases localisation of Ppq1p to discrete foci was observed, although only after prolonged incubation of cells for up to 24 hours under tested conditions. In the case of manganese stress, the Ppq1p foci were also confirmed to co-localise with the mitochondrial marker Cox4p.

Mitochondria in cells grown under foci-promoting conditions did not form reticular networks, but were only present as small foci. The observed fragmentation of mitochondria could be a consequence of stress-induced mitophagy (reviewed in Scherz-Shouval et al., 2007). For example, concentrations of manganese used in this experiment are known to induce mitochondrial respiratory mutations (Putrament et al., 1973), although such mutations were not observed for ethanol at the concentrations used here (Bandas et al., 1980). This hypothesis could easily be tested by examining for the co-localisation of Ppq1p and the vacuole-selective stain FM4-64. Another approach to testing Ppq1p involvement with mitophagy would be to test for genetic interaction between PPQ1 and UTH1 – the latter encodes a protein involved in mitophagy (Kissova et al., 2004). This approach would avoid problems with weak fluorescence of tagged Ppq1 protein.

Ppq1p co-localisation to foci that were initially observed in desiccated slides was likely not caused by the stress conditions tested, since co-localisation occurred within minutes rather than hours. Furthermore, in the various conditions examined, only fragmented mitochondria were observed, while on desiccated slides a minority of observed mitochondria were reticular in structure. On the other hand, Ppq1p never co-localised with DAPI stain, indicating that Ppq1p-labeled 'mitochondria' lack DNA.

Data presented on the localisation of Ppq1p must therefore be considered as preliminary and further experiments will need to be done to confidently establish any physical connection between Ppq1p and mitochondria. In particular, immunofluorescence experiments, where the protein in question is probed for with specific antibodies and fluorescence of the tagged antibody is observed would provide more confidence in results because this approach also enables both amplification of the signal and use of more photostable tags.

In light of the hypothesis that Ppq1p is functionally connected to mitochondria, several tentative links emerge from the data from previous studies of ppq1 mutants. For example, in amino acid starvation conditions in the presence of fermentable carbon sources, Chen et al. (1993) noted that a ppq1Δ strain had an increased cell death rate and these are conditions that strongly promote mitophagy (Kanki et al., 2008). Another link emerges from the observed reduced growth of ppq1Δ strain from spores and mitochondrial remodelling in mature spores (Gorsich et al., 2004). These links are speculative though and further research is needed to confirm involvment of Ppq1p in any mitochondria-related processes.

4.6.4 Mitochondrial morphology and respiration

Mitochondrial organisation was identified as a cellular process affected by a lack of Ppq1p in co-fitness interaction studies using heterozygous deletion strains. This process was not highest on the list and did not appear as an enriched process in other related studies. There were also two potential TFs that were functionally connected to mitochondria: Azf1p and Rtg1p. The link to mitochondria was however tentative since a *ppq1Δ* strain grew as well as wild-type strain on non-fermentative carbon sources such as glycerol. The available evidence from databases therefore did not support the hypothesis that Ppq1p affects mitochondria, however the effect of a *PPQ1* deletion on mitochondria was tested on the basis of the Ppq1p co-localisation study (see section 4.4).

Mitochondrial morphology was not affected by deletion of the *PPQ1* gene in a statistically significant fashion, although the proportion of the reticular type of mitochondria was smaller in both early (24h) and late (48h) stationary phase in *ppq1Δ* strain when compared to the wt parent strain (Figure 4.29). The deletion of the *PPQ1* gene did have an effect on the rate of respiration, although the rate of routine respiration was reduced only slightly and not statistically significantly in the *ppq1* knockout strain. A greater reduction was observed in the rate of uncoupled respiration that is the maximum capacity of the electron transport chain. A reduced respiratory capacity can be caused by variety of mitochondrial factors and elucidating the cause was beyond the scope of this thesis.

Deletion of the *PPQ1* gene therefore caused a reduction in the respiratory capacity of mitochondria. This reduction can be explained in light of proposed hypothesis that Ppq1p affects mitophagy; decreased mitophagy would cause increase in the number of dysfunctional mitochondria, since in normal cells dysfunctional mitochondria are isolated through a fusion-fission process and subsequently degraded. Alternatively, a reduced accuracy of translation could also affect mitochondria although considering the size of the effect this explanation seems less likely.

4.6.5 Summary of findings

In this chapter I confirmed previous conclusions on Ppq1 protein's role in mRNA translation. Deletion of the *PPQ1* gene was shown to increase nonsense suppression and reduce the accuracy of translation. That Ppq1p might be involved in cellular processes beyond translation was deduced by a GO term analysis of genes and proteins that Ppq1p interacts with. Among the processes so identified were those involved in nuclear and

chromosomal organisation and other cytoskeleton related processes. Analysis of the distribution of fluorescently-tagged Ppq1p showed that the protein co-localises with mitochondria although this result was considered to be preliminary and further tests will be needed. A further line of evidence linking Ppq1p to mitochondria was an observed decrease in respiratory capacity of a *ppq1Δ* strain.

Chapter V

The role of the Tsa1p/Tsa2p peroxiredoxins in *de novo* formation of the [*PSI*⁺] prion

5.1   Introduction

Cells living in aerobic environments face external oxidative stress and reactive oxygen species (ROS) produced during normal aerobic metabolism. Cells are protected against oxidative damage by variety of antioxidants such as catalases, peroxidases and superoxide-dismutase. A recently discovered group of antioxidants called the peroxiredoxins use thioredoxin as an electron donor and are present across a wide variety of species (Rhee *et al.*, 2005). The group can be further divided into the 1- and 2-Cys peroxiredoxins.

S. cerevisiae has 5 peroxiredoxins (Prx); cytoplasmic Tsa1p, Tsa2p (both typical 2-Cys), Ahp1p, nuclear Dot5p (two atypical 2-Cys) and mitochondrial Prx1p (1-Cys peroxiredoxin). The Prx proteins show low amino acid sequence similarity (11.5%), but share one highly conserved cysteine residue. Tsa1p and Ahp1p are much more abundant than the other three proteins. All peroxiredoxins except Dot5p form a homodimeric species upon oxidation (Park *et al.*, 2000). Peroxidatic function works through oxidation of the catalytic cysteine residue to sulphenic acid that is unstable and readily forms a disulphide bond with a nearby cysteine. 2-cys peroxiredoxins dimerise and form a disulphide bond between the catalytic cysteine residue of one protein and a resolving cysteine residue from the second protein. The oxidised homodimer is then regenerated by the thioredoxin-thioredoxin reductase system (Chae *et al.*, 1994). Yeast Prxs functions in response to both extracellular and mitochondrial dysfunction-induced oxidative stress overlap (Wong *et al.*, 2004).

Exposure to persistent oxidative stress rapidly inactivates peroxiredoxins. Inactivation happens when the catalytic cysteine residue is "over-oxidized" through sulphenic acid to sulphinic or sulphonic acid rather than forming a disulphide bond. Peroxiredoxin over-oxidation is reversible by Prx1 sulfiredoxin in an ATP-dependent manner (Biteau *et al.*, 2003). Concentrations of hydrogen peroxide required for inactivation are relatively low, for example, Yang *et al.* (2002) showed that for human Prx1 extracellular H_2O_2 concentrations of $100\mu M$ cause a significant shift toward sulphonated Prxs as detected by 2-dimensional gel electrophoresis. The rapid inactivation of peroxiredoxins at low concentrations of peroxides makes peroxidases inefficient compared to other catalases and hints at the possibility of additional roles for these enzymes. Wood *et al.* (2003) proposed a flood-gate model where by inactivation of peroxiredoxins is important for H_2O_2 build-up and its participation in signal transduction. Peroxiredoxins role in diverse processes such as signal transduction, response to DNA damage and cancer development has been reviewed by Morgan *et al.* (2007).

The Tsa1p Prx is a major thioredoxin-dependent peroxidase that catalyses reduction of H_2O_2 and alkyl hydropeoxides. It has two conserved cysteine residues at 47 (catalytic) and 170 (resolving) and both are necessary for its peroxidase function (Chae *et al.*, 1993; Chae *et al.*, 1994). Tsa1p functions with Tsa2p to protect cells against oxidative stress and although Tsa2p is a highly similar protein (86% amino acid identity) it is expressed at much lower levels than Tsa1p (Park *et al.*, 2000). Wong *et al.* (2002) showed that their role in defence against oxidative and nitrosative stress overlap and that while Tsa1p is more abundant compared to Tsa2p, the expression of latter is significantly induced by various stresses. The majority of Tsa1p is found in a soluble fraction, while approximately 5% of the protein associates with ribosomes (Trotter *et al.*, 2008). Tsa2p on the other hand is exclusively found in a ribosomal fraction (Sideri *et al.*, 2010).

Schroder *et al.* (2000) showed that the human Prx, thioredoxin peroxidase B (TPx-B) from erythrocytes forms decameric (5 dimers) complexes, and that the active site cysteines within the oligomers are oxidized to an inactive sulphinic acid form. The oligomers form under a variety of stresses, such as oxidative, heat shock and reductive stress (Schroder *et al.*, 2000; Jang *et al.*, 2004; Rand *et al.*, 2006). Jang *et al.* (2004) showed that the oligomeric complexes function as chaperones *in vitro*, and Rand *et al.* (2006) further showed that these chaperones function to prevent reductive stress-induced ribosomal aggregation *in vivo*. Thioredoxins are necessary for stress induced oligomerisation, while Srx1p is needed for disassembly of Tsa1/2 proteins into a dimeric form.

In yeast the Tsa1p protein plays an additional role in maintaining genomic stability, suppressing a variety of events from single gene mutations, frameshift mutations, and larger deletions to chromosomal rearrangement (Huang *et al.*, 2003). These roles require Tsa1p's peroxidase activity and are unique to Tsa1p within the Prxs, although co-deletion of *TSA2* and other peroxiredoxins genes exacerbates the *tsa1Δ* phenotype. Under normal aerobic growth conditions a small effect on various types of DNA mutation was detected in a *dot5Δ* strain as well (Wong *et al.*, 2004; Iraqui *et al.*, 2009). Tsa1p appears to cooperate with DNA check-point and repair mechanisms, in order to maintain genomic stability (Huang *et al.*, 2005; Iraqui *et al.*, 2009, Tang *et al.*, 2009).

In this chapter the effect of *TSA* genes deletion on the translational apparatus and in particular on the *de novo* misfolding of Sup35p into its [*PSI*⁺] prion form is explored. I show that deletion of both *TSA* genes simultaneously induces [*PSI*⁺] prions that are indistinguishable from typical [*PSI*⁺] prions. However, detection of [*PSI*⁺] by colony colour and the adenine prototrophy assay (as described in Chapter 3) is confounded by the

TSA1 deletion, which induces an increased rate of nuclear *SUP⁺* mutations. This research is part of the project done in collaboration with C. Grant and T. Sideri from Manchester and some of the work presented here was published in Sideri *et al.* (2010). The aim was also to corroborate results on *TSA* genes deletion-induced prion formation obtained by T. Sideri and untangle the effect of *TSA* genes deletion on rates of appearance of [*PSI*⁺] and nuclear *SUP⁺* mutations.

5.2   Phenotype of *tsa1Δ tsa2Δ* deletions in the W303 strain background

While exploring the phenotype of *TSA1* and *TSA2* gene deletions in the W303 background, T. Sideri and C.M. Grant (personal communication) observed that deletion of both genes simultaneously resulted in a colony colour change from red to white. The W303 strain used in their study carries an *ade2-1* mutation, an allele with a premature stop (UAA) codon. The truncated enzyme produced by the *ade2-1* allele is non-functional, resulting in adenine auxotrophy and a build-up of the phosphoribosylamino imidazol intermediate, giving the colonies a distinct red colour. Most white-colony phenotypes that appear in such strains are due to secondary mutations that either increase readthrough of the *ade2-1* premature stop codon (nonsense suppression, chapter 3 section 3.1) or block an earlier step in the biosynthesis of adenosine. Despite a single deletion of the *TSA1* gene increasing DNA mutation rates (see 5.1) it did not induce a red to white colony colour change in the W303 strain indicating that oxidative stress rather than genomic instability is responsible for the appearance of the white colony phenotype in a *TSA* double mutant. Deletion of both the *TSA1* and *TSA2* genes may also damage the translational apparatus and increase the rate of decoding errors since both genes function in protection against oxidative stress and localise to ribosomes (Iraqui *et al.,* 2009; Sideri *et al.,* 2010).

Another mechanism known to cause suppression of the *ade2-1* allele is [*PSI*⁺] prion-induced stop codon readthrough; the red to white colony colour change and associated ability to grow without adenine (Ade⁺) is widely used to assay the *de novo* appearance of this prion (see Chapter 3 section 3.1). Oxidative stress, induced by H_2O_2, has previously been shown to induce [*PSI*⁺] formation (Tyedmers *et al.,* 2008). An efficient [*PSI*⁺] induced Ade⁺ phenotype in an *ade2-1* allele background is usually dependent on the presence of a weak nonsense suppressor allele, *SUQ5* (Cox, 1965). The *SUQ5* allele encodes a mutant tRNA^{Ser} that can decode the UAA stop codon (Waldron *et al.,* 1981). The W303 strain has a wild-type allele *suq5⁺* and therefore the appearance of the Ade⁺ phenotype in the W303

strain is not likely to be caused by any known [*PSI*⁺] variant. Nonetheless, to explore the possibility that the Ade⁺ phenotype is caused by a [*PSI*⁺] prion, we first established whether a *TSA1 TSA2* deletion induced [*PSI*⁺] formation.

5.2.1 Colony colour and growth on media lacking adenine

The W303 strain forms red colonies on rich medium but is unable to grow on adenine deficient media (Figure 5.1a). A similar phenotype was also observed for a *TSA1 tsa2Δ* mutant. The *tsa1Δ TSA2* mutant formed pink colonies and was unable to grow without adenine, although it did generate mutants that reverted to Ade⁺ phenotype with high frequency (Figure 5.1a). Double deletion in the *tsa1Δ tsa2Δ* strain consistently gave white colonies that were adenine prototrophs.

5.2.2 The Ade⁺ phenotype of the W303 *tsa1Δ tsa2Δ* mutant is not affected by guanidine hydrochloride (GndHCl) treatment

[*PSI*⁺], along with other yeast prions, requires the ATPase activity of the Hsp104p chaperone for its continued propagation (Chernoff *et al.*, 1995). Guanidine hydrochloride inhibits the ATPase activity of Hsp104p and consequently cells grown in the presence of guanidine hydrochloride display a block in prion transmission from mother to daughter. The block in transmission eventually eliminates prions from the population (Eaglestone *et al.*, 2000; Byrne *et al.*, 2007). The white colony colour (Figure 5.1b) of the W303-derived *tsa1Δ tsa2Δ* strain and its ability to grow on media lacking adenine were not affected by growth in the presence of 5mM guanidine hydrochloride. The white Ade⁺ phenotype of the *tsa1Δ tsa2Δ* strain therefore was not due to the appearance of the [*PSI*⁺] prion. This result is not surprising since, as mentioned above, the W303 strain does not carry the *SUQ5* allele necessary for efficient suppression of the *ade2-1* mutation by the [*PSI*⁺] prion (Cox 1965). Most likely, the white Ade⁺ phenotype is due to the appearance of efficient nonsense suppressor mutations or possibly other Hsp104p-independent mechanisms, such as continuous *de novo* misfolding of non-heritable Sup35p amyloids (Salnikova *et al.*, 2005).
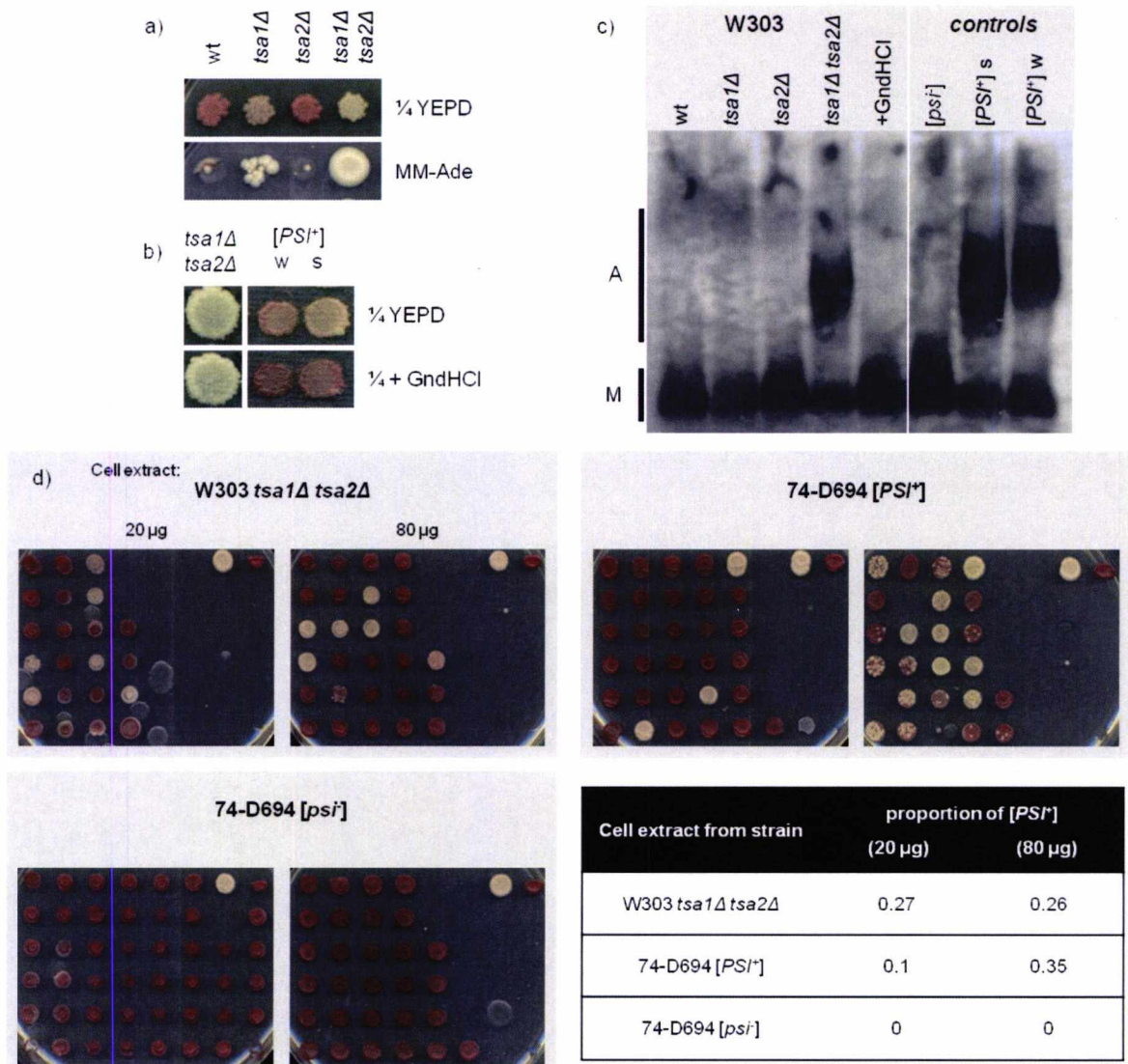
Figure 5.1: Phenotypic analysis of the W303 *tsa1Δ/tsa2Δ* deletion strains and properties of the [*PSI*⁺] prion in a *tsa1Δ tsa2Δ* strain. a) colony colour and adenine auxotrophy of the W303 strain and its *TSA* mutant derivatives. The W303 strain harbours the *ade2-1* allele (premature stop codon) and therefore cannot synthesize adenine. It thus forms red rather than white colonies, and is unable to grow on media lacking adenine. Deletion of the *TSA1* gene causes a slight change in colony colour from red to pink and greatly increases the frequency of Ade⁺ revertants (*SUP*⁺). The *tsa1Δ tsa2Δ* colonies are white and Ade⁺. The YEPD plate was incubated for 3 days and the MM-Ade plate for 7 days; b) the colony colour of the double mutant does not revert to red when grown in the presence of guanidine hydrochloride, in contrast to [*PSI*⁺] strains (74-D694 *ade1-14*). w – weak, s – strong [*PSI*⁺]; c) SDD-AGE of protein extracts from the W303 strains. Only a double deletion strain has SDS-resistant Sup35p aggregates (*tsa1Δ tsa2Δ*) that can be eliminated by growth in the presence of guanidine hydrochloride (+GndHCl). A – SDS-resistant protein aggregates, M – monomers, s – strong and w – weak [*PSI*⁺]. A western blot was probed with αSup35p antibody and developed using the ECL method; d) A [*psi*] strain that was transfected with a W303 *tsa1Δ tsa2Δ* cell extract changes to [*PSI*⁺]; cell extracts were co-transformed with a plasmid carrying the *URA3* marker using a modified protoplast transformation protocol (see methods); two different cell extract protein concentrations were used (20µg on the left and 80µg on the right side of each panel); top right of each plate are [*PSI*⁺] and [*psi*] colony colour controls.

5.2.3 SDS-resistant Sup35p aggregates are present in *tsa1Δ tsa2Δ* strain and can be eliminated by growth in presence of GndHCl

The fact that the above described phenotypes were not caused by the [*PSI*⁺] prion did not exclude the possibility that simultaneous *TSA1* and *TSA2* deletions resulted in *de novo* prion formation that was masked by a high frequency of nuclear-encoded suppressor mutations. Deletion of both *TSA* antioxidants causes oxidative stress (Iraqui *et al.*, 2009), and oxidative stress has been shown to induce prion formation in yeast (H_2O_2, Tyedmers *et al.*, 2008). It is possible that persistent oxidative stress could cause Sup35p to aggregate into non-heritable amyloids, as previously described by Salnikova *et al.* (2005). The difference between [*PSI*⁺] amyloid and non-heritable amyloid is that the latter form spontaneously with very high frequency and are independent of Hsp104p function. SDD-AGE gel analysis of protein extracts from a double deletion *tsa1Δ tsa2Δ* strain revealed the presence of SDS-resistant Sup35p aggregates (Figure 5.1c), a hallmark of the [*PSI*⁺] prion. Furthermore, these aggregates could be eliminated from the strain by passaging cells on 3mM GndHCl plates, suggesting that the aggregates require Hsp104p for their continued propagation. An independent replicate of SDD-AGE presented in Figure 5.1c is presented in Sideri *et al.* (2010).

5.2.4 Sup35p aggregates are infectious

Another characteristic of prions is infectivity, for example, when exposed to external prion-contaminated material, native prion proteins are readily converted to the prion conformation (Tanaka *et al.*, 2004; King *et al.*, 2004). To test whether SDS-resistant Sup35p aggregates isolated from the white Ade⁺ W303 *tsa1Δ tsa2Δ* strains were infectious, they were transformed into a standard 74D-694 [*psi*⁻] [*PIN*⁺] strain using a transfection method first described by Tanaka *et al.* (2004) in which *in vitro* polymerised Sup35p amyloids were used to infect [*psi*⁻] yeast cells.

Two different amounts of total cell extract were used for these experiments; one with 20µg and one with 80µg of protein per transfection. At both concentrations, approximately 25% of the Ura⁺ colonies that had taken up the pUG72 plasmid also changed to [*PSI*⁺] proving that SDS-resistant aggregates from W303 *tsa1Δ tsa2Δ* strain were infectious (Figure 5.1d). Infectivity of aggregates was similar to the standard [*PSI*⁺] strong control at 80µg of cell extract. All [*PSI*⁺] colonies reverted to red colour on guanidine hydrochloride plates. None of the Ura⁺ colonies transfected with cell extracts from 74D-694 [*psi*⁻] [*PIN*⁺] strain

(negative control) were white, and therefore none had changed to [PSI^+]. These results were reported in Sideri *et al.* (2010).

That the W303 *tsa1Δ tsa2Δ* cells have Sup35p aggregates that are SDS-resistant, infectious and dependent on Hsp104p ATPase activity for propagation, strongly indicated that these aggregates are a prion form of Sup35p. The W303 *tsa1Δ tsa2Δ* cells form white colonies and are adenine prototrophs, despite lacking the *SUQ5* suppressor. This phenotype however does not appear to be dependent on [PSI^+] aggregates since elimination of aggregates from the population did not affect the white Ade⁺ phenotype.

5.3   *TSA1/2* gene deletion phenotypes in *SUQ5* and *suq5⁺* backgrounds

The above analysis suggested that the white Ade⁺ phenotype of the *tsa1Δ tsa2Δ* strain was not a consequence of *de novo* formation of [PSI^+] or a non-heritable amyloid form of Sup35p. Rather, the phenotype could be associated with the appearance of a high number of nuclear mutations giving rise to efficient nonsense suppression, or due to non-hereditary mechanisms such as continuous oxidative damage to the translational apparatus caused by deletion of the thioredoxin peroxidase genes (Iraqui *et al.*, 2009; Sideri *et al.*, 2010). To investigate the genetic basis of the white Ade⁺ phenotype, a W303 *tsa1Δ TSA2* [*psi*⁻] strain was crossed with *suq5⁺* and *SUQ5* strains and then crossed back to a W303 *TSA1 tsa2Δ* [*psi*⁻] strain. Two diploid strains were thus created: *TSA1/tsa1Δ TSA2/tsa2Δ suq5⁺/suq5⁺* and *TSA1/tsa1Δ TSA2/tsa2Δ SUQ5/SUQ5*. Both diploids were induced to sporulate and the asci dissected. Colonies grown from spores are presented in Figure 5.2. All genetic crosses and asci dissections were kindly carried out by Dr B.S. Cox.

5.3.1 Nonsense suppression phenotype in *SUQ5* versus *suq5+* background

None of the spores obtained in the crosses, carried out by Dr B.S. Cox, showed the white colony phenotype in *suq5⁺* background (Figure 5.2a, ¼ YEPD plate in bottom left panel). Furthermore, no significant colour differences between spores with different combinations of *TSA* gene deletions were observed, indicating that *TSA* gene deletions and the accompanying increase in mutation rate and oxidative stress do not affect the red Ade⁻ phenotype in a *suq5⁺* background.

Genotype / Revertants	wt	TSA1 tsa2Δ	tsa1ΔTSA2	tsa1Δ tsa2Δ
None	5	12	3	8
Few	1	5	5	2
Many	0	0	1	0
Confluent growth	0	1	1	4

Genotype / Revertants	wt	TSA1 tsa2Δ	tsa1ΔTSA2	tsa1Δ tsa2Δ
None	1	1	0	0
Few	5	4	0	0
Many	0	0	2	0
Confluent growth	0	1	4	1
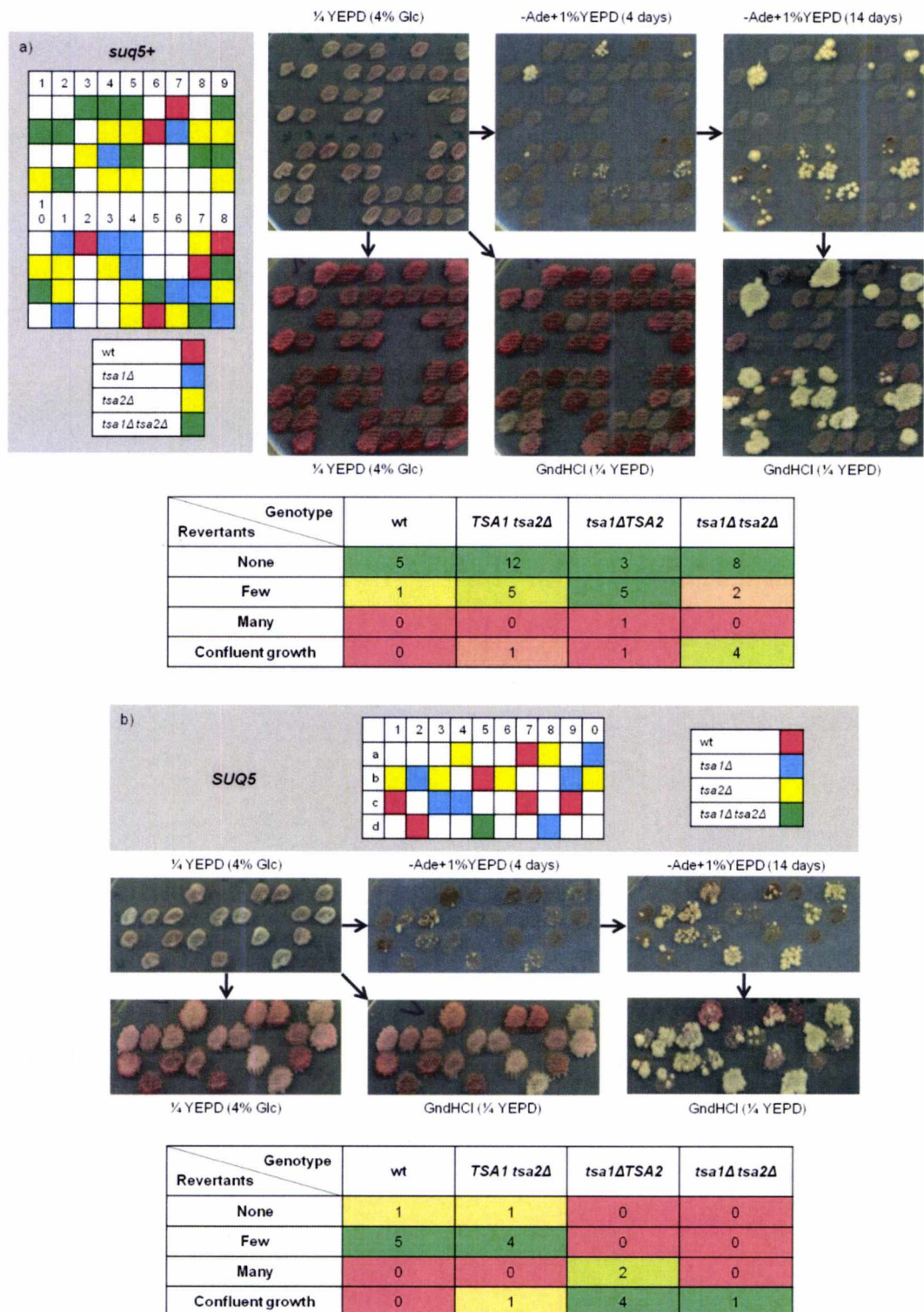
Figure 5.2: Colony colour and adenine auxotrophy in *suq5*⁺ and *SUQ5* tetrads. after sporulation, colonies were restreaked on a ¼ YEPD plate (top left) and replica plated on to YEPD supplemented MM–Ade, ¼ YEPD and ¼ YEPD with added guanidine hydrochloride. Plates were scanned after 4 days of incubation at 30°C (¼ YEPD plates 3+1 day at 4°C). The MM-Ade plate was incubated for another 10 days and replica plated on to a guanidine plate (¼ YEPD; bottom right); tables: growth of *suq5*⁺ (a) or *SUQ5* (b) strains with different combinations of *TSA* genes deleted, grown on minimal media without adenine (supplemented with 1% YEPD). Patches were replica plated from ¼ YEPD

plates. Number of colonies appearing on a patch was scored from none to very high and the number of patches for each category was counted. Note that *TSA* genes did not segregate in a Mendelian fashion between spores of tetrads 4, 5 and 9; the cause for such segregation was not investigated.

Colonies grown from spores of the *SUQ5/SUQ5* parent strain were more diverse in colony colour, ranging from dark red to pink (Figure 5.2b). The colour of colonies did not correspond to the segregation of respective *tsa1Δ* and/or *tsa2Δ* gene knockouts. The spores with the deleted *TSA1* or *TSA2* genes were not lighter in colour than their wt counterparts. More significant was a difference in growth on the adenine-deficient medium, where colonies with *TSA* genes deleted produced higher numbers of Ade⁺ colonies than wt colonies (Figure 5.2b, Table). The *tsa1Δ tsa2Δ* strain had a higher number of Ade⁺ colonies than the *tsa1Δ TSA2* strain, and the *TSA1 tsa2Δ* strain had the lowest number of Ade⁺ colonies. None of the Ade⁺ colonies in all genetic backgrounds studied reverted back to the red colony colour when grown on 5mM GndHCl and therefore the underlying change was not caused by *de novo* [*PSI⁺*] formation.

Comparison between *SUQ5* and *suq5⁺* strains showed that *SUQ5* increased the numbers of Ade⁺ revertants. This effect was most prominent in the *tsa1Δ tsa2Δ* and *tsa1Δ TSA2* strains, but was noticeable even in the wt strain (Figure 5.2a, b). An increase in the number of Ade⁺ revertants in *SUQ5* containing cells was expected since the *SUQ5* allele is a weak suppressor and will therefore enhance the stop codon suppression caused by other weak suppressors and allosuppressors that otherwise would not have a visible phenotype in the *suq5⁺* background. Interestingly, the nonsense suppression effect of the *SUQ5* allele appeared to be toxic in the *tsa1Δ tsa2Δ* strain where only one viable spore was obtained. A number of previous reports have indicated that high efficiency nonsense suppression is lethal in yeast (e.g. Cox, 1971). It is therefore possible that the *tsa1Δ tsa2Δ* mutation acted as an allosuppressor and that this added nonsense suppression was lethal in the *SUQ5* background.

5.3.2 Colony colour stability in *TSA* deletion strains

The *tsa1Δ tsa2Δ* and *tsa1Δ TSA2* colonies (Figure 5.2) showed a high frequency of Ade⁺ revertants, possibly reflecting the continuous oxidative damage or the DNA/genomic instability associated with the *TSA1* deletion (see section 5.1). Thus the Ade⁺ revertants could arise immediately after sporulation, through continuous oxidative stress, or

continuous generation of genetic mutants. Colonies of one full tetrad per *SUQ5* (spores were not from a single tetrad) and *suq5⁺* strain (see top-left plates, Figure 5.2) were restreaked on ¼ YEPD plates to give single colonies (Figure 5.3, left and middle panels). For both the *SUQ5* and *suq5⁺* strains, wt and *tsa2Δ* strains formed only red colonies whereas the *tsa1Δ tsa2Δ* and *tsa1Δ TSA2* strains had significant numbers of white Ade⁺.
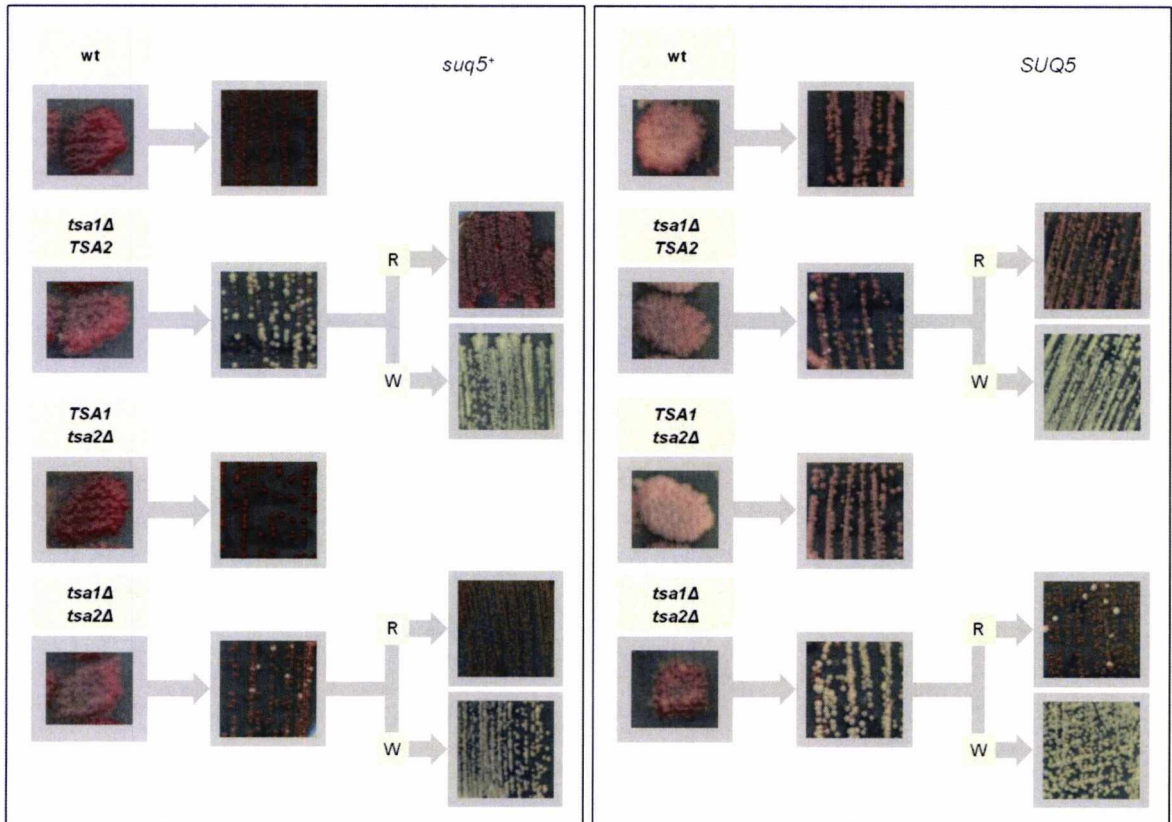
Figure 5.3: Colony colour stability in *suq5⁺* and *SUQ5* strains. Cells were picked up from colonies grown from single spores (left panels) and restreaked on ¼ YEPD plates (middle panels). A red and a white colony from *tsa1Δ tsa2Δ* and *tsa1Δ TSA2* strains were restreaked on new ¼ YEPD plates to test for stability of colony colour (right panels).

Next, one red and one white colony per strain were picked up and streaked on to new ¼ YEPD plates to test the stability of Ade⁺/Ade⁻ phenotypes (Figure 5.3, right panels). Only a few new white colonies appeared in *tsa1Δ tsa2Δ SUQ5* strain and none were observed in the other strains. Red colonies from *tsa1Δ tsa2Δ SUQ5* and *tsa1Δ TSA2 SUQ5* in the right panel plates were picked up, grown in YEPD broth, spread on ¼ YEPD plates and scored for red/white colony colour phenotype. Three percent of colonies were white, and 5 percent of colonies had white sectors in the *tsa1Δ tsa2Δ* strain. Colonies with sectors confirmed that the white sub-population appeared *de novo* rather than originating from a non-clonally purified colony. Cultures made from a *tsa1Δ TSA2* red colony did not give

rise to a single white colony, but had many red colonies with single or multiple white sectors – 11% (11 out of 123) – a similar rate to the *tsa1Δ tsa2Δ* strain. Colony colour of clonally purified colonies corresponded to the adenine phenotype where white colonies were Ade⁺ and red colonies were Ade⁻ (data not shown). No change from white to red colonies was observed throughout these experiments indicating that the white Ade+ phenotype is a genetically stable end point.

The initial colonies grown from *tsa1Δ tsa2Δ* and *tsa1Δ TSA2 SUQ5* spores had a combination of adenine auxotrophs and prototrophs. Red colonies were present in all strains tested and since no change from white to red colonies was observed, it was deduced that the initial spores had a red colony phenotype. Although numbers of white and red colonies from initial patches were not quantified it appears that the frequency of white colonies was much higher than in subsequent restreaking of cells (i.e. ~10%).

The frequency of change of red to white colony colour was similar between *tsa1Δ tsa2Δ* and *tsa1Δ TSA2* strains indicating that the *TSA1* gene deletion alone rather than deletion of both *TSA* genes was responsible for the observed phenotypes. A *TSA1* deletion has been previously shown to cause genomic instability (Wong *et al.,* 2004; Iraqui *et al.,* 2009) although the phenotype is slightly exaggerated in *tsa2Δ* background. Tsa2p associates with ribosomes (Sideri *et al.,* 2010) and although a small fraction of Tsa1p also localises to ribosomes a deletion of both *TSA* genes is required in order to observe damage to the translational apparatus (Wong *et al.,* 2002; Sideri *et al.,* 2011). The red to white colony colour change and the appearance of Ade⁺ revertants is therefore a result of suppression of the *ade2-1* allele, and this is caused by *SUP⁺* mutations rather than oxidative damage to ribosomes.

5.4   Prion properties of *TSA* deletion strains in 74D-694 background

The W303 strain lacks the *SUQ5* allele that would enable efficient assaying of [*PSI⁺*] prion formation. The preferred strain for *de novo* assays of [*PSI⁺*] formation is 74-D694, which carries an *ade1-14* allele with a premature stop codon that [*PSI⁺*] can sufficiently suppress without the need for additional suppressors (see Section 3.1). Consequently, to obtain accurate quantitative estimates of the effects of *TSA1* and *TSA2* gene disruption on *de novo* [*PSI⁺*] formation, the *TSA1/2* genes were deleted from the genome of a 74-D694 [*PIN⁺*] strain (T. Sideri, personal communication). The question addressed in the following section was whether deletion of the *TSA* genes affects prion behaviour and in particular, whether it increases the rate of *de novo* prion formation.

5.4.1 Induced *de novo* formation of the [*PSI*⁺] prion

To test whether deletion of the *TSA1/2* genes increases the rate of *de novo* [*PSI*⁺] formation, plasmid-borne *SUP35NM* under control of the *CUP1* promoter (p6442 plasmid) was expressed (methods section 2.7.1.2) in the 74-D694 wt strain and its *TSA1/2* gene deletion derivatives. High levels of *SUP35NM* expression induce [*PSI*⁺] formation (Chernoff et al., 1993; Derkatch et al., 1996), but unlike the overexpression of full length *SUP35,* overexpression of *SUP35NM* is not toxic to [*psi*⁻] cells (Derkatch *et al.*, 1996).

Deletion of the two *TSA* genes was found to alter the rate of induced, *de novo* formation of the [*PSI*⁺] prion, but surprisingly the rate was lowered rather than increased (Figure 5.4a, red bars). The rate of induced *de novo* formation of [*PSI*⁺] in the *tsa1Δ tsa2Δ* strain was more than 3-fold lower than the rate seen for the wt strain. Although the rate of *de novo* prion formation in the *tsa1Δ TSA2* strain appeared lower than in double *tsa1Δ tsa2Δ* deletion strain, the confidence intervals widely overlap, so it was concluded that the measured rates were not significantly different. The estimated *de novo* [*PSI*⁺] formation rate in the *TSA1 tsa2Δ* strain had a very large 95% confidence intervals and the actual rate could be as high as the rate in the wt strain or similar to the rate of *de novo* [*PSI*⁺] in the *tsa1Δ tsa2Δ* strain.

The 74-D694 *tsa1Δ tsa2Δ* strain had a significantly increased rate of *SUP*⁺ mutations, confirming previous observations in the W303 strain (see section 5.3) as reported by Iraqui *et al.* (2009). Eight- and five- fold increases in *SUP*⁺ mutation rates for *tsa1Δ tsa2Δ* and *tsa1Δ TSA2* strains were observed compared to the wt strain, which are slightly lower than the 14- and 10- fold increases seen for canavanine resistance rates observed by Iraqui et al. (2009). The *SUP*⁺ mutation rate in the *TSA1 tsa2Δ* strain did not differ from the wt rate within the confidence intervals used. This result is in agreement with acquired data on colony colour and Ade⁺ phenotype (see Figure 5.2 and Figure 5.3). Iraqui *et al.* (2009) reported a change in mutation rate for *TSA1 tsa2Δ* strains compared to a wt strain in some but not other assays of spontaneous nuclear gene mutation rates.

Conclusion that the rate of induced *de novo* formation of [*PSI*⁺] is lower in the *tsa1Δ tsa2Δ* strain than in the wt strain is contrary to expectations, since a spontaneously formed [*PSI*⁺] prion was isolated in the W303 *tsa1Δ tsa2Δ* strain, hinting to a higher rate of *de novo* formation in the *tsa1Δ tsa2Δ* strain. It is possible that the mechanism of *de novo* [*PSI*⁺] formation differs between spontaneous and induced formation. To test for this possibility, the rate of spontaneous *de novo* [*PSI*⁺] formation needed to be determined.

rate (×10⁻⁴ / generation)	[PSI+]	SUP+
wt	11.8	1.5
tsa2Δ	5.2	0.6
tsa1Δ	0.9	6.8
tsa1Δ tsa2Δ	3.6	12.4

ratio to wt	[PSI+]	SUP+
tsa2Δ	0.4	0.4
tsa1Δ	0.1	4.5
tsa1Δ tsa2Δ	0.3	8.1
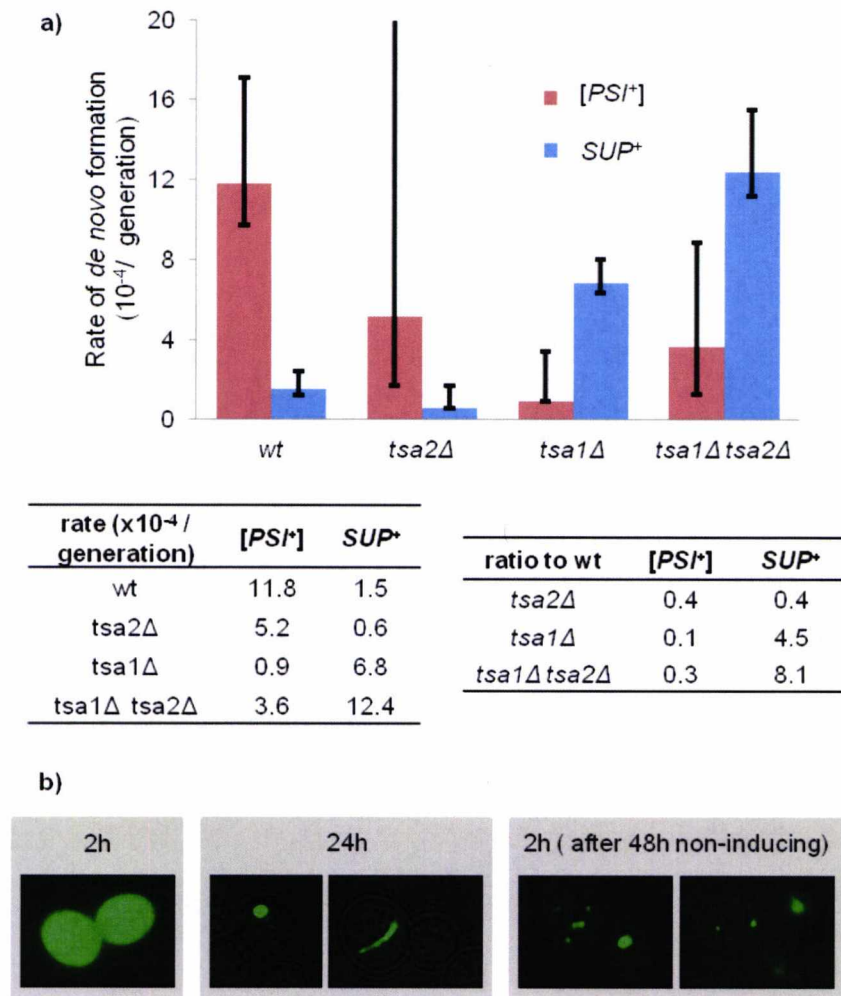
Figure 5.4: Induced de novo [PSI⁺] formation in 74-D694 TSA deletion strains. a) rates of induced *de novo* formation compared to rates of appearance of revertants (*SUP*+). [*PSI*+] colonies were distinguished from *SUP*+ mutants by reversibility of colony colour on plates with guanidine hydrochloride. *tsa1Δ tsa2Δ* strain had a statistically significant lower rate of *de novo* [*PSI*+] formation compared to the wt strain and a very high rate of *SUP*+ (table on the right). Bars indicate 95% confidence intervals; b) induced formation of the [*PSI*+] prion by overexpression of *SUP35NM-GFP* in *tsa1Δ tsa2Δ* strain followed a typical pathway with a ring/worm-like aggregation intermediate and final stabilisation as distinct foci. Hours indicate time of induction that is growth in 25µM CuSO₄ supplemented medium. After 24h of induction cells were diluted and grown in CuSO₄-free media (selecting for retention of the plasmid) for two days before *SUP35NM-GFP* expression was re-induced.

5.4.2 Formation of foci and their propagation during induced [*PSI*+] formation in a *tsa1Δ tsa2Δ* [*psi*⁻] mutant

Induction of [*PSI*+] by overexpression of *Sup35NM-GFP* can be monitored using fluorescence microscopy. Three stages of cellular distribution of Sup35 during *de novo* [*PSI*+] formation have previously been described (Tyedmers *et al.*, 2010). In the *tsa1Δ*

tsa2Δ [*pin⁻*] strain, the Sup35NM-GFP was initially dispersed throughout the cytoplasm (Figure 5.4b, left panel). After prolonged expression (24h), *SUP35NM-GFP* foci and typical worm-like/ring structures began to appear (middle panel). These structures fragmented by the third day into smaller foci. The images shown in Figure 5.5, right panel, were captured after cultures were diluted into a non-inducing medium and left to grow for two days before *SUP35NM-GFP* expression was re-induced. A short induction time (i.e. < 6h) allowed for sufficient expression of Sup35NM-GFP to decorate pre-existing aggregates, while not sufficient for promoting Sup35p aggregation *de novo*.

5.4.3 [*PSI*⁺] colonies contain SDS-resistant aggregates that are GndHCl treatable.

In the experiments with the W303 strain, significant variation and instability in colony colour was observed in the *tsa1Δ tsa2Δ* and *tsa1Δ TSA2* strains (see Figures 5.2 and 5.3). This variability diminished during subsequent re-streaking and 3 or more sequential streaks, approximately 10% of red and none of white colonies changed colour. To determine whether the same colony colour variability occurred in the 74-D694 strain, white, red and pink *tsa1Δ tsa2Δ* colonies obtained from T. Sideri (University of Manchester) were re-streaked on ¼ YEPD plates. No colony change was observed for any of the colour variants streaked out (data not shown) indicating that colony colour instability was only expressed in a *SUQ5* background.

Since colony colour appeared to be stable in the 74-D694 strain, the colony colour assay could be used to distinguish [*PSI*⁺] from *SUP*⁺ cells. The reliability of the assay was confirmed by testing one colony of [*PSI*⁺] and *SUP*⁺ for each of the *TSA* deletion strains (Figure 5.5a). All [*PSI*⁺] colonies tested (one per strain) had SDS-resistant Sup35p aggregates that were eliminated from colony replicas following growth on 5mM GndHCl YEPD plates, in contrast none (one per strain) of the *SUP*⁺ colonies had SDS-resistant aggregates. Figure 5.5a was included in Sideri *et al.* (2010).

5.4.4 Presence of aggregates observed on SDD-AGE coincides with presence of visible foci

A *tsa1Δ tsa2Δ* [*PSI*⁺] colony that had been isolated for SDD-AGE analysis in the experiments described above was also tested for the presence of Sup35pNM-GFP foci. Cells were cultured in medium lacking uracil to select for cells that retained the *URA3-*

based p6442 plasmid. Expression of the *SUP35NM-GFP* was induced by addition of 25µM CuSO$_4$ to the medium and the cells were observed after two hour of induction, as described above.

The *tsa1Δ tsa2Δ* [*PSI*⁺] cells had small Sup35p-containing foci (Figure 5.5b), confirming that the aggregates observed in SDD-AGE were [*PSI*⁺].The foci were smaller and fainter in *tsa1Δ tsa2Δ* [*PSI*⁺] cells than were foci observed in the wt control, possibly because *SUP35NM-GFP* expression is weaker in the former strain. The *CUP1* promoter is "leaky" (Zhou et al., 2001), enabling low levels of Sup35NM-GFP expression. Overexpression, even of the truncated Sup35 protein, is toxic in [*PSI*⁺] cells (Vishveshwara *et al.*, 2009). Cells with *tsa1Δ tsa2Δ* deletion are exposed to oxidative stress and DNA/genomic instability (Sideri *et al.*, 2010, Iraqui *et al.*, 2009) and are probably more sensitive to toxicity caused by *SUP35NM-GFP* expression. In such conditions there would be a strong selection against expression of *SUP35NM-GFP*, which could result in mutations that suppress expression of this gene. Presence of such mutations was not tested for.
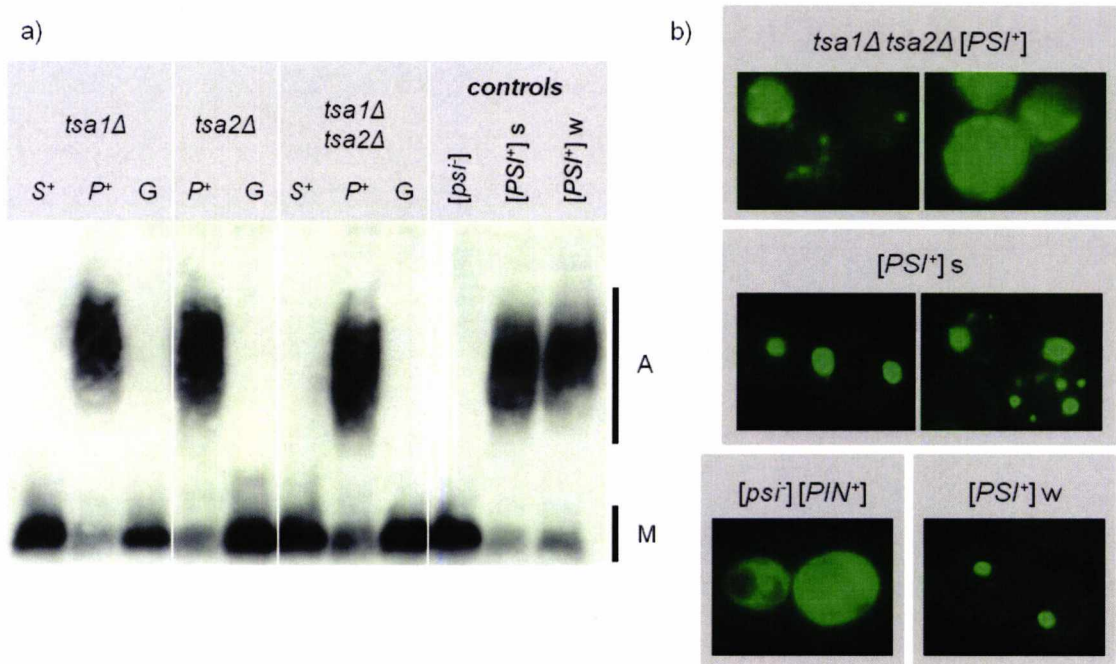
Figure 5.5: Visualisation of Sup35p aggregates from the induced *de novo* [*PSI*⁺] experiment. a) SDD-AGE of 74-D694 colonies. A colony of [*PSI*⁺] and *SUP*⁺ (identified by colony colour assay) per each *TSA* deletion strain was tested, along with guanidine hydrochloride treated replicas of [*PSI*⁺] colonies. All [*PSI*⁺] (P⁺) colonies had SDS-resistant aggregates (A), while in *SUP*⁺ (S⁺) or guanidine hydrochloride treated [*PSI*⁺] colonies (G) only Sup35p monomers were present (M); the blot was probed with αSup35p antibodies and developed using the ECL method; b) Cells from a *tsa1Δ tsa2Δ* [*PSI*⁺] colony were observed under the microscope after 2h induction with CuSO$_4$. Sup35NM-GFP decorated pre-existing aggregates, but did not aggregate on its own. Small aggregates were visible in *tsa1Δ tsa2Δ* [*PSI*⁺] cells; [*PSI*⁺] s/w – strong and weak [*PSI*⁺] strains.

The data obtained on prion formation, propagation, size and shape of Sup35pNM-GFP and Sup35p aggregates further confirm that the *tsa1Δ tsa2Δ* strain forms a typical [*PSI*⁺] prion (see also conclusion of 5.2).

5.4.5 Frequency of spontaneous *de novo* [*PSI*⁺] formation

The rate of induced *de novo* [*PSI*⁺] formation in the *tsa1Δ tsa2Δ* strain was lower than the rate observed in the wt strain (Figure 5.4). This is unexpected since oxidative stress promotes [*PSI*⁺] formation (Tyedmers *et al.*, 2008) and contradicts the observation reported by Sideri *et al.*, (2010, 2011). It is possible that high levels of expression of *SUP35NM* are hindering [*PSI*⁺] formation or are particularly toxic for [*PSI*⁺] in a *tsa1Δ tsa2Δ* strain. A more realistic comparison of *tsa1Δ tsa2Δ* to wt rates would be to compare rates of spontaneous [*PSI*⁺] formation as used by Sideri *et al* (2010). In an experiment, performed as described by Lancaster *et al.* (2010) and in Chapter 3 of this thesis, using adenine deficient media supplemented with 1% (v/v) YEPD, spontaneous rates in *tsa1Δ TSA2* and wt strains were compared (Figure 5.6a). The *tsa1Δ TSA2* strain displayed a much higher rate of *SUP*⁺ mutations, but a comparable rate of [*PSI*⁺] formation.

ratio to wt	[*PSI*⁺]	*SUP*⁺
tsa1Δ	1.5	7.0
tsa1Δ tsa2Δ	-	7.0
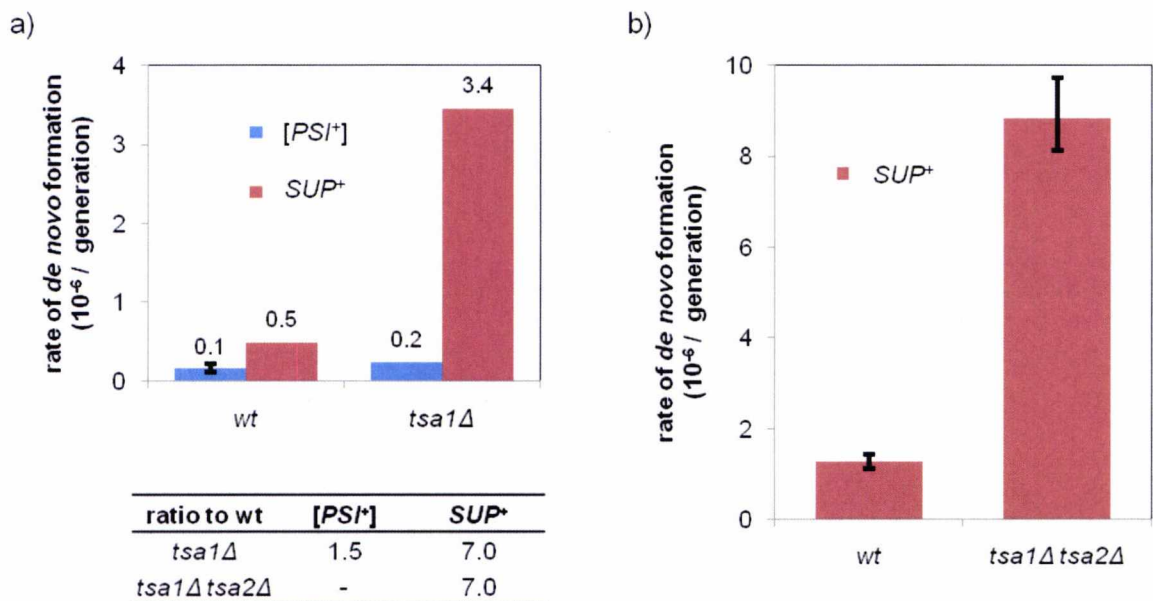
Figure 5.6: Rates of spontaneous *de novo* [*PSI*⁺] formation compared to rates of appearance of *SUP*⁺ in *TSA* deletion strains. a) the rate of [*PSI*⁺] *de novo* formation in a 74-D694 *tsa1Δ TSA2* strain is similar to the wt rate, while the rate of *SUP*⁺ appearance is significantly higher; b) the *tsa1Δ tsa2Δ* strain has a *SUP*⁺ rate similar to the rate in *tsa1Δ TSA2* strain; experiments were designed as described in Lancaster *et al.*, 2010 and analysed with software obtained from Lancaster and Masel; data in a) and b) are from two separate experiments.

The rate of spontaneous *de novo* [*PSI*⁺] formation in a *tsa1Δ tsa2Δ* strain was then quantified using MM-Ade medium without YEPD. As described in Chapter 3 (section 3.3.4) the rates of spontaneous *de novo* [*PSI*⁺] formation on such non-supplemented plates were significantly lower compared to rates on YEPD supplemented plates. The rate for wt strain was below the sensitivity of the assay, but the rate observed for *tsa1Δ tsa2Δ* strain [1.1×10^{-7} ($5 \times 10^{-8} - 3.3 \times 10^{-7}$) per generation] was comparable to that of *ppq1Δ* strain [1.7×10^{-7} ($4.8 \times 10^{-8} - 4.5 \times 10^{-7}$) per generation]. These data, while not allowing for estimation of the actual rate of spontaneous *de novo* formation in *tsa1Δ tsa2Δ* strain (see section 3.3.4 for suppression of growth of [*PSI*⁺] colonies on non-complemented selective medium) strongly suggest that the rate is increased compared to wt, possibly to the same extent as seen in a *ppq1Δ* strain. The rate of *SUP*⁺ mutations was not affected in the experiment (Figure 5.6b), since rates of *SUP*⁺ mutations in wt and *ppq1Δ* strains are comparable to previous experiments (Figure 5.6a, Chapter 3 section 3.3.4 and Lancaster *et al.*, 2010).

5.5   Discussion

5.5.1 Nonsense suppression in *TSA1/2* deletion strains

The suppressor phenotypes observed in the *tsa1Δ tsa2Δ* W303 strain were not caused by appearance of the [*PSI*⁺] prion as they were not reversible through growth on 5mM GdnHCl medium. Further analysis showed that a *tsa1Δ TSA2* strain also had a high frequency appearance of white, Ade⁺ colonies while no change was observed in a *tsa2Δ* strain. These observations agree with previous reports that *TSA1* deletion is necessary to increase genomic instability and that a *TSA2* deletion, although enhancing the instability of *tsa1Δ*, had little effect on its own (Wong *et al.*, 2004, Iraqui *et al.*, 2009). On the other hand, if oxidative stress were responsible for a high frequency appearance of white, Ade⁺ colonies, one would expect the *tsa1Δ tsa2Δ* strain to have a significantly higher frequency of white, Ade⁺ mutants relative to a *tsa1Δ TSA2* strain.

That nuclear gene mutations, rather than stress-induced damage to the translational apparatus, was responsible for the observed nonsense suppression in the W303 strain was further confirmed in a genetically unrelated strain, 74-D694. The rates of appearance of Ade⁺ cells were significantly higher in both the *tsa1Δ tsa2Δ* and *tsa1Δ TSA2* strains compared to wt and *TSA1 tsa2Δ* strains in the 74-D694 background.

Another line of evidence supporting nuclear mutations as the cause for the nonsense suppression phenotype was the difference in the frequency of colony growth/colour

change between *SUQ5* and *suq5*⁺ strains. The latter strains had a much lower frequency of suppressor colonies appearing in all *TSA* backgrounds as expected, since the ability of *SUQ5* to suppress the UAA codon requires the presence of allosuppressor mutations or [*PSI*⁺], while the wild-type *suq5*⁺ allele does not. Although no white colonies were observed to arise from a red *tsa1Δ tsa2Δ suq5*⁺ strain in subsequent streaks, it can be assumed that the frequency was at least 10 times lower since this is the frequency with which dominant suppressor mutations arise compared to allosuppressor mutations (Cox, 1977; see also chapter 3).

The question is how the initial white *tsa1Δ tsa2Δ suq5*⁺ strain was isolated. Results shown in Figure 5.2, where colonies were grown from spores that were replica plated to adenine deficient medium, show that 6 out of 14 spores had a mixture of white and red colonies. This suggests that at least during the initial growth from spores, the rate of appearance of *SUP*⁺ mutants was much higher. Again, the effect was observed in both *tsa1Δ tsa2Δ* and *tsa1Δ TSA2* strains.

5.5.2   [*PSI*⁺] prion formation in *tsa1Δ tsa2Δ* strain:

Simultaneous deletion of the *TSA1* and *TSA2* genes induced [*PSI*⁺] prion formation, as confirmed by the presence of Sup35p aggregates in these cells. The [*PSI*⁺] prion in this strain did not differ from previously described [*PSI*⁺] prion variants, in that it could not suppress the *ade2-1* allele in a *suq5*⁺ background. The size of the SDS-resistant aggregates and their infectivity were similar to strong [*PSI*⁺] prion variants (section 5.2.4, Figure 5.1d).

The rate of spontaneous *de novo* [*PSI*⁺] prion formation was measured only on non-supplemented adenine deficient plates, which partially suppresses the growth of [*PSI*⁺] colonies. Comparison of the rates of [*PSI*⁺] prion formation in wt and *ppq1Δ* strains using the same medium indicated that the rate of [*PSI*⁺] formation in the *ppq1Δ* strain was similar to that observed in the *tsa1Δ tsa2Δ* strain. It is likely that only some [*PSI*⁺] prion variants can grow on MM-Ade medium and since it is possible that *ppq1Δ* and *tsa1Δ tsa2Δ* strains promote different variants, precise estimates of the rate of spontaneous *de novo* [*PSI*⁺] prion formation cannot be made from these data. Sideri *et al.* (2010) observed a much higher frequency of *de novo* [*PSI*⁺] formation (published in Sideri *et al.*, 2010), although the assay used was a qualitative one. That deletion of both *TSA* genes indeed causes prion formation was further confirmed by abolishing the appearance of white, Ade⁺ colonies in *tsa1Δ tsa2Δ* strain by growing them in anoxic conditions. Sideri *et al.* (2010)

also showed that hydrogen peroxide promotes prion formation and that [*PSI*+] appearance is directly correlated to Sup35p oxidation on Met residues (Sideri *et al.*, 2011).

The appearance of *SUP*+ mutants was therefore predominantly a consequence of loss of Tsa1p. Any significant effect on [*PSI*+] prion formation on the other hand was only observed when both *TSA* genes were deleted (section 5.4.5).

The rate of induced *de novo* formation of [*PSI*+] was significantly lower in a *tsa1Δ tsa2Δ* strain compared to a wt strain. There are several possible explanations for this unexpected observation: $CuSO_4$ used to induce expression is toxic to wt cells even at 50μM concentration. In the experiment, copper was used at 25μM, but it is likely that a *TSA* deletion strain was more sensitive to $CuSO_4$ toxicity than a wt strain, since even under normal aerobic conditions, the deletion strain is under severe stress due to DNA/genomic instability (Iraqui *et al.*, 2009) and oxidative stress (Sideri *et al.*, 2010). This hypothesis does not explain why the rate of *SUP*+ mutations was not affected. Alternatively, while overexpression of *SUP35NM* is not toxic in a [*psi*-] background (Derkatch *et al.*, 1996) it is possible that once [*PSI*+] is induced, the 'stressed' *tsa1Δ tsa2Δ* mutant might be particularly susceptible to additional Sup35pNM-induced stress.

Comparison of *SUP*+ *de novo* appearance rates in induced (Figure 5.4) and spontaneous experiments (Figure 5.6) showed that the rates in the former are approximately 100-fold higher for all strains, as originally reported by Chernoff *et al.* (1992). It is unlikely that overexpression of Sup35pNM induces suppressor mutations. Another possibility is that the NM domain binds to the Sup35p protein and prevents the Sup35p interaction with Sup45p (eRF1) that is necessary for efficient termination of translation. Sequestration of Sup35p would allow cells to grow for a few generations on a selective medium inflating the apparent rate of *de novo SUP*+ appearance. *SUP35NM* was only transiently expressed and even if Sup35pNM was not degraded, it would be diluted out within the 7 generations that are necessary to achieve a 100-fold increase in cell number, and therefore a 100-fold increase in *SUP*+ appearance estimates. Alternatively, low level expression of *SUP35NM* gene under *CUP1* promoter control in non-inducing conditions has been reported (Zhou *et al.*, 2001), but it is unknown if low levels of Sup35pNM could sequester high-abundance Sup35 protein sufficiently to induce nonsense suppression. Furthermore, the appearance of white colonies was never observed when non-induced colonies were restreaked. The remaining possibility is that appearance of the [*PSI*+] prion promotes additional *SUP*+ mutations. [*PSI*+] cells growing on adenine deficient plates retain the same rate of *SUP*+ mutations and since such mutants suppress the *ade1-14* allele more efficiently, they would overgrow [*PSI*+] cells in the colony.

5.5.3   Summary of findings

The simultaneous deletion of the *TSA1* and *TSA2* genes promotes the *de novo* appearance of the [*PSI*⁺] prion and undefined *SUP*⁺ nuclear mutations. These consequences of *TSA* gene deletion arise via two independent mechanisms; *TSA1* deletion increases the rate of *SUP*⁺ mutations by increasing intracellular ROS, with the subsequent effect on DNA damage checkpoints and dNTP overexpression (Tang *et al.*, 2009). Increased intracellular levels of ROS do not affect [*PSI*⁺] prion formation (section 5.4.5, Figure 5.6), presumably because levels of the ribosome bound Tsa2p are sufficient to prevent oxidative damage to Sup35p. The rate of [*PSI*⁺] prion formation is elevated only in a *tsa1Δ tsa2Δ* mutant, and is triggered by oxidative damage to Sup35p protein (Sideri *et al.*, 2011).

Chapter VI

General discussion

6.1   Summary

Prions are aggregates of misfolded proteins that have acquired an amyloid-like structure and ability to propagate through recruitment of new proteins. Prion aggregates are infectious and are in mammals linked to neurodegenerative diseases. Several prions have been described to date in budding yeast *S. cerevisiae* and, while not severely detrimental to cells yeast prions have a far-reaching effect on gene expression, translation and nutrient acquisition. Prion formation in yeast can be induced by environmental stress and it has been suggested that yeast prions could represent a mechanism to adapt to changing environment. Yeast prions are stably transmitted from mother to daughter cells and therefore represent a novel form of inheritance.

[*PSI*⁺], a prion form of eukaryotic release factor Sup35 (eRF1) is widely used as a model for research on prion formation and propagation and in this study [*PSI*⁺] is used to explore an effect of three previously identified proteins on *de novo* prion formation. One mechanism proposed to affect prion formation is direct interaction of Sup35p with its binding partners, presumably by preventing Sup35p misfolding. Search for proteins that interact with Sup35p identified Ppq1p, a putative Ser/Thr protein phosphatise (M.F. Tuite and T. von der Haar). Another approach was to identify proteins that function to protect translational apparatus from environmental and endogenous oxidative damage, since deletion of genes coding for these proteins would presumably result in oxidative damage to proteins involved in mRNA translation, including Sup35p. This approach identified two ribosome associated peroxiredoxins, Tsa1p and Tsa2p (T. Sideri and C.M. Grant).

The work presented in this thesis shows that the deletion of *PPQ1* gene greatly increases the rate of *de novo* formation of [*PSI*⁺], but the mechanism by which loss of Ppq1p affects [*PSI*⁺] formation is not known. Although Ppq1p physically interacts with Sup35p, cellular levels of Ppq1p are 300-fold lower than levels of Sup35 (von der Haar, 2008; Ghaemmaghami *et al.*, 2003) and the suppression of *de novo* [*PSI*⁺] formation is therefore not likely to be caused by interaction per se. Phosphorylation of Sup35p has not been observed *in vivo* (Fabret *et al.*, 2008; P. Mugnier, P.M. Herbert, M.F. Tuite, unpublished) and Ppq1p does not seem to directly dephosphorylate Sup35p (T. von der Haar, personal communication). Possible cellular roles of Ppq1p were investigated in an attempt to elucidate the mechanism of Ppq1p-caused suppression of *de novo* [*PSI*⁺] formation. Investigation of Ppq1p role in translation showed that the deletion of the *PPQ1* gene reduces accuracy of translation and increases nonsense suppression, a result that was also observed in the *de novo* formation [*PSI*⁺] assay and was reported previously (Song *et al.*, 1987). Genes and proteins identified through their interactions with Ppq1p, similarity in

gene expression pattern or that cause similar sensitivity to environmental conditions in gene knock-out strains were used in GO term analysis to identify cellular processes Ppq1p might be involved in. Such analysis identified several processes beyond translation, such as processes involved in nuclear and chromosomal organisation and other cytoskeleton related processes. Ppq1p has an unusual N-domain that is biased toward Ser and Asn residues and that could promote aggregation. Fluorescent microscopy study showed that N-domain is unlikely to promote aggregation in a prion-like manner, but is sufficient for co-localisation of Ppq1p with mitochondria under stress, although these results are considered to be preliminary. Link to mitochondria was further supported by an observed reduction in respiratory capacity of a *ppq1Δ* strain. The significance of the link between Ppq1p and mitochondria is not understood and requires further investigation.

That exposure to environmental sources of oxidative stress promotes [*PSI*⁺] prion formation was previously reported (Tyedmers et al., 2008). Results presented in this thesis shows that an endogenous source of oxidative stress, brought about by deleting the ribosomally-associated peroxiredoxins (Prx) encoded by genes *TSA1/2* (Trotter *et al.,* 2008; Sideri *et al.,* 2010), also increases the rate of de novo [*PSI*⁺] formation. This result provides a direct link between oxidative stress and the eukaryotic release factor Sup35p. Sideri *et al.* (2011) subsequently showed that formation of [*PSI*⁺] is directly linked to oxidation of methionine residues in Sup35p. The link between increased rate of de *novo* prion formation and increased oxidative stress in a *tsa1 tsa2* mutant appears to be specific to prions of ribosomally associated proteins ([*PSI*⁺] and [*PIN*⁺]; Sideri *et al.*, 2011).

6.2   Possible mechanisms of Ppq1p suppression of [*PSI*⁺] formation

New data on the effect of *PPQ1* gene deletion and the localisation of Ppq1p within a cell allow proposition of two exclusive hypotheses on the mechanism by which Ppq1p inhibits [*PSI*⁺] formation:

The first hypothesis assumes that Ppq1p functions to prevent Sup35p misfolding at the site of protein synthesis, the ribosome. The mechanism most likely does not involve direct protein structure stabilising interactions between Sup35p and Ppq1p, i.e. the mechanism by which overexpression of *SUP45* is believed to decrease [*PSI*⁺] formation (Derkatch *et al.,* 1998), because Ppq1p is approximately 300-fold less abundant in the cell then Sup35p (von der Haar, 2008; Ghaemmaghami *et al.*, 2003). Direct dephosphorylation of Sup35p by Ppq1p also seems unlikely since Sup35p has not been observed to be

phosphorylated *in vivo* (Fabret *et al.*, 2008; P. Mugnier, P.M. Herbert, M.F. Tuite, unpublished). Ppq1p could however dephosphorylate as of yet unidentified proteins that interact with Sup35p. Dephosphorylation of such proteins could increase their Sup35p-binding affinity and therefore increase the pool of unbound Sup35p within the cell, which would be free to misfold into the prion conformation.

Although the mechanism by which Ppq1p inhibits [*PSI*⁺] formation is not understood, this hypothesis could explain how environmental factors promote [*PSI*⁺] formation. Several chemicals were shown in this thesis (section 4.4.4) to trigger re-localisation of Ppq1p to foci that co-localise with mitochondrial markers. These same chemicals, namely $MnCl_2$, NaCl and H_2O_2, have previously been shown to induce [*PSI*⁺] (Tyedmers *et al.*, 2008). The hypothesis proposes that Ppq1p acts by an as yet unknown mechanism to prevent [*PSI*⁺] formation, but under certain environmental conditions Ppq1p re-locates to cytoplasmic foci, mimicking the effect of *PPQ1* deletion, with re-localised Ppq1p now unable to prevent [*PSI*⁺] formation (section 3.3.2). According to this hypothesis, environmental stress would promote prion formation by sequestering Ppq1p protein. The hypothesis could be tested by exploring whether other [*PSI*⁺] promoting chemicals trigger the re-location of Ppq1p to foci, for example chemicals such as $ZnSO_4$, LiCl, K, Mg-acetate and DTT (Tyedmers *et al.*, 2008). An assumption of this hypothesis is that Sup35p does not re-locate with Ppq1p to foci, so the co-localisation of Ppq1p and Sup35p under conditions that promote re-localisation of Ppq1p to foci should also be tested.

An alternative hypothesis proposes that Ppq1p affects factors that function in actin organisation/endocytotic vesicles formation, but which have also been shown to promote [*PSI*⁺] formation (e.g. Sla1, Sla2, Las17, Vps5, Sac6 proteins; Ganusova *et al.*, 2006; Manogaran *et al.*, 2011). Many links to actin and endocytosis were uncovered in an analysis of available databases: homozygous and heterozygous *ppq1Δ* mutants were both sensitive to the actin polymerisation interfering drug latrunculin (FitDb, Table 4.5); Ppq1p physically interacts with Bzz1p (Tonikian *et al.*, 2009; Biogrid), a protein involved in the regulation of actin polymerisation and that interacts with Las17p (Soulard *et al.*, 2002); and 'cytoskeleton organisation' was an enriched GO process term in an analysis of physically and genetically interacting factors (BioGrid, Table 4.4). It is not yet understood how factors involved in actin organisation and endocytotic vesicle formation promote prion formation, and as such speculation on Ppq1p's contribution to this process is not strictly possible, however, Ppq1p may affect the phosphorylation status of one or more of these factors and consequently alter their activity or interaction with Sup35p.

Finally, while conditions that promoted the co-localisation of Ppq1p with reticular mitochondria were not identified, prolonged exposure to $MnCl_2$, EtOH, NaCl and H_2O_2 did induce the co-localisation of Ppq1p with fragmented mitochondria (sections 4.4.4.2 and 4.4.4.3). The characteristic of this co-localisation was not explored further, but it is possible that fragmented mitochondria were being targeted for degradation. This latter proposition could be tested by repeating the experiments described in sections 4.4.4.2 and 4.4.4.3, in the presence of a vacuole-selective stain such as FM4-64. The absence of further data prevents speculation as to how Ppq1ps localisation with fragmented mitochondria might affect [*PSI*⁺] formation.

6.3   Does Ppq1p affect *de novo* formation of other yeast prions?

One way to explore the effect of Ppq1p on [*PSI*⁺] formation would be to investigate interactions between Ppq1p and other yeast prion proteins, for example Rnq1p and Ure2p, and whether Ppq1p also affects the formation of their respective prions, [*PIN*⁺] and [*URE3*]. Such an experiment could produce one of four different results:

1. Ppq1p does not physically interact with other yeast prion proteins but still affects *de novo* formation of their respective prions. This result would suggest that Ppq1p has a general role in prion formation probably linked to activities of Ppq1p that effect factors involved in actin organisation/endocytotic vesicle formation, which have direct though unexplained roles in prion formation.

2. Ppq1p does not interact with Rnq1p or Ure2p and does not affect the appearance of [*PIN*⁺] or [*URE3*]. This result would indicate that the role of Ppq1p in prion formation is limited to an effect on Sup35p and the [*PSI*⁺] prion, and that Ppq1p probably functions at the site of Sup35p's initial misfolding event, possibly by affecting one or more factors involved in translation.

3. Ppq1p interacts with either one or both Rnq1p and Ure2p and it affects formation of the respective prion. While interaction of Ppq1p with Rnq1p would not be surprising, since both interact with Sup35p (M.F. Tuite and T. von der Haar, personal communication; Tuite *et al.*, 2008) an interaction of Ppq1p with Ure2p would suggest that Ppq1p has a general role in yeast prion formation, probably by directly affecting prion proteins at the site of prion formation.

4. A result that Ppq1p interacts with both proteins, but does not affect [*PIN*⁺] or [*URE3*] would be surprising and not informative in terms of understanding the role of Ppq1p in ([*PSI*⁺]) prion formation.

Exploring the effect of Ppq1p on [*PIN*⁺] *de novo* formation would be particularly interesting because both proteins, Ppq1p and Rnq1p, share several characteristics. Deletion of either *PPQ1* or the *RNQ1* gene has been shown in this study to reduce the rate of uncoupled respiration, the maximum capacity of the electron transport system (Section 4.5.2). The *ppq1Δ* strain also had a decreased growth rate and survival in early stationary phase (Chen *et al.*, 1993; Section 4.3.2.1), while [*PIN*⁺] negatively affects cell survival in stationary phase (G.L. Staniforth, personal communication). In terms of Ppq1p and Rnq1p effecting Sup35p and [*PSI*⁺] prion formation, both proteins have been shown to interact with Sup35p (von der Haar, personal communication; Tuite *et al.*, 2008). Furthermore, it is possible that Ppq1p and Rnq1p physically interact. A yeast 2-hybrid assay failed to detect such an interaction (Section 3.3.5.3), though this result is not conclusive since, within the same experiment, the previously confirmed Rnq1p and Sup35p interaction (Tuite *et al.*, 2008) was also not observed.

[*PIN*⁺] in most cases refers to the prion of Rnq1p and is absolutely necessary for [*PSI*⁺] formation (Derkatch *et al.*, 1997; Derkatch *et al.*, 2001). Ppq1p on the other hand was identified as the strongest suppressor of formation of [*PSI*⁺] (Section 3.3.2; Tyedmers *et al.*, 2008). Ppq1p and Rnq1p both interact with Bzz1p (Tonikian *et al.*, 2009), an interaction that connects them to the presumed site of [*PSI*⁺] formation (Ganusova et al., 2006). The effect of *PPQ1* gene deletion on *de novo* formation of other yeast prions needs to be explored, but evidence uncovered thus far suggests that Ppq1p could negatively control *de novo* prion formation, that is, acts as an anti-[*PIN*⁺] factor.

6.4   Prion formation and filamentous growth

Several lines of evidence suggest that Ppq1p modulates filamentous (or pseudohyphal) growth. A transcription factor called Ste12p that is activated by a MAP kinase signalling pathway and which activates genes involved in filamentous/invasive growth, binds upstream of the *PPQ1* ORF (Liu *et al.*, 1993; Lefrancois *et al.*, 2009; Zheng *et al.*, 2010). In addition, deletion of the *PPQ1* gene promotes filamentous growth (Jin *et al.*, 2008). A condition known to promote filamentous growth, namely a high concentration of manganese (Asleson *et al.*, 2000), was also shown to induce Ppq1p re-localisation to mitochondrial markers (section 4.4.4.3) and to promote [*PSI*⁺] formation (Tyedmers *et al.*,

2008). Ppq1p could therefore represent a novel link between prion formation and filamentous/invasive growth. Filamentous growth represents a switch in growth strategy during nitrogen starvation or growth on poor carbon sources (Kron *et al.*, 1994; Lambrechts *et al.*, 1996). It would be interesting to test whether it is accompanied by a switch in the prion state of one or more yeast prion proteins, since many prions have a global effect on gene expression (Table 1.2). Such a link could be tested by exploring the effect of filamentous growth-inducing chemicals, such as isopropanol and isobutanol (Lorenz *et al.*, 2000) that are produced in nitrogen starvation conditions (Dickinson, 1994), on Ppq1p localisation within a cell and on the rate of [*PSI*$^+$] formation. An effect of prion formation on filamentous growth would be difficult to study, since most laboratory strains carry an *FLO8* allele with a premature stop codon, the *flo8-1*allele, and are consequently not capable of filamentous growth (Liu *et al.*, 1996; Eaglestone *et al.*, 1999). A connection between filamentous growth and prion formation, if uncovered, would suggest a functional role for yeast prions in natural settings.

References

Abdulrehman D., Monteiro P.T., Teixeira M.C., Mira N.P., Lourenco A.B., dos Santos S.C., *et al.* (2011) YEASTRACT: Providing a programmatic access to curated transcriptional regulatory associations in *Saccharomyces cerevisiae* through a web services interface. *Nucleic Acids Res* **39**: D136-40.

Aksenova A., Munoz I., Volkov K., Arino J., and Mironova L. (2007) The *HAL3-PPZ1* dependent regulation of nonsense suppression efficiency in yeast and its influence on manifestation of the yeast prion-like determinant [*ISP*+]. *Genes Cells* **12**: 435-445.

Alberti S., Gitler A.D., and Lindquist S. (2007) A suite of gateway cloning vectors for high-throughput genetic analysis in *Saccharomyces cerevisiae*. *Yeast* **24**: 913-919.

Alberti S., Halfmann R., King O., Kapila A., and Lindquist S. (2009) A systematic survey identifies prions and illuminates sequence features of prionogenic proteins. *Cell* **137**: 146-158.

Allen K.D., Chernova T.A., Tennant E.P., Wilkinson K.D., and Chernoff Y.O. (2007) Effects of ubiquitin system alterations on the formation and loss of a yeast prion. *J Biol Chem* **282**: 3004-13.

Allen K.D., Wegrzyn R.D., Chernova T.A., Muller S., Newnam G.P., Winslett P.A., *et al.* (2005) Hsp70 chaperones as modulators of prion life cycle: Novel effects of ssa and ssb on the *Saccharomyces cerevisiae* prion [*PSI*+]. *Genetics* **169**: 1227-42.

Alper T., Haig D.A., and Clarke M.C. (1966) The exceptionally small size of the scrapie agent. *Biochem Biophys Res Commun* **22**: 278-284.

Asleson C.M., Asleson J.C., Malandra E., Johnston S., and Berman J. (2000) Filamentous growth of *Saccharomyces cerevisiae* is regulated by manganese. *Fungal Genet Biol* **30**: 155-162.

Astbury W.T., and Dickinson S. (1935) The X-ray interpretation of denaturation and the structure of the seed globulins. *Biochem J* **29**: 2351-2360.1.

Bagriantsev S., and Liebman S.W. (2004) Specificity of prion assembly in vivo. [*PSI*+] and [*PIN*+] form separate structures in yeast. *J Biol Chem* **279**: 51042-51048.

Bailleul P.A., Newnam G.P., Steenbergen J.N., and Chernoff Y.O. (1999) Genetic study of interactions between the cytoskeletal assembly protein sla1 and prion-forming domain of the release factor Sup35 (eRF3) in *Saccharomyces cerevisiae*. *Genetics* **153**: 81-94.

Balagopal V., and Parker R. (2009) Polysomes, P bodies and stress granules: States and fates of eukaryotic mRNAs. *Curr Opin Cell Biol* **21**: 403-408.

Ban N., Nissen P., Hansen J., Moore P.B., and Steitz T.A. (2000) The complete atomic structure of the large ribosomal subunit at 2.4 A resolution. *Science* **289**: 905-920.

Bandas E.L., and Zakharov I.A. (1980) Induction of rho⁻ mutations in yeast *Saccharomyces cerevisiae* by ethanol. *Mutat Res* **71**: 193-199.

Bauer H.H., Aebi U., Haner M., Hermann R., Muller M., and Merkle H.P. (1995) Architecture and polymorphism of fibrillar supramolecular assemblies produced by in vitro aggregation of human calcitonin. *J Struct Biol* **115**: 1-15.

Benko A.L., Vaduva G., Martin N.C., and Hopper A.K. (2000) Competition between a sterol biosynthetic enzyme and tRNA modification in addition to changes in the protein synthesis machinery causes altered nonsense suppression. *Proc Natl Acad Sci U S A* **97**: 61-66.

Bessen R.A., and Marsh R.F. (1994) Distinct prp properties suggest the molecular-basis of strain variation in transmissible mink encephalopathy. *Journal of Virology* **68**: 7859-7868.

Biteau B., Labarre J., and Toledano M.B. (2003) ATP-dependent reduction of cysteine-sulphinic acid by S. cerevisiae sulphiredoxin. *Nature* **425**: 980-984.

Blom N., Gammeltoft S., and Brunak S. (1999) Sequence and structure-based prediction of eukaryotic protein phosphorylation sites. *J Mol Biol* **294**: 1351-1362.

Bodenmiller B., Mueller L.N., Mueller M., Domon B., and Aebersold R. (2007) Reproducible isolation of distinct, overlapping segments of the phosphoproteome. *Nat Methods* **4**: 231-237.

Boeke J.D., LaCroute F., and Fink G.R. (1984) A positive selection for mutants lacking orotidine-5'-phosphate decarboxylase activity in yeast: 5-fluoro-orotic acid resistance. *Mol Gen Genet* **197**: 345-346.

Bradley M.E., and Liebman S.W. (2004) The Sup35 domains required for maintenance of weak, strong or undifferentiated yeast [*PSI*⁺] prions. *Mol Microbiol* **51**: 1649-1659.

Bradley M.E., and Liebman S.W. (2003) Destabilizing interactions among [*PSI*⁺] and [*PIN*⁺] yeast prion variants. *Genetics* **165**: 1675-85.

Bradley M.E., Edskes H.K., Hong J.Y., Wickner R.B., and Liebman S.W. (2002) Interactions among prions and prion "strains" in yeast. *Proc Natl Acad Sci U S A* **99 Suppl 4**: 16392-9.

Burck C.L., Chernoff Y.O., Liu R., Farabaugh P.J., and Liebman S.W. (1999) Translational suppressors and antisuppressors alter the efficiency of the Ty1 programmed translational frameshift. *RNA* **5**: 1451-1457.

Burston H.E., Maldonado-Baez L., Davey M., Montpetit B., Schluter C., Wendland B., and Conibear E. (2009) Regulators of yeast endocytosis identified by systematic quantitative analysis. *J Cell Biol* **185**: 1097-1110.

Byrne L.J., Cox B.S., Cole D.J., Ridout M.S., Morgan B.J., and Tuite M.F. (2007) Cell division is essential for elimination of the yeast [*PSI*⁺] prion by guanidine hydrochloride. *Proc Natl Acad Sci U S A* **104**: 11688-93.

Cardenas M.E., Cutler N.S., Lorenz M.C., Di Como C.J., and Heitman J. (1999) The TOR signaling cascade regulates gene expression in response to nutrients. *Genes & Dev.* **13**: 3271-3279

Cerveny K.L., and Jensen R.E. (2003) The WD-repeats of Net2p interact with Dnm1p and Fis1p to regulate division of mitochondria. *Mol Biol Cell* **14**: 4126-4139.

Chacinska A., Szczesniak B., Kochneva-Pervukhova N.V., Kushnirov V.V., Ter-Avanesyan M.D., and Boguta M. (2001) Ssb1 chaperone is a [*PSI*⁺] prion-curing factor. *Curr Genet* **39**: 62-7.

Chae H.Z., Chung S.J., and Rhee S.G. (1994) Thioredoxin-dependent peroxide reductase from yeast. *J Biol Chem* **269**: 27670-27678.

Chae H.Z., Kim I.H., Kim K., and Rhee S.G. (1993) Cloning, sequencing, and mutation of thiol-specific antioxidant gene of *Saccharomyces cerevisiae*. *J Biol Chem* **268**: 16815-16821.

Chan J.C., Oyler N.A., Yau W.M., and Tycko R. (2005) Parallel beta-sheets and polar zippers in amyloid fibrils formed by residues 10-39 of the yeast prion protein Ure2p. *Biochemistry* **44**: 10669-10680.

Chandler R.L. (1961) Encephalopathy in mice produced by inoculation with scrapie brain material. *Lancet* **1**: 1378-9.

Chen B., Newnam G.P., and Chernoff Y.O. (2007) Prion species barrier between the closely related yeast proteins is detected despite coaggregation. *Proc Natl Acad Sci U S A* **104**: 2791-2796.

Chen M.X., Chen Y.H., and Cohen P.T. (1993) PPQ, a novel protein phosphatase containing a ser + asn-rich amino-terminal domain, is involved in the regulation of protein synthesis. *Eur J Biochem* **218**: 689-699.

Chernoff Y.O., Derkach I.L., and Inge-Vechtomov S.G. (1993) Multicopy *SUP35* gene induces de-novo appearance of psi-like factors in the yeast *Saccharomyces cerevisiae*. *Curr Genet* **24**: 268-70.

Chernoff Y.O., Newnam G.P., Kumar J., Allen K., and Zink A.D. (1999) Evidence for a protein mutator in yeast: Role of the Hsp70-related chaperone ssb in formation, stability, and toxicity of the [*PSI*⁺] prion. *Mol Cell Biol* **19**: 8103-12.

Chernoff Y.O., Lindquist S.L., Ono B., Inge-Vechtomov S.G., and Liebman S.W. (1995) Role of the chaperone protein Hsp104 in propagation of the yeast prion-like factor [*PSI*⁺]. *Science* **268**: 880-4.

Chernoff Y.O., Inge-Vechtomov S.G., Derkach I.L., Ptyushkina M.V., Tarunina O.V., Dagkesamanskaya A.R., and Ter-Avanesyan M.D. (1992) Dosage-dependent translational suppression in yeast *Saccharomyces cerevisiae*. *Yeast* **8**: 489-499.

Chien P., and Weissman J.S. (2001) Conformational diversity in a yeast prion dictates its seeding specificity. *Nature* **410**: 223-227.

Chiti F., and Dobson C.M. (2006) Protein misfolding, functional amyloid, and human disease. *Annu Rev Biochem* **75**: 333-366.

Choe Y.J., Ryu Y., Kim H.J., and Seok Y.J. (2009) Increased [*PSI*⁺] appearance by fusion of Rnq1 with the prion domain of Sup35 in *Saccharomyces cerevisiae*. *Eukaryot Cell* **8**: 968-976.

Chua G., Morris Q.D., Sopko R., Robinson M.D., Ryan O., Chan E.T., *et al.* (2006) Identifying transcription factor functions and targets by phenotypic activation. *Proc Natl Acad Sci U S A* **103:** 12045-12050.

Clotet J., Gari E., Aldea M., and Arino J. (1999) The yeast ser/thr phosphatases Sit4 and Ppz1 play opposite roles in regulation of the cell cycle. *Mol Cell Biol* **19:** 2408-2415.

Clotet J., Posas F., de Nadal E., and Arino J. (1996) The NH2-terminal extension of protein phosphatase *PPZ1* has an essential functional role. *J Biol Chem* **271:** 26349-26355.

Collins S.R., Douglass A., Vale R.D., and Weissman J.S. (2004) Mechanism of prion propagation: Amyloid growth occurs by monomer addition. *PLoS Biol* **2:** e321.

Costanzo M., Baryshnikova A., Bellay J., Kim Y., Spear E.D., Sevier C.S., *et al.* (2010) The genetic landscape of a cell. *Science* **327:** 425-431.

Courchesne W.E., and Magasanik B. (1988) Regulation of nitrogen assimilation in *Saccharomyces cerevisiae*: Roles of the *URE2* and *GLN3* genes. *J Bacteriol* **170:** 708-713.

Coustou V., Deleu C., Saupe S., and Begueret J. (1997) The protein product of the het-s heterokaryon incompatibility gene of the fungus podospora anserina behaves as a prion analog. *Proc Natl Acad Sci U S A* **94:** 9773-8.

Cou M., Brenner S.L., Spector I., Korn E.D. (1987) Inhibition of actin polymerization by latrunculin A. *FEBS letters* **213**: 316-318.

Cox B., Ness F., and Tuite M. (2003) Analysis of the generation and segregation of propagons: Entities that propagate the [*PSI*$^+$] prion in yeast. *Genetics* **165:** 23-33.

Cox B.S. (1965) *PSI*, a cytoplasmic suppressor of supersuppressor in yeast. *Heredity* **20:** 505-521.

Crick F. (1970) Central dogma of molecular biology. *Nature* **227:** 561-563.

Cunningham T.S., Andhare R., and Cooper T.G. (2000) Nitrogen catabolite repression of DAL80 expression depends on the relative levels of Gat1p and Ure2p production in *Saccharomyces cerevisiae*. *J Biol Chem* **275:** 14408-14414.

Dagkesamanskaya A.R., and Ter-Avanesyan M.D. (1991) Interaction of the yeast omnipotent suppressors *SUP1* (*SUP45*) and *SUP2* (*SUP35*) with non-mendelian factors. *Genetics* **128:** 513-520.

de Nadal E., Fadden R.P., Ruiz A., Haystead T., and Arino J. (2001) A role for the ppz Ser/Thr protein phosphatases in the regulation of translation elongation factor 1Balpha. *J Biol Chem* **276:** 14829-14834.

DePace A.H., Santoso A., Hillner P., and Weissman J.S. (1998) A critical role for amino-terminal glutamine/asparagine repeats in the formation and propagation of a yeast prion. *Cell* **93:** 1241-1252.

Derkatch I.L., Bradley M.E., and Liebman S.W. (1998) Overexpression of the *SUP45* gene encoding a Sup35p-binding protein inhibits the induction of the *de novo* appearance of the [*PSI*+] prion. *Proc Natl Acad Sci U S A* **95**: 2400-5.

Derkatch I.L., Bradley M.E., Hong J.Y., and Liebman S.W. (2001) Prions affect the appearance of other prions: The story of [*PIN*+]. *Cell* **106**: 171-182.

Derkatch I.L., Bradley M.E., Zhou P., Chernoff Y.O., and Liebman S.W. (1997) Genetic and environmental factors affecting the de novo appearance of the [*PSI*+] prion in *Saccharomyces cerevisiae*. *Genetics* **147**: 507-519.

Derkatch I.L., Chernoff Y.O., Kushnirov V.V., Inge-Vechtomov S.G., and Liebman S.W. (1996) Genesis and variability of [*PSI*+] prion factors in *Saccharomyces cerevisiae*. *Genetics* **144**: 1375-1386.

Derkatch I.L., Uptain S.M., Outeiro T.F., Krishnan R., Lindquist S.L., and Liebman S.W. (2004) Effects of Q/N-rich, polyQ, and non-polyQ amyloids on the de novo formation of the [*PSI*+] prion in yeast and aggregation of Sup35 in vitro. *Proc Natl Acad Sci U S A* **101**: 12934-9.

Derkatch I.L., Bradley M.E., Masse S.V., Zadorsky S.P., Polozkov G.V., Inge-Vechtomov S.G., and Liebman S.W. (2000) Dependence and independence of [*PSI*+] and [*PIN*+]: A two-prion system in yeast? *EMBO J* **19**: 1942-52.

Dickinson J.R. (1994) Irreversible formation of pseudohyphae by haploid *Saccharomyces cerevisiae*. *FEMS Microbiol Lett* **119**: 99-103.

Dobson C.M. (2003) Protein folding and misfolding. *Nature* **426**: 884-890.

Doel S.M., McCready S.J., Nierras C.R., and Cox B.S. (1994) The dominant *PNM2*-mutation which eliminates the psi factor of *Saccharomyces cerevisiae* is the result of a missense mutation in the *SUP35* gene. *Genetics* **137**: 659-670.

Du Z., Park K.W., Yu H., Fan Q., and Li L. (2008) Newly identified prion linked to the chromatin-remodeling factor Swi1 in *Saccharomyces cerevisiae*. *Nat Genet* **40**: 460-465.

DuBay K.F., Pawar A.P., Chiti F., Zurdo J., Dobson C.M., and Vendruscolo M. (2004) Prediction of the absolute aggregation rates of amyloidogenic polypeptide chains. *J Mol Biol* **341**: 1317-1326.

Dyczkowski J., and Vingron M. (2005) Comparative analysis of cell cycle regulated genes in eukaryotes. *Genome Inform* **16**: 125-131.

Eaglestone S.S., Cox B.S., and Tuite M.F. (1999) Translation termination efficiency can be regulated in *Saccharomyces cerevisiae* by environmental stress through a prion-mediated mechanism. *EMBO J* **18**: 1974-1981.

Eaglestone S.S., Ruddock L.W., Cox B.S., and Tuite M.F. (2000) Guanidine hydrochloride blocks a critical step in the propagation of the prion-like determinant [*PSI*+] of *Saccharomyces cerevisiae*. *Proc Natl Acad Sci U S A* **97**: 240-244.

Eurwilaichitr L., Graves F.M., Stansfield I., and Tuite M.F. (1999) The C-terminus of eRF1 defines a functionally important domain for translation termination in *Saccharomyces cerevisiae*. *Mol Microbiol* **32:** 485-96.

Fabret C., Cosnier B., Lekomtsev S., Gillet S., Hatin I., Le Marechal P., and Rousset J.P. (2008) A novel mutant of the Sup35 protein of *Saccharomyces cerevisiae* defective in translation termination and in GTPase activity still supports cell viability. *BMC Mol Biol* **9:** 22.

Fan Q., Park K.W., Du Z., Morano K.A., and Li L. (2007) The role of Sse1 in the de novo formation and variant determination of the [*PSI*⁺] prion. *Genetics* **177:** 1583-93.

Fandrich M., Fletcher M.A., and Dobson C.M. (2001) Amyloid fibrils from muscle myoglobin. *Nature* **410:** 165-166.

Fernandez-Escamilla A.M., Rousseau F., Schymkowitz J., and Serrano L. (2004) Prediction of sequence-dependent and mutational effects on the aggregation of peptides and proteins. *Nat Biotechnol* **22:** 1302-1306.

Ferreira P.C., Ness F., Edwards S.R., Cox B.S., and Tuite M.F. (2001) The elimination of the yeast [*PSI*⁺] prion by guanidine hydrochloride is the result of Hsp104 inactivation. *Mol Microbiol* **40:** 1357-69.

Ferris J.P. (2006) Montmorillonite-catalysed formation of RNA oligomers: The possible role of catalysis in the origins of life. *Philos Trans R Soc Lond B Biol Sci* **361:** 1777-86; discussion 1786.

Frolova L.Y., Merkulova T.I., and Kisselev L.L. (2000) Translation termination in eukaryotes: Polypeptide release factor eRF1 is composed of functionally and structurally distinct domains. *RNA* **6:** 381-90.

Gajdusek D.C., Gibbs C.J., and Alpers M. (1966) Experimental transmission of a kuru-like syndrome to chimpanzees. *Nature* **209:** 794-6.

Galletta B.J., and Cooper J.A. (2009) Actin and endocytosis: Mechanisms and phylogeny. *Curr Opin Cell Biol* **21:** 20-27.

Ganusova E.E., Ozolins L.N., Bhagat S., Newnam G.P., Wegrzyn R.D., Sherman M.Y., and Chernoff Y.O. (2006) Modulation of prion formation, aggregation, and toxicity by the actin cytoskeleton in yeast. *Mol Cell Biol* **26:** 617-629.

Ghaemmaghami S., Huh W.K., Bower K., Howson R.W., Belle A., Dephoure N., *et al.* (2003) Global analysis of protein expression in yeast. *Nature* **425:** 737-741.

Gietz R.D., and Schiestl R.H. (2007) High-efficiency yeast transformation using the LiAc/SS carrier DNA/PEG method. *Nat Protoc* **2:** 31-34.

Gilks N., Kedersha N., Ayodele M., Shen L., Stoecklin G., Dember L.M., and Anderson P. (2004) Stress granule assembly is mediated by prion-like aggregation of TIA-1. *Mol Biol Cell* **15:** 5383-5398.

Glover J.R., and Lindquist S. (1998) Hsp104, Hsp70, and Hsp40: A novel chaperone system that rescues previously aggregated proteins. *Cell* **94:** 73-82.

Glover J.R., Kowal A.S., Schirmer E.C., Patino M.M., Liu J.J., and Lindquist S. (1997) Self-seeded fibers formed by Sup35, the protein determinant of [*PSI*⁺], a heritable prion-like factor of S. cerevisiae. *Cell* **89:** 811-819.

Goggin K., Bissonnette C., Grenier C., Volkov L., and Roucou X. (2007) Aggregation of cellular prion protein is initiated by proximity-induced dimerization. *Journal of Neurochemistry* **102:** 1195-1205.

Goldfarb L.G., Brown P., McCombie W.R., Goldgaber D., Swergold G.D., Wills P.R., *et al.* (1991) Transmissible familial Creutzfeldt-Jakob disease associated with five, seven, and eight extra octapeptide coding repeats in the PRNP gene. *Proc Natl Acad Sci U S A* **88:** 10926-10930.

Gorsich S.W., and Shaw J.M. (2004) Importance of mitochondrial dynamics during meiosis and sporulation *Mol Biol Cell* **15:** 4369-4381.

Govaerts C., Wille H., Prusiner S.B., and Cohen F.E. (2004) Evidence for assembly of prions with left-handed beta-helices into trimers. *Proc Natl Acad Sci U S A* **101:** 8342-8347.

Griffith J.S. (1967) Self-replication and scrapie. *Nature* **215:** 1043-4.

Grishin A.V., Rothenberg M., Downs M.A., and Blumer K.J. (1998) Mot3, a zn finger transcription factor that modulates gene expression and attenuates mating pheromone signaling in *Saccharomyces cerevisiae*. *Genetics* **149:** 879-892.

Grousl T., Ivanov P., Frydlova I., Vasicova P., Janda F., Vojtova J., *et al.* (2009) Robust heat shock induces eIF2alpha-phosphorylation-independent assembly of stress granules containing eIF3 and 40S ribosomal subunits in budding yeast, *Saccharomyces cerevisiae*. *J Cell Sci* **122:** 2078-2088.

Gruhler A., Olsen J.V., Mohammed S., Mortensen P., Faergeman N.J., Mann M., and Jensen O.N. (2005) Quantitative phosphoproteomics applied to the yeast pheromone signaling pathway. *Mol Cell Proteomics* **4:** 310-327.

Güldener U., Heck S., Fiedler T., Beinhauer J., and Hegemann J.H. (1996) A new efficient gene disruption cassette for repeated use in budding yeast. *Nucleic Acids Res* **24:** e13.

Gueldener U., Heinisch J., Koehler G.J., Voss D., and Hegemann J.H. (2002) A second set of loxP marker cassettes for cre-mediated multiple gene knockouts in budding yeast. *Nucleic Acids Res* **30:** e23.

Halfmann R., Alberti S., Krishnan R., Lyle N., O'Donnell C.W., King O.D., *et al.* (2011) Opposing effects of glutamine and asparagine govern prion formation by intrinsically disordered proteins. *Mol Cell* **43:** 72-84.

Harger J.W., and Dinman J.D. (2003) An in vivo dual-luciferase assay system for studying translational recoding in the yeast *Saccharomyces cerevisiae*. *RNA* **9:** 1019-1024.

Harper J.D., Wong S.S., Lieber C.M., and Lansbury P.T. (1997) Observation of metastable abeta amyloid protofibrils by atomic force microscopy. *Chem Biol* **4:** 119-125.

Harrison L.B., Yu Z., Stajich J.E., Dietrich F.S., and Harrison P.M. (2007) Evolution of budding yeast prion-determinant sequences across diverse fungi. *J Mol Biol* **368**: 273-282.

Hermann G.J., Thatcher J.W., Mills J.P., Hales K.G., Fuller M.T., Nunnari J., and Shaw J.M. (1998) Mitochondrial fusion in yeast requires the transmembrane GTPase Fzo1p *J Cell Biol* **143**: 359-373.

Hibbs M.A., Hess D.C., Myers C.L., Huttenhower C., Li K., and Troyanskaya O.G. (2007) Exploring the functional landscape of gene expression: Directed search of large microarray compendia *Bioinformatics* **23**: 2692-2699.

Hillenmeyer M.E., Fung E., Wildenhain J., Pierce S.E., Hoon S., Lee W., *et al.* (2008) The chemical genomic portrait of yeast: Uncovering a phenotype for all genes. *Science* **320**: 362-365.

Hosoda N., Kobayashi T., Uchida N., Funakoshi Y., Kikuchi Y., Hoshino S., and Katada T. (2003) Translation termination factor eRF3 mediates mRNA decay through the regulation of deadenylation. *J Biol Chem* **278**: 38287-38291.

Huang M.E., and Kolodner R.D. (2005) A biological network in *Saccharomyces cerevisiae* prevents the deleterious effects of endogenous oxidative DNA damage. *Mol Cell* **17**: 709-720.

Huang M.E., Rio A.G., Nicolas A., and Kolodner R.D. (2003) A genomewide screen in *Saccharomyces cerevisiae* for genes that suppress the accumulation of mutations. *Proc Natl Acad Sci U S A* **100**: 11529-11534.

Hughes V., Muller A., Stark M.J., and Cohen P.T. (1993) Both isoforms of protein phosphatase Z are essential for the maintenance of cell size and integrity in *Saccharomyces cerevisiae* in response to osmotic stress. *Eur J Biochem* **216**: 269-279.

Hurst L.D., and Smith N.G. (1999) Do essential genes evolve slowly? *Curr Biol* **9**: 747-750.

Inge-Vechtomov S.G., Tikhodeev O.N., and Karpova T.S. (1988) Selective systems for obtaining recessive ribosomal suppressors in saccharomycete yeasts. *Genetika* **24**: 1159-1165.

Iraqui I., Kienda G., Soeur J., Faye G., Baldacci G., Kolodner R.D., and Huang M.E. (2009) Peroxiredoxin Tsa1 is the key peroxidase suppressing genome instability and protecting against cell death in *Saccharomyces cerevisiae*. *PLoS Genet* **5**: e1000524.

Ivanov M.S., Aksenova A.I., Burdaeva I., Radchenko E.A., and Mironova L.N. (2008) Overexpression of gene PPZ1 in the yeast *Saccharomyces cerevisiae* affects the efficiency of nonsense suppression. *Genetika* **44**: 177-184.

James P., Halladay J., and Craig E.A. (1996) Genomic libraries and a host strain designed for highly efficient two-hybrid selection in yeast. *Genetics* **144**: 1425-1436.

Jang H.H., Lee K.O., Chi Y.H., Jung B.G., Park S.K., Park J.H., *et al.* (2004) Two enzymes in one; two yeast peroxiredoxins display oxidative stress-dependent switching from a peroxidase to a molecular chaperone function. *Cell* **117**: 625-635.

Jin L.W., Claborn K.A., Kurimoto M., Geday M.A., Maezawa I., Sohraby F., *et al.* (2003) Imaging linear birefringence and dichroism in cerebral amyloid pathologies. *Proc Natl Acad Sci U S A* **100**: 15294-15298.

Jin R., Dobry C.J., McCown P.J., and Kumar A. (2008) Large-scale analysis of yeast filamentous growth by systematic gene disruption and overexpression. *Mol Biol Cell* **19**: 284-296.

Jones G.W., Song Y., and Masison D.C. (2003) Deletion of the Hsp70 chaperone gene SSB causes hypersensitivity to guanidine toxicity and curing of the [*PSI$^+$*] prion by increasing guanidine uptake in yeast. *Mol Genet Genomics* **269**: 304-311.

Jordan I.K., Rogozin I.B., Wolf Y.I., and Koonin E.V. (2002) Essential genes are more evolutionarily conserved than are nonessential genes in bacteria. *Genome Res* **12**: 962-968.

Jung G., Jones G., and Masison D.C. (2002) Amino acid residue 184 of yeast Hsp104 chaperone is critical for prion-curing by guanidine, prion propagation, and thermotolerance. *Proc Natl Acad Sci U S A* **99**: 9936-9941.

Kaganovich D., Kopito R., and Frydman J. (2008) Misfolded proteins partition between two distinct quality control compartments. *Nature* **454**: 1088-1095.

Kajava A.V., Baxa U., Wickner R.B., and Steven A.C. (2004) A model for Ure2p prion filaments and other amyloids: The parallel superpleated beta-structure. *Proc Natl Acad Sci U S A* **101**: 7885-7890.

Kallmeyer A.K., Keeling K.M., and Bedwell D.M. (2006) Eukaryotic release factor 1 phosphorylation by CK2 protein kinase is dynamic but has little effect on the efficiency of translation termination in *Saccharomyces cerevisiae*. *Eukaryot Cell* **5**: 1378-1387.

Kanki T., and Klionsky D.J. (2008) Mitophagy in yeast occurs through a selective mechanism. *J Biol Chem* **283**: 32386-32393.

Kawai-Noma S., Pack C.G., Kojidani T., Asakawa H., Hiraoka Y., Kinjo M., *et al.* (2010) In vivo evidence for the fibrillar structures of Sup35 prions in yeast cells. *J Cell Biol* **190**: 223-231.

Kayed R., Head E., Thompson J.L., McIntire T.M., Milton S.C., Cotman C.W., and Glabe C.G. (2003) Common structure of soluble amyloid oligomers implies common mechanism of pathogenesis. *Science* **300**: 486-489.

Keeling K.M., Lanier J., Du M., Salas-Marco J., Gao L., Kaenjak-Angeletti A., and Bedwell D.M. (2004) Leaky termination at premature stop codons antagonizes nonsense-mediated mRNA decay in S. cerevisiae *RNA* **10**: 691-703.

Kent W.J., Sugnet C.W., Furey T.S., Roskin K.M., Pringle T.H., Zahler A.M., and Haussler D. (2002) The human genome browser at UCSC *Genome Res* **12**: 996-1006.

Kimura Y., Koitabashi S., and Fujita T. (2003) Analysis of yeast prion aggregates with amyloid-staining compound in vivo. *Cell Struct Funct* **28**: 187-193.

King C.Y., and Diaz-Avalos R. (2004) Protein-only transmission of three yeast prion strains. *Nature* **428:** 319-323.

King C.Y., Tittmann P., Gross H., Gebert R., Aebi M., and Wuthrich K. (1997) Prion-inducing domain 2-114 of yeast Sup35 protein transforms in vitro into amyloid-like filaments. *Proc Natl Acad Sci U S A* **94:** 6618-6622.

Kishimoto A., Hasegawa K., Suzuki H., Taguchi H., Namba K., and Yoshida M. (2004) Beta-helix is a likely core structure of yeast prion Sup35 amyloid fibers. *Biochem Biophys Res Commun* **315:** 739-745.

Kissova I., Deffieu M., Manon S., and Camougrand N. (2004) Uth1p is involved in the autophagic degradation of mitochondria. *J Biol Chem* **279:** 39068-39074.

Krishnan R., and Lindquist S.L. (2005) Structural insights into a yeast prion illuminate nucleation and strain diversity. *Nature* **435:** 765-772.

Kron S.J., Styles C.A., and Fink G.R. (1994) Symmetric cell division in pseudohyphae of the yeast *Saccharomyces cerevisiae. Mol Biol Cell* **5:** 1003-1022.

Kryndushkin D.S., Alexandrov I.M., Ter-Avanesyan M.D., and Kushnirov V.V. (2003) Yeast [*PSI*+] prion aggregates are formed by small Sup35 polymers fragmented by Hsp104. *J Biol Chem* **278:** 49636-43.

Krzewska J., Tanaka M., Burston S.G., and Melki R. (2007) Biochemical and functional analysis of the assembly of full-length Sup35p and its prion-forming domain. *J Biol Chem* **282:** 1679-1686.

Kushnirov V.V., Kryndushkin D.S., Boguta M., Smirnov V.N., and Ter-Avanesyan M.D. (2000) Chaperones that cure yeast artificial [*PSI*+] and their prion-specific effects. *Curr Biol* **10:** 1443-6.

Kushnirov V.V., Ter-Avanesyan M.D., Telckov M.V., Surguchov A.P., Smirnov V.N., and Inge-Vechtomov S.G. (1988) Nucleotide sequence of the *SUP2* (*SUP35*) gene of *Saccharomyces cerevisiae. Gene* **66:** 45-54.

Lacroute F. (1971) Non-mendelian mutation allowing ureidosuccinic acid uptake in yeast *J Bacteriol* **106:** 519-522.

Laemmli U.K. (1970) Cleavage of structural proteins during the assembly of the head of bacteriophage T4. *Nature* **227:** 680-685.

Lambrechts M.G., Bauer F.F., Marmur J., and Pretorius I.S. (1996) Muc1, a mucin-like protein that is regulated by Mss10, is critical for pseudohyphal differentiation in yeast. *Proc Natl Acad Sci U S A* **93:** 8419-8424.

Lancaster A.K., Bardill J.P., True H.L., and Masel J. (2010) The spontaneous appearance rate of the yeast prion [*PSI*+] and its implications for the evolution of the evolvability properties of the [PSI+] system. *Genetics* **184:** 393-400.

Leadsham J.E., Miller K., Ayscough K.R., Colombo S., Martegani E., Sudbery P., and Gourlay C.W. (2009) Whi2p links nutritional sensing to actin-dependent ras-cAMP-PKA regulation and apoptosis in yeast. *J Cell Sci* **122:** 706-715.

Lefrancois P., Euskirchen G.M., Auerbach R.K., Rozowsky J., Gibson T., Yellman C.M., *et al.* (2009) Efficient yeast ChIP-seq using multiplex short-read DNA sequencing. *BMC Genomics* **10:** 37.

Liti G., Carter D.M., Moses A.M., Warringer J., Parts L., James S.A., *et al.* (2009) Population genomics of domestic and wild yeasts. *Nature* **458:** 337-341.

Liu H., Styles C.A., and Fink G.R. (1996) *Saccharomyces cerevisiae* S288C has a mutation in *FLO8*, a gene required for filamentous growth. *Genetics* **144:** 967-978.

Liu H., Styles C.A., and Fink G.R. (1993) Elements of the yeast pheromone response pathway required for filamentous growth of diploids. *Science* **262:** 1741-1744.

Liu J.J., and Lindquist S. (1999) Oligopeptide-repeat expansions modulate 'protein-only' inheritance in yeast. *Nature* **400:** 573-576.

Liu J.J., Sondheimer N., and Lindquist S.L. (2002) Changes in the middle region of Sup35 profoundly alter the nature of epigenetic inheritance for the yeast prion [*PSI*⁺]. *Proc Natl Acad Sci U S A* **99 Suppl 4:** 16446-53.

Lorenz M.C., Cutler N.S., and Heitman J. (2000) Characterization of alcohol-induced filamentous growth in *Saccharomyces cerevisiae*. *Mol Biol Cell* **11:** 183-199.

Lund P.M., and Cox B.S. (1981) Reversion analysis of [psi-] mutations in *Saccharomyces cerevisiae*. *Genet Res* **37:** 173-182.

Luria S.E., and Delbruck M. (1943) Mutations of bacteria from virus sensitivity to virus resistance. *Genetics* **28:** 491-511.

Madeo F., Herker E., Maldener C., Wissing S., Lachelt S., Herlan M., *et al.* (2002) A caspase-related protease regulates apoptosis in yeast. *Mol Cell* **9:** 911-917.

Mann D.J., Dombradi V., and Cohen P.T. (1993) Drosophila protein phosphatase V functionally complements a SIT4 mutant in *Saccharomyces cerevisiae* and its amino-terminal region can confer this complementation to a heterologous phosphatase catalytic domain. *EMBO J* **12:** 4833-4842.

Manogaran A.L., Kirkland K.T., and Liebman S.W. (2006) An engineered nonsense *URA3* allele provides a versatile system to detect the presence, absence and appearance of the [*PSI*⁺] prion in *Saccharomyces cerevisiae*. *Yeast* **23:** 141-147.

Manogaran A.L., Hong J.Y., Hufana J., Tyedmers J., Lindquist S., and Liebman S.W. (2011) Prion formation and polyglutamine aggregation are controlled by two classes of genes. *PLoS Genet* **7:** e1001386.

Manuelidis L., Yu Z.X., Banquero N., and Mullins B. (2007) Cells infected with scrapie and creutzfeldt-jakob disease agents produce intracellular 25-nm virus-like particles. *Proceedings of the National Academy of Sciences of the United States of America* **104:** 1965-1970.

Mathur V., Taneja V., Sun Y., and Liebman S.W. (2010) Analyzing the birth and propagation of two distinct prions, [*PSI*⁺] and [het-s]ᵧ, in yeast. *Mol Biol Cell* **21:** 1449-1461.

Mendl N., Occhipinti A., Muller M., Wild P., Dikic I., and Reichert A.S. (2011) Mitophagy in yeast is independent of mitochondrial fission and requires the stress response gene *WHI2*. *J Cell Sci* **124**: 1339-1350.

Meriin A.B., Zhang X., He X., Newnam G.P., Chernoff Y.O., and Sherman M.Y. (2002) Huntington toxicity in yeast model depends on polyglutamine aggregation mediated by a prion-like protein Rnq1. *J Cell Biol* **157**: 997-1004.

Michelitsch M.D., and Weissman J.S. (2000) A census of glutamine/asparagine-rich regions: Implications for their conserved function and the prediction of novel prions. *Proc Natl Acad Sci U S A* **97**: 11910-11915.

Monti M., Garolla di Bard B.L., Calloni G., Chiti F., Amoresano A., Ramponi G., and Pucci P. (2004) The regions of the sequence most exposed to the solvent within the amyloidogenic state of a protein initiate the aggregation process. *J Mol Biol* **336**: 253-262.

Morgan B.A., and Veal E.A. (2007) Functions of typical 2-cys peroxiredoxins in yeast. *Subcell Biochem* **44**: 253-265.

Morozova-Roche L.A., Zamotin V., Malisauskas M., Ohman A., Chertkova R., Lavrikova M.A., *et al.* (2004) Fibrillation of carrier protein albebetin and its biologically active constructs. multiple oligomeric intermediates and pathways. *Biochemistry* **43**: 9610-9619.

Nakayashiki T., Kurtzman C.P., Edskes H.K., and Wickner R.B. (2005) Yeast prions [*URE3*] and [*PSI*⁺] are diseases. *Proc Natl Acad Sci U S A* **102**: 10575-10580.

Namy O., Hatin I., and Rousset J.P. (2001) Impact of the six nucleotides downstream of the stop codon on translation termination. *EMBO Rep* **2**: 787-793.

Nelson R., Sawaya M.R., Balbirnie M., Madsen A.O., Riekel C., Grothe R., and Eisenberg D. (2005) Structure of the cross-beta spine of amyloid-like fibrils. *Nature* **435**: 773-778.

Nemecek J., Nakayashiki T., and Wickner R.B. (2009) A prion of yeast metacaspase homolog (Mca1p) detected by a genetic screen. *Proc Natl Acad Sci U S A* **106**: 1892-1896.

Ness F., Ferreira P., Cox B.S., and Tuite M.F. (2002) Guanidine hydrochloride inhibits the generation of prion "seeds" but not prion protein aggregation in yeast. *Mol Cell Biol* **22**: 5593-605.

Newnam G.P., Wegrzyn R.D., Lindquist S.L., and Chernoff Y.O. (1999) Antagonistic interactions between yeast chaperones Hsp104 and Hsp70 in prion curing. *Mol Cell Biol* **19**: 1325-33.

Nissen P., Hansen J., Ban N., Moore P.B., and Steitz T.A. (2000) The structural basis of ribosome activity in peptide bond synthesis. *Science* **289**: 920-930.

Ono B.I., Ishino Y., and Shinoda S. (1983) Nonsense mutations in the *can1* locus of *Saccharomyces cerevisiae*. *J Bacteriol* **154**: 1476-1479.

Orlowska-Matuszewska G., and Wawrzycka D. (2006) A novel phenotype of eight spores asci in deletants of the prion-like Rnq1p in *Saccharomyces cerevisiae*. *Biochem Biophys Res Commun* **340**: 190-193.

Osherovich L.Z., and Weissman J.S. (2001) Multiple Gln/Asn-rich prion domains confer susceptibility to induction of the yeast [*PSI*⁺] prion. *Cell* **106**: 183-194.

Osherovich L.Z., Cox B.S., Tuite M.F., and Weissman J.S. (2004) Dissection and design of yeast prions. *PLoS Biol* **2**: E86.

Paoletti M., and Saupe S.J. (2009) Fungal incompatibility: Evolutionary origin in pathogen defense? *Bioessays* **31**: 1201-1210.

Parham S.N., Resende C.G., and Tuite M.F. (2001) Oligopeptide repeats in the yeast protein Sup35p stabilize intermolecular prion interactions. *EMBO J* **20**: 2111-2119.

Park S.G., Cha M.K., Jeong W., and Kim I.H. (2000) Distinct physiological functions of thiol peroxidase isoenzymes in *Saccharomyces cerevisiae*. *J Biol Chem* **275**: 5723-5732.

Parsell D.A., Kowal A.S., Singer M.A., and Lindquist S. (1994) Protein disaggregation mediated by heat-shock protein Hsp104. *Nature* **372**: 475-8.

Patel B.K., Gavin-Smyth J., and Liebman S.W. (2009) The yeast global transcriptional co-repressor protein Cyc8 can propagate as a prion. *Nat Cell Biol* **11**: 344-349.

Patino M.M., Liu J.J., Glover J.R., and Lindquist S. (1996) Support for the prion hypothesis for inheritance of a phenotypic trait in yeast. *Science* **273**: 622-626.

Paushkin S.V., Kushnirov V.V., Smirnov V.N., and Ter-Avanesyan M.D. (1997) Interaction between yeast Sup45p (eRF1) and Sup35p (eRF3) polypeptide chain release factors: Implications for prion-dependent regulation. *Mol Cell Biol* **17**: 2798-805.

Pedersen J.S., Dikov D., Flink J.L., Hjuler H.A., Christiansen G., and Otzen D.E. (2006) The changing face of glucagon fibrillation: Structural polymorphism and conformational imprinting. *J Mol Biol* **355**: 501-523.

Perutz M.F., Johnson T., Suzuki M., and Finch J.T. (1994) Glutamine repeats as polar zippers: Their possible role in inherited neurodegenerative diseases. *Proc Natl Acad Sci U S A* **91**: 5355-5358.

Plakoutsi G., Taddei N., Stefani M., and Chiti F. (2004) Aggregation of the acylphosphatase from sulfolobus solfataricus: The folded and partially unfolded states can both be precursors for amyloid formation. *J Biol Chem* **279**: 14111-14119.

Posas F., Casamayor A., Morral N., and Arino J. (1992) Molecular cloning and analysis of a yeast protein phosphatase with an unusual amino-terminal region. *J Biol Chem* **267**: 11734-11740.

Posas F., Clotet J., Muns M.T., Corominas J., Casamayor A., and Arino J. (1993) The gene *PPG* encodes a novel yeast protein phosphatase involved in glycogen accumulation. *J Biol Chem* **268**: 1349-1354.

Prusiner S.B. (1982) Novel proteinaceous infectious particles cause scrapie. *Science* **216**: 136-44.

Prusiner S.B., Bolton D.C., Groth D.F., Bowman K.A., Cochran S.P., and McKinley M.P. (1982) Further purification and characterization of scrapie prions. *Biochemistry* **21**: 6942-50.

Putrament A., Baranowska H., and Prazmo W. (1973) Induction by manganese of mitochondrial antibiotic resistance mutations in yeast. *Mol Gen Genet* **126**: 357-366.

Rand J.D., and Grant C.M. (2006) The thioredoxin system protects ribosomes against stress-induced aggregation. *Mol Biol Cell* **17**: 387-401.

Reijns M.A., Alexander R.D., Spiller M.P., and Beggs J.D. (2008) A role for Q/N-rich aggregation-prone regions in P-body localization. *J Cell Sci* **121**: 2463-2472.

Ren J., Wen L., Gao X., Jin C., Xue Y., and Yao X. (2008) CSS-palm 2.0: An updated software for palmitoylation sites prediction. *Protein Eng Des Sel* **21**: 639-644.

Resende C.G., Outeiro T.F., Sands L., Lindquist S., and Tuite M.F. (2003) Prion protein gene polymorphisms in *Saccharomyces cerevisiae*. *Mol Microbiol* **49**: 1005-17.

Rhee S.G., Chae H.Z., and Kim K. (2005) Peroxiredoxins: A historical overview and speculative preview of novel mechanisms and emerging concepts in cell signaling. *Free Radic Biol Med* **38**: 1543-1552.

Roberts R.L., and Fink G.R. (1994) Elements of a single MAP kinase cascade in *Saccharomyces cerevisiae* mediate two developmental programs in the same cell type: Mating and invasive growth. *Genes Dev* **8**: 2974-2985.

Rogoza T., Goginashvili A., Rodionova S., Ivanov M., Viktorovskaya O., Rubel A., *et al.* (2010) Non-mendelian determinant [*ISP*$^+$] in yeast is a nuclear-residing prion form of the global transcriptional regulator Sfp1. *Proc Natl Acad Sci U S A* **107**: 10573-10577.

Roostaee A., Cote S., and Roucou X. (2009) Aggregation and amyloid fibril formation induced by chemical dimerization of recombinant prion protein in physiological-like conditions *J Biol Chem* **284**: 30907-30916.

Ross E.D., Minton A., and Wickner R.B. (2005a) Prion domains: Sequences, structures and interactions. *Nat Cell Biol* **7**: 1039-1044.

Ross E.D., Edskes H.K., Terry M.J., and Wickner R.B. (2005b) Primary sequence independence for prion formation. *Proc Natl Acad Sci U S A* **102**: 12825-12830.

Saiki M., Honda S., Kawasaki K., Zhou D., Kaito A., Konakahara T., and Morii H. (2005) Higher-order molecular packing in amyloid-like fibrils constructed with linear arrangements of hydrophobic and hydrogen-bonding side-chains. *J Mol Biol* **348**: 983-998.

Salas-Marco J., and Bedwell D.M. (2005) Discrimination between defects in elongation fidelity and termination efficiency provides mechanistic insights into translational readthrough. *J Mol Biol* **348**: 801-815.

Salnikova A.B., Kryndushkin D.S., Smirnov V.N., Kushnirov V.V., and Ter-Avanesyan M.D. (2005) Nonsense suppression in yeast cells overproducing Sup35 (eRF3) is caused by its non-heritable amyloids. *J Biol Chem* **280**: 8808-8812.

Scherz-Shouval R., Elazar Z. (2007) ROS, mitochondria and the regulation of autophagy. *Trends in Cell Biology* **17**: 422-427.

Schroder E., Littlechild J.A., Lebedev A.A., Errington N., Vagin A.A., and Isupov M.N. (2000) Crystal structure of decameric 2-cys peroxiredoxin from human erythrocytes at 1.7 A resolution. *Structure* **8**: 605-615.

Schwimmer C., and Masison D.C. (2002) Antagonistic interactions between yeast [*PSI*⁺] and [*URE3*] prions and curing of [*URE3*] by Hsp70 protein chaperone Ssa1p but not by Ssa2p. *Mol Cell Biol* **22**: 3590-8.

Serio T.R., Cashikar A.G., Kowal A.S., Sawicki G.J., Moslehi J.J., Serpell L., *et al.* (2000) Nucleated conformational conversion and the replication of conformational information by a prion determinant. *Science* **289**: 1317-1321.

Shannon P., Markiel A., Ozier O., Baliga N.S., Wang J.T., Ramage D., *et al.* (2003) Cytoscape: A software environment for integrated models of biomolecular interaction networks *Genome Res* **13**: 2498-2504.

Shapiro R. (2006) Small molecule interactions were central to the origin of life. *Q Rev Biol* **81**: 105-125.

Shewmaker F., and Wickner R.B. (2006) Ageing in yeast does not enhance prion generation. *Yeast* **23**: 1123-1128.

Shewmaker F., Ross E.D., Tycko R., and Wickner R.B. (2008) Amyloids of shuffled prion domains that form prions have a parallel in-register beta-sheet structure. *Biochemistry* **47**: 4000-4007.

Shkundina I.S., Kushnirov V.V., Tuite M.F., and Ter-Avanesyan M.D. (2006) The role of the N-terminal oligopeptide repeats of the yeast Sup35 prion protein in propagation and transmission of prion variants. *Genetics* **172**: 827-835.

Shorter J., and Lindquist S. (2006) Destruction or potentiation of different prions catalyzed by similar Hsp104 remodeling activities. *Mol Cell* **23**: 425-38.

Shorter J., and Lindquist S. (2004) Hsp104 catalyzes formation and elimination of self-replicating Sup35 prion conformers. *Science* **304**: 1793-7.

Sideri T.C., Koloteva-Levine N., Tuite M.F., and Grant C.M. (2011) Methionine oxidation of Sup35 induces formation of the [*PSI*⁺] prion in a yeast peroxiredoxin mutant. *J Biol Chem* .

Sideri T.C., Stojanovski K., Tuite M.F., and Grant C.M. (2010) Ribosome-associated peroxiredoxins suppress oxidative stress-induced de novo formation of the [*PSI*⁺] prion in yeast. *Proc Natl Acad Sci U S A* **107**: 6394-6399.

Smirnov V.N., Kreier V.G., Lizlova L.V., Andrianova V.M., and Inge-Vechtomov S.G. (1974) Recessive super-suppression in yeast. *Mol Gen Genet* **129**: 105-121.

Sondheimer N., and Lindquist S. (2000) Rnq1: An epigenetic modifier of protein function in yeast. *Mol Cell* **5**: 163-72.

Song J.M., and Liebman S.W. (1987) Allosuppressors that enhance the efficiency of omnipotent suppressors in *Saccharomyces cerevisiae. Genetics* **115:** 451-460.

Sopko R., Huang D., Preston N., Chua G., Papp B., Kafadar K., *et al.* (2006) Mapping pathways and phenotypes by systematic gene overexpression. *Mol Cell* **21:** 319-330.

Soulard A., Lechler T., Spiridonov V., Shevchenko A., Shevchenko A., Li R., and Winsor B. (2002) *Saccharomyces cerevisiae* Bzz1p is implicated with type I myosins in actin patch polarization and is able to recruit actin-polymerizing machinery in vitro. *Mol Cell Biol* **22:** 7889-7906.

Stansfield I., Jones K.M., Kushnirov V.V., Dagkesamanskaya A.R., Poznyakovski A.I., Paushkin S.V., *et al.* (1995) The products of the *SUP45* (eRF1) and *SUP35* genes interact to mediate translation termination in *Saccharomyces cerevisiae. EMBO J* **14:** 4365-73.

Stark C., Su T.C., Breitkreutz A., Lourenco P., Dahabieh M., Breitkreutz B.J., *et al.* (2010) PhosphoGRID: A database of experimentally verified in vivo protein phosphorylation sites from the budding yeast *Saccharomyces cerevisiae. Database (Oxford)* **2010:** bap026.

Sunde M., Serpell L.C., Bartlam M., Fraser P.E., Pepys M.B., and Blake C.C. (1997) Common core structure of amyloid fibrils by synchrotron X-ray diffraction. *J Mol Biol* **273:** 729-739.

Sutton A., Immanuel D., and Arndt K.T. (1991) The SIT4 protein phosphatase functions in late G1 for progression into S phase. *Mol Cell Biol* **11:** 2133-2148.

Tanaka M., Collins S.R., Toyama B.H., and Weissman J.S. (2006) The physical basis of how prion conformations determine strain phenotypes. *Nature* **442:** 585-589.

Tanaka M., Chien P., Naber N., Cooke R., and Weissman J.S. (2004) Conformational variations in an infectious protein determine prion strain differences. *Nature* **428:** 323-328.

Tang H.M., Siu K.L., Wong C.M., and Jin D.Y. (2009) Loss of yeast peroxiredoxin Tsa1p induces genome instability through activation of the DNA damage checkpoint and elevation of dNTP levels. *PLoS Genet* **5:** e1000697.

Tartaglia G.G., Cavalli A., Pellarin R., and Caflisch A. (2004) The role of aromaticity, exposed surface, and dipole moment in determining protein aggregation rates. *Protein Sci* **13:** 1939-1941.

Teravanesyan M.D., Kushnirov V.V., Dagkesamanskaya A.R., Didichenko S.A., Chernoff Y.O., Ingevechtomov S.G., and Smirnov V.N. (1993) Deletion analysis of the Sup35 gene of the yeast saccharomyces-cerevisiae reveals 2 nonoverlapping functional regions in the encoded protein. *Molecular Microbiology* **7:** 683-692.

Ter-Avanesyan M.D., Dagkesamanskaya A.R., Kushnirov V.V., and Smirnov V.N. (1994) The *SUP35* omnipotent suppressor gene is involved in the maintenance of the non-mendelian determinant [psi+] in the yeast *Saccharomyces cerevisiae. Genetics* **137:** 671-676.

Tonikian R., Xin X., Toret C.P., Gfeller D., Landgraf C., Panni S., *et al.* (2009) Bayesian modeling of the yeast SH3 domain interactome predicts spatiotemporal dynamics of endocytosis proteins. *PLoS Biol* **7:** e1000218.

Toyama B.H., Kelly M.J., Gross J.D., and Weissman J.S. (2007) The structural basis of yeast prion strain variants. *Nature* **449**: 233-237.

Trotter E.W., Rand J.D., Vickerstaff J., and Grant C.M. (2008) The yeast Tsa1 peroxiredoxin is a ribosome-associated antioxidant. *Biochem J* **412**: 73-80.

True H.L., and Lindquist S.L. (2000) A yeast prion provides a mechanism for genetic variation and phenotypic diversity. *Nature* **407**: 477-483.

Tuite M., Stojanovski K., Ness F., Merritt G., and Koloteva-Levine N. (2008) Cellular factors important for the de novo formation of yeast prions. *Biochem Soc Trans* **36**: 1083-1087.

Tuite M.F., and Serio T.R. (2010) The prion hypothesis: From biological anomaly to basic regulatory mechanism. *Nat Rev Mol Cell Biol* **11**: 823-833.

Tuite M.F., Mundy C.R., and Cox B.S. (1981) Agents that cause a high frequency of genetic change from [psi+] to [psi-] in *Saccharomyces cerevisiae*. *Genetics* **98**: 691-711.

Tyedmers J., Madariaga M.L., and Lindquist S. (2008) Prion switching in response to environmental stress. *PLoS Biol* **6**: e294.

Tyedmers J., Treusch S., Dong J., McCaffery J.M., Bevis B., and Lindquist S. (2010) Prion induction involves an ancient system for the sequestration of aggregated proteins and heritable changes in prion fragmentation. *Proc Natl Acad Sci U S A* **107**: 8633-8638.

Uptain S.M., Sawicki G.J., Caughey B., and Lindquist S. (2001) Strains of [*PSI*$^+$] are distinguished by their efficiencies of prion-mediated conformational conversion. *EMBO J* **20**: 6236-6245.

Urakov V.N., Valouev I.A., Kochneva-Pervukhova N.V., Packeiser A.N., Vishnevsky A.Y., Glebov O.O., *et al.* (2006) N-terminal region of *Saccharomyces cerevisiae* eRF3 is essential for the functioning of the eRF1/eRF3 complex beyond translation termination. *BMC Mol Biol* **7**: 34.

van der Wel P.C., Lewandowski J.R., and Griffin R.G. (2007) Solid-state NMR study of amyloid nanocrystals and fibrils formed by the peptide GNNQQNY from yeast prion protein Sup35p. *J Am Chem Soc* **129**: 5117-5130.

Venturi G.M., Bloecher A., Williams-Hart T., and Tatchell K. (2000) Genetic interactions between *GLC7*, *PPZ1* and *PPZ2* in *Saccharomyces cerevisiae*. *Genetics* **155**: 69-83.

Vincent A., Newnam G., and Liebman S.W. (1994) The yeast translational allosuppressor, *SAL6*: A new member of the PP1-like phosphatase family with a long serine-rich N-terminal extension. *Genetics* **138**: 597-608.

Vishveshwara N., Bradley M.E., and Liebman S.W. (2009) Sequestration of essential proteins causes prion associated toxicity in yeast. *Mol Microbiol* **73**: 1101-1114.

Visser W., van Spronsen E.A., Nanninga N., Pronk J.T., Gijs Kuenen J., and van Dijken J.P. (1995) Effects of growth conditions on mitochondrial morphology in *Saccharomyces cerevisiae*. *Antonie Van Leeuwenhoek* **67**: 243-253.

Vitrenko Y.A., Pavon M.E., Stone S.I., and Liebman S.W. (2007a) Propagation of the [*PIN⁺*] prion by fragments of Rnq1 fused to GFP. *Curr Genet* **51:** 309-19.

Vitrenko Y.A., Gracheva E.O., Richmond J.E., and Liebman S.W. (2007b) Visualization of aggregation of the Rnq1 prion domain and cross-seeding interactions with Sup35NM. *J Biol Chem* **282:** 1779-87.

Volkov K., Osipov K., Valouev I., Inge-Vechtomov S., and Mironova L. (2007) N-terminal extension of *Saccharomyces cerevisiae* translation termination factor eRF3 influences the suppression efficiency of sup35 mutations. *FEMS Yeast Res* **7:** 357-365.

Volkov K.V., Aksenova A.Y., Soom M.J., Osipov K.V., Svitin A.V., Kurischko C., *et al.* (2002) Novel non-mendelian determinant involved in the control of translation accuracy in *Saccharomyces cerevisiae*. *Genetics* **160:** 25-36.

von der Haar T. (2008) A quantitative estimation of the global translational activity in logarithmically growing yeast cells. *BMC Syst Biol* **2:** 87.

von der Haar T. (2007) Optimized protein extraction for quantitative proteomics of yeasts. *PLoS One* **2:** e1078.

Waldron C., Cox B.S., Wills N., Gesteland R.F., Piper P.W., Colby D., and Guthrie C. (1981) Yeast ochre suppressor SUQ5-ol is an altered tRNA ser UCA. *Nucleic Acids Res* **9:** 3077-3088.

Walsh D.M., Hartley D.M., Kusumoto Y., Fezoui Y., Condron M.M., Lomakin A., *et al.* (1999) Amyloid beta-protein fibrillogenesis. structure and biological activity of protofibrillar intermediates. *J Biol Chem* **274:** 25945-25952.

Westermann B., and Neupert W. (2000) Mitochondria-targeted green fluorescent proteins: Convenient tools for the study of organelle biogenesis in *Saccharomyces cerevisiae*. *Yeast* **16:** 1421-1427.

Wickner R.B. (1994) URE3] as an altered *URE2* protein: Evidence for a prion analog in *Saccharomyces cerevisiae*. *Science* **264:** 566-569.

Wong C.M., Siu K.L., and Jin D.Y. (2004) Peroxiredoxin-null yeast cells are hypersensitive to oxidative stress and are genomically unstable. *J Biol Chem* **279:** 23207-23213.

Wong C.M., Zhou Y., Ng R.W., Kung Hf H.F., and Jin D.Y. (2002) Cooperation of yeast peroxiredoxins Tsa1p and Tsa2p in the cellular defense against oxidative and nitrosative stress *J Biol Chem* **277:** 5385-5394.

Wood Z.A., Poole L.B., and Karplus P.A. (2003) Peroxiredoxin evolution and the regulation of hydrogen peroxide signaling. *Science* **300:** 650-653.

Yang J., Roe S.M., Cliff M.J., Williams M.A., Ladbury J.E., Cohen P.T., and Barford D. (2005) Molecular basis for TPR domain-mediated regulation of protein phosphatase 5. *EMBO J* **24:** 1-10.

Yang K.S., Kang S.W., Woo H.A., Hwang S.C., Chae H.Z., Kim K., and Rhee S.G. (2002) Inactivation of human peroxiredoxin I during catalysis as the result of the oxidation of the catalytic site cysteine to cysteine-sulfinic acid. *J Biol Chem* **277:** 38029-38036.

Yonemoto W., McGlone M.L., and Taylor S.S. (1993) N-myristylation of the catalytic subunit of cAMP-dependent protein kinase conveys structural stability. *J Biol Chem* **268:** 2348-2352.

Yoshikawa K., Tanaka T., Ida Y., Furusawa C., Hirasawa T., and Shimizu H. (2011) Comprehensive phenotypic analysis of single-gene deletion and overexpression strains of *Saccharomyces cerevisiae. Yeast* **28:** 349-361.

Young C.S., and Cox B.S. (1975) Extrachromosomal elements in a super-suppression system of yeast. III. enhanced detection of weak suppressors in certain non-suppressed psi-strains. *Heredity* **34:** 83-93.

Zhang Y. (2008) I-TASSER server for protein 3D structure prediction. *BMC Bioinformatics* **9:** 40.

Zheng W., Zhao H., Mancera E., Steinmetz L.M., and Snyder M. (2010) Genetic analysis of variation in transcription factor binding in yeast. *Nature* **464:** 1187-1191.

Zhou P., Derkatch I.L., and Liebman S.W. (2001) The relationship between visible intracellular aggregates that appear after overexpression of Sup35 and the yeast prion-like elements [*PSI*⁺] and [*PIN*⁺]. *Mol Microbiol* **39:** 37-46.

Zhou P., Derkatch I.L., Uptain S.M., Patino M.M., Lindquist S., and Liebman S.W. (1999) The yeast non-mendelian factor [*ETA*⁺] is a variant of [*PSI*⁺], a prion-like form of release factor eRF3. *EMBO J* **18:** 1182-1191.

Zhouravleva G., Frolova L., Le Goff X., Le Guellec R., Inge-Vechtomov S., Kisselev L., and Philippe M. (1995) Termination of translation in eukaryotes is governed by two interacting polypeptide chain release factors, eRF1 and eRF3. *EMBO J* **14:** 4065-4072.